ISSN 0971-6777 (Print)
ISSN 2277-8934 (Online)

JOURNAL OF CAMEL PRACTICE AND RESEARCH

www.camelsandcamelids.com • www.indianjournals.com

Volume 29 August 2022 Number 2

In This Issue

JOURNAL OF CAMEL PRACTICE AND RESEARCH

EDITOR
TARUN KUMAR GAHLOT
Camel Publishing House
Bikaner - 334001, INDIA
Email : tkcamelvet@yahoo.com
Website : www.camelsandcamelids.com • www.tkgahlotcamelvet.com • www.indianjournals.com

CAMEL PUBLISHING HOUSE
Bikaner - 334001, INDIA

Manuscripts and other related correspondence may be made to :

Dr. Tarun Kumar Gahlot
Editor, Journal of Camel Practice and Research
67, Gandhi Nagar West
Near Lalgarh Palace
Bikaner-334001, INDIA

Mobile : 0091-9414137029
Email : tkcamelvet@yahoo.com
Website : www.camelsandcamelids.com • www.tkgahlotcamelvet.com • www.indianjournals.com

Scope of Journal of Camel Practice and Research

Journal of Camel Practice and Research (JCPR) publishes only research and clinical manuscripts related to the Camelids (Old and New World camelids), hence published contents are consistent with the title and scope of the journal. Review articles on emerging research are invited and published. JCPR also publishes the news related to the New or Old World Camelids, specially those related to new products, conferences, books, trainings or workshops etc.

SUBSCRIPTION RATE - 2022

ANNUAL Rs. 4500/- or US $ 450

Note : *Subscription in Rupees is applicable to Indian subscribers only.*

Publisher : The **Journal of Camel Practice and Research** (Triannual) is published by the **"Camel Publishing House"** 67, Gandhi Nagar West, Near Lalgarh Palace, Bikaner-334001, India. email: tkcamelvet@yahoo.com

Cover Design: Tarun Kumar Gahlot

Cover Photo: Camels at King Abdulaziz Camel Festival, Saudi Arabia

Courtesy: Tarun Kumar Gahlot

Printer: Sankhla Printers, Vinayak Shikhar, Near Polytechnic College, Bikaner-334003, India.

Phone: 0091 - 151 - 2242023

CONTENTS

Volume 29 **August 2022** **Number 2**

CONTENTS

Volume 29 **August 2022** **Number 2**

EDITORIAL

SAVING THE CAMELS

"Saving the camels" is drawing attention in few countries where either population is on decline or camels die of toxicity or plastic pollution. However, to a lesser extent camels are saved from road accidents also by putting several signboards at camel crossing prone areas and imposing fine if camels are hit by automobiles. The present large camelid population in the world is probably more than 40 million**. The Indian dromedary camel population is still in decline, especially since the 2010s, a reverse trend developed in China. In countries marked by a regular or drastic decline of their camelid population, a tendency to re-increase has been in force since the beginning of the century, except in India**. It needs an urgent population crisis management at government level. While deciding the policies to save the camels in India, it should be pondered upon that how best the population sustainability and a gradual increase in camel population is taking place in other countries including China. The camel population in India is in mortal decline. The economic benefits of rearing a camel have all but disappeared. The road network in Rajasthan has grown by almost 30 times since 1951, slowly but surely eliminating the need for the "ship of the desert". Camels, or camel carts carrying people or goods — so common even a few decades ago — can rarely be seen now. Till the 1960s, Civil Admininstrative officers in Rajasthan routinely toured their districts on camels. Camel owners in India perhaps lost interest in rearing and breeding camels because of poor economical returns. In fact, the effort made by the Government of Rajasthan — enacting The Rajasthan Camel (Prohibition of Slaughter and Regulation of Temporary Migration or Export) Act, 2015 — has had just the opposite effect. Forced by economic reality, the Raika sold their camels to any buyer, including those whom they suspected of buying it for meat, and even sold in grey market for a meagre price. The ban has benefitted only the meat traders and corrupt officials. Camels in India are unlikely to survive as just milch animals either, despite the many demonstrated benefits of camel milk, for several reasons. Neither production nor demand could possibly sustain an economically successful dairy model*. The dromedary camels in Arabian Peninsula are best thriving as a race animal which is additionally used for meat and milk purposes also. These camels are surplus as feral camels in Australia where their use is not much exploited.

A group of scientists recently published papers on plastic pollution. Camels residing in the UAE are experiencing a regional 1% mortality rate from ingesting plastic pollution***. Polybezoars, the tightly packed collection of indigestible materials, which can include plastics, ropes other litter and salt deposits, that is trapped in the stomach or digestive tract, forming a large stone-like mass, lead to gastrointestinal blockages, sepsis from increased populations of gut bacteria, dehydration and malnutrition.

It is imperative to discuss the pertinent topic "Saving the camels" through this plarform to bring a growing awareness among the cameleers, camel scientists and government authorities for saving this desert creature.

(*Decline in India's camel population is worrying written by Rajiv Mehrishi, former civil servant, Rajasthan cadre, The Indian Express, July 7, 2022; **Faye, B. How many large camelids in the world? A synthetic analysis of the world camel demographic changes. Pastoralism 10, 25 (2020). https://doi.org/10.1186/s13570-020-00176-z, ***(Marcus Eriksen, Amy Lusher, Mia Nixon and Ulrich Wernery. The plight of camels eating plastic waste. Journal of Arid Environments, 2021; Volume 185)

(Dr. Tarun Kumar Gahlot)
Editor

SUBSCRIPTION - 2022

FOR

JOURNAL OF CAMEL PRACTICE AND RESEARCH

(Triannual In English Language, April, August and December Issue Every Year)

SUBSCRIPTION RATE - 2022

ANNUAL Rs. 4500/- or US $ 450

Note : *Subscription in Rupees is applicable to Indian subscribers only.*

Subscription Form

I want to become annual subscriber of the **Journal of Camel Practice and Research**, for/from the year 2022 ..... For this purpose I am enclosing herewith a cheque / demand draft number ..... dated ..... for Rs./US $..... in favour of "**Camel Publishing House**". The cheque or D.D. should be payable at State Bank of India, Code No. 7260, Bikaner. Payment may be made through payment portal of website www.camelsandcamelids.com or money transfer to bank account.

Name : .....

Permanent Address : .....

: .....

Country : .....

Signature : .....

Mail to :

Camel Publishing House
67, Gandhi Nagar West
Near Lalgarh Palace
Bikaner - 334001, INDIA
Phone : 0091-151-2527029
email : tkcamelvet@yahoo.com
website : www.camelsandcamelids.com

BACK ISSUES OF JCPR AVAILABLE

ISSN 0971-6777

JOURNAL OF CAMEL PRACTICE AND RESEARCH

www.camelsandcamelids.com

Volume 17 June 2010 Number 1

In This Issue

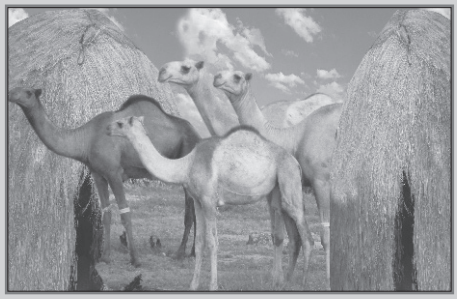

ISSN 0971-6777

JOURNAL OF CAMEL PRACTICE AND RESEARCH

www.camelsandcamelids.com

Volume 17 December 2010 Number 2

In This Issue

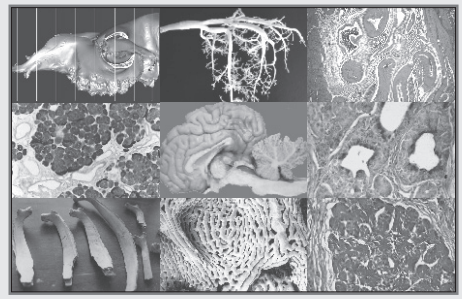

ISSN 0971-6777

JOURNAL OF CAMEL PRACTICE AND RESEARCH

www.camelsandcamelids.com

Volume 18 June 2011 Number 1

In This Issue

ISSN 0971-6777 (Print)
ISSN 2277-8934 (Online)

JOURNAL OF CAMEL PRACTICE AND RESEARCH

www.camelsandcamelids.com

Volume 18 December 2011 Number 2

In This Issue

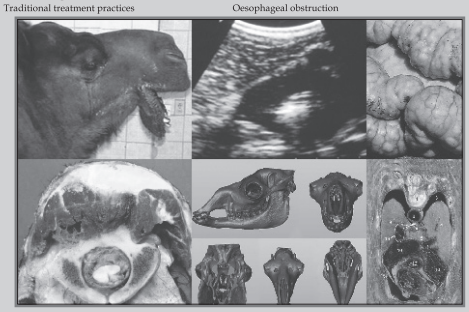

See the details of list of contents of all previous issues of JCPR on our website www.camelsandcamelids.com

Kindly refer querries to: Dr. T.K. GAHLOT, Editor, JCPR
email: tkcamelvet@yahoo.com

BACK ISSUES OF JCPR AVAILABLE

ISSN 0971-6777 (Print)
ISSN 2277-8934 (Online)

JOURNAL OF CAMEL PRACTICE AND RESEARCH

www.camelsandcamelids.com

Volume 19 June 2012 Number 1

In This Issue

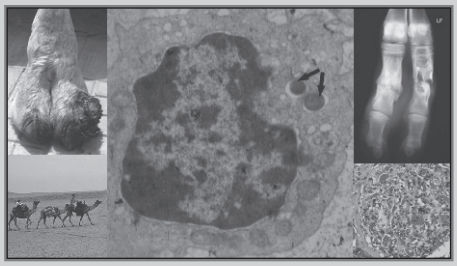

ISSN 0971-6777 (Print)
ISSN 2277-8934 (Online)

JOURNAL OF CAMEL PRACTICE AND RESEARCH

www.camelsandcamelids.com

Volume 19 December 2012 Number 2

In This Issue

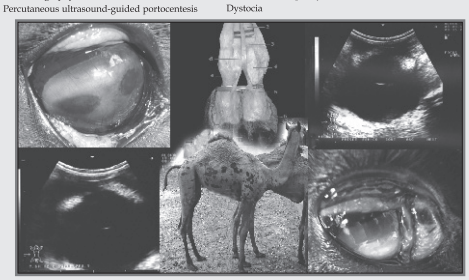

ISSN 0971-6777 (Print)
ISSN 2277-8934 (Online)

JOURNAL OF CAMEL PRACTICE AND RESEARCH

www.camelsandcamelids.com • www.indianjournals.com

Volume 20 June 2013 Number 1

FIRST FROZEN SEMEN CALF

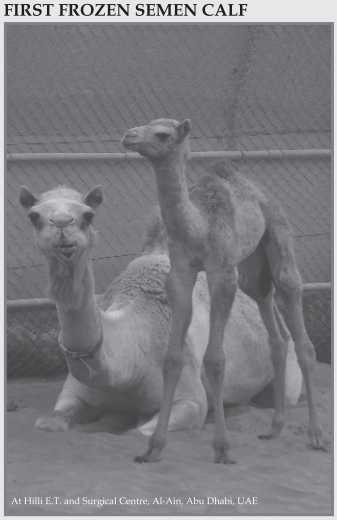

At Hilli E.T. and Surgical Centre, Al-Ain, Abu Dhabi, UAE

In This Issue

ISSN 0971-6777 (Print)
ISSN 2277-8934 (Online)

JOURNAL OF CAMEL PRACTICE AND RESEARCH

www.camelsandcamelids.com • www.indianjournals.com

Volume 20 December 2013 Number 2

In This Issue

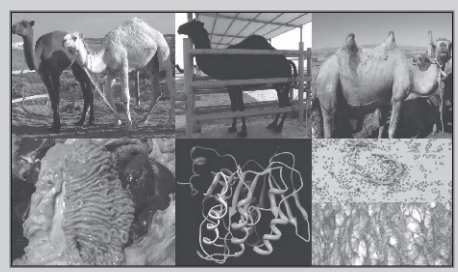

See the details of list of contents of all previous issues of JCPR on our website
www.camelsandcamelids.com

Kindly refer querries to: Dr. T.K. GAHLOT, Editor, JCPR
email: tkcamelvet@yahoo.com

DOI : 10.5958/2277-8934.2022.00014.5 Vol 29 No 2, p 105-110

MERS-COV IN DROMEDARY CAMELS: SEQUENCE-BASED COMPARISON OF ANTIGENICITY AND PATHOGENICITY OF STRUCTURAL AND NON-STRUCTURAL PROTEINS

Sabry M. El-Bahr[1,2], Mahmoud Kandeel[1,3], I.F. Albokhadaim[1], M. Al-Nazawi[1] and Hafiz Ahmed[4]

[1]Department of Biomedical Sciences, College of Veterinary Medicine, King Faisal University, Al-Ahsa 31982, P.O. 400, Saudi Arabia

[2]Department of Biochemistry, Faculty of Veterinary Medicine, Alexandria University, Alexandria 21523, Egypt

[3]Department of Pharmacology, Faculty of Veterinary Medicine, Kafr Elsheikh University, Egypt

[4]GlycoMentra Inc., 1450 South Rolling Road, Baltimore, MD 21227, USA

ABSTRACT

The goal of this researcher was to map the camel MERS-CoV structural and non-structural proteins and track changes in antigenicity and pathogenicity from 2013 to 2018. This is critical for developing effective diagnostic and control methods. Therefore, the sequences of MERS-CoV structural proteins such as Spike (S), Membrane (M), Nucleocapsid (N) and Envelope (E) and nonstructural proteins, comprising polyprotein-ab (polyab) and Open reading frame-3 (ORF3) were retrieved. The amino acid sequences of each of these proteins were analysed to estimate their antigenic and pathogenic properties from 2013 to 2018. The antigenicity profiles showed variations in antigenicity minimum, maximum, range, and average from 2013 to 2018. MERS-CoV proteins' maximum antigenicity score was declining in the examined time frame. In 2013, the maximum score was 0.86, and by 2018, it had dropped to 0.6. This resulted in a greater range of antigenicity with the onset of MERS-CoV in 2013, with a range of 0.56, which eventually decreased to 0.22 in 2018. The net effect on the mean value of antigenicity score revealed that MERS-CoV antigenicity decreased gradually. Between 2013 and 2018, the mean antigenicity score of structural and non-structural proteins decreased. Non-structural proteins, on the other hand, had the greatest alterations, with a mean value of 0.52 in 2013 and 0.42 in 2018, representing a loss of 19.2 per cent of their antigenicity score. In contrast, the structural protein showed a mean value of 0.55 in 2013 and 0.53 in 2018, i.e. lost only 3.6% of its antigenicity score. Given that ORF3 was nonantigenic, therefore, all changes in antigenicity changes were attributed to polyab protein. Pathogenicity score has decreased from 0.81 in 2013 to 0.78 in 2018. Further studies are required to map these changes on the virus-host cell interaction level.

Key words: Antigenicity, camels, MERS-CoV, pathogenicity, proteins

MERS-CoV was first identified in Saudi Arabia in 2012 in a patient with severe pneumonia (Zaki *et al,* 2012). Initially the virus was termed as "human coronavirus Erasmus Medical Centre (EMC) or EMC-CoV". This novel coronavirus later was termed as Middle East respiratory syndrome coronavirus (MERS-CoV) according to the announcement of the Coronavirus Study Group of the International Committee on Taxonomy of Viruses (ICTV) (de Groot *et al*, 2013). The MERS-genome CoV is 30 kb (30,119nt) long and encodes four structural proteins (Spike, Envelope, Membrane, and Nucleocapsid) as well as 16 nonstructural proteins (van Boheemen *et al,* 2012).

MERS-CoV infection has a 35.4 per cent fatality rate, and new cases and deaths have continued till the end of 2018 (WHO, 2018). According to current research, many coronaviruses that are phylogenetically similar to MERS-CoV, such as BatCoV-HKU4, BatCoV-HKU5, and other MERS-related coronaviruses, are considered to have originated in bats (Woo *et al,* 2012; van Boheemen *et al,* 2012; Corman *et al,* 2014; Anthony *et al,* 2017). The BatCoV-HKU4 has also been discovered to be capable of activating the MERS-CoV cellular receptor, bolstering the bat origin theory (Wang *et al,* 2014). There is, however, no direct evidence that MERS-CoV may be isolated from bats (Xu *et al,* 2019). Because camel isolates are nearly identical to human isolates and many domestic camels are MERS-CoV seropositive, dromedary camels are thought to be the animal reservoir for MERS-CoV (Xu

SEND REPRINT REQUEST TO SABRY MOHAMED EL-BAHR email: selbahar@kfu.edu.sa; sabryelbahr@hotmail.com

et al, 2019). Camels in the Middle East and northern Africa contain antibodies to MERS-CoV or a virus that is quite similar to it, according to serological evidence dating back to the 1980s (Alagaili *et al,* 2014; Corman *et al,* 2014; Müller *et al,* 2014). These findings are not applicable to Bactrian camels or dromedaries from other countries, such as Australia and Kazakhstan (Hemida *et al,* 2014a). While these findings support the theory that camels can transmit illnesses to humans, initial MERS cases may not have had any interaction with camels. Furthermore, because the MERS-CoV receptor, dipeptidyl peptidase 4, is highly conserved in mammals, other mammalian hosts may be involved (van Doremalen *et al,* 2017). In this study, the changes in MERS-CoV antigenicity and pathogenicity were be evaluated from 2013 to 2018. The results were further analysed in the light of structural and non-structural protein components, as well as, the specific proteins used in the analysis.

Materials and Methods

Retrieval of input protein data and analytical programs

The sequences of the input proteins of interest (polyab, ORF3, S, M, N, and E) were retrieved from the GenBank at NCBI.

Prediction of the antigenic properties of MERS-CoV proteins

The amino acid sequences of proteins of interest (polyab, ORF3, S, M, N, and E) were utilised for antigenic property analysis, and the VaxiJen v2.0 server (Doytchinova and Flower, 2007) with a threshold of 0.4 was employed (http://www.ddg-pharmfac.net/vaxijen/VaxiJen/VaxiJen.html). A summary of antigenicity statistics for MERS-CoV 2013-2018 is presented in Table 1. The antigenicity score for each of the proteins of interest: polyab, S, M, N, and E was recorded. The algorithm was used to analyse the antigenic property after inserting a threshold value of 0.4.

Prediction of pathogenic and antigenic properties

Using the protein sequences of each chosen MERS-CoV isolate, we used the MP3 program (http://metagenomics.iiserb.ac.in/mp3/application.php) with default settings to estimate pathogenicity scores (Gupta *et al,* 2014). The hybrid findings (SVM+HMM) were taken into account, and the SVM scores were employed in the analysis. The pathogenic score for each of the proteins of interest (polyab, ORF3, S, M, N, and E) was recorded (Table 2). For each isolate, the average scores of all these proteins were also computed.

Statistical analysis

All data handling and presentation were done by MS excel and GraphPad Prism software. The results were presented in Mean±SD or, in some cases, the mean + range is provided. Descriptive statistics were used to express changes in each isolate parameter.

Results and Discussion

MERS-CoV is an emerging infectious virus that is exceedingly dangerous to humans and is zoonotic in nature. Effective vaccination and diagnostic methods for this virus are still mostly unknown. Gaps in our understanding of these pathogens' protective immunity and antigenicity offer obstacles to the development of vaccines and diagnostics. Respiratory sickness caused by the MERS-CoV virus continues to grow for unnoticeable reasons. Since SARS-CoV-2 has emerged, it has become clear that effective therapies against extremely deadly human coronaviruses developed quickly. Despite this fact, the efforts to develop efficient vaccines and diagnostics against MERS-CoV are still in their primary stages. There has been a surge in R&D efforts to produce diagnostic, preventive, and therapeutic solutions for SARS-CoV-2, which has caused millions of affections. In contrast, MERS-CoV with more than 1,700 acetate cases of sickness and 600 deaths in 27 countries has less attention in developing vaccines and diagnostics.

Table 1. Summary of antigenicity statistics for MERS-CoV 2013-2018.

Year	2013	2014	2015	2016	2017	2018
Antigenicity scores (Mean ± SD)	0.5271 ± 0.1305	0.503 ± 0.1091	0.4891 ± 0.09007	0.4911 ± 0.08907	0.4941 ± 0.08299	0.4911 ± 0.07723

Table 2. Summary of pathogenicity statistics for MERS-CoV 2013-2018.

Year	2013	2014	2015	2016	2017	2018
Pathogenicity scores (Mean ± SD)	0.8115 ± 0.5868	0.7722 ± 0.6045	0.7227 ± 0.6039	0.7529 ± 0.5104	0.7775 ± 0.5217	0.776 ± 0.531

A summary of MERS-CoV antigenicity and its statistics during 2013-2018 is provided in Fig 1. The number of data entries each year ranged from 12-84 with the highest hits in 2014 followed by 2015. Surprisingly, the antigenicity profiles shoed variations in antigenicity minimum, maximum, range, and average from 2013 to 2018. MERS-CoV proteins' maximum antigenicity score decreased. In 2013, the maximum score was 0.86, and by 2018, it had dropped to 0.6. (Fig 2). This resulted in a greater range of antigenicity with the onset of MERS-CoV in 2013, with a range of 0.56, which eventually decreased to 0.22 in 2018. (Fig 1A, Fig 2). The net effect on the mean value of antigenicity score revealed that MERS-CoV antigenicity decreased gradually. In 2013, the antigenicity score was 0.5271 ± 0.1305 which decreased to 0.4911 ± 0.077 in 2018. As the initial data showed declining antigenicity of MERS-CoV, we further investigated the changes in antigenicity in the protein components of MERS-CoV (Fig 3). Both structural and non-structural proteins showed declining mean antigenicity scores from 2013-2018. However, the greater changes were with NS, which showed a mean value of 0.52 in 2013 and 0.42 in 2018, i.e. lost about 19.2% of its antigenicity score. In contrast, the structural protein

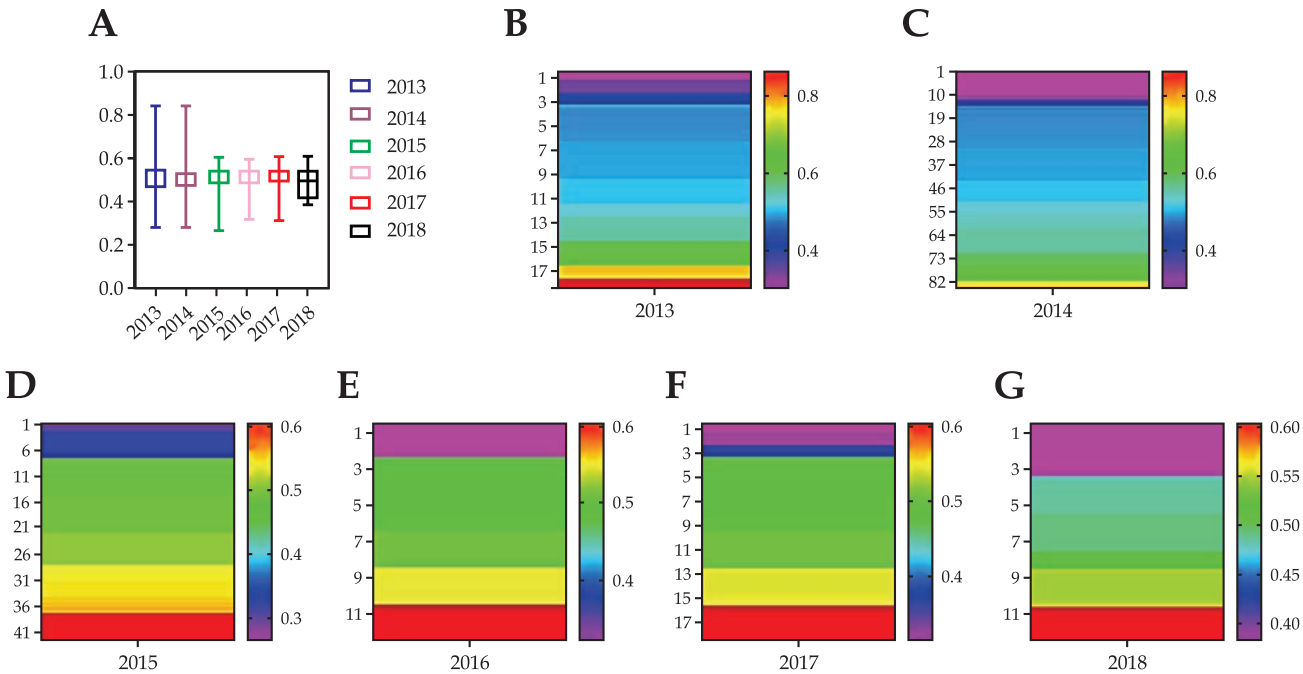

Fig 1. MERS-CoV antigenicity scores. (A) Box and whiskers plot showing the range of antigenicity with cross-line at mean values (B) Heat map representation of antigenicity score in the year 2013. A colour scale from red to pink (right panel) to imply the estimated antigenicity score. (C) The same plot as in B for 2014 (D) 2015 (E) 2016 (F) 2017 (G). 2018.

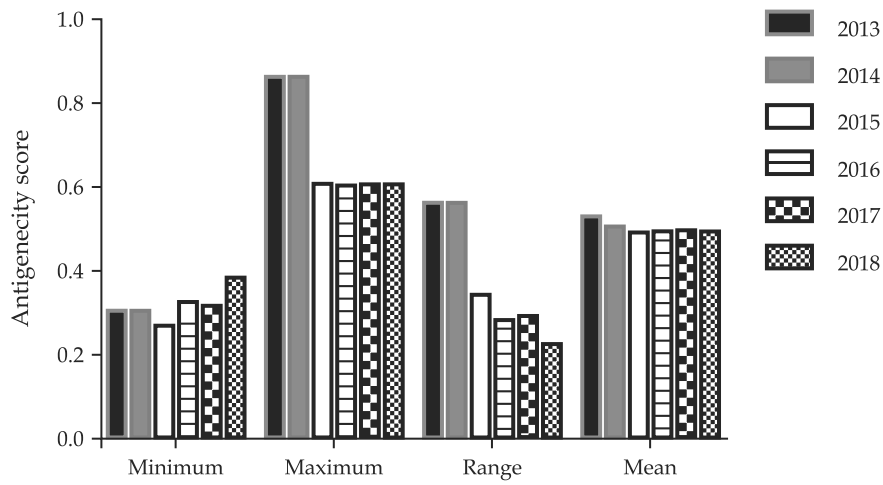

Fig 2. The mean and range for MERS-CoV 2013-2018.

showed a mean value of 0.55 in 2013 and 0.53 in 2018, i.e. lost only 3.6% of its antigenicity score. In this study, we used only two NS proteins in all procedures, polyab and ORF3. Given that ORF3 was nonantigenic, therefore, all changes in antigenicity were attributed to polyab. The analysis of MERS-CoV pathogenicity scores from 2013 to 2018 demonstrated a moderate decline. Pathogenicity score has decreased from 0.8115 ± 0.5868 in 2013 to 0.776 ± 0.531 in 2018. The range of pathogenicity of viral proteins was broad in the early years of MERS-CoV emergence, but it narrowed in subsequent years (Fig 4). The changes in the pathogenicity of MERS-CoV proteins were further analysed according to the protein components, comprising S, N, E, M and Polyab (Fig 5). Among these proteins, polyab and E proteins showed a gradual decrease in pathogenicity.

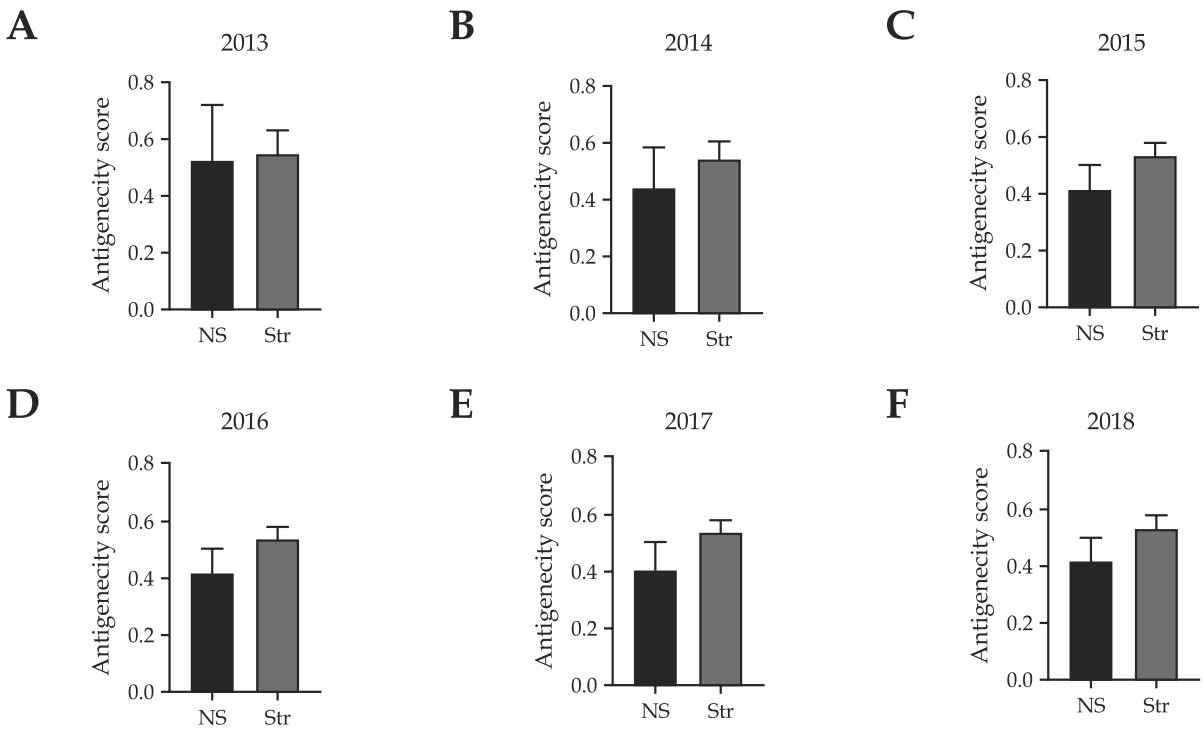

Fig 3. MERS-CoV nonstructural (NS) and structural (Str) proteins antigenicity scores. (A) Column bar graph showing the NS and Str proteins antigenicity scores during 2013 (B) 2014 (C) 2015 (D) 2016 (E) 2017 (F) 2018.

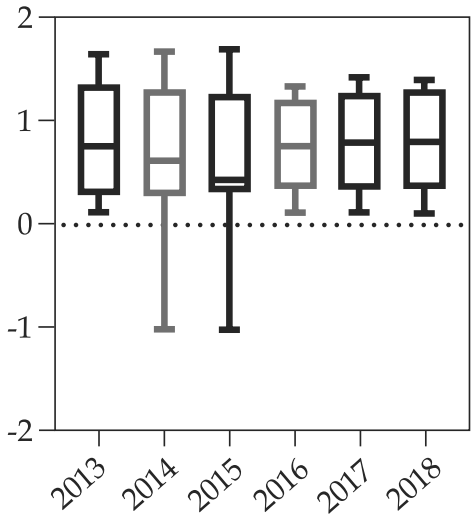

Fig 4. MERS-CoV pathogenicity scores. Box and whiskers plot showing the range of pathogenicity with cross-line at mean values.

In 2015, molecular diagnostic approaches and their global performances for the sensitive and specific detection of MERS-CoV RNA are well-illustrated in the first external quality evaluation MERS-CoV panel (Pas *et al,* 2015). MERS-CoV could be detected in all laboratories, but with varying degrees of sensitivity. The fact that 8% of labs reported false positives for MERS-CoV in a single assay demonstrates that there is potential for improvement and that confirmatory targets are important. This fact highlights the need for continued assessment of the accuracy of detection methods. In this work, we showed a decreasing antigenicity of MERS-CoV proteins. The impact of these changes on the accuracy of current diagnostics is to be elucidated.

Conflict of interest

The authors declare no conflict of interest.

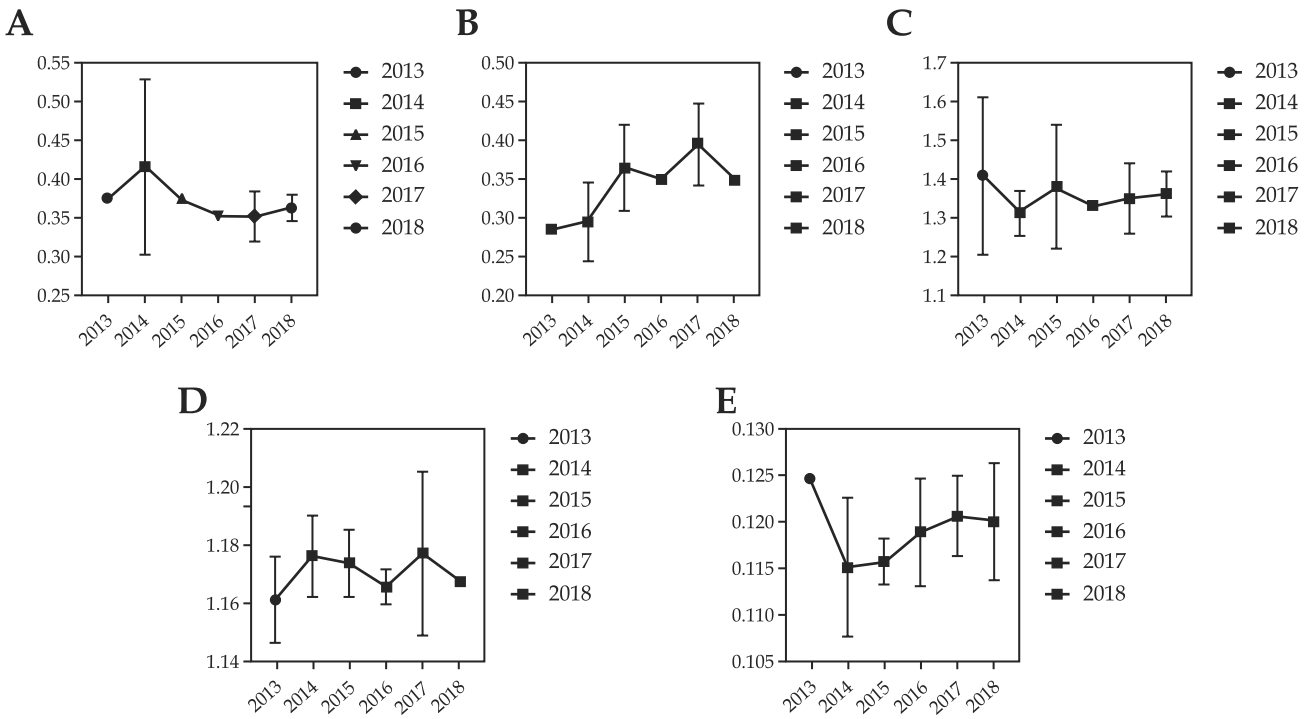

Fig 5. MERS-CoV proteins pathogenicity scores. (A) E protein (B) M protein (C) E protein (D) S protein (E) Polyab.

Acknowledgements

This work was supported by the Deanship of Scientific Research, Vice Presidency for Graduate Studies and Scientific Research, King Faisal University, Saudi Arabia (Project # 171002; Grant 271).

References

Alagaili AN, Briese T, Mishra N, Kapoor V, Sameroff SC, Burbelo PD, de Wit E, Munster VJ, Hensley LE, Zalmout IS, Kapoor A, Epstein JH, Karesh WB, Daszak P, Mohammed OB and Lipkin WI. Middle East respiratory syndrome coronavirus infection in dromedary camels in Saudi Arabia. mBio. 2014; 5:884-814. DOI:10.1128/mBio.00884-14.

Anthony SJ, Gilardi K, Menachery VD, Goldstein T, Ssebide B, Mbabazi R, Navarrete-Macias I, Liang E, Wells H, Hicks A, Petrosov A, Byarugaba DK, Debbink K, Dinnon KH, Scobey T, Randell SH, Yount BL, Cranfield M, Johnson CK, Baric RS, Lipkin WI and Mazet JA. Further evidence for bats as the evolutionary source of Middle East respiratory syndrome coronavirus. mBio. 2017; 8(2). Doi:10.1128/mBio.00373-17.

Corman VM, Ithete NL, Richards LR, Schoeman MC, Preiser W, Drosten C and Drexler JF. Rooting the phylogenetic tree of middle east respiratory syndrome coronavirus by characterization of a conspecific virus from an African Bat. Journal of Virology. 2014; 88(19):11297–11303. Doi:10.1128/jvi.01498-14.

de Groot RJ, Baker SC, Baric RS, Brown CS, Drosten C, Enjuanes L, Fouchier RA, Galiano M, Gorbalenya AE, Memish ZA, Perlman S, Poon LL, Snijder EJ, Stephens GM, Woo PC, Zaki AM, Zambon M and Ziebuhr J. Middle East respiratory syndrome coronavirus (MERS-CoV): announcement of the coronavirus study group. Journal of Virology. 2013; 87(14):7790-7792. Doi:10.1128/jvi.01244-13.

Doytchinova IA and Flower DR. VaxiJen: a server for prediction of protective antigens, tumour antigens and subunit vaccines. BMC bioinformatics. 2007; 8(1):1-7.

Gupta A, Kapil R, Dhakan DB and Sharma VK. MP3: a software tool for the prediction of pathogenic proteins in genomic and metagenomic data. PloS one. 2014; 9(4), e93907.

Hemida MG, Chu DK, Poon LL, Perera RA, Alhammadi MA, Ng HY, Siu LY, Guan Y, Alnaeem A, Peiris M. MERS coronavirus in dromedary camel herd, Saudi Arabia. Emerging Infectious Diseases. 2014; 20(7):1231-4. doi: 10.3201/eid2007.140571.

Müller MA, Corman VM, Jores J, Meyer B, Younan M, Liljander A, Bosch BJ, Lattwein E, Hilali M, Musa BE, Bornstein S and Drosten C. MERS coronavirus neutralizing antibodies in camels, Eastern Africa, 1983-1997. Emerging Infectious Diseases. 2014; 20:2093-2095. DOI:10.3201/eid2012.141026.

Pas SD, Patel P, Reusken C, Domingo C, Corman VM, Drosten C, Dijkman R, Thiel V, Nowotny N, Koopmans MP and Niedrig M. First international external quality assessment of molecular diagnostics for Mers-CoV. Journal of Clinical Virology. 2015; 69:81-85. Doi: 10.1016/j.jcv.2015.05.022.

van Boheemen S, de Graaf M, Lauber C, Bestebroer TM, Raj VS, Zaki AM, Osterhaus AD, Haagmans BL, Gorbalenya AE, Snijder EJ and Fouchier RA. Genomic characterization of a newly discovered coronavirus associated with acute respiratory distress syndrome in humans. mBio. 2012; 3(6):00473–12.

van Doremalen N, Hijazeen ZS, Holloway P, Al Omari B, McDowell C, Adney D, Talafha HA, Guitian J, Steel J, Amarin N, Tibbo M, Abu-Basha E, Al-Majali AM, Munster VJ and Richt JA. High Prevalence of Middle East Respiratory Coronavirus in Young Dromedary Camels in Jordan. Vector Borne Zoonotic Diseases. 2017; 17:155-159. DOI:10.1089/vbz.2016.2062.

Wang Q, Qi J, Yuan Y, Xuan Y, Han P, Wan Y, Ji W, Li Y, Wu Y, Wang J, Iwamoto A, Woo PC, Yuen KY, Yan J, Lu G and Gao GF. Bat origins of MERS-CoV supported by bat coronavirus HKU4 usage of human receptor CD26. Cell Host Microbe. 2014; 16(3):328-337. Doi:10.1016/j.chom.2014.08.009.

WHO. Middle East respiratory syndrome coronavirus (MERS-CoV) 2018 [cited 2019 Mar 26]. Available from: http://www.who.int/emergencies/mers-cov/en/

Woo PC, Lau SK, Li KS, Tsang AK and Yuen KY. Genetic relatedness of the novel human group C betacoronavirus to Tylonycteris bat coronavirus HKU4 and Pipistrellus bat coronavirus HKU5. Emerging Microbes and Infections. 2012; 1(11):e35. Doi: 10.1038/emi.2012.45.

Xu J, Jia W, Wang P, Zhang S, Shi X, Wang X and Zhang L. Antibodies and vaccines against Middle East respiratory syndrome coronavirus. Emerging Microbes and Infections. 2019; 8(1):841-856. Doi: 10.1080/22221751.2019.1624482.

Zaki AM, van Boheemen S, Bestebroer TM, Osterhaus AD and Fouchier RA. Isolation of a novel coronavirus from a man with pneumonia in Saudi Arabia. The New England Journal of Medicine. 2012; 367:1814-1820. DOI:10.1056/NEJMoa1211721.

DOI : 10.5958/2277-8934.2022.00015.7 Vol 29 No 2, p 111-116

SPATIAL EXPRESSION OF OSTEOPONTIN IN TESTIS, EPIDIDYMIS AND SPERMATOZOA IN DROMEDARY CAMEL

Khalid Alkhodair and Abdelhay Mohamed Ali
Department of Anatomy, College of Veterinary Medicine, King Faisal University, P.O Box: 400. Al-Ahsa, 31982, Saudi Arabia

ABSTRACT

The aim of this study is to clarify the function of osteopontin (OPN) through its expression and localisation in male testis, epididymis and sperm cell of dromedary camel during rutting season. Testis and epididymis parts (caput, corpus and cauda) specimens were obtained from 8 mature male camels and semen was collected from 4 another fertile camels for sperms. OPN mRNA expression and its location was analysed using quantitative real-time polymerase chain reaction (qRT-PCR) and immunohistochemistry (IHC) techniques, respectively. OPN mRNA expression was significantly ($P < 0.05$) higher in the cauda of epididymis than other epididymal parts and testis. Immunolocalisation revealed high immunoreaction intensity in the elongated spermatids in seminiferous tubules and Leydig cells in interstitial tissue. However, a faint immunostaining was seen in spermatogonia and Sertoli cells. Along the epididymis tract, intense immunoreactivity of OPN was localised in the cytoplasm of the epithelial cells with high concentration in the apical region nearby lumen and the acrosomal part of the cauda epididymal sperms. Immunofluorescence and immunochromogenic staining of OPN was detected on the acrosomal cap and neck of epididymal sperms. These findings suggested that OPN might play an important role in the sperm protection, migration and fertilisation in dromedary camels.

Key words: Dromedary camel, epididymis, expression, osteopontin, spermatozoa, testis

Osteopontin (OPN), also named as Secreted Phosphoprotein1 (SPP1), is an indispensable highly phosphorylated glycoprotein in mammalian reproduction. Firstly, it was isolated from the mineralised matrix of bovine bone (Denhardt and Guo, 1993; Franzen and Heinegård, 1985). Thereafter, it was found in different tissues such as brain (Shin *et al,* 2005), kidney (Xie *et al,* 2001) and body secretions like male seminal fluids (Cancel *et al,* 1999). The function of OPN has been determined according to the expressed cells in the tissues and it thought to play a role in cell adhesion (Wai and Kuo, 2004). Moreover, it was observed in different male reproductive tissues such as testis, epididymis as well as sperm (Lin *et al,* 2006; RodrÍguez *et al,* 2000; Siiteri *et al,* 1995; Wilson *et al,* 2005; Souza *et al,* 2009; Kang *et al,* 2014). Meanwhile, it has been discovered to contribute in several reproductive processes such as sperm-egg interaction, fertilisation and early embryonic development (Erikson *et al,* 2007; Souza *et al,* 2009; Monaco *et al,* 2009). It has been suggested that the OPN has a potential role in fertilisation (Erikson *et al,* 2007); spermatogenesis and spermatozoa function (Zhang *et al,* 2016) and was considered as one of the decapacitation factors to prevent premature sperm motility activation (Goncalves *et al,* 2007). In addition, OPN has been stated as a sperm surface molecule; where it was found in testes, epididymis and on the surface of epididymal spermatozoa. Therefore, OPN could play a role in maturation during spermatogenesis (Siiteri *et al,* 1995).

In different mammalians, spatial expression of OPN has been thoroughly investigated. The OPN mRNA has been detected in the germ cells of spermatids, epididymis and spermatozoa of the bull (RodrÍguez *et al,* 2000); Sertoli cells of the mouse (Wilson *et al,* 2005); both germ and Sertoli cells in the rat testis (Siiteri *et al,* 1995) and in the testicular interstitium, acrosomes of testicular spermatids and epididymis of the sheep (Zhang *et al,* 2016). Meanwhile, immunolocalisation of OPN was detected in different locations; in the epididymal sperm, testis and cauda epididymal fluid of bull (Erikson *et al,* 2007); testes in both rat and mouse (Wilson *et al,* 2005; Siiteri *et al,* 1995); spermatogonia, different stages of spermatocytes, acrosomes of spermatids and few sertoli cells of boar; testis, epididymis and cauda epididymal spermatozoa in the sheep (Zhang *et al,*

SEND REPRINT REQUEST TO KHALID ALKHODAIR email: kalkhodair@kfu.edu.sa

2016) and it has been detected in the seminal plasma of the dromedary camel and its high concentrations was positively correlated with fertility of camels (Waheed *et al*, 2015).

According to previous studies, the expression pattern of OPN has distinct interspecies differences, which indicated that OPN might contribute in several biological processes in various species. Although, there are several studies on detection of OPN in the reproductive system of domestic animal species, but the role of OPN in camel reproductive system has not been reported yet. Therefore, the present study was under taken to clarify the expression and localisation of OPN in dromedary testis, epididymis and epididymal sperm during rutting season to understand its activity in spermatogenesis.

Materials and Methods

Animals and sample collection

Twelve male reproductive tracts of clinically healthy dromedary camels (4-12 years) were obtained from local abattoirs in Saudi Arabia during rutting season (November to April). The testes and caput, corpus and cauda of epididymis were collected from 8 animals. First specimen's part was immediately snap freeze in liquid nitrogen and kept at –80°C for qrt-PCR analyses and the 2nd part was fixed in 10% buffered formalin for immunohistochemistry. In addition, epididymal sperms were collected from the cauda epididymis of the rest 4 males. Sperm samples washed with phosphate-buffered saline (PBS) and suspended sperms were smeared on Superfrost slides, air-dried and then stored at –20°C until use for immunohistochemistry and immunofluorescence.

Gene expression analysis

Briefly, total RNA was extracted using TRIzol Reagent (Invitrogen, Carlsbad, CA, USA) according to the instructions, then RNA pellets were resuspended in UltraPure™ DEPC-Treated Water (Invitrogen, USA). BioTek Synergy MX reader (BioTek, USA) was used to measure RNA concentration and purity at optical density value 260:280 nm absorbance, which was between 1.8 and 2.0. Reverse transcription reactions were performed using iScriptcDNA Synthesis Kit (BioRad, Hercules, CA, USA). The total of reaction (20 µL) was a mixture of 2 µg RNA templates, 4 µL iScript Reaction Mix, 1 µL iScript Reverse Transcriptase and nuclease-free distilled water. Reaction thermocycle was at 25°C for 5 min, 46°C for 20 min, then at 95°C for 60 seconds to inactivate the reverse transcriptase according to manufacturer's protocol. Gene-specific primers were designed for dromedary camel OPN and glyceraldehyde 3-phosphate dehydrogenase (GAPDH), reference gene, using NCBI primer-blast website (http://www.ncbi.nlm.nih.gov/tools/primer-blast/) and Gen-Bank accession numbers and amplicon length of target genes were presented in table 1. Quantitative real-time PCR (qRT-PCR) carried out using CFX96 Touch Real-time PCR (BioRad, USA). SsoAdvanced SYBR Green Supermix (BioRad, USA) was used to detect the fluorescence emission in a reaction volume of 20 µL. All cDNA templates were run in duplicate and relative quantification was done by the $2^{-\Delta\Delta CT}$ method. Relative quantifications were calculated to the reference gene (GAPDH) directly via CFX Manager™ software V3.1 (BioRad, Hercules, CA, USA).

Table 1. Designed primer sequences, Genbank accession numbers and product sizes used for qRT-PCR.

Gene name	Sequences	Accession number	Amplicon Length (bp)
OPN	F: AAGACA CAC AAG ATG GCC GA	XM_010983105.1	187
	R: TGG CTG TTC CAG TCA GAA GC		
GAPDH	F: CCT GGA GAA ACC TGC CAA ATA	XM_010990867.2	207
	R: TCG TTG TCG TAC CAG GAA ATG		

Tissues immunostaining

Sections of paraffin block samples (5µm thick) were cut and placed on Superfrost slides. After deparaffinised and rehydration, antigen-retrieval buffer was applied at 100°C for 15 min. After cooling, the slides were immersed with 3% hydrogen peroxide following by blocking buffer for 10 min after washing 0.1% (v/v) Tween 20 in Tris-buffered saline (TBST: 3×5min). Sections were then incubated with Rabbit anti-Osteopontin (Abcam, Inc., ab8448, 1:100) over night at 4°C. After washing (TBST: 3×5min), the goat anti-rabbit biotinylated secondary antibody (Abcam, Inc., ab64256) was added to the sections for 1 hour at room temperature then were washed again with TBST. Next, the slides were incubated with streptavidin-HRP conjugate (Abcam, Inc., ab64269) for 20 min then washed 3×5 min TBST. Colour was developed by adding a suitable amount of 3,3'-diaminobenzidine tetrahydrochloridechromogen substrate for 5 min. Slides were counterstained with haematoxylin, dehydrated and cleared, mounted by cover slip and visualised using a Leica DM6000 B

light microscope. Primary antibody was omitted in the negative control sections.

Sperm immunostaining

Sperm-smeared slides were surrounded by Hydrophobic Barrier Pap Pen, then incubated in PBS for 5 min followed by blocking buffer for 15 min at RT. Slides were then incubated with rabbit anti-Osteopontin (Abcam, Inc., ab8448, 1:50) for 1 hour at RT followed by washing (3×5 min PBS). All slides were incubated with goat anti-rabbit fluorescent secondary antibody (FITC) (Abcam, Inc., ab6717, 1;100) for 2 hours in a dark place at RT. After washing (3×5 min PBS), a cover slip was mounted on the slides using aqueous antifade mounting medium. Then slides were visualised immediately using Leica DM6000 B fluorescent microscope. In addition, chromogenic immunostaining of sperm slides were performed similar to that conducted on tissue slides.

Statistical analysis

Data were analysed using SPSS software version 16. Comparisons were made among different tissues with varying expressions as means ± standard errors *via* a one-way analysis of variance with post hoc analysis. Data were shown as means ± standard errors.

Results and Discussion

Relative gene expression of OPN in the testis and epididymis

As shown in fig 1, relative gene expression of OPN revealed differences mRNA expression between testis and epididymis parts. Meanwhile, the highest expression of OPN was detected in the cauda of epididymis. The data indicated that OPN mRNA expression in the cauda of epididymis was significantly ($P < 0.05$) higher compared to the other tissues. However, no significant differences were seen between testis, caput and corpus of epididymis.

Immunolocalisation of OPN in the testis and epididymis

In seminiferous tubules, a highly intense immune-reactivity of OPN was observed in the elongated spermatids. However, spermatogonia and Sertoli cells revealed a faint immune-intensity. In addition, Leydig cells in the interstitial tissue showed strong OPN immune-intensity (Fig 2A). The caput, corpus and cauda of epididymis, revealed intense immune-reactivity of OPN in the cytoplasm of epithelial cells with a highly concentrated intensity in the apical region nearby lumen of epididymis (Figs 2B, C and D). Meanwhile, a strong immune-reactivity was observed in the sperm's acrosome of cauda epididymidis (Fig 2D). No positive immune reaction was observed in all control sections (Figs 2, A1, B1, C1 and D1).

Immunolocalisation of OPN of epididymal sperm

Positive OPN immuno-reactivity was found in the epididymal sperm. Specific immune-localisation of OPN was detected in both acrosomal cap and neck of epididymal sperm in fluorescent (Fig 3A) and chromogenic immunostaining (Fig 3B). However, in other parts of the sperm, no positive immuno-reaction was observed.

OPN is an indispensable highly phosphorylated glycoprotein in mammalian reproduction that was observed in different male reproductive tissues such as testis, epididymis and sperm cells (Lin *et al,* 2006; RodrÍguez *et al,* 2000; Siiteri *et al,* 1995; Wilson *et al,* 2005; Souza *et al,* 2009; Kang *et al,* 2014). Our study examined for the first time the spatial expression of OPN in the male dromedary camel reproductive tract.

In this study, mRNA transcription of OPN was expressed in the testis and all parts of epididymis. Moreover, the highest expression was in the tail (cauda) of the epididymis. OPN expression in different locations along the reproductive tract implies to the need of this vital protein for the supportive and protective function during sperm journey. However, the concentration of this protein at the last trip (storage) is also suggested to have a strong protective role with integrity adhesion

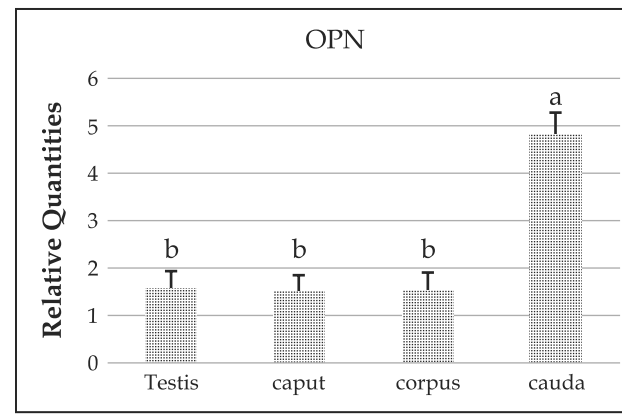

Fig 1. Comparison of OPN expression level in the testis, caput, corpus and cauda epididymis of dromedary camels by qRT-PCR. The gene expressions were normalised to GAPDH and showed as means ± standard errors. The significance was set to $P<0.05$ and different letters (a, b) indicate significance among examined tissues. The cauda epididymis showed a high expression in comparison with other reproductive tissues.

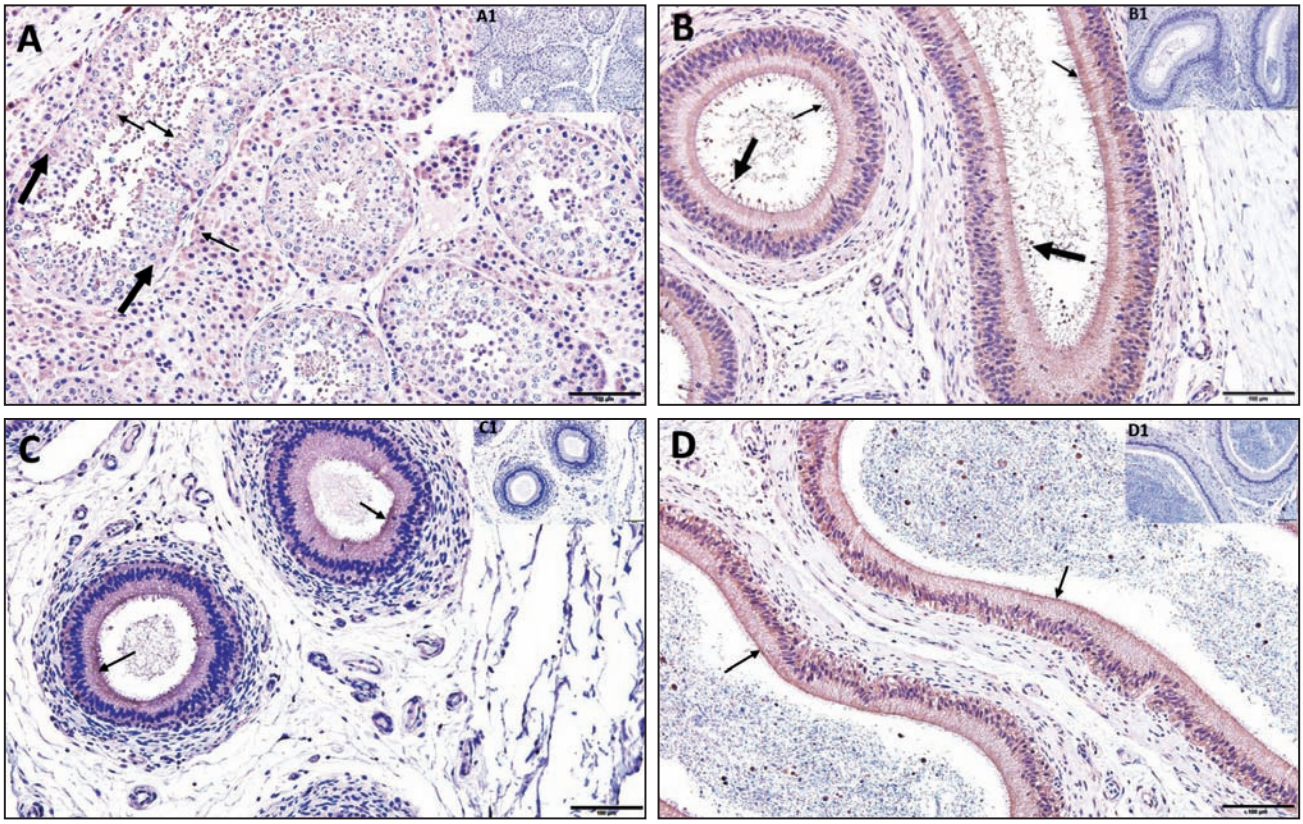

Fig 2. Immuno-staining of the OPN in the testis and epididymis of male dromedary camels. (**A**) Testis, showing highly intense immuno-reactivity in both elongated spermatids and interstitial Leydig cells (thin arrows), while less faint immuno-reactivity appeared in spermatogonia and Sertoli cells (thick arrows). (**B**) Caput epididymis, (**C**) Corpus epididymis and (**D**) Cauda epididymis showing highly concentrated intensity in the apical region nearby lumen of epididymis (thin arrows); meanwhile, strong immune-reactivity was observed in the sperm's acrosome of cauda epididymis (thick arrows). (A1-D1) negative control Section. Scale bar, 100 µm.

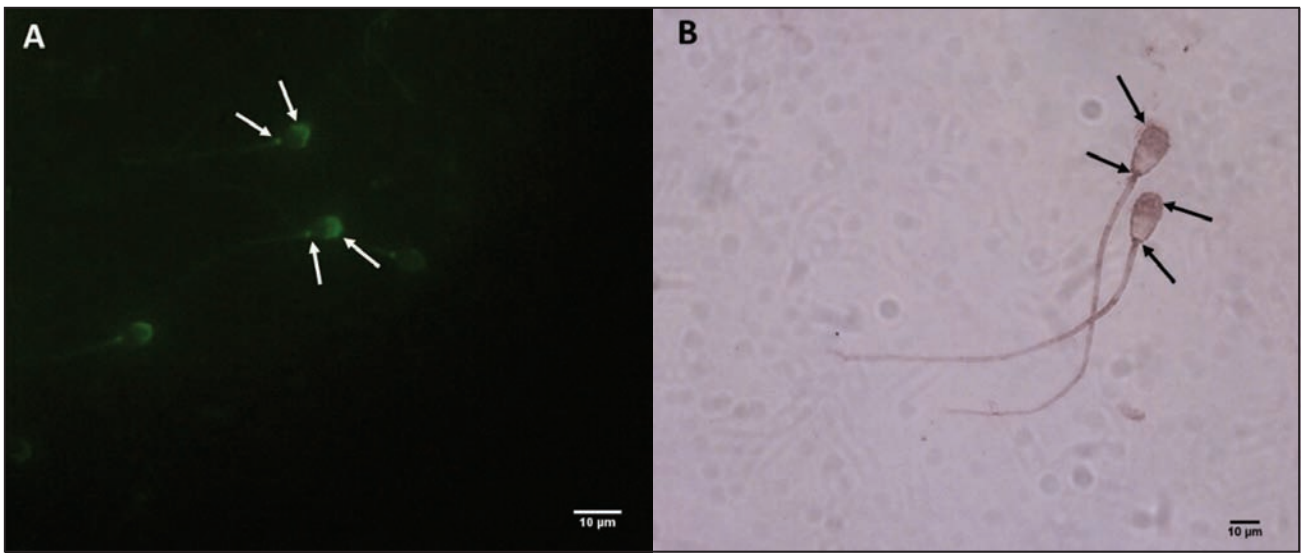

Fig 3. Fluorescent (**A**) and chromogenic (**B**) immunostaining of OPN in epididymal camel sperm. Both acrosomal cap and neck (arrows) of epididymal sperm showing positive immuno-reactivity of OPN. Scale bar, 10 µm.

function that required for sperm maturation, storage and migration. In the same context, similar results were found in other species such as rat and bull by (RodrÍguez *et al,* 2000; Siiteri *et al,* 1995).

In previous studies, the OPN immunolocalisation has been detected in the testis and epididymis of different mammalians such as boar, bovine and rat (Lin *et al,* 2006; RodrÍguez *et al,* 2000;

Siiteri *et al,* 1995). In the present study, OPN was localised on several regions of the camel testis. The highest signals were localised in the elongating spermatids of seminiferous tubules and testicular interstitium (Leydig cells). However, the low signals were observed in some spermatogonia and Sertoli cell. Presence of OPN in various localised stages of testicular tissue particularly the seminiferous tubules might indicate that it may play a key role in spermatogenesis. Previously, it has been documented that the OPN protein binds to a variety of cell surface integrins (transmembrane receptors) which promote cell-cell and cell-ECM adhesion resulting in cytoskeletal organisation and cellular transduction (Burghardt *et al,* 2002; Sodek *et al,* 2000; Johnson *et al,* 2014). Meanwhile, Sertoli cells to germ cells and germ cells to germ cells adhesion and communication are required to provoke and regulate the spermatogenesis (Jégou and Pineau, 1995). Therefore, OPN seems to share in Sertoli-germ cells, germ-germ cells or both adhesion and communication in the seminiferous tubules.

In similar previous studies, OPN was detected in spermatogonia, different stages of spermatocytes, acrosomes of spermatids, some Sertoli cells and Leydig cells in the boar testis (Kim and Shin, 2007). However, in the sheep testis, it was detected in the acrosomes of spermatids near the lumen of the seminiferous tubule (Zhang *et al,* 2016). In addition, OPN has been presented in both sertoli cells and germ cells in the rat (Siiteri *et al,* 1995; Luedtke *et al,* 2002) and mouse (Wilson *et al,* 2005). Interestingly, these results are closely resembling to that found in our present study. However, in contrast, Cancel *et al* (1999) reported that the OPN was undetected in the testis of bovine.

In the present study, the epididymis of the camel showed clear immunostaining of OPN in the epithelial layer. However, highly concentrated intensity was detected in the apical region nearby lumen of epididymis. Meanwhile, a strong immune-reactivity was observed in the sperm's acrosome of cauda epididymidis. Beside cell-cell and cell-ECM adhesion and communication functions, OPN has been reported to promote cell migration, cell death reduction and intracellular calcium alteration (Butler, 1989; Johnson *et al,* 2014). It is therefore, believed that OPN localisation in the epididymis parts particularly in cauda epididymidis and sperm acrosome promote spermatozoa migration and protect it from death during the long journey and may contribute in ova penetration during fertilisation process. In comparison, similar data have been reported in the rat by Luedtke *et al* (2002). However, in the sheep, it was concentrated on the apical region of the principal cells in the epididymis and on the caudal epididymal spermatozoa (Zhang *et al,* 2016). However, in contrast, OPN was undetected in the epididymis of bovine (Cancel *et al,* 1999).

In the sperm cell, we found OPN in the acrosomal cap and neck of epididymal sperm of camel. Harmonically, Waheed *et al* (2015) reported that the OPN was detected in the seminal plasma of dromedary camel suggesting that OPN has an important role in male's fertility. In another species, OPN was located in the post-acrosomal region and on the midpiece of epididymal sperm of bull (Erikson *et al,* 2007). Furthermore, OPN was observed in the surface of epididymal sperm and epididymal fluid in the rat (Siiteri *et al,* 1995). Therefore, detection of OPN in acrosomal and neck of sperm may provide biofuels to migrate and penetrate during reproductive process.

In conclusion, spatial expression patterns of OPN in testis, epididymis and sperm cell of dromedary camel could play a role in spermatozoal vital functions and spermatogenesis. In addition, the localisation of OPN on the acrosomal cap and neck of camel sperm might carry out a function in the migration, fertilisation and early embryonic development.

Acknowledgement

The authors acknowledge the Deanship of Scientific Research, Vice Presidency for Graduate Studies and Scientific Research, King Faisal University for the financial support through the Annual Funding track (Project No. 180046).

References

Burghardt RC, Johnson GA, Jaeger LA, Ka H, Garlow JE, Spencer TE and Bazer FW. Integrins and extracellular matrix proteins at the maternal-foetal interface in domestic animals. Cells Tissues Organs. 2002; 172:202-217.

Butler WT. The nature and significance of osteopontin. Connective Tissue Research. 1989; 23:123-136.

Cancel AM, Chapman DA and Killian GJ. Osteopontin localisation in the holstein bull reproductive tract. Biology of Reproduction. 1999; 60:454-460.

Denhardt DT and Guo X. Osteopontin: a protein with diverse functions. The FASEB Journal. 1993; 7:1475-1482.

Erikson DW, Way AL, Chapman DA and Killian GJ. Detection of osteopontin on holstein bull spermatozoa, in cauda epididymal fluid and testis homogenates and its potential role in bovine fertilisation. Reproduction. 2007; 133:909-917.

Franzen A and Heinegård D. Isolation and characterisation of two sialoproteins present only in bone calcified matrix. Biochemical Journal. 1985; 232:715-724.

Goncalves R, Wolinetz C and Killian G. Influence of arginine-glycine-aspartic acid (rgd), integrins (αv and α5) and osteopontin on bovine sperm–egg binding and fertilisation *in vitro*. Theriogenology. 2007; 67:468-474.

Jégou B and Pineau C. Current aspects of autocrine and paracrine regulation of spermatogenesis. Tissue Renin-Angiotensin Systems. 1995; 67-86.

Johnson GA, Burghardt RC and Bazer FW. Osteopontin: A leading candidate adhesion molecule for implantation in pigs and sheep. Journal of Animal Science and Biotechnology. 2014; 5:1-14.

Kang Y-J, Forbes K, Carver J and Aplin JD. The role of the osteopontin–integrin αvβ3 interaction at implantation: Functional analysis using three different *in vitro* models. Human Reproduction. 2014; 29:739-749.

Kim S and Shin T. Immunohistochemical study of osteopontin in boar testis. Journal of Veterinary Science. 2007; 8:107-110.

Lin C, Tholen E, Jennen D, Ponsuksili S, Schellander K and Wimmers K. Evidence for effects of testis and epididymis expressed genes on sperm quality and boar fertility traits. Reproduction in Domestic Animals. 2006; 41:538-543.

Luedtke CC, McKee MD, Cyr DG, Gregory M, Kaartinen MT, Mui J and Hermo L. Osteopontin expression and regulation in the testis, efferent ducts and epididymis of rats during postnatal development through to adulthood. Biology of Reproduction. 2002; 66:1437-1448.

Monaco E, Gasparrini B, Boccia L, De Rosa A, Attanasio L, Zicarelli L and Killian G. Effect of osteopontin (OPN) on *in vitro* embryo development in cattle. Theriogenology. 2009; 71:450-457.

RodrÍguez CM, day JR and Killian GJ. Osteopontin gene expression in the holstein bull reproductive tract. Journal of Andrology. 2000; 21:414-420.

Shin T, Ahn M, Kim H, Moon C, Kang T-Y, Lee J-M, Sim K-B and Hyun J-W. Temporal expression of osteopontin and cd44 in rat brains with experimental cryolesions. Brain Research. 2005; 1041:95-101.

Siiteri JE, Ensrud KM, Moore A and Hamilton DW. Identification of osteopontin (opn) mrna and protein in the rat testis and epididymis and on sperm. Molecular Reproduction and Development. 1995; 40:16-28.

Sodek J, Ganss B and McKee M. Osteopontin. Critical Reviews in Oral Biology and Medicine. 2000; 11:279-303.

Souza FFd, Chirinea V, Martins M and Lopes MD. Osteopontin in seminal plasma and sperm membrane of dogs. Reproduction in Domestic Animals. 2009; 44:283-286.

Waheed M, Ghoneim I and Alhaider A. Seminal plasma and serum fertility biomarkers in dromedary camels (*Camelus dromedarius*). Theriogenology. 2015; 83:650-654.

Wai PY and Kuo PC. The role of osteopontin in tumour metastasis. Journal of Surgical Research. 2004; 121:228-241.

Wilson MJ, Liaw L and Koopman P. Osteopontin and related sibling glycoprotein genes are expressed by sertoli cells during mouse testis development. Developmental Dynamics: An Official Publication of the American Association of Anatomists. 2005; 233:1488-1495.

Xie Y, Sakatsume M, Nishi S, Narita I, Arakawa M and Gejyo F. Expression, roles, receptors and regulation of osteopontin in the kidney. Kidney International. 2001; 60:1645-1657.

Zhang G-M, Lan S, Jia R-X, Yan G-Y, Wang L-Z, Nie H-T, Lei Z-H and Wang F. Age-associated and tissue-specific expression of osteopontin in male Hu sheep reproductive tract. Tissue and Cell. 2016; 48:496-502.

DOI : 10.5958/2277-8934.2022.00016.9 *Vol 29 No 2, p 117-125*

REVERSE DIAGNOSTIC WORKFLOW TO SHORTLIST MERS-COV SPIKE ANTIGENIC EPITOPES IN DROMEDARY CAMELS

Sabry M. El-Bahr[1,2], Mahmoud Kandeel[1,3], I.F. Albokhadaim[1], M. Al-Nazawi[1] and Hafiz Ahmed[4]

[1]Department of Biomedical Sciences, College of Veterinary Medicine, King Faisal University, Al-Ahsa 31982, P.O. 400, Saudi Arabia

[2]Department of Biochemistry, Faculty of Veterinary Medicine, Alexandria University, Alexandria 21523, Egypt

[3]Department of Pharmacology, Faculty of Veterinary Medicine, Kafr Elsheikh University, Egypt

[4]GlycoMentra Inc., 1450 South Rolling Road, Baltimore, MD 21227, USA

ABSTRACT

In this study, we provide a comprehensive reverse diagnostic workflow, in which, the *in-silico* amino acid composition was employed retrogradely to shortlist the viral spike antigenic epitopes to infer diagnostics efficiency. This study was aimed to explore the analytical estimates of changes in epitope composition among MERS-CoV lineages. This can be used as a predictor of the effectiveness of rapid diagnostic testing. Therefore, MERS-CoV lineage-specific spike protein sequences were extracted, aligned and compared. In addition, the degree of sequence similarity, as well as pairwise comparison, phylogenetic relations and antigenic epitopes analysis, have been conducted. The current findings indicated that no differences were observed in length and range of epitopes for each virus among all studied lineages. Most of epitopes sequences were conserved. However, few sequences showed few single amino acid mutations. About 20% of epitopes were located at the receptor-binding domain (RBD) and 80% of these were located in the other Spike`s domains. These mutations were related to lineage 2 and 3 and not for lineage 1, 4 and 5. The number of difference among viruses accession no (ALA49781, ALA49594, ALA49440, ALA50001, ALA49935, ALA49847, ALA49825, ALA49561, ALA49374, ALA49803, ALA49660, ALA49352, ALA49671, ALA49341, AHX00711, AHY22565, AJG44124, AJG44091, ALA49429, ALA49418, ALA49902, AHY22525, AHX71946, AHE78108.1, AHI48672.1, AHI48550) was maximum of 8. No gaps were observed in the epitopes alignment. The identity of spike protein among the lineages ranged from 99.5 -100%. The study concluded that any of studied epitopes are suitable for production of rapid tests of MERS CoV in dromedary camels, particularly that produced from lineages 1, 4 and 5.

Key words: MERS CoV, camels, epitopes, viral lineage, rapid test

The Middle East respiratory syndrome coronavirus (MERS-CoV) was initially discovered in a patient with acute respiratory distress syndrome in the Kingdom of Saudi Arabia in October 2012 (Zaki *et al,* 2012). MERS-CoV is diagnosed primarily by molecular methods, i.e. Real-time reverse transcriptase-polymerase amplification (RT-PCR) (Corman *et al,* 2012a; 2012b), reverse transcription–loop-mediated isothermal amplification (RTLAMP) and reverse transcription–recombinase polymerase amplification (RT-RTPA) (Shirato *et al,* 2014; Abd El Wahed *et al,* 2013). MERS-CoV or closely related viruses have also been detected in seropositive camels using a variety of serological techniques. Protein microarrays (Reusken *et al,* 2013a, 2013b; Meyer *et al,* 2013), a recombinant spike immunofluorescent assay (Buchholz *et al,* 2013; Annan *et al,* 2013), an indirect enzyme-linked immunosorbent assay (ELISA) (Alexandersen *et al,* 2014), microneutralisation, and spike pseudoparticle neutralisation are some of the techniques used (Perera *et al,* 2013). Molecular tests are relatively expensive and considered problematic for screening large numbers of animals in a short period of time; therefore, a rapid, inexpensive, sensitive, and specific test for the diagnosis of MERS-CoV in camels is required. MERS-CoV antigen was detected in the nasal swabs of dromedary camels using a fast immunochromatographic technique (Song *et al,* 2015). The identification of MERS-CoV nucleocapsid protein in a short time period utilising highly specific monoclonal antibodies at room temperature is the basis of this assay. The viral spike protein of MERS-CoV, which has both conserved and highly mutable or variable regions in its sequence, is the focus of most contemporary fast diagnostic assays. The accuracy of such testing is then jeopardised by mutations,

SEND REPRINT REQUEST TO SABRY M. EL-BAHR email: selbahar@kfu.edu.sa; sabryelbahr@hotmail.com

particularly in the virus's antigenic epitopes. This study presents analytical estimates of changes in epitope composition among MERS-CoV lineages.

Materials and Methods

Retrieval of input protein data and analytical programs

The sequences of the input spike protein were retrieved from the previously analysed MERS-CoV lineages (Chu *et al,* 2018; Sabir *et al,* 2016). Table 1 provides an overview of the genomes and proteins utilised in the study. CLC Genomics Workbench 12.0 (QIAGEN, Aarhus, Denmark) and Geneious prime were used to process the sequences (Kearse *et al,* 2012).

Sequence alignment and retrieval of the spike protein

The CLC genomics program's protein sequence capabilities were used to handle the spike protein sequence. With 10 gaps open and one gap extension cost, a very accurate alignment was achieved using the protein alignment wizard's alignment parameters. To compare the sequences, a pairwise comparison matrix was created. The identity matrix was created after calculating the differences, identity percentage, gaps and mutations.

Phylogenetics

The phylogenetic tree was built using the neighbour-joining (NJ) technique and then evaluated for evolutionary links. Using the default settings, the CLC genomics program was utilised. Distances were calculated using the JTT substitution model. The neighbour-joining method was tested to 100 Bootstrap resampling repeats. (Romesburg, 2004).

Spike`s antigenic epitopes

The potential antigenic epitopes in studied MERS-CoV lineages were searched at EMBOSS

Table 1. The accession numbers (no.) and description of the genomes and proteins used in this study.

Lineage	Accession no. of full genome	Accession no. of Spike	Description
5	Camel/Jeddah/Jd87/2015	ALA49781	Spike protein [Middle East respiratory syndrome-related coronavirus].
5	Camel/Jeddah/N62(b)/2014	ALA49594	Spike protein [Middle East respiratory syndrome-related coronavirus].
5	Camel/Jeddah/D38/2014	ALA49440	Spike protein [Middle East respiratory syndrome-related coronavirus].
5	Camel/Taif/T68/2015	ALA50001	Spike protein [Middle East respiratory syndrome-related coronavirus].
5	Camel/Riyadh/Ry79/2015	ALA49935	Spike protein [Middle East respiratory syndrome-related coronavirus].
5	Camel/Riyadh/Ry159/2015	ALA49847	Spike protein [Middle East respiratory syndrome-related coronavirus].
5	Camel/Riyadh/Ry136/2015	ALA49825	Spike protein [Middle East respiratory syndrome-related coronavirus].
3	Camel/Jeddah/D90/2014	ALA49561	Spike protein [Middle East respiratory syndrome-related coronavirus].
3	Camel/Jeddah/401/2014	ALA49374	Spike protein [Middle East respiratory syndrome-related coronavirus].
3	Camel/Jeddah/Jd175/2015	ALA49803	Spike protein [Middle East respiratory syndrome-related coronavirus].
3	Camel/Jeddah/S100/2014	ALA49660	Spike protein [Middle East respiratory syndrome-related coronavirus].
3	Camel/Riyadh/Ry23N/2014	ALA49352	Spike protein [Middle East respiratory syndrome-related coronavirus].
3	Camel/Jeddah/S73/2014	ALA49671	Spike protein [Middle East respiratory syndrome-related coronavirus].
3	Camel/Jeddah/F13A/2014	ALA49341	Spike protein [Middle East respiratory syndrome-related coronavirus].
2	KFU-HKU/13/2013	AHX00711	Spike protein [Middle East respiratory syndrome-related coronavirus].
2	Camel/KSA/376/2013	AHY22565	Spike protein [Middle East respiratory syndrome-related coronavirus].
2	Camel/UAE/D1209/2014	AJG44124	S [Middle East respiratory syndrome-related coronavirus].
2	Camel/UAE/D1164.14/2014	AJG44091	S [Middle East respiratory syndrome-related coronavirus].
4	Camel/Jeddah/D36/2014	ALA49429	Spike protein [Middle East respiratory syndrome-related coronavirus].
4	Camel/Jeddah/D35/2014	ALA49418	Spike protein [Middle East respiratory syndrome-related coronavirus].
4	Camel/Riyadh/Ry179/2015	ALA49902	Spike protein [Middle East respiratory syndrome-related coronavirus].
4	Camel/KSA/505/2014	AHY22525	Spike protein [Middle East respiratory syndrome-related coronavirus].
4	Camel/Qatar/2/2014	AHX71946	Spike protein [Middle East respiratory syndrome-related coronavirus].
1	Camel/Jeddah-Camel-1/2013	AHE78108.1	S [Middle East respiratory syndrome-related coronavirus]
1	Taif/1/2013	AHI48672.1	S protein [Middle East respiratory syndrome-related coronavirus]
1	Wadi-Ad-Dawasir_1/2013	AHI48550	S protein [Middle East respiratory syndrome-related coronavirus]

antigenic prediction tool (Kolaskar and Tongaonkar, 1990). The antigenic determination is based on a semi-empirical approach based on physicochemical properties of amino acid residues and their frequencies of occurrence in experimentally known segmental epitopes. The minimal length of antigenic region was set to six. The output format was set to EMBOSS motif.

Results

Antigenic epitopes

Antigenic epitope analysis requests were sent to the EMBOSS antigenic prediction tool. Based on the output epitopes, the 15 epitopes with the highest epitope score were extracted and compared among MERS-CoV lineages. Table 2 summarises the

Table 2. The antigenic epitopes predicted by EMBOSS antigenic detection in MERS-CoV lineages. The epitopes are in descending order according to the predicted score. Top 15 epitopes for each virus were selected.

Virus	#	In RBD (YES/ No)	Sequence	length	range	Conserved/ mutations no.	score
AHE78108.1 AHI48550.1 AHX71946.1 AHY22525 AHY22565.1 AJG44124.1 ALA49341.1 ALA49352.1 ALA49418.1 ALA49429.1 ALA49440.1 ALA49561.1 ALA49594.1 ALA49660.1 ALA49671.1 ALA49781.1 ALA49803.1 ALA49825.1 ALA49847.1 ALA49902.1 ALA49935.1 ALA50001.1	1	No	YIWLGFIAGLVALALCVFFILCCTGCGTN	29	1298->1326	Conserved	1.258
	2	No	NYYCLRACVSVPVSVIYD	18	647->664	Conserved	1.243
	3	No	SGFCGQGTHIVSFVVNAP	18	1114->1131	Conserved	1.216
	4	Yes	YSPCVSIVPST	11	523->533	Conserved	1.210
	5	No	ARDLICAQYVAGYKVLPPLM	20	920->939	Conserved	1.205
	6	No	YGPLQTPVGCVLGLVNSSLFVEDCKLPL GQSLCALPDTP	39	704->742	Conserved	1.204
	7	Yes	NPTCLILATVPHNLT	15	475->489	Conserved	1.203
	8	No	TTLLDLTYEMLSLQQVVKALNESYIDLK	28	1257->1284	Conserved	1.187
	9	Yes	NYNLTKLLSLFSVNDFTCSQISPAAIASN CYSSLILDYFSYPLS	44	408->451	T424I (ALA49341.1) L411F (ALA49374.1)	1.178
	10	No	SVFLLMFLLTPTESYVDVGPDSVKSACIEVDIQQT	35	4->38	Conserved	1.178
	11	No	ASQLGNCVEYSLYGVSGRG	19	597->615	Conserved	1.176
	12	No	NHTLVLLPDGCGTLLRAFYCILEP	24	166->189	Conserved	1.173
	13	No	TLNAFVAQQLVRSESAALSAQLAKD	25	1077->1101	Conserved	1.172
	14	No	SFGVTQEYIQTTIQKVTVDCKQYVCNGF	28	787->814	V810I (AJG44091.1) V810I (AHX00711.1)	1.168
	15	No	GLYFMHVGYYPSNHIEVVSAYGLCDAA	27	1133->1159	A1159S (AHY22565.1)	1.165
AHX00711.1 AJG44091.1	1	No	YIWLGFIAGLVALALCVFFILCCTGCGTN	29	1298->1326	Conserved	1.258
	2	No	NYYCLRACVSVPVSVIYD	18	647->664	Conserved	1.243
	3	No	SGFCGQGTHIVSFVVNAP	18	1114->1131	Conserved	1.216
	4	Yes	YSPCVSIVPST	11	523->533	Conserved	1.210
	5	No	ARDLICAQYVAGYKVLPPLM	20	920->939	Conserved	1.205
	6	No	YGPLQTPVGCVLGLVNSSLFVEDCKLPLGQSLCAL PDTP	39	704->742	Conserved	1.204
	7	Yes	NPTCLILATVPHNLT	15	475->489	Conserved	1.203
	8	No	TTLLDLTYEMLSLQQVVKALNESYIDLK	28	1257->1284	Conserved	1.187
	9	Yes	NYNLTKLLSLFSVNDFTCSQISPAAIASN CYSSLILDYFSYPLS	44	408->451	T424I (ALA49341.1) L411F (ALA49374.1)	1.178
	10	No	SVFLLMFLLTPTESYVDVGPDSVKSACIEVDIQQT	35	4->38	Conserved	1.178
	11	No	ASQLGNCVEYSLYGVSGRG	19	597->615	Conserved	1.176
	12	No	NHTLVLLPDGCGTLLRAFYCILEP	24	166->189	Conserved	1.173
	13	No	TLNAFVAQQLVRSESAALSAQLAKD	25	1077->1101	Conserved	1.172
	14	No	GLYFMHVGYYPSNHIEVVSAYGLCDAA	27	1133->1159	A1159S (AHY22565.1)	1.165
	15	No	HATLFGSVACEHI	13	670->682	Conserved	1.155

Table 2 continued....

ALA49374.1	1	No	YIWLGFIAGLVALALCVFFILCCTGCGTN	29	1298->1326	Conserved	1.258
	2	No	NYYCLRACVSVPVSVIYD	18	647->664	Conserved	1.243
	3	No	SGFCGQGTHIVSFVVNAP	18	1114->1131	Conserved	1.216
	4	Yes	YSPCVSIVPST	11	523->533	Conserved	1.210
	5	No	ARDLICAQYVAGYKVLPPLM	20	920->939	Conserved	1.205
	6	No	YGPLQTPVGCVLGLVNSSLFVEDCKLPLGQSLCA LPDTP	39	704->742	Conserved	1.204
	7	Yes	NPTCLILATVPHNLT	15	475->489	Conserved	1.203
	8	No	TTLLDLTYEMLSLQQVVKALNESYIDLK	28	1257->1284	Conserved	1.187
	9	Yes	TKLLSLFSVNDFTCSQISPAAIASNCYSSLILDYFSYPLS	40	412->451	T424I (ALA49341.1)	1.178
	10	No	SVFLLMFLLTPTESYVDVGPDSVKSACIEVDIQQT	35	4->38	Conserved	1.178
	11	No	ASQLGNCVEYSLYGVSGRG	19	597->615	Conserved	1.176
	12	No	NHTLVLLPDGCGTLLRAFYCILEP	24	166->189	Conserved	1.173
	13	No	TLNAFVAQQLVRSESAALSAQLAKD	25	1077->1101	Conserved	1.172
	14	No	SFGVTQEYIQTTIQKVTVDCKQYVCNGF	28	787->814	V810I (AJG44091.1) V810I (AHX00711.1)	1.168
	15	No	GLYFMHVGYYPSNHIEVVSAYGLCDAA	27	1133->1159	A1159S (AHY22565.1)	1.165

epitopes sequences, their respective location on either RBD or other S protein domains, the range of amino acid, conservation among lineages and the predicted mutations. The epitopes were arranged in descending order, according to their antigenic scores.

Spike alignment

The spike protein sequences of various MERS-CoV lineages were aligned (Fig 1). The alignment showed a mostly conserved amino acid sequence with few mutations, which are summarised in table 3. These mutations were related to lineage 2 and 3. However, these mutations were few and involved only single amino acid. The current findings indicated that there were no differences observed in length and range of epitopes for each virus among all studied lineages (Table 2). Most of epitopes sequences were conserved. However, few sequences underwent little mutation involving single amino acids (Table 2). Except for AHX00711.1 and AJG44091.1, single amino acid mutations were observed at epitope no. 9, 14 and 15 (Table 2). At epitope 9, these mutations were T424I (ALA49341.1) and L411F (ALA49374.1) (Table 2). At epitope 14, these mutations were V810I (AJG44091.1) and V810I (AHX00711.1) (Table 2). At epitope 15, this mutation was A1159S (AHY22565.1) (Table 2). For AHX00711.1 and AJG44091.1, the single amino acid mutations were at epitopes no. 9 and 14 (Table 2). At epitope 9, these mutations were T424I (ALA49341.1) and L411F (ALA49374.1). At epitope 14, this mutation was A1159S (AHY22565.1) (Table 2). Data summarised in table 3 indicated that 20% of epitopes sequences are located at the receptor-binding domain (RBD) and 80% of these sequences are located away from the RBD. This finding suggests the reliability of using a rapid test based on spike protein epitopes in dromedary camels by targeting multiple domains epitopes on the surface of MERS-CoV spike.

Table 3. List of observed mutations in virus spike in the studied lineages.

Mutation	Present in all lineages (Yes/No)	lineage	Accession number of mutants
T424I	No	3	ALA49341.1
L411F	Yes	3	ALA49374.1
V810I	Yes	2	AJG44091.1
V810I	Yes	2	AHX00711.1
A1159S	Yes	2	AHY22565.1

Pairwise comparison matrix

Pairwise comparison matrix revealed the absence of gaps in the alignment that indicates the lack of amino acid insertions or deletions in the spike protein among the lineages (Fig 2). In addition, the number of differences among viruses was a maximum of 8. The highest difference was 8 and it was among virus no 25 when matched with virus no 23 and 22 (Fig 2). Fortunately, most of these mutations are not involved in the antigenic epitopes. Pairwise comparison matrix revealed a higher identity of the spike protein among the lineages which ranged from 99.5 -100% (Fig 3).

Phylogenetic analysis

The spike protein of MERS-CoV was clustered in 3 main lineages (Fig 4). This indicates that the virus diversity is less common in virus spike, compared with the full genome.

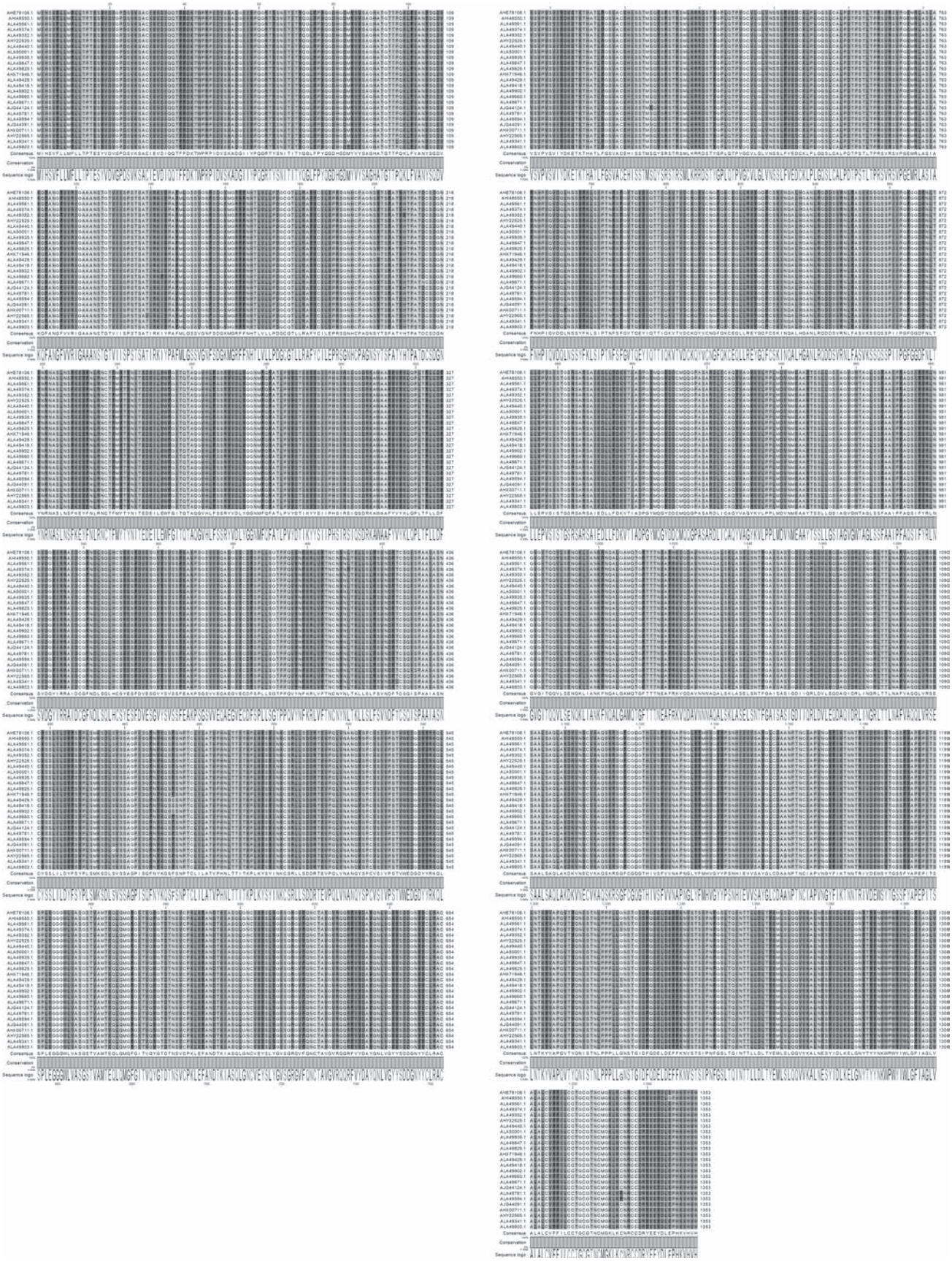

Fig 1. Sequence alignment of spike protein from different MERS-CoV lineages.

	1	2	3	4	5	6	7	8	9	10	11	12	13	14	15	16	17	18	19	20	21	22	23	24	25
AHE78108.1	1		0	0	0	0	0	0	0	0	0	0	0	0	0	0	0	0	0	0	0	0	0	0	0
AHI48550.1	2	1		0	0	0	0	0	0	0	0	0	0	0	0	0	0	0	0	0	0	0	0	0	0
ALA49561.1	3	2	3		0	0	0	0	0	0	0	0	0	0	0	0	0	0	0	0	0	0	0	0	0
ALA49374.1	4	3	4	1		0	0	0	0	0	0	0	0	0	0	0	0	0	0	0	0	0	0	0	0
ALA49352.1	5	2	3	2	3		0	0	0	0	0	0	0	0	0	0	0	0	0	0	0	0	0	0	0
AHY22525.1	6	1	2	1	2	1		0	0	0	0	0	0	0	0	0	0	0	0	0	0	0	0	0	0
ALA49440.1	7	1	2	1	2	1	0		0	0	0	0	0	0	0	0	0	0	0	0	0	0	0	0	0
ALA50001.1	8	1	2	1	2	1	0	0		0	0	0	0	0	0	0	0	0	0	0	0	0	0	0	0
ALA49935.1	9	1	2	1	2	1	0	0	0		0	0	0	0	0	0	0	0	0	0	0	0	0	0	0
ALA49847.1	10	1	2	1	2	1	0	0	0	0		0	0	0	0	0	0	0	0	0	0	0	0	0	0
ALA49825.1	11	1	2	1	2	1	0	0	0	0	0		0	0	0	0	0	0	0	0	0	0	0	0	0
AHX71946.1	12	2	3	2	3	2	1	1	1	1	1	1		0	0	0	0	0	0	0	0	0	0	0	0
ALA49429.1	13	3	4	1	2	3	2	2	2	2	2	2	3		0	0	0	0	0	0	0	0	0	0	0
ALA49418.1	14	3	4	1	2	3	2	2	2	2	2	2	3	0		0	0	0	0	0	0	0	0	0	0
ALA49902.1	15	2	3	2	3	2	1	1	1	1	1	1	2	1	1		0	0	0	0	0	0	0	0	0
ALA49660.1	16	4	5	2	3	4	3	3	3	3	3	3	4	3	3	4		0	0	0	0	0	0	0	0
ALA49671.1	17	4	5	2	3	4	3	3	3	3	3	3	4	3	3	4	2		0	0	0	0	0	0	0
AJG44124.1	18	3	4	3	4	3	2	2	2	2	2	2	3	4	4	3	5	5		0	0	0	0	0	0
ALA49781.1	19	2	3	2	3	2	1	1	1	1	1	1	2	3	3	2	4	4	3		0	0	0	0	0
ALA49594.1	20	2	3	2	3	2	1	1	1	1	1	1	2	3	3	2	4	4	3	0		0	0	0	0
AJG44091.1	21	4	5	4	5	4	3	3	3	3	3	3	4	5	5	4	6	6	3	4	4		0	0	0
AHX00711.1	22	5	6	5	6	5	4	4	4	4	4	4	5	6	6	5	7	7	4	5	5	3		0	0
AHY22565.1	23	5	6	5	6	5	4	4	4	4	4	4	5	6	6	5	7	7	4	5	5	5	6		0
ALA49341.1	24	3	4	3	4	3	2	2	2	2	2	2	3	4	4	3	5	5	4	3	3	5	6	6	
ALA49803.1	25	5	6	3	4	5	4	4	4	4	4	4	5	4	4	5	5	5	6	5	5	7	8	8	6

Fig 2. Comparative pairwise matrix for sequences of spike protein from different MERS-CoV lineages. The upper diagonal panel is the number of gaps. The lower diagonal panel is the number of amino acid differences.

	1	2	3	4	5	6	7	8	9	10	11	12	13	14	15	16	17	18	19	20	21	22	23	24	25
AHE78108.1	1		7.3939E-4	0.0015	0.0022	0.0015	7.3939E-4	7.3939E-4	7.3939E-4	7.3939E-4	7.3939E-4	7.3939E-4	0.0015	0.0022	0.0022	0.0015	0.0030	0.0030	0.0022	0.0015	0.0015	0.0030	0.0037	0.0037	0.0022	0.0037
AHI48550.1	2	99.9261		0.0022	0.0030	0.0022	0.0015	0.0015	0.0015	0.0015	0.0015	0.0015	0.0022	0.0030	0.0030	0.0022	0.0037	0.0037	0.0030	0.0022	0.0022	0.0037	0.0044	0.0044	0.0030	0.0044
ALA49561.1	3	99.8522	99.7783		7.3939E-4	0.0015	7.3939E-4	7.3939E-4	7.3939E-4	7.3939E-4	7.3939E-4	7.3939E-4	0.0015	7.3939E-4	7.3939E-4	0.0015	0.0015	0.0015	0.0022	0.0015	0.0015	0.0030	0.0037	0.0037	0.0022	0.0022
ALA49374.1	4	99.7783	99.7044	99.9261		0.0022	0.0015	0.0015	0.0015	0.0015	0.0015	0.0015	0.0022	0.0015	0.0015	0.0022	0.0022	0.0022	0.0030	0.0022	0.0022	0.0037	0.0044	0.0044	0.0030	0.0030
ALA49352.1	5	99.8522	99.7783	99.8522	99.7783		7.3939E-4	7.3939E-4	7.3939E-4	7.3939E-4	7.3939E-4	7.3939E-4	0.0015	0.0022	0.0022	0.0015	0.0030	0.0030	0.0022	0.0015	0.0015	0.0030	0.0037	0.0037	0.0022	0.0037
AHY22525.1	6	99.9261	99.8522	99.9261	99.8522	99.9261		1.0547E-16	1.0547E-16	1.0547E-16	1.0547E-16	1.0547E-16	7.3939E-4	0.0015	0.0015	7.3939E-4	0.0022	0.0022	0.0015	7.3939E-4	7.3939E-4	0.0022	0.0030	0.0030	0.0015	0.0030
ALA49440.1	7	99.9261	99.8522	99.9261	99.8522	99.9261	100.0000		1.0547E-16	1.0547E-16	1.0547E-16	1.0547E-16	7.3939E-4	0.0015	0.0015	7.3939E-4	0.0022	0.0022	0.0015	7.3939E-4	7.3939E-4	0.0022	0.0030	0.0030	0.0015	0.0030
ALA50001.1	8	99.9261	99.8522	99.9261	99.8522	99.9261	100.0000	100.0000		1.0547E-16	1.0547E-16	1.0547E-16	7.3939E-4	0.0015	0.0015	7.3939E-4	0.0022	0.0022	0.0015	7.3939E-4	7.3939E-4	0.0022	0.0030	0.0030	0.0015	0.0030
ALA49935.1	9	99.9261	99.8522	99.9261	99.8522	99.9261	100.0000	100.0000	100.0000		1.0547E-16	1.0547E-16	7.3939E-4	0.0015	0.0015	7.3939E-4	0.0022	0.0022	0.0015	7.3939E-4	7.3939E-4	0.0022	0.0030	0.0030	0.0015	0.0030
ALA49847.1	10	99.9261	99.8522	99.9261	99.8522	99.9261	100.0000	100.0000	100.0000	100.0000		1.0547E-16	7.3939E-4	0.0015	0.0015	7.3939E-4	0.0022	0.0022	0.0015	7.3939E-4	7.3939E-4	0.0022	0.0030	0.0030	0.0015	0.0030
ALA49825.1	11	99.9261	99.8522	99.9261	99.8522	99.9261	100.0000	100.0000	100.0000	100.0000	100.0000		7.3939E-4	0.0015	0.0015	7.3939E-4	0.0022	0.0022	0.0015	7.3939E-4	7.3939E-4	0.0022	0.0030	0.0030	0.0015	0.0030
AHX71946.1	12	99.8522	99.7783	99.8522	99.7783	99.8522	99.9261	99.9261	99.9261	99.9261	99.9261	99.9261		0.0022	0.0022	0.0015	0.0030	0.0030	0.0022	0.0015	0.0015	0.0030	0.0037	0.0037	0.0022	0.0037
ALA49429.1	13	99.7783	99.7044	99.9261	99.8522	99.7783	99.8522	99.8522	99.8522	99.8522	99.8522	99.8522	99.7783		1.0547E-16	7.3939E-4	0.0022	0.0022	0.0030	0.0022	0.0022	0.0037	0.0044	0.0044	0.0030	0.0030
ALA49418.1	14	99.7783	99.7044	99.9261	99.8522	99.7783	99.8522	99.8522	99.8522	99.8522	99.8522	99.8522	99.7783	100.0000		7.3939E-4	0.0022	0.0022	0.0030	0.0022	0.0022	0.0037	0.0044	0.0044	0.0030	0.0030
ALA49902.1	15	99.8522	99.7783	99.8522	99.7783	99.8522	99.9261	99.9261	99.9261	99.9261	99.9261	99.8522	99.9261	99.9261		0.0030	0.0030	0.0022	0.0015	0.0015	0.0030	0.0037	0.0037	0.0022	0.0037
ALA49660.1	16	99.7044	99.6305	99.8522	99.7783	99.7044	99.7783	99.7783	99.7783	99.7783	99.7783	99.7044	99.7783	99.7783	99.7044		0.0015	0.0037	0.0030	0.0030	0.0044	0.0052	0.0052	0.0037	0.0037
ALA49671.1	17	99.7044	99.6305	99.8522	99.7783	99.7044	99.7783	99.7783	99.7783	99.7783	99.7783	99.7044	99.7783	99.7783	99.7044	99.8522		0.0037	0.0030	0.0030	0.0044	0.0052	0.0052	0.0037	0.0037
AJG44124.1	18	99.7783	99.7044	99.7783	99.7044	99.7783	99.8522	99.8522	99.8522	99.8522	99.8522	99.8522	99.7783	99.7044	99.7044	99.7783	99.6305	99.6305		0.0022	0.0022	0.0022	0.0030	0.0030	0.0030	0.0044
ALA49781.1	19	99.8522	99.7783	99.8522	99.7783	99.8522	99.9261	99.9261	99.9261	99.9261	99.9261	99.9261	99.8522	99.7783	99.7783	99.8522	99.7044	99.7044	99.7783		1.0547E-16	0.0030	0.0037	0.0037	0.0022	0.0037
ALA49594.1	20	99.8522	99.7783	99.8522	99.7783	99.8522	99.9261	99.9261	99.9261	99.9261	99.9261	99.9261	99.8522	99.7783	99.7783	99.8522	99.7044	99.7044	99.7783	100.0000		0.0030	0.0037	0.0037	0.0022	0.0037
AJG44091.1	21	99.7044	99.6305	99.7044	99.6305	99.7044	99.7783	99.7783	99.7783	99.7783	99.7783	99.7044	99.6305	99.6305	99.7044	99.5565	99.5565	99.7783	99.7044	99.7044		0.0022	0.0037	0.0037	0.0037	0.0052
AHX00711.1	22	99.6305	99.5565	99.6305	99.5565	99.6305	99.7044	99.7044	99.7044	99.7044	99.7044	99.7044	99.6305	99.5565	99.5565	99.6305	99.4826	99.4826	99.7044	99.6305	99.6305	99.7783		0.0044	0.0044	0.0059
AHY22565.1	23	99.6305	99.5565	99.6305	99.5565	99.6305	99.7044	99.7044	99.7044	99.7044	99.7044	99.7044	99.6305	99.5565	99.5565	99.6305	99.4826	99.4826	99.7044	99.6305	99.6305	99.6305	99.5565		0.0044	0.0059
ALA49341.1	24	99.7783	99.7044	99.7783	99.7044	99.7783	99.8522	99.8522	99.8522	99.8522	99.8522	99.8522	99.7783	99.7044	99.7044	99.7783	99.6305	99.6305	99.7044	99.7783	99.7783	99.6305	99.5565	99.5565		0.0044
ALA49803.1	25	99.6305	99.5565	99.7783	99.7044	99.6305	99.7044	99.7044	99.7044	99.7044	99.7044	99.7044	99.6305	99.7044	99.7044	99.6305	99.6305	99.6305	99.5565	99.6305	99.6305	99.4826	99.4087	99.4087	99.5565	

Fig 3. Comparative pairwise matrix for sequences of spike protein from different MERS-CoV lineages. The upper diagonal panel is the distance. The lower diagonal panel is the identity per cent.

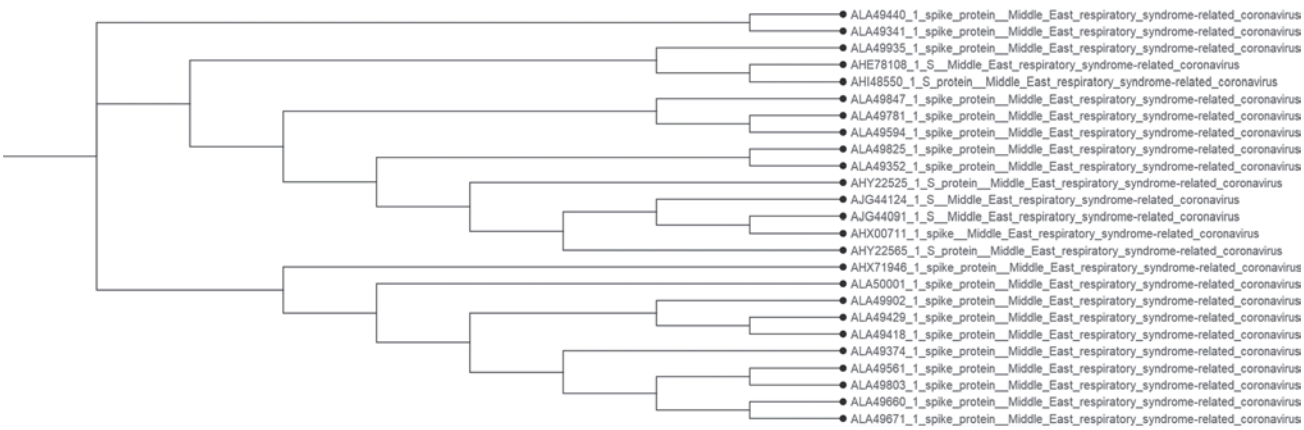

Fig 4. Cladogram of spike protein from different MERS-CoV lineages.

Discussion

MERS-CoVs have been sequenced and classified in both humans and camels since the first human MERS-CoV was discovered (Cotten *et al*, 2014; Lau *et al*, 2016; Sabir *et al*, 2016). Sabir *et al* (2016) sequenced and analysed typical MERS-CoV genomes from Saudi Arabia, including 67 from camels and discovered different clade B MERS-CoV lineages. Co-

infections with MERS-CoV and other coronaviruses were prevalent, as were additional non-MERS-CoVs. Another study sequenced 10 different camel MERS-CoVs from Abu Dhabi and discovered viruses in many clade B lineages, including a 6th lineage and a camel MERS-CoV within clade A. The clade A MERS-CoVs are assumed to be older and not circulating today, therefore, this study provides valuable insight into camel MERS-CoV variety in nature (Lau *et al,* 2016). Additional efforts to sequence MERS-CoV from camels have focused on nucleocapsid and spike genes as possible locations for finding genetic diversity (van Doremalen *et al,* 2017). Several human coronaviruses are known to have originated from zoonotic sources (Millet *et al,* 2016; Muhairi *et al,* 2016). At a live animal market in the Emirate of Abu Dhabi's eastern region, 376 camels were checked for MERS-Cov (Yusof *et al,* 2017). From 139 samples, 126 whole genomes and 3 nearly complete genomes were recovered. Five of the remaining 10 samples yielded spike gene sequences. Within clade B, the genomes of camel MERS-CoV represented 3 recognised and 2 potentially novel lineages. Camel and human MERS-CoV sequences are jumbled together within lineages. In the camel samples, the researchers discovered 10 recombination events. The junctions between ORF1b and S were the most common recombination breakpoints. MERS-CoV infection in humans may have resulted from the continual transfer of various MERS-CoV lineages from camels, according to evidence. The camel MERS-CoV genomes sequenced in this investigation support this idea (Yusof *et al,* 2017).

The current findings indicated that there were no differences observed in length and range of epitopes for each virus among all studied lineages. Most of epitopes sequences were conserved. However, few sequences underwent little mutation involving single amino acids. The top 15 epitopes in dromedary camels have a conserved sequence, indicating that a quick test based on spike protein epitopes is reliable. According to the present data, 20% of epitope sequences are found near the RBD, whereas the remaining 80% are found distant from the RBD. In dromedary camels, this research proved the reliability of the previously mentioned rapid test based on spike protein epitopes. In the current study, the alignment of spike protein sequences from several MERS-CoV lineages indicated a small number of alterations. Lineages 2 and 3 were affected by these changes. Using rapid testing for MERS-CoV detection based on epitopes from lineages 1, 4, and 5 seems to be effective, based on the current findings. Furthermore, given the changes in lineages 2 and 3 were rare and involved just a single amino acid, these quick tests may be successful when employing any epitope from these lineages.

The current findings revealed the absence of gaps in the alignment that indicates the lack of amino acid insertions or deletions in the spike protein among the lineages. This finding confirmed the effectiveness of any of studied epitopes for rapid test designing in dromedary camels. The current finding indicated that, the number of difference among viruses accession number was a maximum of 8, most of them were not involved in the antigenic epitopes. This finding confirmed the suitability of any of the studied epitopes for production of rapid tests of MERS CoV in dromedary camels. The current findings indicated a higher identity of the spike protein among the lineages which ranged from 99.5 -100%. This finding provides new evidence of the effectiveness of any of the studied epitopes for the production of rapid tests of MERS CoV in dromedary camels as illustrated above.

Because identifying antigens and epitopes using an experimental method may be difficult, expensive, and time-consuming, using an *in-silico* strategy to uncover novel epitopes has become the preferred alternative. This approach is recognised as one of the most effective in identifying antigens because it screens the whole microbial proteome using a variety of prediction algorithms. In conclusion, our comprehensive technique encompasses antigenic epitope screening both horizontally (through the whole coding areas of the Spike) and vertically (across various MERS-CoV lineages). Mutations in the targeted epitopes might have an influence on the diagnostics' population coverage and efficiency. After examining current MERS-CoV mutants across lineages, we evaluated for immunogenicity conservation in the chosen epitopes to provide more diagnostic options. The efficiency of diagnostics based on the provided configurations is expected to be high due to the observed low mutagenicity rate of MERS-CoV. Combining the present findings with experimental confirmation is a pre requisite for successful diagnostics.

Acknowledgements

This work was supported by the Deanship of Scientific Research, Vice Presidency for Graduate Studies and Scientific Research, King Faisal University, Saudi Arabia (Project # 171002; Grant 271).

References

Abd El Wahed A, Patel P, Heidenreich D, Hufert FT and Weidmann M. Reverse transcription recombinase polymerase amplification assay for the detection of Middle East respiratory syndrome coronavirus. PLOS Currents. 2013; 12;5:ecurrents.DOI:10.1371/currents.outbreaks.

Alexandersen S1, Kobinger GP, Soule G and Wernery U. Middle East respiratory syndrome coronavirus antibody reactors among camels in Dubai, United Arab Emirates, in 2005. Transboundary and Emerging Diseases. 2014; 61:105-108.

Annan A, Baldwin HJ, Corman VM, Klose SM, Owusu M, Nkrumah EE, Badu EK, Anti P, Agbenyega O, Meyer B, Oppong S, Sarkodie YA, Kalko EK, Lina PH, Godlevska EV, Reusken C, Seebens A, Gloza-Rausch F, Vallo P, Tschapka M, Drosten C and Drexler JF. Human betacoronavirus 2c EMC/2012-related viruses in bats, Ghana and Europe. Emerging Infectious Diseases. 2013; 19:456-459.

Buchholz U, Muller MA, Nitsche A, Sanewski A, Wevering N, Bauer- Balci T, Bonin F, Drosten C, Schweiger B, Wolff T, Muth D, Meyer B, Buda S, Krause G, Schaade L and Haas W. Contact investigation of a case of human novel coronavirus infection treated in a German hospital, October-November 2012. Eurosurveillance. 2013; 18(8):20406.

Chu DKW, Hui KPY, Perera R, Miguel E, Niemeyer D, Zhao J, Channappanavar R, Dudas G, Oladipo JO, Traoré A, Fassi-Fihri O, Ali A, Demissié GF, Muth D, Chan MCW, Nicholls JM, Meyerholz DK, Kuranga SA, Mamo G, Zhou Z, So RTY, Hemida MG, Webby RJ, Roger F, Rambaut A, Poon LLM, Perlman S, Drosten C, Chevalier V and Peiris M. MERS coronaviruses from camels in Africa exhibit region-dependent genetic diversity. Proceedings of the National Academy of Sciences. 2018; 115:3144-3149.

Corman V, Eckerle I, Bleicker T, Zaki A, Landt O, Eschbach-Bludau M, van Boheemen S, Gopal R, Ballhause M, Bestebroer T, Muth D, Muller M, Drexler J, Zambon M, Osterhaus A, Fouchier R and Drosten C. Detection of a novel human coronavirus by real-time reversetranscription polymerase chain reaction. Eurosurveillance. 2012a; 17:pii20285.

Corman VM, Muller MA, Costabel U, Timm J, Binger T, Meyer B, Kreher P, Lattwein E, Eschbach-Bludau M, Nitsche A, Bleicker T, Landt O, Schweiger B, Drexler JF, Osterhaus AD, Haagmans BL, Dittmer U, Bonin F, Wolff T and Drosten C. Assays for laboratory confirmation of novel human coronavirus (hCoV-EMC) infections. Eurosurveillance. 2012b; 17(49):20334.

Cotten M, Watson SJ, Zumla AI, Makhdoom HQ, Palser AL, Ong SH, Al Rabeeah AA, Alhakeem RF, Assiri A, Al-Tawfiq JA, Albarrak A, Barry M, Shibl A, Alrabiah FA, Hajjar S, Balkhy HH, Flemban H, Rambaut A, Kellam P and Memish ZA. Spread, circulation, and evolution of the Middle East respiratory syndrome coronavirus. mBio. 2014; 5(1):e01062-13. DOI:10.1128/mBio.01062-13.

Kearse M, Moir R, Wilson A, Stones-Havas S, Cheung M, Sturrock S, Buxton S, Cooper A, Markowitz S, Duran C, Thierer T, Ashton B, Meintjes P and Drummond A. Geneious Basic: an integrated and extendable desktop software platform for the organisation and analysis of sequence data. Bioinformatics. 2012; 28:1647-1649.

Kolaskar AS and Tongaonkar PC. A semi-empirical method for prediction of antigenic determinants on protein antigens. FEBS Letters. 1990; 276:172-174.

Lau SK, Wernery R, Wong EY, Joseph S, Tsang AK, Patteril NA, Elizabeth SK, Chan KH, Muhammed R, Kinne J, Yuen KY, Wernery U and Woo PC. Polyphyletic origin of MERS coronaviruses and isolation of a novel clade A strain from dromedary camels in the United Arab Emirates. Emerging Microbes and Infections. 2016; 5(1):1-9.

Meyer B, Müller MA, Corman VM, Reusken CBEM, Ritz D, Godeke GJ, Lattwein E, Kallies S, Siemens A, van Beek J, Drexler JF, Muth D, Bosch B-J, Wernery U, Koopmans MPG, Wernery R and Drosten C. Antibodies against MERS coronavirus in dromedary camels, United Arab Emirates, 2003 and 2013. Emerging Infectious Diseases. 2003; 20:552-559. DOI:10.3201/eid2004.131746.

Millet JK, Goldstein ME, Labitt RN, Hsu HL, Daniel S and Whittaker GR. A camel-derived MERS-CoV with a variant spike protein cleavage site and distinct fusion activation properties. Emerging Microbes and Infections. 2016; 5(1):1-9.

Muhairi SA, Hosani FA, Eltahir YM, Mulla MA, Yusof MF, Serhan WS, Hashem FM, Elsayed EA, Marzoug BA and Abdelazim AS. Epidemiological investigation of Middle East respiratory syndrome coronavirus in dromedary camel farms linked with human infection in Abu Dhabi Emirate, United Arab Emirates. Virus Genes. 2016; 52: 848-854. DOI:10.1007/s11262-016-1367-1.

Perera RA, Wang P, Gomaa MR, El-Shesheny R, Kandeil A, Bagato O, Siu LY, Shehata MM, Kayed AS, Moatasim Y, Li M, Poon LL, Guan Y, Webby RJ, Ali MA, Peiris JS and Kayali G. Seroepidemiology for MERS coronavirus using microneutralisation and pseudoparticle virus neutralisation assays reveal a high prevalence of antibody in dromedary camels in Egypt. Eurosurveillance. 2013; 5;18(36):pii20574. DOI:10.2807/1560-7917.es2013.18.36.20574.

Reusken C, Mou H, Godeke GJ, van der Hoek L, Meyer B, Muller MA, Haagmans B, de Sousa R, Schuurman N, Dittmer U, Rottier P, Osterhaus A, Drosten C, Bosch BJ and Koopmans M. Specific serology for emerging human coronaviruses by protein microarray. Eurosurveillance. 2013b; 18(14):20441. DOI: 10.2807/1560-7917.es2013.18.14.20441.

Reusken CB, Haagmans BL, Muller MA, Gutierrez C, Godeke GJ, Meyer B, Muth D, Raj VS, Smits-De Vries L, Corman VM, Drexler J-F, Smits SL, El Tahir YE, De Sousa R, van Beek J, Nowotny N, van Maanen K, Hidalgo-Hermoso E, Bosch B-J, Rottier P, Osterhaus A, Gortazar-Schmidt C, Drosten C and Koopmans MPG. Middle East respiratory syndrome coronavirus neutralising serum antibodies in dromedary camels: a comparative serological study. The Lancet Infectious Diseases. 2013a; 13:859-866. DOI:10.1016/S1473-3099(13)70164-6.

Romesburg C. Cluster analysis for researchers. Lulu. com. (2004).

Sabir JS, Lam TT, Ahmed MM, Li L, Shen Y, Abo-Aba SE, Qureshi MI, Abu-Zeid M, Zhang Y, Khiyami MA, Alharbi NS, Hajrah NH, Sabir MJ, Mutwakil MH, Kabli SA, Alsulaimany FA, Obaid AY, Zhou B, Smith DK, Holmes EC, Zhu H and Guan Y. Co-circulation of three camel coronavirus species and recombination of MERS-CoVs in Saudi Arabia. Science. 2016; 351:81-84.

Shirato K, Yano T, Senba S, Akachi S, Kobayashi T, Nishinaka T, Notomi T and Matsuyama S. Detection of Middle East respiratory syndrome coronavirus using reverse transcription loop-mediated isothermal amplification (RT-LAMP). Virology Journal. 2014; 11(1):1-11.

Song D, Ha G, Serhan W, Eltahir Y, Yusof M, Hashem F, Elsayed E, Marzoug B, Abdelazim A and Al Muhairi S. Development and validation of a rapid immunochromatographic assay for detection of Middle East respiratory syndrome coronavirus antigen in dromedary camels. Journal of Clinical Microbiology. 2015; (4):1178-82.

van Doremalen N, Hijazeen ZS, Holloway P, Al Omari B, McDowell C, Adney D, Talafha HA, Guitian J, Steel J, Amarin N, Tibbo M, Abu-Basha E, Al-Majali AM, Munster VJ and Richt JA. High prevalence of middle east respiratory coronavirus in young dromedary camels in Jordan. Vector Borne Zoonotic Diseases. 2017; 17:155-159.

Yusof MF, Queen K, Eltahir YM, Paden CR, Al Hammadi ZMAH, Tao Y, Li Y, Khalafalla AI, Shi M, Zhang J, Mohamed MSAE, Abd Elaal Ahmed MH, Azeez IA, Bensalah OK, Eldahab ZS, Al Hosani FI, Gerber SI, Hall AJ, Tong S and Al Muhairi SS. Diversity of Middle East respiratory syndrome coronaviruses in 109 dromedary camels based on full-genome sequencing, Abu Dhabi, United Arab Emirates. Emerging Microbes and Infections. 2017; 6(11): 101-111.

Zaki AM, van Boheemen S, Bestebroer TM, Osterhaus AD and Fouchier RA. Isolation of a novel coronavirus from a man with pneumonia in Saudi Arabia. The New England Journal of Medicine. 2012; 367:1814-1820.

HEMOGLOBIN PLAYS A VITAL ROLE IN PHYSIOLOGICAL PROCESS

SHARKOFERROL® VET

True hematinic for all types of anemia in Livestock

Salient feature

- **Immunity Booster** : Improves humoral immunity by promoting formation of blood cells and maintains optimum haemoglobin level.
- **Instant Energy** : Malt extract and Nicotinamide provides instant energy.
- **Growth Promoter** : Vitamin B complex and rich carbohydrate source serves as growth promoter.
- **Stress reliever** : Helps to relieve environmental and physiological stress.

Dosage:

Cattle, Buffaloes & Horses : 30 to 50 gm daily
Calves, Sheep & goats : 10 to 15 gm daily
Camel: 10 gm per 100 kg B. Wt. daily

450 g *1 kg* *2.50 kg*

Alembic

For further details please contact:
Alembic Pharmaceuticals Ltd. Prime Corporate Park, 2nd Floor, Behind ITC Grand Maratha Sheraton, Sahar Road, Andheri (E), Mumbai - 400 099 • Tel: 022 30611666 Fax: 022 30611682

DOI : 10.5958/2277-8934.2022.00017.0 Vol 29 No 2, p 127-132

VIRULENCE GENES AND ANTIMICROBIAL RESISTANCE PROFILE OF *Escherichia coli* ISOLATES FROM DIARRHOEIC NEONATAL DROMEDARY CAMELS

Shirish Dadarao Narnaware, Rakesh Ranjan, Basanti Jyotsana and Artabandhu Sahoo
ICAR- National Research Centre on Camel, Bikaner, Rajasthan 334001, India

ABSTRACT

In the present study, *Escherichia coli* were isolated from rectal swabs of total 48 (20.68%) diarrhoeic neonatal dromedary camels during the five years study period in an organised farm. The PCR for amplification of virulence genes revealed that 31 (64.58%) isolates harboured at least one virulence gene. The detection rates of *stx1, stx2, eae, F41, K99* and *sta* virulence genes were 4.16%, 2.08%, 35.41%, 14.58%, 18.75% and 16.66%, respectively. Based on occurrence of these virulence genes the isolates were pathotyped into shigatoxigenic *E. coli* (STEC) (6.25%), enteropathogenic *E. coli* (EPEC) (20.83%) and enterotoxigenic *E. coli* (ETEC) (29.16%). Atypical combinations of EPEC+ETEC (8.33%) were also detected. The *E. coli* isolates from all three neonatal camels having acute haemorrhagic enteritis and mortality were found to be of STEC type. In antibiotic sensitivity test, most prevalent resistance was observed against amoxicillin, cloxacillin, erythromycin and lincomycin whereas lowest resistance was observed against gentamicin and amikacin. Findings of this study indicate that neonatal camels are the probable reservoir of multidrug resistant and zoonotic STEC. Young age (below 7 days), housing system with loose sandy ground and winter season were identified as important risk factors for high incidence of neonatal camel calf diarrhoea in the present study.

Key words: Antimicrobial resistance, camel, *Escherichia coli*, neonatal diarrhoea, PCR, virulence genes

The occurrence of neonatal diarrhoea or colibacillosis caused by *Escherichia coli* in neonatal camels is one of the important infectious diseases as it incurs significant economic losses due to high morbidity and mortality rate resulting from severe diarrhoea and septicemia (Mohammed *et al*, 2003). It was believed that strains of *E. coli* colonise the host's intestine with different virulence factors and induce diarrhoea by escaping the immune system (Cho and Yoon, 2014; Desvaux *et al,* 2020). *E. coli* causing neonatal calf diarrhoea were mainly pathotyped on the basis of presence of virulence factors as enteropathogenic *E. coli* (EPEC), enterotoxigenic *E. coli* (ETEC) and shigatoxigenic *E. coli* (STEC) which include subgroup enterohaemorrhagic (EHEC), enteroinvasive (EIEC), enteroaggregative (EAEC) and enteroadherent *E. coli* (EAdEC) (Andrade *et al,* 2012). These pathotypes have mostly been related to mild to severe diarrhoea causing high rates of morbidity and mortality particularly during the early neonatal period in calves (Andrade *et al,* 2012). Each diarrhoeagenic *E. coli* pathotype represents a collection of strains that possess similar virulence factors and cause similar diseases with similar pathology (Robins-Browne *et al,* 2016). The STEC is considered as zoonotic pathogen causing haemorrhagic colitis and haemorrhagic uraemic syndrome in human beings (Nataro and Kaper, 1998). The pathogenicity of STEC is mediated mainly through Shiga toxins 1 and 2 encoded by stx1 and stx2 genes, respectively (Paton and Paton, 1998). The pathogenicity of ETEC is attributed to the expression of fimbrial antigens F41, F5 and F17, and the elaboration of one or more enterotoxins like heat-stable enterotoxins (sta) and heat-labile enterotoxins (LT) (Ryu *et al,* 2020). The EPEC pathotype involved in young calf diarrhoea and dysentery induce attaching and effacing (AE) lesions on intestinal cells due to the production of the protein intimin (eae) (Mainil and Fairbrother, 2014).

During the past decade, drug resistance in enterobacteriaceae has increased worldwide which is considered as potential threat for public health (Prestinaci *et al,* 2015). Since *E. coli* is present as gut commensal in humans and animals, it has become one of the microorganisms that are commonly resistant to

SEND REPRINT REQUEST TO SHIRISH DADARAO NARNAWARE email: sdnarnaware1@gmail.com

antimicrobials due to the selective pressure imposed by the antimicrobial drugs used in the treatment of food animals and humans (Zhao *et al,* 2012). In present study, characterisation of *E. coli* pathotypes isolated from diarrhoeic neonatal dromedary camels and their antimicrobial resistance pattern was investigated.

Materials and Methods

Animals, sample collection and pathological studies

This study was conducted during the period from 2016 to 2020 in an organised dromedary camel farm situated at Bikaner, India which is an arid region within Thar desert. The neonatal camels of the farm were kept along with their dam in a corral having loose sandy soil with free access to colostrum since birth. The faecal swabs were directly collected from the rectum of the diarrhoeic neonatal camels using sterile cotton swabs for bacterial culture. These calves were not given any antimicrobials before sampling. The faecal samples were also collected in sterile containers (sterile clinicol™, Himedia, India) and investigated for presence of oocysts of coccidia and cryptosporidia and eggs of helminths using direct wet mount examination method. The necropsy was performed on 3 diarrhoeic neonatal camels having mortality and tissue samples from internal organs were collected in 10% formal saline for histopathology. The formalin fixed tissue samples were embedded in paraffin, cut into 4–5 micron sections using a semi automatic microtome (Wewox®, India) and stained with haematoxylin and eosin (HE) stain.

Bacterial culture and antimicrobial susceptibility testing

The rectal swab samples collected from diarrhoeic neonatal camels were inoculated on MacConkey and Eosin Methylene Blue (EMB) agar media and incubated at 37 °C for 18-24 hours. These *E. coli* colonies were further cultured on Mueller Hinton agar for determination of antimicrobial susceptibility using the agar disc diffusion method (Humphries *et al,* 2018). The antibiotic discs were chosen keeping in mind their common use in livestock farming in India. The antibiotic discs (HiMedia, India) included in the present study were: amoxicillin (AMX) (10µg), cloxacillin (COX) (5µg), cefotaxime (CTX) (30µg), tetracycline (TE) (30µg), doxycycline hydrochloride (DO) (30µg), erythromycin (E) (15µg), lincomycin (10µg), gentamicin (GEN) (10µg), amikacin (AK) (30µg), streptomycin (S) (10µg), amoxicillin/ sulbactum (AMS) (30/15µg), trimethoprim (TR) (5µg), ciprofloxacin (CIP) (5µg), enrofloxacin (EX) (10µg), ceftriaxone (CTR) (30µg) and chloramphenicol (C) (30µg). The diameter of the zones of inhibition was measured by antibiotic zone scale™ (HiMedia, India) and the zones were graded as sensitive and resistant to the drugs tested by referring to Zone Size Interpretative Chart (HiMedia, India) in accordance to Performance Standards for Antimicrobial Disk Susceptibility Tests, Clinical and Laboratory Standards Institute (CLSI) (Humphries *et al,* 2018). Multiple-antibiotic resistance was defined as resistance to 2 or more antibiotic classes.

DNA extraction and PCR for detection of virulence genes

Pure and characteristic lactose fermenting pink coloured colonies from MacConkey agar were selected for DNA extraction using Mericon™ DNA bacteria kit (Qiagen, Germany). The PCR for molecular identification of *E. coli* isolates was carried out using the primer sequence targeting uidA gene encoding β- glucuronidase of *E. coli* to amplify a 486-bp fragment (Heininger *et al*, 1999). For detection of different virulence genes (*stx1, stx2, eae, K99, F41* and *sta*), multiple PCR was performed using different primer sets (Table 1) and PCR cycling conditions described previously (Franck *et al,* 1998).

Results

Incidence, clinical and pathological findings

In the present study, *E. coli* was isolated from rectal swab samples of 48 (20.68%) diarrhoeic neonatal camels over the period of 4 years with case fatality rate of 6.25%. No significant difference was found in occurrence of diarrhoea in male and female neonatal camels. No evidence of any parasitic infection was found in any of the faecal samples collected from these diarrhoeic neonatal camels. An association between age of neonatal camels and occurrence of diarrhoea was observed. The incidence of diarrhoea was appreciably more in camels of age group below 7 days (n=41) compared to camels of age group 7 days and above (n=7) (Table 2). The important clinical signs in diarrhoeic neonatal camels were profuse, foul-smelling, yellow to pale yellow or greenish, watery to pasty diarrhoea soiling the tail and hindquarters. In 3 neonatal camels having mortality, the severity of the symptoms were more pronounced and characterised by anorexia, weakness and mucous and blood mixed faeces.

The necropsy of these neonatal camels showed gross lesions of dark red diffusely congested small and large intestinal mucosa with presence of moderate amount of mucous and blood mixed contents in the lumen (Fig 1). The abomasum also showed dark red congested mucosa with blood mixed contents. The liver was enlarged and showed multifocal pale areas throughout its surface. Kidneys were enlarged with moderate to severe congestion. The other organs were not showing any significant gross changes. Histopathology of small intestine revealed areas of desquamation with presence of free epithelial cells in lumen, mucosal epithelial necrosis, hyperemia of the villi, villus stunting and fusion, and mild to moderate infiltration of eosinophils in the lamina propria and crypt region (Fig 2). The submucosa showed mild to moderate thickening, oedema and dilatation and congestion of submucosal capillaries. Histopathology of liver showed prominent vacuolar degenerative changes in hepatocytes with congestion of central vein and sinusoidal capillaries. Histopathology of kidney showed congestion of glomerular capillaries and occasionally atrophied and distorted glomeruli.

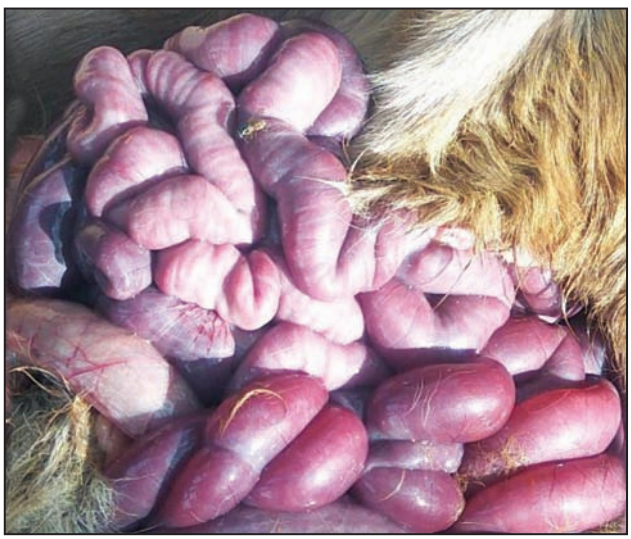

Fig 1. Moderate to severely congested small intestinal loops.

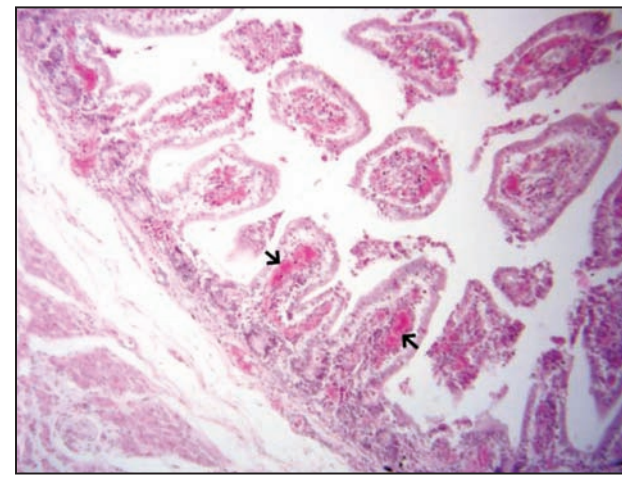

Fig 2. Histopathology of small intestine showing desquamation of villous epithelium and atrophied villi with hyperemic blood vessels (arrow). HE X 100.

Table 1. Details of primers used for amplification of different virulence genes.

Pathotype	Target virulence gene	Oligonucleotide sequences (5′-3′)	Product size (bp)	References
STEC	*stx1*	F: TTCGCTCTGCAATAGGTA R: TTCCCCAGTTCAATGTAAGAT	555	Paton *et al*, 1995
	stx2	F: GTGCCTGTTACTGGGTTTTTCTTC R: AGGGGTCGATATCTCTGTCC	118	Paton *et al*, 1993
EPEC	*eae*	F: ATATCCGTTTTAATGGCTATCT R: AATCTTCTGCGTACTGTGTTCA	425	Yu and Kaper, 1992
ETEC	*F41*	F: GCATCAGCGGCAGTATCT R: GTCCCTAGCTCAGTATTATCACCT	380	Fidock *et al*, 1989
	K99	F: TATTATCTTAGGTGGTATGG R: GGTATCCTTTAGCAGCAGTATTTC	314	Roosendaal *et al*, 1984
	sta	GCTAATGTTGGCAATTTTTATTTCTGTA AGGATTACAACAAAGTTCACAGCAGTAA	190	Sekizaki *et al*, 1985

Table 2. Summary of age, sex and result of virulence gene PCR in diarrhoeic neonatal camels.

Total camels	Sex		Age (days)		Result of virulence gene PCR					
	Male	Female	<7 days	≥7 days	*stx1*	*stx 2*	*eae*	*F41*	*K99*	*sta*
48	21	27	41	7	2 (4.16%)	1 (2.08%)	17 (35.41%)	7 (14.58%)	9 (18.75%)	8 (16.66%)

Table 3. Summary of virulence gene profile and pathotypes of *E. coli* isolates from diarrhoeic neonatal camels.

Pathotype	Virulence genes	No. of isolates (%)	Total No. of isolates (%)
STEC	*stx1+eae*	2 (4.16%)	3 (6.25%)
	stx2+eae	1 (2.08%)	
EPEC	*eae*	10 (20.83%)	10 (20.83%)
ETEC	*F41*	5 (10.41%)	14 (29.16%)
	K99	1 (2.08%)	
	K99+ sta	6 (12.5%)	
	sta	2 (4.16%)	
Mixed (EPEC+ETEC)	*eae+ F41*	2 (4.16%)	4 (8.33%)
	eae+ K99	2 (4.76%)	
None	None	17 (35.41%)	17 (35.41%)

Distribution of virulence genes and pathotypes

The screening for presence of virulence genes in *E. coli* isolates from diarrhoeic neonatal camels revealed 31 (64.58%) isolates possess one or more virulence genes, whereas in 17 (35.41%) of the isolates no virulence genes could be detected and considered non-pathogenic (Table 3). The individual incidence of virulence genes *viz*., stx1, stx2, eae, F41, K99 and sta in *E. coli* isolates were 2 (4.16%), 1 (2.08%), 17 (35.41%), 7 (14.58%), 9 (18.75%) and 8 (16.66%), respectively (Table 2). Based on the distribution of virulence genes, the *E. coli* isolates were pathotyped as STEC (6.25%), EPEC (20.83%), ETEC (29.16%) and mixed type (8.33%) (Table 3). The *E. coli* isolates from all the 3 neonatal camels having acute haemorrhagic enteritis and mortality were found to be of STEC type.

Antimicrobial resistance

The antimicrobial resistance profiles of all *E. coli* isolates against the tested antibiotics are summarised in Table 4.

Discussion

In this study, a high incidence of neonatal camel calf diarrhoea was observed which was mainly attributed to unhygienic living conditions, overcrowding and damp floors which support and shelter infectious agents (Cho and Yoon, 2014). Since camels are seasonal breeders, maximum calving in India usually took place in winter season particularly in the months of January and February. Moreover, the calving shed of the present study had loose sandy soil in which wet conditions prevailed for longer time due to winter months. Highest prevalence rate of *E. coli* infection during winter season was also recorded in cattle and buffalo calves in earlier studies (Awad *et al,* 2020). The neonatal calves below 7 days showed maximum incidence of calf diarrhoea which was mainly attributed to the non appearance of humoural immunity and pessimistic response to cell mediated immunity in calves (Mohan *et al,* 1990). The clinical signs of yellowish or greenish diarrhoea with occasional presence of mucous and blood in *E. coli* infected camels of the present study were in agreement with camel calf diarrhoea cases reported earlier (Yeshiwas and Fentahun, 2017). Similarly, the pathological lesions of acute enteritis with desquamation of mucosal epithelium and atrophy of villi were frequently reported in intestine of diarrhoeic calves due to *E. coli* infection (Awad *et al,* 2020).

Table 4. Summary of antimicrobial resistance profile of *E. coli* isolates.

Antimicrobial group	Antimicrobial agents	No. of resistant *E. coli* isolates (%)
β- lactams	Amoxicillin	48 (100%)
	Cloxacillin	48 (100%)
	Cefotaxime	6 (12.5%)
	Cephoxitin	12 (25%)
Tetracyclines	Tetracycline	27 (56.25%)
	Doxycycline	24 (50%)
Macrolides	Erythromycin	48 (100%)
	Lincomycin	48 (100%)
Aminoglycosides	Gentamicin	5 (10.41%)
	Amikacin	5 (10.41%)
	Streptomycin	22 (45.83%)
β- lactamase inhibitor	Amoxicillin/ sulbactum	21 (43.75%)
Folate inhibitor	Trimethoprim	40 (83.33%)
Quinolones	Ciprofloxacin	20 (41.66%)
	Enrofloxacin	21 (43.75%)
Cephalosporins	Ceftriaxone	11 (22.91%)
Chloramphenicol	Chloramphenicol	33 (70.83%)

The antimicrobials used for susceptibility testing in the present study were routinely used in veterinary practice as therapeutics or as growth promoters in India. The antibiotic resistance pattern observed in *E. coli* isolates of the present study was comparable with those observed in *E. coli* isolates from camel and cattle calves from Tunisia and India (Bessalah *et al,* 2016; Sharma *et al,* 2017). The high prevalence of antimicrobial resistance against commonly used drugs in human medicine in *E. coli* isolates of the present study pointed to the judicious use of antimicrobials in livestock farms. Although, there was difference in occurrence of virulence factors in *E. coli* isolates, however, the antimicrobial susceptibility pattern was more or less similar among them. This may be due to the fact that all diarrhoeic neonatal camels of the present study were from a farm where continuous use of these antibiotics for various types of ailments was practicsed since long time.

Characterisation and identification of genes encoding virulence factors and subdivision of diarrhoeic *E. coli* into pathotypes were necessary for understanding the disease epidemiology and pathogenesis (Garcia *et al,* 2020). The majority of diarrhoeic neonatal camels of the present study were found infected with ETEC infection during first 6 days after birth was in agreement with earlier studies (Guler *et al,* 2008; Foster and Smith, 2009). The 2nd most prevalent pathotype in diarrhoeic neonatal camels was EPEC with detection rate of 20.83% which was comparable with previous studies in diarrhoeic cattle and buffalo calves (Guler *et al,* 2008; Awad *et al,* 2020). However, Foster and Smith (2009) claimed that the significance of EPEC as a calf pathogen was questionable as it can be isolated from both healthy and diarrhoeic calves. The STEC pathotypes were detected in 6.25% of *E. coli* isolates which was lower than those reported in previous studies in diarrhoeic cattle and buffalo calves (Awad *et al,* 2020). In the present study, the *E. coli* isolated from neonatal camels having acute haemorrhagic enteritis and mortality were found to be of STEC type. Globally, STEC was an important cause of life threatening diarrhoeal disease in both animals and humans and association of STEC pathotype in causing haemorrhagic dysentery in young calves had been frequently reported (Robins-Browne *et al,* 2016). The shiga toxins destroyed intestinal microvilli resulting into haemorrhagic diarrhoea in calves (Nataro and Kaper, 1998). Mixed pathotypes with combinations of EPEC with ETEC were frequently reported in earlier studies (Awad *et al,* 2020; Ryu *et al,* 2020). It was speculated that these atypical combinations may result in the emergence of new pathotypes which may be more pathogenic and cause severe diarrhoea in calves (Awad *et al,* 2020).

Among diarrhoeic neonatal camels of the present study, ETEC were the most common pathotype, whereas STEC were found responsible for acute haemorrhagic enteritis and mortality. Young age (less than 7 days), calving pen with loose sandy ground and peak winter season were found associated with high incidence of neonatal camel calf diarrhoea in the present study. The studies on virulence genes and antimicrobial resistance pattern in *E. coli* isolates from diarrhoeic neonatal camels can be crucial for camel farmers and veterinarians in selection of antimicrobials for effective management and prevention of the disease and to minimise the emergence of multidrug resistant *E. coli* which may pose health risks to both animals and humans.

References

Andrade GI, Coura FM, Santos ELS, Ferreira MG, Galinari GCF, Facury Filho EJ, de Carvalho AU, Lage AP and Heinemann MB. Identification of virulence factors by multiplex PCR in *Escherichia coli* isolated from calves in Minas Gerais, Brazil. Tropical Animal Health and Production. 2012; 44:1783-1790.

Awad WS, El-Sayed AA, Mohammed FF, Bakry NM, Abdou NMI and Kamel MS. Molecular characterisation of pathogenic *Escherichia coli* isolated from diarrhoeic and in-contact cattle and buffalo calves. Tropical Animal Health and Production. 2020; 52:3173-3185.

Bessalah S, Fairbrother JM, Salhi, I, Vanier G, Khorchani T, Seddik MM and Hammadi M. Antimicrobial resistance and molecular characterisation of virulence genes, phylogenetic groups of *Escherichia coli* isolated from diarrhoeic and healthy camel-calves in Tunisia. Comporative Immunology, Microbiology and Infectious Diseases. 2016; 49:1-7.

Cho YI and Yoon KJ. An overview of calf diarrhoea - infectious etiology, diagnosis, and intervention. Journal of Veterinary Science. 2014; 15:1-17.

Desvaux M, Dalmasso G, Beyrouthy R, Barnich N, Delmas J and Bonnet R. Pathogenicity factors of genomic islands in intestinal and extraintestinal *Escherichia coli*. Frontiers in Microbiology. 2020; 11:2065.

Fidock DA, McNicholas PA and Lehrbach PR. Nucleotide sequence of the F41 fimbriae subunit gene in *Escherichia coli* B41. Nucleic Acids Research. 1989; 17:2849.

Foster DM and Smith GW. Pathophysiology of diarrhoea in calves. Veterinary Clinics of North America. Food Animal Practice. 2009; 25:13-36.

Franck SM, Bosworth BT and Moon HW. Multiplex PCR for enterotoxigenic, attaching and effacing, and Shiga toxin-producing *Escherichia coli* strains from calves. Journal of Clinical Microbiology. 1998; 36:1795-1797.

Garcia V, Gambino M, Pedersen K, Haugegaard S, Olsen JE and Herrero-Fresno A. F4- and F18-Positive Enterotoxigenic *Escherichia coli* isolates from diarrhoea of postweaning pigs: genomic characterisation. Applied and Environmental Microbiology. 2020; 86:e01913-20.

Guler L, Gunduz K and Ok U. Virulence factors and antimicrobial susceptibility of *Escherichia coli* isolated from calves in Turkey. Zoonoses and Public Health. 2008; 55:249-257.

Heininger A, Binder M, Schmidt S, Unertl K, Botzenhart K, Döring G. PCR and blood culture for detection of *Escherichia coli* bacteremia in rats. Journal of Clinical Microbiology. 1999; 37:2479-2482.

Humphries R, Ambler J, Mitchell SL, Castanheira M, Dingle T, Hindler JA, Koeth L, Sei K, Hardy D and Zimmer B. CLSI methods development and standardisation working group best practices for evaluation of antimicrobial susceptibility tests. Journal of Clinical Microbiology. 2018; 56:e01934-17.

Mainil J and Fairbrother J. *Escherichia coli* in Domestic Mammals and Birds, In: Morabito S (Eds), Pathogenic *Escherichia coli*: Molecular and Cellular Microbiology, Ciaster Academic Press, Norwich, UK. 2014; pp 19-44.

Mohammed, ME, Hart CA and Kadden OR. Viruses and bacteria associated with neonatal camel calf diarrhoea in eastern Sudan. Emirates Journal of Agricultural Sciences. 2003; 15:56-62.

Mohan RS, Rao R, Raghavan RS anbd Gaffar AA. Studies on neonatal diarrhoea in buffalo calves with special reference to epizootiology and fluid therapy. Indian Veterinary Journal. 1990; 67:1057-1059.

Nataro JP and Kaper JB. Diarrhoeagenic *Escherichia coli*. Clinical Microbiology Reviews. 1998; 11:142-201.

Paton AW, Paton JC and Manning PA. Polymerase chain reaction amplification, cloning and sequencing of variant *Escherichia coli* Shiga-like toxin type II operons. Microbial Pathogenesis. 1993; 15:77-82.

Paton AW, Beutin L and Paton JC. Heterogeneity of the amino acid sequences of *Escherichia coli* Shiga-like toxin type-I operons. Gene. 1995; 153:71–74.

Paton AW and Paton JC. Detection and characterisation of Shiga toxigenic *E. coli* by using multiplex PCR assays for stx1, stx2, eaeA, Enterohaemorrhagic *E. coli* hlyA, rfbO11, and rfbO157. Journal of Clinical Microbiology. 1998; 36:598-602.

Prestinaci F, Pezzotti P and Pantosti A. Antimicrobial resistance: a global multifaceted phenomenon. Pathogens and Global Health. 2015; 109:309-318.

Robins-Browne RM, Holt KE, Ingle DJ, Hocking DM, Yang J and Tauschek M. Are *Escherichia coli* pathotypes still relevant in the era of whole-genome sequencing? Frontiers in Cellular and Infection Microbiology. 2016; 6:141.

Roosendaal B, Gaastra W and de Graaf FK. The nucleotide sequence of the gene encoding the K99 subunit of enterotoxigenic *Escherichia coli*. FEMS Microbiology Letters. 1984; 22:253-258.

Ryu JH, Kim S, Park J and Choi KS. Characterisation of virulence genes in *Escherichia coli* strains isolated from pre-weaned calves in the Republic of Korea. Acta Veterinaria Scandinavica. 2020; 62:45.

Sekizaki T, Akashi H and Terakado N. Nucleotide sequences of the genes for *Escherichia coli* heat-stable enterotoxin I of bovine, avian, and porcine origins. American Journal of Veterinary Research. 1985; 46:909-912.

Sharma RK, Taku AK, Malik A, Bhat MA, Javed R, Badroo GA and Kour A. Molecular characterisation and antimicrobial profiling of *Escherichia coli* isolates from diarrhoeic calves. Indian Journal of Animal Sciences. 2017; 87:1467-1471.

Yeshiwas WM and Fentahun WM. The prevalence of *E. coli* from diarrhoeic calves and their antibiotic sensitivity test in selected dairy farms of Debre Zeit, Ethiopia. Advances in Biotechnology and Microbiology. 2017; 6:555680.

Yu J and Kaper JB. Cloning and characterisation of the eae gene of enterohaemorrhagic *Escherichia coli* O157:H7. Molecular Microbiology. 1992; 6:411-417.

Zhao S, Blickenstaff K, Bodeis- Jones S, Gaines SA, Tong E and McDermott PF. Comparison of the prevalence and antimicrobial resistances of *Escherichia coli* isolates from different retail meats in the Unites States, 2002 to 2008. Applied and Environmental Microbiology. 2012; 78:1702-1707.

DOI : 10.5958/2277-8934.2022.00018.2 Vol 29 No 2, p 133-140

ANTIBACTERIAL PROPERTIES OF *Ocimum sanctum, Moringa oleifera* AND *Murraya koenigii* LEAF EXTRACTS AGAINST *Corynebacterium pseudotuberculosis* ISOLATED FROM CAMEL (*Camelus dromedarius*)

Jeeshan Nabi[1], Amita Ranjan[1], Pratishtha Sharma[1], Rakesh Ranjan[2], Neetu Pareek[2] and Dinesh Harsh[2]

[1]Department of Veterinary Pharmacology and Toxicology, College of Veterinary and Animal Science, Rajasthan University of Veterinary and Animal Sciences, Bikaner-334001, Rajasthan, India
[2]ICAR-National Research Centre on Camel Bikaner-334001, Rajasthan, India

ABSTRACT

In the present study, antibacterial properties of methanolic and chloroform extracts of *Ocimum sanctum*, *Moringa oleifera* and *Murraya koenigii* leaves against *Corynebacterium pseudotuberculosis* (CPs) isolated from abscess in dromedary camel were screened using agar well diffusion assay and minimum bactericidal concentration (MBC) were determined using broth microdilution technique. MBC of selected plant extracts varied from 3.125 to 12.5 mg/ml. Chloroform extracts of *Ocimum sanctum* and *Murraya koenigii* had highest antibacterial properties; while it was lowest in methanolic extract of *Moringa oleifera* and *Murraya koenigii* leaves.

Key words: Antimicrobial, Camel, Corynebacterium, Moringa, Murraya, Ocimum

Corynebacterium pseudotuberculosis (CPs) is an important pathogen of domestic animals including sheep, goat, horses, cattle and camel (Dorella *et al,* 2006). In camel, it causes enlargement and suppuration of peripheral and visceral lymph nodes (Tejedor-Junco *et al,* 2004; Wernery and Kinne, 2016; Ranjan *et al,* 2018) and plays an important role in superficial septic wounds (Zidan *et al,* 2013). *In vitro* sensitivity tests suggest that CPs isolated from different animal species are sensitive for most of the common antibiotics (Judson and Songer, 1991). However, after growing CPs as biofilm, in an attempt to mimic the environment of natural infection, the bacterium was found highly resistant to all the tested antimicrobials (Olson *et al,* 2002). Research reports published in the recent past also suggest emergence of drug resistance problem in CPs (Abdel-Wahab and Shigidi, 2013; Algammal, 2016).

There are many medicinal plants containing useful phytochemical constituents which have antibacterial properties and their therapeutic values help in treating many bacterial infections (Abuga *et al*, 2021). Masese *et al* (2016) found *Moringa oleifera, Murraya koingii and Ocimum sanctumare* as an effective reducing agent for the synthesis of AgNPs which were highly stable and had significant activity against *Escherichia coli* and *Staphylococcus aureus*. Moodley *et al* (2018) found that the biosynthesised nanoparticle preparations from *M. oleifera* leaf extracts exhibit potential for application as broad-spectrum antimicrobial agents. The extract of leaves of *Ocimum sanctum* has demonstrated effective antimicrobial property against *A. actinomycetemcomitans*, suggesting its possible use as an effective and affordable "adjunct" in the management of periodontal conditions in humans (Mallikarjun *et al*, 2016). *Murraya koenigii* extracts have demonstrated antibacterial effects particularly on *E. coli* and *Staphylococcus* as compared to antibiotics such as Gentamycin and Amikacin (Irfan *et al,* 2016). Fouad (2019) found antibacterial efficacy of *Moringa oleifera* leaf extract against pyogenic bacteria isolated from a dromedary camel (*Camelus dromedarius*) abscess. Zubair (2020) evaluated the inhibitory effect and anti-biofilm activity of *Moringa oleifera* and *Citrus sinensis* extracts against those of pathogenic *Pseudomonas*

SEND REPRINT REQUEST TO AMITA RANJAN email: amita_pharma@rediffmail.com

aeruginosa and *Staphylococcus aureus* and found that extracts have effectively blocked MRSA and ESBL development in the biofilm matrix. However, studies on antibacterial properties of medicinal plant extracts in camels is meager. The present investigation is, therefore, undertaken to study the antibacterial properties of *Ocimum sanctum, Moringa oleifera* and *Murraya koenigii* leaf extracts against *Corynebacterium pseudotuberculosis* isolated from an abscess of a camel (*Camelus dromedarius*).

Materials and Methods

Bacterial culture and characterisation

The pure colonies of CPs were isolated from pus sample from enlarged, suppurated, cervical lymph node of a dromedary camel housed at ICAR-National Research Centre on Camel, Bikaner, India. The organism was identified on the basis of culture characteristics, morphological features after Grams staining, result of various biochemical tests (Nabi, 2021) and quadruplex PCR test (Almeida *et al,* 2017).

Collection of plants, identification and extract preparation

Fresh leaves of *Ocimum sanctum*, *Moringa oleifera* and *Murraya koenigii* were collected from different localities of Bikaner, Rajasthan and were authenticated by scientists from ICAR-Central Institute for Arid Horticulture, Bikaner. Collected leaves were rinsed with distilled water, dried in shed at room temperature for 15 days and ground to obtain a coarse powder. Methanolic and chloroform extracts of each plant leaves were prepared. Fifty gram dried leaf powder was soaked overnight in 200 ml methanol/ chloroform and the mixture was shaken vigorously several times in between. Next day, the mixture was filtered with Whatman filter paper number one. The filtrate was evaporated to dryness *in vaccuo* at 50°C using rotary film evaporator, and stored at -20°C till further use. Extractability or yield (%) of each extract was calculated using a formula: Extractability or yield (%) = (weight of extract obtained in gram/ weight of leaf powder taken in gram) *100 (Mazhangara *et al,* 2020).

The extract obtained was dissolved in 10% dimethylsulfoxide (DMSO; HiMedia Laboratories Private Limited, Mumbai, India) to a desired concentration and sterilised by passing through a 22 µm (pore size) filter (HiMedia Laboratories Pvt Ltd., Mumbai, India) before use.

Evaluation of anti-microbial properties of plant extracts

The antimicrobial activities of plant-extracts were screened using agar well diffusion test (Kavitha, 2017) with slight modifications. Briefly, 0.2 ml of diluted inoculum ($1X10^5$ CFU/ml) of the CPs was swabbed on the Brain Heart Infusion (BHI) Agar supplemented with 5% defibrinated sheep blood. Thereafter, using a sterilised cork borer, wells of 5 mm diameter were punched. Using a micropipette, 100 µl of the plant extract solution (100 mg/ml) were added to the wells. The plates were incubated aerobically at 37±2 °C for 24 to 48 h and the zone of inhibition (in mm) was measured with the help of a Vernier caliper. The test was performed in triplicates with controls.

The minimum bactericidal concentrations (MBC) of the methanolic and chloroform extracts were determined using broth micro-dilution technique as per the standard CLSI methods (Wayne, 2008) with slight modifications (Jahan *et al,* 2011).

Standardisation of inoculum size

To ensure an exact number of bacteria present in the inoculum, one or two isolated colonies were inoculated into 5 ml of BHI broth (supplemented with 0.1% Tween 20 to prevent clumping of colonies) and inoculated at 37°C for 24-48 hours. Thereafter, the inoculum was centrifuged at 4,000 rpm for 5 minutes with appropriate aseptic precautions. The supernatant was discarded and the pellet was re-suspended in sterile Phosphate Buffer Saline (PBS) pH 7.4 and centrifuged again at 4000 rpm for 5 min. The process was repeated until the supernatant was clear. The pellet, thereafter was suspended in 5 ml sterile PBS and optical density was recorded at 500 nm. Serial dilutions (two-fold) were done in PBS under aseptic conditions until the optical density was in a range of 0.8 to 1.0. The actual number of colony forming units was estimated after inoculating 100 µl of the bacterial suspension over BHI Agar with 5% defibrinated sheep blood and incubating at 37°C for 24-48 hours. The required dilution factor was calculated and the dilution was carried out to obtain a final concentration of $5 X 10^6$ cfu/ ml (Norman *et al,* 2014).

Preparation of the microplate

In a sterile 96 micro well plate, different test herbal solutions (200 µl each) were pipetted into the first row under aseptic conditions. To all other wells, 100 µl of BHI broth was added. Serial dilutions were performed by transferring 100 µl from the corresponding wells in the first row to the next row

so that at the end, 100 µl of the test herbal extract was present in each well in a serially descending concentration (50, 25, 12.5, 6.25, 3.125, 1.562, 0.781, 0.391, 0.195 and 0.098 mg/ml). Now, 60 µl of 3.3 X strength BHI broth, 20 µl sterile PBS and 20 µl of bacterial suspension (5 X 10^6 cfu/ ml) was poured into each well to obtain a concentration of 5 X 10^5 cfu/ ml and a final volume 200 µl in each well. In addition, one media control (herbal extract and bacterial culture), one bacterial control (herbal extract and BHI broth) and one extract control (BHI broth plus bacterial culture) were also run simultaneously. The micro well plate was covered with lid and sealed with tape and incubated at 37°C for 48 hours. The MBC value was determined by sub-culturing each test dilutions (by transferring 100 µl) on BHI agar with 5% defibrinated sheep blood plates at 37°C for 24-48 hours. The highest dilution (or lowest extract concentration) showing no bacterial growth was taken as MBC (Norman *et al*, 2014).

Statistical analysis

The values obtained were analysed by one-way ANOVA using computer software Statistical Package of Social Sciences (SPSS-20).

Results and Discussion

Plant extracts

The colour, consistency and extractability percentage of different plant extracts are given in table 1. The methanolic extract of *Ocimum sanctum* appeared as blackish, semi-solid paste like with extractability 5.58%. The chloroform extract was brown-black coloured flakes with extraction per cent 2.80. In corroboration with the present findings Agarwal *et al* (2010) reported extractability of ethanolic *O. sanctum* leaf extract to be 6%. Likewise, Shafi *et al* (2018) reported the extraction percentage for hydro-alcoholic extract (1:1 water and ethanol) to be 9.6%.

Methanolic *M. oleifera* leaf extract obtained was brown-blackish, semi solid mass with 7.32 % yield. The chloroform extract was dark green in colour with extractability 2.32%. Nikkon *et al* (2003) reported extraction percentage of *M. oleifera* root barks to be 3.33 % using ethanol as extraction media.

Methanolic leaf extract of *Murraya koenigii* was brown-black solid mass with 0.81 % extractability. The chloroform extract was also similar in colour and consistency with extractability was 1.70%. Vats *et al* (2011) reported extraction percentage of *M. koenigii* roots as 4.03, 1.31, 0.59 and 9.4% for petroleum ether, chloroform, ethyl acetate and ethanol extracts, respectively. Kavitha (2017) reported that organic extracts obtained were viscous in nature and brownish in colour, but yield percentage recorded was 7.0, 6.5 and 9.2 % (v/w) for hexane, chloroform and ethanol, respectively.

Evaluation of antibacterial property

Results of agar well diffusion test and estimation of Minimum Bactericidal Concentration

Table 1. Colour, consistency and extractability percentage of different plant extracts used with methanol and chloroform as solvents.

S. No.	Plant	Solvent used	Colour	Consistency	Extractability %
1.	*Ocimum sanctm*	Methanol	Blackish	Semi-solid (Paste like)	5.58
		Chloroform	Brown-black	Powder (Flakes)	2.80
2.	*Moringa oleifera*	Methanol	Brown-black	Semi-solid	7.32
		Chloroform	Dark green	Semi-solid	2.32
3.	*Murraya koenigii*	Methanol	Brown-black	Semi-solid	0.81
		Chloroform	Brown-black	Semi-solid	1.70

Table 2. Zone of inhibition and MBC of different plant extracts against *C. pseudotuberculosis*.

S.No	Plant	Solvent used	Zone of inhibition(mm)*	MBC (mg/ml)
1	*Ocimum sanctum*	Methanol	12.667 ± 0.667^{a}	6.25
		Chloroform	14.000 ± 1.000^{ab}	3.125
2	*Moringa oleifera*	Methanol	14.667 ± 0.667^{abc}	12.5
		Chloroform	16.00 ± 1.555^{bc}	6.25
3	*Murraya koenigii*	Methanol	14.667 ± 0.667^{abc}	12.5
		Chloroform	17.000 ± 0.577^{c}	3.125

*Data are presented as mean ±S.E. as measurement of inhibition zone (mm). Means and standard errors determined from 3 biological replications. The values with different superscript differ significantly ($P< 0.05$) within a column.

(MBC) are given in table 2. In the wake of emerging problem of multidrug resistant bacteria there is a continuing need for new preparations particularly low cost natural products as they are readily accepted by patients (Martin and Ernst, 2013). Nevertheless, antibacterial properties of a plant extract in *in vitro* tests is reported to vary with several factors like type and strain of bacteria, inoculum size, type of media, type of solvent and extraction procedure, part of the plant used and time of collection and total amount of herbal extract used (Mandal *et al,* 2012).

Osmium sanctum

The zone of inhibition for methanolic and chloroform extracts of *O. sanctum* varied from 12 to 15 mm in diameter. In corroboration of the present findings, Aqil *et al* (2005) reported that inhibition zone for ethanolic extract of *O. sanctum* leaves against methicillin resistant *Staph. aureus* (MRSA) varied from 11 to 18 mm in diameter when 100 µl of plant extract with concentration 100 mg/ml was used. An inhibition zone of 10 mm diameter was reported when aqueous or ethanolic extracts of *O. sanctum* were used in concentration 10 mg/ml against *Aeromonas hydrophila* (Harikrishan and Balasundaram, 2008). Agarwal *et al* (2010) reported that inhibition zone of ethanolic extract (at concentration 10 mg/ml) of *O. sanctum* varies from 12 to 19 mm in diameter against *Strepto. mutans*. Jahan *et al* (2011) also recorded zone of inhibition of ethanolic extract of *O. sanctum* against *Staph. aureus* to vary between 10.66 to 15.66 mm.

MBC for methanolic and chloroform extract of *O. sanctum* were found to be 6.25 and 3.125 mg/ml, respectively. MIC of ethanolic extract against different strains of MRSA turned to vary from 1.3 to 8.2 mg/ml (Aqil *et al,* 2005). Likewise, initial MIC of ethanolic extract of *O. sanctum* leaves ranged from 2.4- 9.4 mg/ml and 4.7- 18.8 mg/ml for resistant and sensitive *Staph. aureus* strains, respectively (Jahan *et al,* 2011). Goyal and Kaushik (2011) reported that MIC of ethanolic and methanolic extracts of *O. sanctum* leaves varied from 1024 to > 4096 µg/ml. In the present study, chloroform extract of *O. sanctum* had more potent antibacterial activity than methanolic extract. In concurrence with this observation, Shokeen *et al* (2005) also recorded that chloroform extract of leaves of *O. sanctum* have highest percentage of inhibition of *Neisseria gonorrhoeae* among hexane, benzene, chloroform, ethyl acetate, acetone and 70% ethanol extracts. However, perusal of available reports suggests large variation in MIC and MBC values of *O. sanctum* leaf extracts against different bacteria. MIC as low as 0.25 mg/ml was reported by Adiguzel *et al* (2005) and 0.02 mg/ml by Akinvemi *et al* (2005). On the other hand, Shafi *et al* (2018) reported MIC to vary from 62.5 to 125 mg/ml for hydro-alcoholic extract of *O. sanctum* leaves against common mastitis pathogens like *Staph. aureus*, *Strepto.* spp, *E. coli*, *Coryne.* spp, *Pseudomonas* spp and *Klebsiella* spp. They further reported that MIC for *Coryne.* spp was 62.5 mg/ml.

O. sanctum, a plant from family Labiatae, known as *Tulsi* in hindi, have several pharmacological activities, like hypoglycemic, antipyretic, analgesic, anti-inflammatory, antistress, immune-modulatory, radio-protective, anti-tumour and anti-bacterial (Bhargava and Singh, 1981; Godhwani *et al,* 1987).

Moringa oleifera

Mean diameter of inhibition zone for methanolic and chloroform extract of *M. oleifera* recorded was 14.68 and 16.00 mm, respectively. Rahman *et al* (2009) studied antibacterial activity *M. oleifera* leaves against 4 gram negative and 6 gram positive bacteria and found that zone of inhibition for fresh leaf juice varied between 15.23 to 25.2 mm, for powder from fresh leaf juice was 29.25 to 42.3 mm and ethanol extract of fresh leaves was 16.25 to 21.5 mm. Peixoto *et al* (2011) also reported that mean diameter of zone of inhibition for aqueous and ethanolic extract of *M. oleifera* leaves varied from 14.4 to 30.0 mm depending upon the type and concentration of extract used and genus of the test bacteria. Among ethanol, chloroform and hexane extracts of *M. oleifera* leaves, methanolic extract was found most effective against *E. Coli*, *S. dysenteriae*, *Salmonella* spp., *Enterobacter* spp., *K. pneumonia*e and *S. marcescens* (Rahman *et al,* 2010). Large variation in MIC has been reported (from 0.041 to 50 mg/ml) for crude seed extracts (ethanolic or chloroform extracts) against gram negative organisms (Chandrasekhar *et al,* 2020).

MBC of methanolic and chloroform extract of *M. oleifera* was found to be 12.5 and 6.25 mg/ml, respectively. Likewise, Fouad *et al* (2019) reported that MIC values of cold water extract and ethanolic extract of *M. oleifera* leaves were 25 mg/ml and 390 µg/ ml, respectively against CPs isolated from pus in camel. However, lower MIC values were reported in several other studies. For example, the MIC values of methanolic, ethyl acetate and hexane extracts of *M. oleifera* leaves against some Gram negative bacteria were reported to vary from 62.5 to 1000 µg/mL (Rahman *et al,* 2010). Recently, Garcia-

Beltran *et al* (2020) reported significant antibacterial activity of ethanolic and aqueous extracts against pathogenic *Vibrio anguillarum* and *Photobacterium damselae* strains at a concentration ranging from 0.25 to 1.00 mg/ml. They further opined that antibacterial activity of *M. oleifera* extracts could be attributed to certain active components that might act in a synergistic way to inhibit the bacterial growth and viability. Deoxy-niazimicine extracted from *M. oleifera* leaves is reported to be effective against several pathogenic bacteria (Nikkon *et al,* 2003). Flavonoids and glucomoringin present in *M. oleifera* also attribute antibacterial potential against certain bacteria (Onsare and Arora, 2015; Galuppo *et al,* 2013). Low levels of the isothiocyanate derivative compounds are some additional constituents that inhibit some Gram-negative and Gram-positive bacteria.

Moringa or *Drumstick tree* (*Moringa oleifera*) is widely cultivated in tropical to subtropical regions across the world (García-Beltran *et al,* 2020). The dry leaves of the plant contain high concentration of macro and micronutrients, tannins, sterols, saponins, trepenoids, phenolics, alkaloids and flavanoids (Gopalkrishnan *et al,* 2016). Antibacterial activity of *M. oleifera* leaf extract could be attributed to phenolic compounds, flavonoids, saponin, tannin and cyanogenic glycosides (Rauha *et al,* 2000; Doughari *et al,* 2007; Verma *et al,* 2009; Garcia-Beltran *et al,* 2020). However, marked variation in phytochemical composition and thereby antioxidant and antimicrobial activities of 13 different cultivars of *Moringa oleifera* obtained from different locations across the globe has been reported (Ndhlala *et al,* 2014) that may result into variation in antibacterial potential of different extracts.

Murraya koenigii

Zone of inhibition for methanolic and chloroform extracts of *M. koenigii* leaves varied from 14 to 21 mm in diameter. Likewise, in a study zone of activity (inhibition zone) ranged from 6 to 20 mm in diameter depending upon the organic solvent used and species of bacteria (Naz *et al,* 2015). In this study methanolic leaf extract showed most promising antibacterial agent among n-hexane, acetone and methanolic extract. Nagappan *et al* (2011) also reported that the diameter of inhibition zone for carbazole alkaloids and essential oil of *Murraya koenigii* varies from 8.0 mm to 18.0 mm and highest susceptibility with inhibition zone of 18.5 ± 0.5 mm, 18.5 ± 0.5 mm and 18.0 ± 0.5 mm was recorded against *S. aureus*, *P. aeruginosa* and *S. pneumoniae*, respectively.

The MBC of *M. koenigii* leaf extracts was recorded as 3.125 and 12.5 mg/ml for chloroform and methanolic extracts, respectively. Present study indicated that chloroform extract of *M. koenigii* leaves has higher antimicrobial activity than methanolic extract. MIC of chloroform extract of *M. koenigii* leaves was 125µg/ ml against *Kleb. pneumoniae*, while methanolic extract had no antimicrobial activity against tested bacteria and fungi (Panghal *et al,* 2011). On the contrary, Kavitha (2017) reported that ethyl alcohol extract displayed highest antibacterial activity when compared to hexane and chloroform extracts of *M. koenigii* leaves. They recorded MIC and MBC of ethyl alcohol extract of *M. koenigii* leaves against different bacteria which varied from 12.05 to 25 mg/ml and 25 to 50 mg/ml, respectively. Likewise, Rath and Padhy (2014) observed that MIC and MBC of methanolic extract of *M. koenigii* leaves against different multidrug resistant gram positive and gram negative bacteria causing urinary tract infections in humans varied from 1.41 to 21.67 mg/ml.

Murraya koenigii (Linn) *Spreng.,* commonly known as "*Curry patta*" in Hindi, is a member of the family Rutaceae. The antimicrobial activity of *M. koenigii* leaves is largely attributed to several carbazole alkaloids present in it (Naz *et al,* 2015; Nalli *et al,* 2016). Seven pyranocarbazoles with antibacterial activities were extracted from methanolic extract of *Murraya koenigii* (L.) through bioassay guided fractionation (Joshi *et al,* 2017).

In the present study, highest antibacterial activity is recorded in chloroform extract of *Ocimum sanctum* and *Murraya koenigii* and lowest in methanolic extract of *Moringa oleifera* and *Murraya koenigii* leaves. Variations in the phytochemical levels of the different cultivars may be an important factor behind variation recorded in antibacterial activity. The antibacterial compounds from these plants may be used as a constituent of topical antiseptic preparations.

References

Abdel-Wahab MB and Shigidi MTA. Susceptibility of *Corynebacterium pseudotuberculosis* isolated from sheep and goats with caseous lymphadenitis to some antimicrobial agents. Sudan Journal of Veterinary Research. 2013; 28:10-12.

Abuga I, Sulaiman SF, Wahab RA, Ooi KL and Rasad MSBA. Phytochemical constituents and antibacterial activities of 45 Malay traditional medicinal plants. Journal of Herbal Medicine. 2021; https://doi.org/10.1016/j.hermed.2021.100496.

Adiguzel A, Gulluce M, Sengul M, Ogutcu H, Sahin F and Karaman I. Antimicrobial effects of *Ocimum basilicum* (Labiatae). Turkish Journal of Biology. (2005); 29:155-160.

Agarwal P, Nagesh L and Murlikrishnan. Evaluation of the antimicrobial activity of various concentrations of *Tulsi* (*Ocimum sanctum*) against *Streptococcus mutans*: An *in vitro* study. Indian Journal of Dental Research. 2010; 21:327-3593.

Akinvemi KO, Oladopo O, Okwara CE and Fasure CKA. Screening of crude extracts of 6 medicinal plants used in South-West Nigerian unorthodox medicine for anti-methicillin resistant *Staphylococcus aureus* activity. BMC Complementary Medicine and Therapies. 2005; 5:6-13.

Algammal AM. Molecular characterisation and antibiotic susceptibility of *Corynebacterium pseudotuberculosis* isolated from sheep and goats suffering from caseous lymphadenitis. Zagazig Veterinary Journal. 2016; 44:1-8.

Almeida S, Dorneles EMS, Diniz C, Abreu V, Sousa C, Alves J, Carneiro A, Bagano P, Spier S, Barh D, Lage, AP, Figueiredo H and Azevedo V. Quadruplex PCR assay for identification of *Corynebacterium pseudotuberculosis* differentiating biovar *Ovis* and *Equi*. BMC Veterinary Research. 2017; 13:290.

Aqil F, Khan MSA, Owais M and Ahmad I. Effect of certain bioactive plant extracts on clinical isolates of β-lactamase producing methicillin resistant *Staphylococcus aureus*. Journal of Basic Microbiology. 2005; 45:106-114.

Bhargava KP and Singh N. Anti-stress activity of *Ocimum sanctum* Linn. Indian Journal of Medical Research. 1981; 73:443-451.

Chandrasekhar S, Vijaykumar R, Chelliah R and Oh DH. Identification and purification of potential bioactive peptide of *Moringa oleifera* seed extracts. Plants. 2020; 9:1445.

Dorella FA, Pacheco LG, Oliveira SC, Miyoshi A and Azevedo A. *Corynebacterium pseudotuberculosis*: microbiology, biochemical properties, pathogenesis and molecular studies of virulence. Veterinary Research. 2006;37: 201-218.

Doughari JH, Pukuma MS and De N. Antibacterial effects of *Balanites aegyptiaca* L. Drel and *Moringa oleifera* Lam on Salmonella typhi. African Journal of Biotechnology. 2007; 62:2212-2215.

Fouad EA, Elnaga ASMA and Kandil MM. Antibacterial efficacy of *Moringa oleifera* leaf extract against pyogenic bacteria isolated from a dromedary camel (*Camelus dromedarius*) abscess. Veterinary World. 2019; 12:802-808.

Galuppo M, Nicola GRD, Iori R, Dell'Utri P, Bramanti P and Mazzon E. Antibacterial activity of glucomoringin bioactivated with myrosinase against two important pathogens affecting the health of long-term patients in hospitals. Molecules. 2013; 18:14340-14348.

Garcia-Beltran JM, Mansour AT, Alsaqufi AS, Ali HM and Esteban MA. Effects of aqueous and ethanolic leaf extracts from drumstick tree (*Moringa oleifera*) on gilthead seabream (*Sparus aurata* L.) leukocytes, and their cytotoxic, antitumor, bactericidal and antioxidant activities. Fish and Shellfish Immunology. 2020; 106: 44-55.

Godhwani S, Godhwani JL and Vyas DS. *Ocimum sanctum*: an experimental study evaluating its anti-inflammatory, analgesic and antipyretic activity in animals. Journal of Ethnopharmacology. 1987; 21:153-163.

Gopalkrishnan L, Doriya K and Kumar DS. *Moringa oleifera*: a review on nutritive importance and its medicinal application. Food Science and Human Wellness. 2016; 5:49-56.

Goyal P and Kaushik P. *In vitro* evaluation of antibacterial activity of various crude leaf extracts of Indian scared plant, *Ocimum sanctum* L. British Microbiology Research Journal. 2011; 1:70-78.

Harikrishan R and Balasundaram C. *In vitro* and In vivo studies of the use of some medicinal herbs against the pathogen *Aeromonas hydrophila* in Goldfish. Journal of Aquatic Animal Health. 2008; 20:165-176.

Irfan Uma and Ali Sarah. The antibacterial effect of curry leaves (Murraya Koenigii). European Journal of Pharmaceutical and Medical Research. 2016; 3. 382-387.

Jahan F, Lawrence R, Kumar V and Junaid M. Evaluation of antimicrobial activity of plant extracts on antibiotic susceptible and resistant *Staphylococcus aureus* strains. Journal of Chemical and Pharmaceutical Research. 2011; 3:777-789.

Joshi T, Jain T, Mahar R, Singh SK, Srivastava P, Shukla SK, Mishra DK, Bhatta RS, Banerjee D and Kanojiya S. Pyranocarbazoles from *Murraya koenigii* (L.) Spreng as antimicrobial agents. Natural Product Research. 2017; 10.1080/14786419. 2017.1308363.

Judson R and Songer JG. *Corynaebacterium pseudotuberculosis: in vitro* susceptibility to 39 antimicrobial agents. Veterinary Microbiology. 1991; 27:145-150.

Kavitha M. Antibacterial and antioxidant activity of leaf organic extracts of local cultivars of *Murraya koenigii* (L.) *spreng* from Tamilnadu. Bioscience Biotechnology Research Communications. 2017; 10:359-364.

Mallikarjun S, Rao A, Rajesh G, Shenoy R and Pai M. Antimicrobial efficacy of Tulsi leaf (Ocimum sanctum) extract on periodontal pathogens: An in vitro study. J Indian Soc Periodontol. 2016; 20(2):145-150. doi:10.4103/0972-124X.175177

Mandal S, Mandal MD and Pal NK. Enhancing chloramphenicol and trimethoprim *in vitro* activity by *Ocimum sanctum* Linn (Lamiaceae) leaf extract against *Salmonella enterica* serovar *Typhi*. Asian Pacific Journal of Tropical Medicine. 2012; 5:220-224.

Martin KW and Ernst E. Herbal medicines for treatment of bacterial infections: a review of controlled clinical trials. Journal of Antimicrobial Chemotherapy. 2013; 51:241-246.

Masese Osoro Brian , Hemachitra P., Deepa R. and V. Senthamarai Selvi. Synthesis of silver nanoparticles and its antibacterial activity from Moringa oleifera, Murraya koingii and Ocimum sanctum against *E. coli* and *S. aureus*. Der Pharmacia Lettre. 2016; 8(10):150-160.

Mazhangara IR, Masika PJ, Mupangwa JF, Chivandi E, Jaja IF and Muchenje V. *In vitro* efficacy of *Elephantorrhiza*

elephantina root extracts against adult *Paramphistomum cervi* in goats. Parasite Epidemiology and Control. 2020; 10 e00157, https://doi. org/10.1016/j.parepi.2020. e00157

Moodley Jerushka S, Naidu Krishna Suresh Babu, Pillay Karen, Sershen and Govender Patrick. Green synthesis of silver nanoparticles from Moringa oleifera leaf extracts and its antimicrobial potential. Advances in Natural Sciences: Nanoscience and Nanotechnology. 2018; 9(1):015011

Nabi J. Evaluation of antibacterial activity of selected plant extracts against *Corynebacterium pseudotuberculosis* isolated from *Camelus dromedarius*. Unpublished Masters Thesis (M.V.Sc.), Rajasthan University of Veterinary and Animal Sciences, Bikaner, Rajasthan, India. 2021.

Nagappan T, Ramasamy P, Effendy M, Wahid A, Segaran TC and Vairappan CS. Biological activity of carbazole alkaloids and essential oil of *Murraya koenigii* against antibiotic resistant microbes and cancer cell lines. Molecules. 2011; 16: 9651-9664.

Nalli Y, Khajuria V, Gupta S, Arora P, Ul-Hassan SR, Ahmed Z and Ali A. Four new carbazole alkaloids from *Murraya koenigii* that display anti-inflammatory and anti-microbial activities. Organic and Biomolecular Chemistry. 2016; 10.1039/c6ob00267f.

Naz S, Saied S, Ahmed A and Shahid SM. Three new carbazole alkaloids and biological activities of *Murraya koenigii*. Journal of Asian Natural Products Research. 2015; 17: 7-13.

Ndhlala AR, Mulaudzi R, Ncube B, Abdelgadir HA, Plooy CPD and Staden JV. Antioxidant, antimicrobial and phytochemical variations in 13 *Moringa oleifera* Lam. cultivars. Molecules. 2014; 19:10480-10949.

Nikkon F, Saud ZA, Rahman MH and Haque MK. *In vitro* antimicrobial activity of the compound isolated from chloroform extract of *Moringa oleifera* Lam. Pakistan Journal of Biological Sciences. 2003; 6:1888-1890.

Norman TE, Batisa M, Lawhon SD, Zhang S, Kuskie KR, Swinford AK, Bernstein LR and Cohen ND. *In vitro* susceptibility of Equine-obtained isolates of *Corynebacterium pseudotuberculosis* to gallium maltolate and 20 other antimicrobial agents. 2014; Journal of Clinical Microbiology 52:2684-2685.

Olson ME, Ceri H, Morck DW, Buret AG and Read RR. Biofilm bacteria: formation and comparative susceptibility to antibiotics. Canadian Journal of Veterinary Research. 2002; 66:86-92.

Onsare J and Arora D. Antibiofilm potential of flavonoids extracted from *Moringa oleifera* seed coat against *Staphylococcus aureus*, *Pseudomonas aeruginosa* and *Candida albicans*. Journal of Applied Microbiology. 2015; 118:313-325.

Panghal M, Kaushal V and Yadav JP. *In vitro* antimicrobial activity of ten medicinal plants against clinical isolates of oral cancer cases. Annals of Clinical Microbiology and Antimicrobials. 2011; 10:21.

Peixoto JRO, Silva GC, Costa RA, Fontenelle JLDS, Vieira GHF and Vieira HSDF. *In vitro* antibacterial effect of aqueous and ethanolic Moringa leaf extracts. Asian Pacific Journal of Tropical Medicine. 2011; 3:201-204.

Rahman MM, Rahman MM, Akhter S, Jamal MAHM, Pandeya DR, Haque MA, Alam MF and Rahman A. Control of coliform bacteria detected from diarrhoea associated patients by extracts of *Moringa oleifera*. Nepal Medical College Journal. 2010; 12:12-19.

Rahman MM, Sheikh MMI, Sharmin SA, Islam MS, Rahman MA, Rahman MM and Alam MF. Antibacterial activity of leaf juice and extracts of *Moringa oleifera* Lam against some human pathogenic bacteria. Chiang Mai University Journal of Natural Sciences. 2009; 8:219-227.

Ranjan R, Vyas S, Kashinath, Sonawane GG and Patil NV. Lymphadenitis caused by *Corynebacterium pseudotuberculosis* in a dromedary (*Camelus dromedarius*) herd. Journal of Camel Practice and Research. 2018; 25:45-48.

Rath S and Padhy RN. Monitoring *in vitro* antibacterial efficacy of 26 Indian species against multidrug resistant urinary tract infecting bacteria. Integrative Medicine Research. 2014; 3:133-141.

Rauha JP, Remes S, Heinonen M, Hopia A, Kähkönen M, Kujala T and Vuorela P. Antimicrobial effects of Finnish plant extracts containing flavonoids and other phenolic compounds. International Journal of Food Microbiology. 2000; 56:3-12.

Shafi TA, Bansal BK and Gupta DK. *In vitro* antibacterial activity and minimum inhibitory concentration of *Ocimum sanctum* leaves against common bovine pathogens. Journal of Dairy, Veterinary and Animal Research. 2018; 7:322-324.

Shokeen P, Ray K, Bala M and Tandon V. Preliminary studies on activity of *Ocimum sanctum*, *Drynaria quercifolia* and *Annona squamosa* against *Neisseria gonorrhoeae*. Journal of Phytomedicine. 2005; 32:106-111.

Tejedor-Junco MT, Martin JL, Corbera JA, Shulz U and Gutierrez C. Pseudotuberculosis in dromedary camels in the Canary Islands. Tropical Animal Health and Production. 2004; 36:459-562.

Vats M, Singh H and Sardana S. Phytochemical screening and antimicrobial activity of roots of *Murraya koenigii* (Linn.) spreng (Rutaceae). Brazilian Journal of Microbiology. 2011; 42:1569-1573.

Verma AR, Vijayakumar M, Mathela, CS and Rao CV. *In vitro* and in vivo antioxidant properties of different fractions of *Moringa oleifera* leaves. Food and Chemical Toxicology. 2009; 47:2196-2201.

Wayne PA. Performance standards for antimicrobial susceptibility testing; 18th informational supplement, CLSI document M100-18. Clinical and Laboratory Standards Institute, USA. 2008.

Wernery U and Kinne J. Caseous lymphadenitis (Pseudotuberculosis) in camelids: A review. Austin Journal of Veterinary Science and Animal Husbandry. 2016; 3:1022.

Zidan KH, Mazloum K, Saran MA and Haltem ME (2013). Abscesses in dromedary camels, sheep and goats: etiology and pathology. Proceedings of the 1st International Scientific Conference of Pathology

Department, Faculty of Veterinary Medicine, Cairo University, Egypt; pp 47-69.
Zubair M. Antimicrobial and Anti-Biofilm Activities of *Citrus sinensis* and *Moringa oleifera* Against the Pathogenic *Pseudomonas aeruginosa* and *Staphylococcus aureus*. Cureus. 2020 Dec 28;12(12):e12337. doi: 10.7759/cureus.12337. PMID: 33520533; PMCID: PMC7839279.

News

ICAR SATELLITE MEETING ON CAMELID REPRODUCTION

The Satellite Meeting took place from 1 (Friday) to 3 (Sunday) July 2022 following the ICAR 2020 conference at the University of Bologna, Italy. The official language of the meeting was English and no translation was provided. The scientific program includes original and review presentations on all aspects of reproduction, genetics, production and welfare in New and Old World Camelids. The major topics covered were male and female reproductive physiology and endocrinology, gynecology, theriogenology and reproductive efficiency; andrology and artificial insemination; superovulation and embryo transfer; cryo-preservation of gametes and other assisted reproductive methods; gestation, parturition and neonatology; mammary gland and milk production; camelid breeding and genetics; interaction between genotype and phenotype and camel behaviour and welfare. The papers were presented in 8 sessions, i.e. embryology, female reproduction, male reproduction (two sessions), nutrition, milking, welfare, cell culture and genetics. A field trip to Ferrara and visit of Azienda Caretti dairy and Parmigiano cheese factory also took place.

INTERNATIONAL CONFERENCE ON THE SAFETY OF CAMELS

The First International Conference on the Safety of Camels will be organised jointly by Camel Club and International Camel Organisation on 27th July 2022 at Riyadh. The opening session will be on the concept of tampering in camels followed by first session on the effect of plastic surgery on camels and session two on the effect of drugs and hormones on behaviors and appearance. The invited speakers are from USA, Saudi Arabia, Egypt, Sudan and Bahrain.

CAMEL DAIRY MARKET 2022-2027

The global camel dairy market size reached a value of US$ 6.9 Billion in 2021. Looking forward, IMARC Group expects the market to reach US$ 8.6 Billion by 2027, exhibiting a CAGR of 3.1% during 2022-2027. On a regional level, the market has been classified into Middle East, Africa, Asia, Oceania, and Rest of the world, where Africa currently dominates the global market. Some of the major players in the global camel dairy market include Camelicious, Al Ain Dairy, Desert Farms, Vital Camel Milk, Tiviski Dairy, Camilk Dairy, Camel Dairy Farm Smits, Camel Milk Co Australia and Camel Milk South Africa.

DOI : 10.5958/2277-8934.2022.00019.4 Vol 29 No 2, p 141-146

ANTIGENIC COMPONENTS OF *Echinococcus granulosus* HYDATID CYST FLUID FROM DROMEDARY CAMELS (*Camelus dromedarius*)

E.M. El Hassan[1] and Sabry M. El-Bahr[2,3]
Department of Microbiology[1], Biomedical Sciences[2] College of Veterinary Medicine,
King Faisal University, Al-Ahsa, 31982, P.O. Box: 400, Saudi Arabia
Department of Biochemistry[3], Faculty of Veterinary Medicine, Alexandria University, Alexandria, Egypt

ABSTRACT

This study is designed to investigate the components of hydatid cyst fluid (HCF), the larval stage of *Echinococcus granulosus*, that acted as antigens during infection in dromedary camels and to identify the antigenic fractions specific to this metacestode. Hydatid cysts were obtained from an infected slaughtered camel in Al-Ahsa central abattoir, Kingdom of Saudi Arabia. Crude antigen extract was prepared from hydatid cyst fluid (HCF). SDS-PAGE fractionation of HCF on 7-20% acrylamide gel revealed 11 protein fractions when stained by Commassie blue stain. The molecular weight of these fractions ranged from ~180 to 22KDa. Western immunoblotting against serum from the camel infected with hydatid cyst identified 4 antigenic components of molecular weight of ~180, 55, 48 and 22KDa. Reaction with sera collected from camels with parasitic infections other than *E. granulosus* and from healthy camels free from parasitic infections failed to identify any antigenic component of HCF apart from one component of 58kDa with serum from camels suffering from mixed infection of *Nematodirus* and strongyle worms. The rest of antigenic components identified by HCF infection serum seems to be specific to this larval stage.

Key words: Dromedary camels, electrophoresis, *Echinococcus granulosus,* hydatidosis, immunoblots

Hydatidosis is a disease caused by infection of intermediate hosts with the larval stage (hydatid cyst) of the dog tapeworm *Echinococcus granulosus*. The disease is present in many African and Middle East countries (Kamhawi, 1995; Shambesh *et al,* 1997; Battelli *et al,* 2002; Sadjjadi, 2006). It is endemic in the Kingdom of Saudi Arabia affecting both humans and their domestic animals (Abu-Eshy, 1998; Al Mofleh *et al,* 2000; Adewunmi and Basilingappa, 2004; Fahim and Al Salamah, 2007; Ibrahim, 2010; Rashed *et al,* 2004). Diagnosis of the disease, particularly human cases were improved lately by the use of imaging techniques including ultrasonography, computed tomography (CT scanning) and magnetic resonance imaging (MRI) and immunological assays (WHO, 2003; Zhang *et al,* 2003). Immunological assays depends on hydatid cyst fluid (HCF) antigens as a source of antigenic material (Burgu *et al,* 2000; Kanwar *et al,* 1994; Musiani *et al,* 1978; Oriol *et al,* 1971; Piantelli *et al,* 1977; Pozzuoli *et al,* 1974). These immunoassays are used to detect antibodies to HCF antigens but they lack sensitivity and specificity (Babba *et al,* 1994). In addition, they do not discriminate between current and previous infection. Nevertheless, western blotting has been used extensively for the study of parasite systems. Enzyme-linked immunoelectrotransfer blot (EITB) was reported to be the most sensitive serological assay for confirmation of hydatidosis (Verastegui *et al,* 1992). It also showed high specificity due to the high resolution of HCF antigenic components (Kharebov *et al,* 1997).

The detection of circulating parasite antigens in host's blood, would be an ideal approach for diagnosis of the disease and is more superior than antibody detection assay as it can provide specific parasitic diagnosis (Chaya and Parija, 2013). It is also considered a useful approach for assessment of treatment efficacy and has a high degree of specificity compared to antibody detection assays (Sadjjadi *et al,* 2009). Soluble antigens of other parasites circulating in body fluids have been detected using antigen-detection immunoassays (Janardhan *et al* 2011; Cai *et al* 2014) serving as a confirmatory guide for current infection.

In the present study, the HCF components that acted as antigens during the course of infection

SEND REPRINT REQUEST TO SABRY M. EL-BAHR email: selbahar@kfu.edu.sa; sabryelbahr@hotmail.com

were investigated. The antigenic fractions specific to HCF that will react potently, in western blotting, with serum from naturally infected camels and could identify possible candidates for diagnosis of infection.

Materials and Methods

Parasitological methods

One hundred faecal samples were obtained from slaughtered camels in Al-Ahsa central abattoir and these were examined for parasitic infections other than *E. granulosus* hydatid cyst using faecal flotation technique (Dryden *et al,* 2005) utilising magnesium sulfate as a flotation solution as well as sedimentation method.

Crude hydatid cyst fluid (HCF) extract

Hydatid cysts fluid was obtained from an infected camel slaughtered in Al-Ahsa central abattoir, Kingdom of Saudi Arabia. Crude antigen extract was prepared from hydatid cyst fluid (HCF) according to Al-Olayan and Helmy (2012). The HCF was aspirated aseptically and 25x protease inhibitor cocktail in 100 mM phosphate buffer, pH 7.0 immediately added. HCF was then centrifuged at 3000g for 30 min at 4°C and the supernatant was collected and dialysed, using cellulose membrane with molecular weight cut-off of 3.5kDa, against 3 changes of deionised water per 24 h. The dialysate then centrifuged again at 3000g for 30 min at 4°C and the supernatant was collected. Protein contents were estimated and antigen extracts were aliquoted and stored at -70°C until needed.

Serum samples

Serum samples were collected from eight camels infected with hydatid cyst at the slaughterhouse. These had mixed infection of *Nematodirus*/strongyle, while one camel had *Trichuris* infection and 2 camels had *Eimeria* spp. infection. Serum from a healthy camel calf free from parasitic infections was also collected. Samples from camels with the mixed infections and those with *Eimeria* spp. infection were pooled together. Serum samples were aliquoted and stored at -20°C until needed.

SDS-PAGE fractionation of hydatid cyst fluid (HCF)

The HCF crude extract was subjected to SDS-PAGE gradient gel electrophoresis (Laemmli, 1970) on 7 – 20% gradient gel. Coomassie Blue stain was used for visualisation of the gel protein banding pattern. A calibration curve based on the molecular weight markers was constructed and used to calibrate the molecular weight of individual HCF proteins. For permanent records, the gel was rinsed in distilled water and photographed.

Electrophoretic transfer of HCF proteins on NC membrane

An unstained gel containing HCF proteins separated by SDS-PAGE was soaked in transfer buffer (Electrode buffer, methanol and D.W) and laid on two pieces of filter paper (6µm pore size, Whatman) pre-soaked in transfer buffer and laid on top of the anode plate of a Sartoblot II-S semi-dry electroblotter (Sartorius Ltd., Germany). A nitrocellulose membrane (0.45µm pore size, Sartorius Ltd., Germany) previously cut to the size of the gel and soaked in transfer buffer then laid on top of the gel and again covered by two soaked filter papers at the cathode side. Electrophoretic transfer to nitrocellulose membrane was conducted for 90 minutes at room temperature with a constant current of 0.8 mA per cm^2 of gel.

Detection of antigenic components of HCF

Following the transfer of HCF proteins onto nitrocellulose membrane, the membrane was transferred into a sandwich box and the excess protein binding sites were blocked in 5% dried milk in blocking buffer, pH 7.4 overnight with gentle shaking. The blocked membrane then was rinsed with PBS. The reactivity of the separated proteins was examined by incubation of strips of the membrane overnight at room temperature with 1/50 dilution in blocking buffer of serum collected. The negative control serum from the healthy camel calf was also included in the run. The unbound antibodies were then removed by washing the membranes with seven changes of PBS over a period of 2 hours, before a peroxidase labelled goat anti-camel IgG (Alpha Diagnostic INTL, INC, USA) diluted to 1/2500 in blocking buffer was added and incubated for 2 hours. After washing, the membrane in PBS as above to remove excess conjugate, the labelled antigen/antibody complexes was visualised by incubation in 4-chlro-1-α-naphthol substrate solution, pH 7.5. Colour development was allowed to occur over 20 – 30 minutes, and the reaction then stopped by washing in distilled water and permanent records were made by photography.

Results

Parasitological finding

Faecal examination of slaughter camels revealed the presence of a mixed infection with *Nematodirus* and strongyle eggs in 8 camels (Fig 1a), *Trichuris* sp.

eggs in a single camel (Fig 1b) and *Eimeria* oocyst in 2 of the surveyed camels (Fig c).

Hydatid cyst fluid (HCF) protein profile

Crude HCF extract showed 11 individual protein bands with molecular weight ranging from 180 - 22k.Da in 7 – 20% gradient polyacrylamide gel stained with Coomassie blue stain (Fig 2, lane 2). Three of the detected components were in the high molecular weight part of the gel (180 – 130kDa). The 48, 42 and 22 components showed the highest staining intensity.

Antigenic components of hydatid cyst fluid (HCF)

Infection serum from the camel naturally infected with hydatid cyst reacted with 4 antigenic components of HCF with molecular weight of ~180, 55, 48 and 22kDa (Fig 3, lane 2). Serum from camels with mixed infection of *Nematodirus* and strongyle worms reacted with one antigenic component of HCF with molecular weight of ~58kDa (Fig 3, lane 3). Serum collected from healthy camels and camels infected with *Trichuris* and/or *Eimeria* spp. failed to recognise any of the HCF components (Fig 3, lanes 1, 4 and 5).

Discussion

Hydatidosis in farm animals is generally asymptomatic (Urquhart *et al,* 2006) and a definitive diagnosis can only be made by necropsy. The identification of antigenic components of this larval stage of *Echinococcus granulosus* is important for diagnosis of the disease in these intermediate hosts. In the present study, the components of the hydatid cyst fluid obtained from naturally infected dromedary camels have been characterised using SDS-PAGE on gradient 7-20% polyacrylamide gels. Coomassie blue staining of fractionated HCF components revealed the presence of 11 protein bands ranging from 180 to 22kDa. Similarly, Hassanain *et al* (2021) using 10% homogenous gel, detected 10 protein bands ranging from 200 to 14kDa in HCF from naturally infected camels. The slight difference in the number and molecular range of these components probably attributed to difference in gels used. Doganay *et al* (2013) using 15% homogenous gels stained with silver stain detected 11 and 10 protein bands ranging from 200 to about 6.5kDa in HCF originated from sheep and donkey, respectively; however, Kordafshari *et al* (2010) using 5% homogenous gels detected 9 bands in HCF from sheep.

In order to determine the components of the cyst fluid that acted as antigens during infection and to allocate those specific to this larval stage, sera from camels naturally infected with hydatid cyst, camels infected with *Nematodirus*/*strongyle*, *Trichuris* and *Eimeria* spp. and also negative control serum from healthy camels free from parasitic infections were analysed by western immuoblotting. Results showed that four of the cyst fluid components with molecular weight ranging from ~180 to ~22kDa are antigenic during infection as indicated by their reaction to infection serum and confirming the usefulness of this technique in diagnosis of infection in intermediate hosts. Two of these antigens, namely 48 and 22kDa reacted potently with this serum. Hassanain *et al* (2021) also detected 4 antigenic components with molecular weight ranging from 200 to 22kDa by sera from infected camels and 6 bands ranging from 200 to 14kDa using serum from confirmed human cases. Al-Olayan and Helmy (2012) using sera from confirmed that human cases were able to detect 11 bands in HCF originated from camels with molecular weight ranging from 110 to 16.8kDa. Sera from confirmed human cases when probed with hydatid cyst fluids from sheep and donkey identified 3 components with molecular weight ranging from 56 to 24kDa and only one component with molecular weight of 24kDa, respectively (Doganay *et al,* 2013).

Serum from dromedary camels having mixed infection with *Nematodirus*/strongyle worms in the present study was able to react with a single component with molecular weight of 58kDa of HCF indicating a possible shared epitope between the antigenic components of these parasites. This 58kDa antigen was not present in the Coomassie blue stained gel, yet was detected by western immunoblotting, possibly due to the fact that this technique is more sensitive than Coomassie blue. Coomassie blue has a detection limit of 1µg protein (Greenfield, 2014), while as little as 100pg of protein can be detected by immunoblotting (Towbin *et al,* 1979). Sera from animals with other parasitic infection such as *Haemonchus contortus, Spirocerca lupi* and *Oesophagostomum radiatum* have been reported to be detected antigenic components of HCF obtained from cattle (Kagiko, 1985). Similarly, sera from animals infected with other larval cestodes were able to react with HCF antigens (Kordafshari *et al,* 2010).

Negative control sera from dromedary camels infected with *Trichuris* or *Eimeria* sp. in the present study failed to react with any of the HCF antigenic components. This is probably due to lack of HCF components in these parasites. Antiserum raised against HCF antigens was unable to react with any

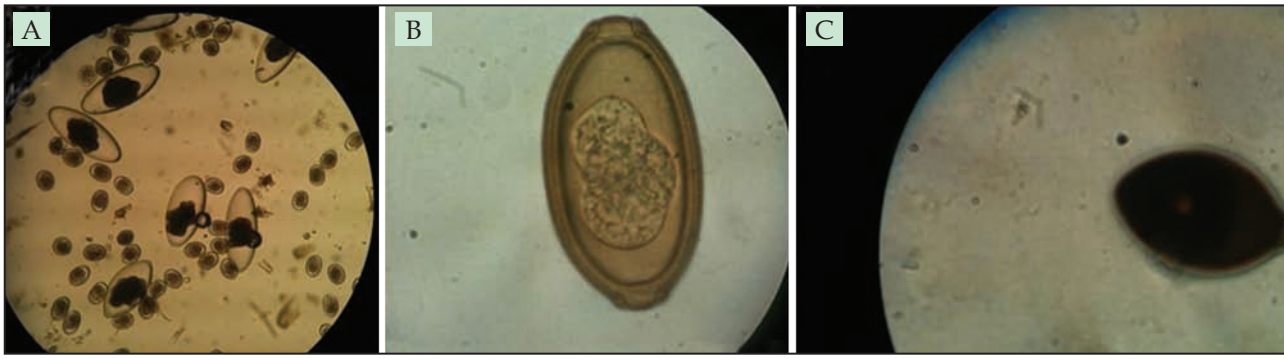

Fig 1. Parasitological findings. (a) Mixed *Nematodirus* and strongyle worms eggs (b) *Trichuris* spp., Egg (c) *Eimeria* spp. oocyst.

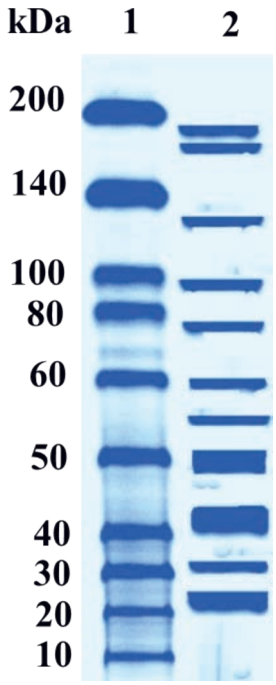

Fig 2. Protein profile of hydatid cyst fluid (HCF) on 7-20% polyacrylamide gel stained by Coomassie blue. **Lane 1**- Molecular weight markers. **Lane 2**- HCF extract.

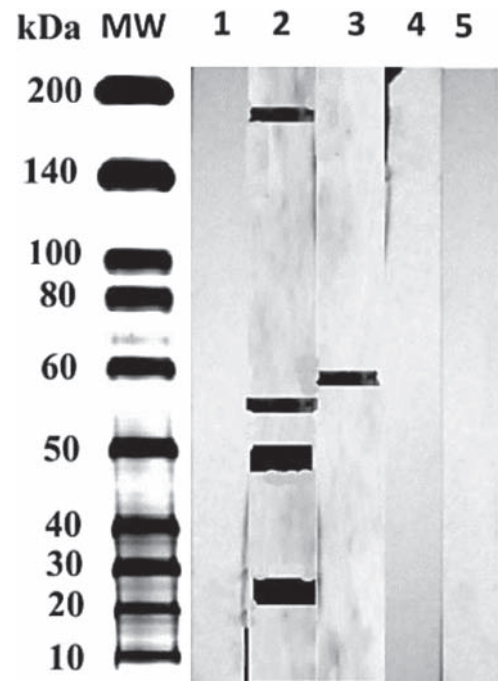

Fig 3. Hydatid cyst fluid (HCF) antigenic components identified by: **Lane 1**- Negative control serum. MM- Molecular weight markers. **Lane 2**- Infection serum from camels naturally infected with hydatid cyst. **Lane 3**- Serum from camels with mixed infection of *Nematodirus* and strongyle worms. **Lane 4**- Serum from camels infected with *Trichuris* spp. **Lane 5**- Serum from camels infected with *Eimeria* spp.

antigenic components of *Trichuris vulpis, Bonostomum phlebotomum* and *Ascaris suum* (Kagiko, 1985).

The 4 antigenic components detected by sera from dromedary camels naturally infected with hydatid cyst seems to be unique to this parasite at least under the condition used in the present study.

In conclusion, the present study confirms the usefulness of western immunoblotting in serodiagnosis of hydatidosis in intermediate hosts and identifies the antigenic components of this larval stage of *E. granulosus* in dromedary camels. The study also allocated antigenic components specific to this parasite under the circumstances used in the present experiment, of which the 48 and 22kDa fractions that reacted potently with this serum may represent possible candidates for specific diagnosis of this infection.

Acknowledgements

The authors would like to express a deep gratitude and thanks to the Deanship of Scientific Research, King Faisal University, Saudi Arabia for support and funding of this research (Project # 180040; GRANT231).

References

Abu-Eshy SA. Some rare presentations of hydatid cyst

(*Echinococcus granulosus*). Journal of Royal College of Surgery, Edinburgh. 1998; 43:347-352.

Adewunmi OA and Basilingappa HM. Primary ovarian hydatid disease in the Kingdom of Saudi Arabia. Saudi Medical Journal. 2004; 25:1697-1700.

Al Mofleh IA, Al Rashed RS, Ayoola EA, Al Faleh FZ, Al Amri SM, Al Rikabi AC, Al Sohaibani MO and Reyes AH. Hepatic granulomas in an arab population: a retrospective study from a teaching hospital in Riyadh. Saudi Journal of Gastroenterology. 2000; 6:41-46.

Al-Olayan EM and Helmy H. Diagnostic value of different antigenic fractions of hydatid cyst fluid from camel and sheep in Kingdom of Saudi Arabia. Journal of Saudi Chemical Society. 2012; 16:203-207.

Babba H, Messedi A, Masmoudi S, Zribi M, Grillot R, Ambriose-Thomas P, Beyrouti I and Sahnoun Y. Diagnosis of human hydatidosis: comparison between imagery and six serologic techniques. American Journal of Tropical Medicine and Hygiene. 1994; 50:64-68.

Battelli G, Mantovani A and Seimenis A. Cystic echinococcosis and the Mediterranean region: a long-lasting association. Parassitologia. 2002; 44:43-57.

Burgu A, Douanay A, Gonenc B, Sarimehmetoulu HO and Kalinbacak F. Analysis of fluids of hydatid cysts from sheep by SDS-PAGE, and determination of specific antigens in protein structure by Western blotting. Turkish Journal of Veterinary and Animal Science. 2000; 24:493-500.

Cai YC, Xu JF, Steinmann P, Chen SH, Chu YH, Tian LG, Chen MX, Li H, Lu Y, Zhang LL, Zhou Y and Chen JX. Field comparison of circulating antibody assays *versus* circulating antigen assays for the detection of *Schistosoma japonica* in endemic areas of China. Parasites and Vectors. 2014; 7:138-146.

Chaya DR and Parija SC. Evaluation of a newly designed sandwich enzyme linked immunosorbent assay for the detection of hydatid antigen in serum, urine and cyst fluid for diagnosis of cystic echinococcosis. Tropical Parasitology. 2013; 3:125-131.

Doganay A, Gonenc B, Sarimehmetoglu HO, Oge H, Oge S, Adanir R, Avcioglu H and Tanyuksel M. Analysis of cyst fluid antigens from different hosts for the serodiagnosis of hydatidosis. Ankara Univ Vet Fak Derg. 2013; 60:33-37.

Dryden MW, Payne PA, Ridley R and Smith V. Comparison of common faecal flotation techniques for the recovery of parasite eggs and oocysts. Veterinary Therapeutics. 2005; 6:15-28.

Fahim F and Al Salamah SM. Cystic Echinococcosis in Central Saudi Arabia: a 5-year experience. Turkish Journal of Gastroenterology. 2007; 18:22-27.

Greenfield EA. Antibodies: A Laboratory Manual, 2nd edn. Cold Spring Harbor Laboratory Press. 2014.

Hassanain MA, Toeleb NI, Shaapan RM, Hassanain NA, Maher A and Yousif AB. Immunological detection of human and camel cystic echinococcosis using different antigens of hydatid cyst fluid, protoscoleces and germinal layers. Veterinary World. 2021; 14:270-275.

Ibrahim MM. Study of cystic echinococcosis in slaughtered animals in Al Baha region, Saudi Arabia: interaction between some biotic and abiotic factors. Acta Tropica. 2010; 113:26-33.

Janardhan S, Pandiaraja P, Pandey V, Karande A and Kaliraj P. Development and characterisation of monoclonal antibodies against WbSXP-1 for the detection of circulating filarial antigens. Journal of Helminthology. 2011; 85:1-6.

Kagiko MM. Characterisation of hydatid cyst antigens by crossed Immunoelectrophoresis and its implications for the serodiagnosis of hydatid disease in livestock. A PhD thesis. University of Nairobi. 1985.

Kamhawi S. A retrospective study of human cystic echinococcosis in Jordan. Annual of Tropical Medicine and Parasitology. 1995; 89:409-414.

Kanwar JR, Kanwar RK, Grewal AS and Vinayak VK. Significance of detection of immune-complexed 8 kDa hydatid specific antigen for immunodiagnosis of hydatidosis. FEMS Immunology and Medical Microbiology. 1994; 9:231-236.

Kharebov A, Nahmias J and El-On J. Cellular and humoural immune responses of hydatidosis patients to *Echinococcus granulosus* purified antigen. American Journal of Tropical Medicine and Hygiene. 1997; 57:619-625.

Kordafshari S, Hosseini SH, Meshgi B and Youssefi MR. Comparison of electrophoretic patterns of larval stages of Taeniidae and determination of specific antigens of hydatid cyst by western blotting technique. Global Veterinaria. 2010; 4:601-606.

Laemmli UK. Cleavage of structural proteins during the assembly of the head of bacteriophage T4. Nature. 1970; 227:680-685.

Musiani P, Piantelli M, Lauriola L, Arru E and Pozzuoli R. *Echinococcus granulosus*: specific quantification of the two most immunoreactive antigens in hydatid fluids. Journal of Clinical Pathology. 1978; 31:475-478.

Oriol R, Williams JF, Esandi MVP and Oriol C. Purification of lipoprotein antigens of *Echinococcus granulosus* from sheep hydatid fluid. American Journal of Tropical Medicine and Hygiene. 1971; 20:569-574.

Piantelli M, Pozzuoli R, Arru E and Musiani P. *Echinococcus granulosus*: identification of subunits of the major antigens. Journal of Immunology. 1977; 119:1382-1386.

Pozzuoli R, Musiani P, Arru E, Patrono C and Piantelli M. *Echinococcus granulosus*: evaluation of purified antigens immunoreactivity. Experimental Parasitology. 1974; 35:52-60.

Rashed AA, Omer HM, Fouad MA and Al Shareef AM. The effect of severe cystic hydatidosis on the liver of a Najdi sheep with special reference to the cyst histology and histochemistry. Journal of Egyptian Society for Parasitology. 2004; 34(1):297-304.

Sadjjadi SM. Present situation of echinococcosis in the Middle East and Arabic North Africa. Parasitology International. 2006; 55:197-202.

Sadjjadi SM, Sedaghat F, Hosseini SV and Sarkari B. Serum antigen and antibody detection in echinococcosus:

application in serodiagnosis of human hydatidosis. Korean Journal of Parasitology. 2009; 47:153-157.

Shambesh MK, Craig PS, Ibrahem MM, Gusbi AM and Echtuish EF. A high prevalence of cystic hydatid disease in North Africa. Annal of Tropical Medicine and Parasitology. 1997; 91:957-959.

Soulsby EJL. Helminthes, Arthropods and Protozoa of Domesticated Animals. 7th edn., Bailliere Tindall, England. 1986. ISBN 0-7020-0820-6.

Towbin H, Stachelin T and Gordon J. Electrophoretic transfer of proteins from polyacrylamide gels to nitrocellulose sheetsa: procedure and some applications. Proceedings of the National Academy of Science, USA. 1979; 76:4350-4354.

Urquhart GM, Armour J, Duncan JL, Dunn AM and Jennings FW. Veterinary Parasitology. Longman Scientific and Technical England, UK. 2006.

Verastegui M, Moro P, Guevara A, Rodriguez T, Miranda E and Gilman RH. Enzyme-linked immunoelectrotransfer blot test for diagnosis of human hydatid disease. Journal of Clinical Microbiology. 1992; 30:1557-1561.

WHO Informal Working Group. International classification of ultrasound images in cystic echinococcosis for application in clinical and field epidemiological settings. Acta Tropica. 2003; 85:253-261.

Zhang W, Li J and McManus DP. Concepts in immunology and diagnosis of hydatid disease. Clinical Microbiology Review. 2003; pp 18-36.

DOI : 10.5958/2277-8934.2022.00020.0 Vol 29 No 2, p 147-153

COMPARATIVE ANALYSIS OF SELECTED IMMUNE PARAMETERS IN BLOOD OF THE MAJAHEEM AND MAGATEER DROMEDARY CAMEL BREEDS

Jamal Hussen[1], Ahmed I. El sheikh[2] and Faisal Almathen[2,3]

[1]Department of Microbiology, [2]Department of Veterinary Public Health, College of Veterinary Medicine,
[3]The Camel Research Centre, King Faisal University, Al-Ahsa, Saudi Arabia

ABSTRACT

The present study investigated the composition of blood leukocytes in the Magateer and Majaheem camel breeds using immune cell labeling and flow cytometry. In addition, the phagocytosis activity of blood neutrophils and monocytes were compared between the two breeds. Although the total number of leukocytes did not differ significantly between the two camel breeds, a significantly higher fraction and absolute number of neutrophils was observed in blood of the Majaheem breed compared to the Magateer breed. In contrast to this, the fraction of eosinophils was significantly lower in blood of the Majaheem than the Magateer breed. The comparison of lymphocyte composition between the two breeds revealed significantly more B cells (relative and absolute count) in blood of the Magateer breed camel than the Majaheem camels. The two breeds showed comparable phagocytosis activity for their neutrophils and monocytes. Collectively, the present study compared selected cellular immune parameters between the two main breeds of the dromedary camel and identified similarities and differences.

Key words: Breed, dromedary camel, immune parameters, flow cytometry, leukocytes, Magateer, Majaheem

The impact of animal breed on innate and adaptive immunity has been investigated for several species (Schilling *et al,* 2019; Khatab *et al,* 2021; Lin *et al,* 2022; Ordonez *et al,* 2022; Ortega *et al,* 2022). In the dromedary camel, several components of the immune system have been recently characterised (Hussen and Schuberth, 2020). The phenotype and function of leukocytes are influenced by several physiologic (Gaashan *et al,* 2020) and pathologic factors (Hussen *et al,* 2018 and Hussen, 2019). Animal breed is one of the most important factors with key effect on the immune competence.

In the dromedary camel, several immuno-genomic studies have described the genomic diversity of immunity-related genes in domesticated and wild camels, including genes encoding for B cell receptors, T cell receptors and MHC molecules (Antonacci *et al,* 2011; Vaccarelli *et al,* 2012; Ciccarese *et al,* 2014; Plasil *et al,* 2016; Futas *et al,* 2019; Plasil *et al,* 2019; Lado *et al,* 2020; Ming *et al,* 2020). Animal breeding programmes have traditionally focused on animal selection based on animal production capacity. However, intensive research is currently undertaken on selecting animal breeds with higher immune competence and disease resistance (Gavora and Spencer, 1983; Nino-Soto *et al,* 2008; Begley *et al,* 2009; Cartwright *et al,* 2011). For the dromedary camel, several breeds have been characterised based on animal size, coat colour and linear measurements (Kohler-Rollefson, 1993; Al-Atiyat *et al,* 2016; Meghelli *et al,* 2020).

Studies on the impact of dromedary camels breed on the cellular immune system are scarce. Therefore, the aim of the present study was to comparatively analyse the cellular composition of leukocytes in blood samples collected from the Magateer and the Majaheem dromedary camel breeds. In addition, the phagocytosis activity of blood phagocytes, including neutrophils and monocytes was compared between the two breeds.

Materials and Methods

Animals and blood sampling

Blood samples from jugular vein were collected into vacutainer tubes containing EDTA from 33 apparently healthy dromedary camels (n=33) including 15 animals of the Magateer breed (n=15) (mean age 9.3 ± 2.4 years) and Majaheem breed (n=18) (mean age 9.6 ± 2.1 yeras) from three camel farms in Al-Ahsa region in eastern Saudi Arabia. Cell separation from the collected blood samples was performed within one hour from the sampling.

SEND REPRINT REQUEST TO JAMAL HUSSEN email: jhussen@kfu.edu.sa

Cell separation

Leukocytes were separated from blood samples after hypotonic lysis of red blood cells. The lysis was performed by incubating 1 mL blood in 5 mL distilled water for 20 sec followed by the addition of 5ml double concentrated PBS to restore tonicity. This haemolysis procedure was repeated until complete lysis of red blood cells. The cells were washed two times in PBS (500×g, 250×g, 10 min, 10°C). Separated leukocytes were finally suspended in staining puffer (PBS containing 5 g/L BSA, 100 mg /L NaN_3) at 5 x 10^6 cells/mL.

Flow cytometry

Cell labeling was performed in round-bottomed 96-well microtitre plate using 5 × 10^5 leukocytes per well as previously described (Hussen, 2021). All incubation and centrifugation steps were performed at 4°C. Separated leukocytes were incubated with unlabeled primary monoclonal antibodies (mAbs) specific for the cell surface molecules, CD4, WC-1, MHCII and CD14 (Hussen and Schuberth, 2020) for 15 min in the dark. After two washings in staining buffer, the cells were incubated with fluorochrome-labeled anti mouse IgM, IgG1 and IgG2a secondary antibodies (Invitrogen) for 15 min in the dark. After two washings, labeled cells were analysed on an Accurie C6 flow cytometer (BD Biosciences) by acquisition of at least 100 000 total leukocytes. Collected flow cytometric data was analysed using the CFlow Software (V 1.0.264.21; BD Biosciences). Leukocyte count was estimated and under microscope using the Neubauer counting chamber after staining of blood sample with Türk Solution.

Flow cytometric analysis of bacterial phagocytosis

For monocyte identification, separated leukocytes were firstly labeled with APC-conjugated mouse IgG2a against CD14. Labeled leukocytes were then incubated in 96 well plates (1×10^5/well) with FITC-labeled S. aureus (50 bacteria/cell) for 45 minutes at 37°C and 5% CO_2. After incubation (15 min; 4°C), the percentage of monocytes and neutrophils with elevated green fluorescence among total cells was calculated after flow cytometric analysis.

Statistical Analyses

The statistical software program GraphPad Prism was used for statistical analysis. Differences between means were tested with the unpaired student's t test with significant differences if the *p* value was less than 0.05.

Results and Discussion

Based on animal size, coat colour and linear measurements, several breeds have been characterised within the dromedary camel species (Kohler-Rollefson, 1993; Al-Atiyat *et al,* 2016; Meghelli *et al,* 2020). However, the most common classification of the Arabian camel differentiates between the Majaheem breed (black camel) and the Magateer breed (white camel). In the dromedary camel, several myeloid and lymphoid immune cell populations and subpopulations were characterised during the recent years using flow cytometric analysis (Hussen, 2019; Hussen and Schuberth, 2020; Hussen *et al,* 2020; Hussen, 2021).

The comparison between the two camel breeds regarding their relative composition of leukocytes (Fig 1A) revealed significantly higher fraction of neutrophils in blood of the Majaheem (72.0 ± 1.2% of leukocytes) than the Magateer (67.8 ± 1.4% of leukocytes) breed ($p < 0.05$). In contrast to this, the fraction of eosinophils was significantly lower in blood of the Majaheem (5.5 ± 0.5% of leukocytes) than the Magateer (7.9 ± 1.3% of leukocytes) breed ($p < 0.05$). However, the fraction of monocytes and lymphocytes did not show any significant differences between the two breeds (Fig 1B). With exception of the absolute number of neutrophils, the absolute counting of total leukocytes and their populations did not show any significant difference between the two breeds ($p > 0.05$). The Majaheem camels (8565.9 ± 456 cell / µl blood) had significantly ($p < 0.05$) more numbers of neutrophils in their blood than the Magateer breed (7658.5 ± 748 cell / µl blood) camels (Fig 1C). The numbers of eosinophils, lymphocytes and monocytes were comparable between the two breeds ($p > 0.05$).

Although the percentage of lymphocytes and their absolute numbers did not differ between the two breeds, the Magateer breed camel showed more B cells in their blood than the Majaheem camels. This difference was significant for both the relative fraction of B cells (18.8 ± 1.4 versus 15.2 ± 1.1% of lymphoctres for the Majaheem breed) and their absolute numbers (271.9 ± 42 versus 201.0 ± 38 cell / µL blood for the Majaheem breed) (Fig 2).

Given the role of B cells in the humoral immune response through the production of antigen-specific antibodies (Cyster and Allen, 2019; Dhenni and Phan, 2020), the reduced numbers of B cells in blood of the Majaheem breed may have an impact on their response to B cell stimulating antigens. To test this hypothesis, further studies are needed to comparatively analyse B cell functional

responsiveness (proliferation, antibody production) toward monoclonal and polyclonal stimulation in different camel breeds.

To investigate the breed-related effect on the immune cell function in camels, we analysed the phagocytosis activity of neutrophils and monocytes in blood from the Magateer and Majaheem camels *in vitro*. The incubation of camel leukocytes with FITC-conjugated *Staphylococcus aureus* (*S. aureus*) bacteria (Fig 3A) resulted in similar phagocytosis activity for

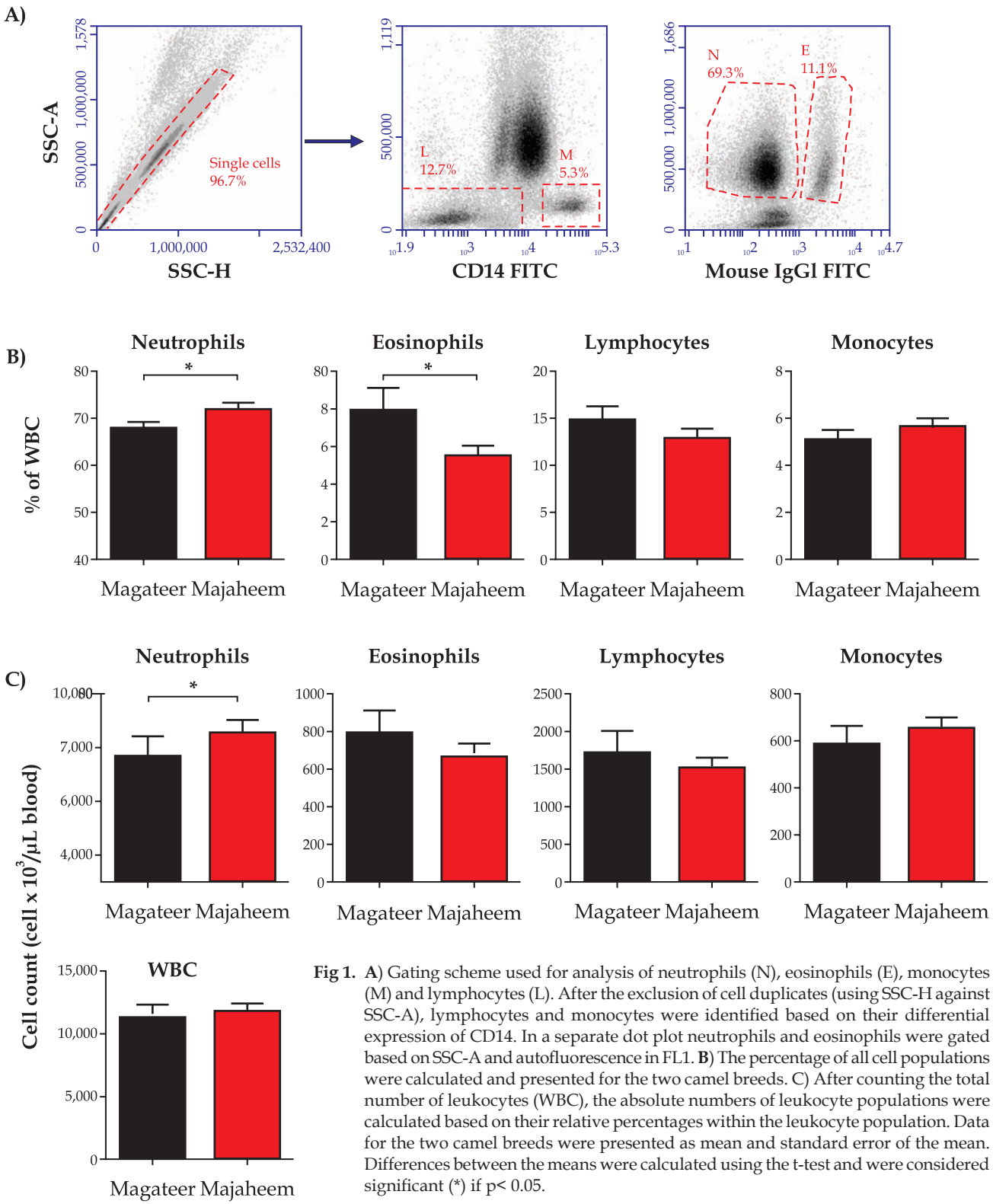

Fig 1. **A**) Gating scheme used for analysis of neutrophils (N), eosinophils (E), monocytes (M) and lymphocytes (L). After the exclusion of cell duplicates (using SSC-H against SSC-A), lymphocytes and monocytes were identified based on their differential expression of CD14. In a separate dot plot neutrophils and eosinophils were gated based on SSC-A and autofluorescence in FL1. **B**) The percentage of all cell populations were calculated and presented for the two camel breeds. C) After counting the total number of leukocytes (WBC), the absolute numbers of leukocyte populations were calculated based on their relative percentages within the leukocyte population. Data for the two camel breeds were presented as mean and standard error of the mean. Differences between the means were calculated using the t-test and were considered significant (*) if $p < 0.05$.

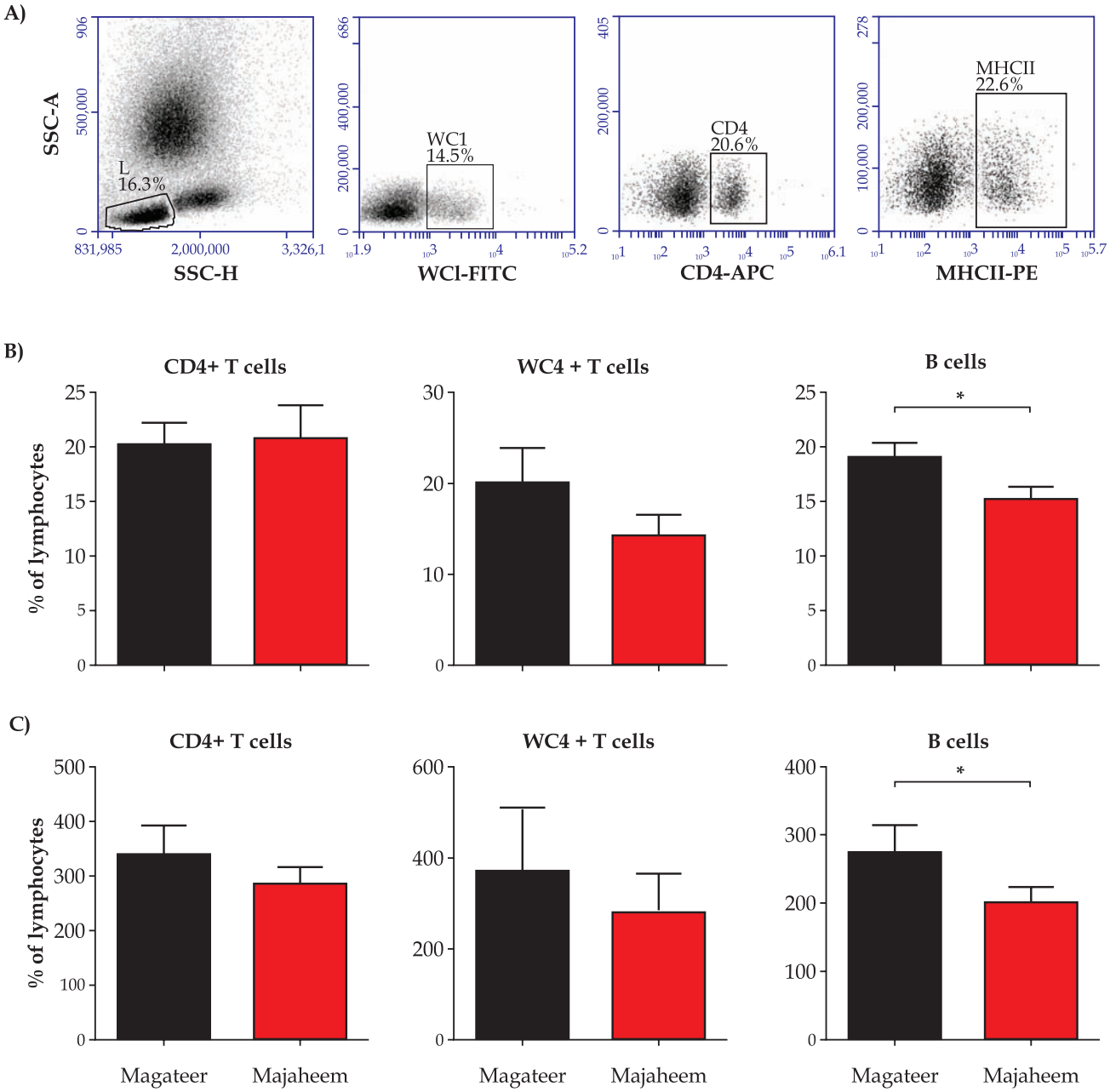

Fig 2. **A)** Separated camel leukocytes were labeled with monoclonal antibodies to the lymphocyte markers CD4, WC1 and MHCII. **B)** The relative fractions of CD4-positive helper T cells, gamma delta T cells and B cells were estimated by flow cytometry based on the cell-staining with CD4, WC1 and MHCII, respectively. **C)** The absolute cell numbers of lymphocyte subsets were calculated by multiplication of the estimated cell percentage within total lymphocytes with the total lymphocyte count. Data for the two camel breeds were presented as mean and standard error of the mean. Differences between the means were calculated using the t-test and were considered significant (*) if $p < 0.05$.

the two breeds. The proportions of neutrophils and monocytes that have ingested the bacteria did not differ significantly between the two camel breeds (Fig 3B).

The identification and selection of camel breeds with the superior capacity to mount effective immune responses would significantly contribute to reduced disease occurrence and improved camel production and reproduction. Studies on bovine breeds indicated that dairy cows could be classified based on their genetic background as high, moderate, or low immune responders (Mallard *et al,* 2015). The more balanced and robust immune responses in high responder animals could be linked to lower disease occurrence. An effective immune response was regulated by the balanced response of both

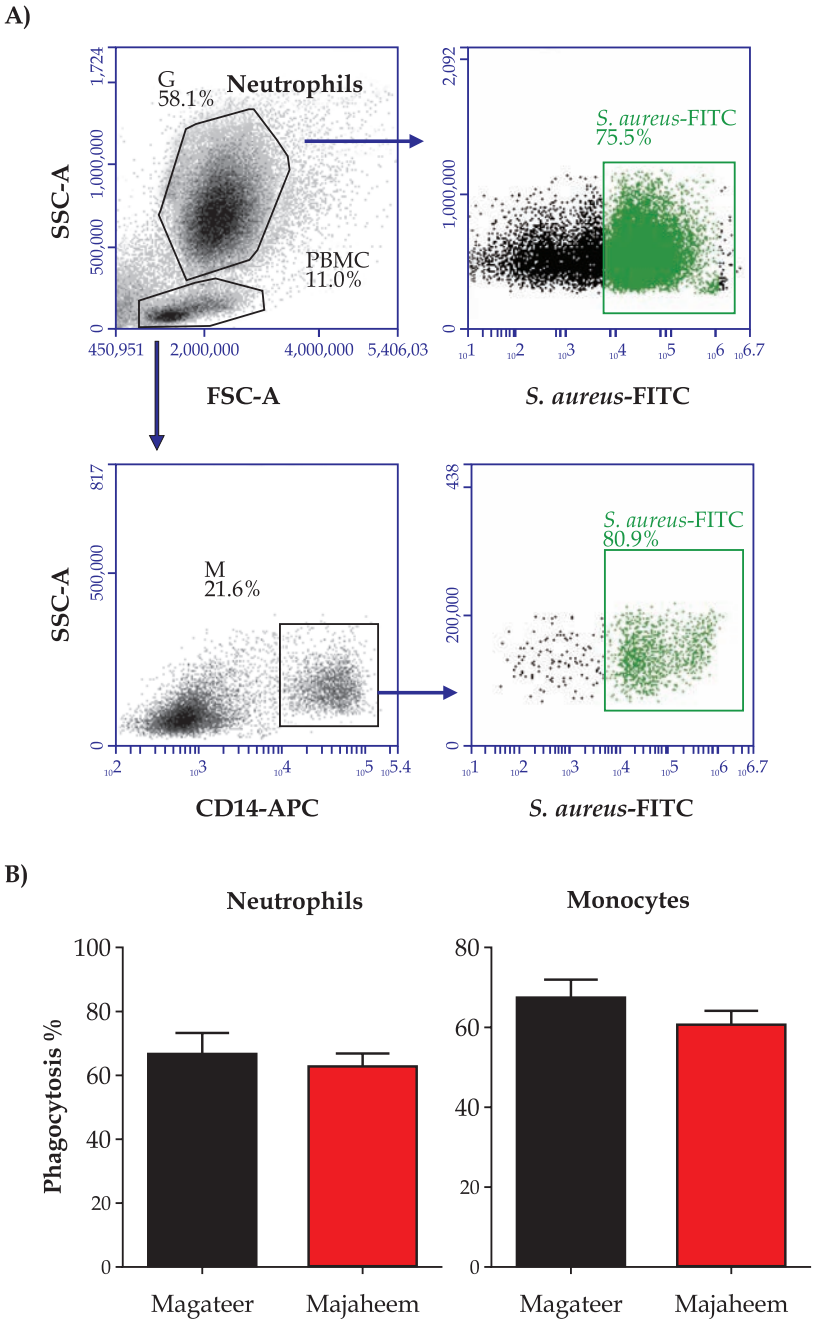

Fig 3. Flow cytometric analysis of phagocytosis. A) Separated camel leukocytes were incubated with staphylococcus aureus conjugated with FITC and labeled cells were analysed by flow cytometry. After gating on granulocytes or monocytes, the phagocytosis activity was analyzed based on the enhanced fluorescence in the green fluorescence channel (FL1). B) The percentage of phagocytosis-positive cells was calculated for neutrophils and monocytes and the two camel breeds. Differences between the means were calculated using the t-test and were considered significant (*) if $p< 0.05$.

innate and adaptive immune arms of the immune system. Cytokines and chemokines are key players in the regulation of immune responses and the communication between immune cells (Kimber *et al*, 2000; Gatla *et al*, 2019). Although the present study identified some differences in selected immune parameters between the two main camel breeds, the characterisation of camel breeds with higher immune responsiveness and disease resistance requires the analysis of a wide range of humoral and cellular components of the camel immune system. Especially the characterisation of cytokines responsible for polarisation of the camel innate and adaptive immune responses toward type 1, type 2, or type 17 immune responses which would improve our understanding of immune competence in camel.

Collectively, the present study compared selected cellular immune parameters between the two main breeds of the dromedary camel and identified similarities and differences. The Magateer dromedary camels had more neutrophils but less B cells in their blood than the Majaheem camels. The two breeds showed comparable phagocytosis activity for their neutrophils and monocytes. The clinical relevance of these differences on the camel immune response to pathogens should be evaluated using *in vivo* and *ex vivo* future studies.

Acknowledgements

This work was supported through the Annual Funding track by the Deanship of Scientific Research, Vice Presidency for Graduate Studies and Scientific Research, King Faisal University, Saudi Arabia (Project No. AN00309).

References

Al-Atiyat RM, Suliman G, Al-Suhaibani E, El-Waziry A, Al-Owaimer A and Basmaeil S. The differentiation of camel breeds based on meat measurements using discriminant analysis. Tropical Animal Health and Production. 2016; 48(5): 871-878 DOI: 10.1007/s11250-015-0990-5.

Antonacci R, Mineccia M, Lefranc MP, Ashmaoui HM, Lanave C, Piccinni B, Pesole G, Hassanane MS, Massari S and Ciccarese S. Expression and genomic analyses of *Camelus dromedarius* T cell receptor delta (TRD) genes reveal a variable domain repertoire enlargement due

to CDR3 diversification and somatic mutation. Mol Immunol. 2011; 48(12-13):1384-1396 DOI: 10.1016/j.molimm.2011.03.011.

Begley N, Buckley F, Burnside EB, Schaeffer L, Pierce K and Mallard BA. Immune responses of Holstein and Norwegian Red x Holstein calves on Canadian dairy farms. Journal of Dairy Science. 2009; 92(2):518-525 DOI: 10.3168/jds.2008-1300.

Cartwright SL, Begley N, Schaeffer LR, Burnside EB and Mallard BA. Antibody and cell-mediated immune responses and survival between Holstein and Norwegian Red x Holstein Canadian calves. Journal of Dairy Science. 2011; 94(3):1576-1585 DOI: 10.3168/jds.2010-3502.

Ciccarese S, Vaccarelli G, Lefranc MP, Tasco G, Consiglio A, Casadio R, Linguiti G and Antonacci R. Characteristics of the somatic hypermutation in the *Camelus dromedarius* T cell receptor gamma (TRG) and delta (TRD) variable domains. Developmental & Comparative Immunology. 2014; 46(2):300-313 DOI: 10.1016/j.dci.2014.05.001.

Cyster JG and Allen CDC. B Cell Responses: Cell interaction dynamics and decisions. Cell. 2019; 177(3):524-540 DOI: 10.1016/j.cell.2019.03.016.

Dhenni R and Phan TG. The geography of memory B cell reactivation in vaccine-induced immunity and in autoimmune disease relapses. Immunological Reviews. 2020; 296(1):62-86 DOI: 10.1111/imr.12862.

Futas J, Oppelt J, Jelinek A, Elbers JP, Wijacki J, Knoll A, Burger PA and Horin P. Natural Killer Cell Receptor Genes in Camels: Another Mammalian Model. Front Genet. 2019; 10:620 DOI: 10.3389/fgene.2019.00620.

Gaashan MM, Al-Mubarak AI and Hussen J. Leukocyte populations and their cell adhesion molecules expression in newborn dromedary camel calves. Veterinary World. 2020; 13(9):1863-1869 DOI: 10.14202/vetworld.2020.1863-1869.

Gatla HR, Muniraj N, Thevkar P, Yavvari S, Sukhavasi S and Makena MR. Regulation of Chemokines and Cytokines by Histone Deacetylases and an Update on Histone Decetylase Inhibitors in Human Diseases. International Journal of Molecular Sciences. 2019; 20(5) DOI: 10.3390/ijms20051110.

Gavora JS and Spencer JL. Breeding for immune responsiveness and disease resistance. Animal Blood Groups and Biochemical Genetics. 1983; 14(3):159-180 DOI: 10.1111/j.1365-2052.1983.tb01070.x.

Hussen J. Antibacterial functions of neutrophil and monocyte in newborn dromedary camel calves. Journal of Camel Practice And Research. 2019; 26(3):251-254.

Hussen J. Bacterial species-specific modulatory effects on phenotype and function of camel blood leukocytes. BMC Veterinary Research. 2021; 17(1):241 DOI: 10.1186/s12917-021-02939-1.

Hussen J and Schuberth HJ. Recent advances in camel immunology. Frontiers in Immunology. 2020; 11:614150 DOI: 10.3389/fimmu.2020.614150.

Hussen J, Shawaf T, Al-herz AI, Alturaifi HR, Al Khamees M and Alluwaimi AM. Expression patterns of cell adhesion molecules on CD4+ T cells and WC1+ T cells in the peripheral blood of dromedary camels. Pakistan Veterinary Journal. 2018; 38(3):231-236 DOI: 10.29261/pakvetj/2018.055.

Hussen J, Shawaf T, Al-Mubarak AIA, Al Humam NA, Almathen F and Schuberth HJ. Dromedary camel CD14(high) MHCII(high) monocytes display inflammatory properties and are reduced in newborn camel calves. BMC Veterinary Research. 2020; 16(1):62 DOI: 10.1186/s12917-020-02285-8.

Khatab SA, Hemeda SA, El-Nahas AF, Abd El Naby WSH, Hassan S, Alorabi JA and Dawood MAO. Intra- and inter-breed variation in immune response to acute and sub-chronic Salmonella infection and commercial immune-stimulant in two-layer breeds. Veterinary Medicine and Science. 2021; 7(6):2353-2361 DOI: 10.1002/vms3.621.

Kimber I, Cumberbatch M, Dearman RJ, Bhushan M and Griffiths CE. Cytokines and chemokines in the initiation and regulation of epidermal Langerhans cell mobilisation. British Journal of Dermatology. 2000; 142(3):401-412 DOI: 10.1046/j.1365-2133.2000.03349.x.

Kohler-Rollefson I. About camel breeds: A reevaluation of current classification systems. Journal of Animal Breeding and Genetics. 1993; 110(1-6):66-73 DOI: 10.1111/j.1439-0388.1993.tb00717.x.

Lado S, Elbers JP, Rogers MF, Melo-Ferreira J, Yadamsuren A, Corander J, Horin P and Burger PA. Nucleotide diversity of functionally different groups of immune response genes in Old World camels based on newly annotated and reference-guided assemblies. BMC Genomics. 2020; 21(1):606 DOI: 10.1186/s12864-020-06990-4.

Lin S, Ke C, Liu L, Gao Y, Xu L, Han B, Zhao Y, Zhang S and Sun D. Genome-wide association studies for immunoglobulin concentrations in colostrum and serum in Chinese Holstein." BMC Genomics. 2022; 23(1):41 DOI: 10.1186/s12864-021-08250-5.

Mallard BA, Emam M, Paibomesai M, Thompson-Crispi K and Wagter-Lesperance L. Genetic selection of cattle for improved immunity and health. Japanese Journal of Veterinary Research. 2015; 63 Suppl 1:S37-44.

Meghelli I, Kaouadji Z, Yilmaz O, Cemal I, Karaca O and Gaouar SBS. Morphometric characterisation and estimating body weight of two Algerian camel breeds using morphometric measurements. Tropical Animal Health and Production. 2020; 52(5):2505-2512 DOI: 10.1007/s11250-020-02204-x.

Ming L, Wang Z, Yi L, Batmunkh M, Liu T, Siren D, He J, Juramt N, Jambl T, Li Y and Jirimutu. Chromosome-level assembly of wild Bactrian camel genome reveals organisation of immune gene loci. Molecular Ecology Resources. 2020; 20(3) DOI: 10.1111/1755-0998.13141.

Nino-Soto MI, Heriazon A, Quinton M, Miglior F, Thompson K and Mallard BA. Differential gene expression of high and low immune responder Canadian Holstein dairy cows. Developmental Biology (Basel). 2008; 132:315-320 DOI: 10.1159/000317277.

Ordonez D, Bohorquez MD, Avendano C and Patarroyo MA. Comparing Class II MHC DRB3 Diversity in

Colombian Simmental and Simbrah Cattle Across Worldwide Bovine Populations. Frontiers in Genetics. 2022; 13:772885 DOI: 10.3389/fgene.2022.772885.

Ortega L, Quesada J, Ruiz A, Conde-Felipe MM, Ferrer O, Rodriguez F and Molina JM. Local immune response of Canarian Majorera goats infected with Teladorsagia circumcincta. Parasites and Vectors. 2022; 15(1):25 DOI: 10.1186/s13071-021-05145-y.

Plasil M, Mohandesan E, Fitak RR, Musilova P, Kubickova S, Burger PA and Horin P. The major histocompatibility complex in Old World camelids and low polymorphism of its class II genes. BMC Genomics. 2016; 17:167 DOI: 10.1186/s12864-016-2500-1.

Plasil M, Wijkmark S, Elbers JP, Oppelt J, Burger PA and Horin P. The major histocompatibility complex of Old World camelids: Class I and class I-related genes. HLA. 2019; 93(4):203-215 DOI: 10.1111/tan.13510.

Schilling MA, Memari S, Cavanaugh M, Katani R, Deist MS, Radzio-Basu J, Lamont SJ, Buza JJ and Kapur V. "Conserved, breed-dependent and subline-dependent innate immune responses of Fayoumi and Leghorn chicken embryos to Newcastle disease virus infection. Scientific Reports. 2019; 9(1):7209 DOI: 10.1038/s41598-019-43483-1.

Vaccarelli G, Antonacci R, Tasco G, Yang F, Giordano L, El Ashmaoui HM, Hassanane MS, Massari S, Casadio R and Ciccarese S. Generation of diversity by somatic mutation in the *Camelus dromedarius* T-cell receptor gamma variable domains. European Journal of Immunology. 2012; 42(12):3416-3428 DOI: 10.1002/eji.201142176.

Yousif OK and Babiker SA. The desert camel as a meat animal. Meat Science. 1989; 26(4):245-254 DOI: 10.1016/0309-1740(89)90010-7.

SELECTED RESEARCH ON
GROSS ANATOMY AND HISTOLOGY OF CAMELS

Hard bound, 452 pages, few figures coloured

Selected Research on Gross Anatomy and Histology of Camels is a unique reference book on anatomy of dromedary and bactrian camels. This book contains a first ever wide spectrum of histological description of various organs of camels which is depicted by special stains and scanning electronmicroscopy in addition to the gross anatomy, histochemical and immunohistochemical studies. The book has 92 manuscripts in 9 sections, e.g. radiographic anatomy, anatomy of various systems (skeletal, digestive, respiratory, circulatory, urogenital and nervous), common integument and miscellaneous. These manuscripts were published by 158 authors working in 37 laboratories or colleges or institutions from 14 countries in the Journal of Camel Practice and Research between June 1994 to June 2010. Bactrian camel anatomy research was exclusively contributed by the researchers of China. The countries involved in camel anatomy research were China, Egypt, India, Iran, Saudi Arabia, Iraq, Jordan, Japan, Pakistan, Sweden, United Arab Emirates, United States of America, France and Germany. Camel Publishing House has taken a step forward to compile this knowledge in form of a book and this herculian task was accomplished by its dedicated editors, viz. T.K. Gahlot (India), S.K. Nagpal (India), A.S. Saber (Egypt) and Jianlin Wang (China). This classic reference book will serve as a one stop resource for scientific information on gross anatomy and histology of camels.

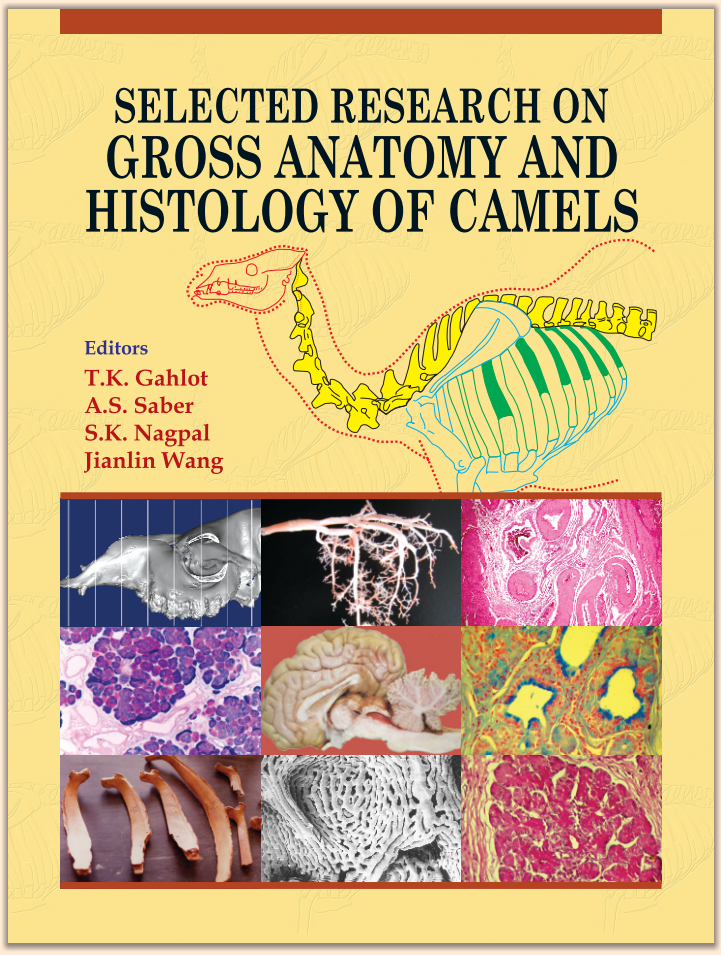

Editors:
T.K. Gahlot, A.S. Saber, S.K. Nagpal and Jianlin Wang

Edition: 2011

Publisher: **Camel Publishing House**
67, Gandhi Nagar West,
Near Lalgarh Palace
Bikaner 334001 Rajasthan,
India
email: tkcamelvet@yahoo.com
website: www.camelsandcamelids.com

Price: US $ 375 (Abroad)
INR 7500 (India)

ISBN: 81-903140-1-7

DOI : 10.5958/2277-8934.2022.00021.2 Vol 29 No 2, p 155-159

NEUTROPHILS EXTRACELLULAR TRAPS FORMATION AND REACTIVE OXYGEN SPECIES (ROS) PRODUCTION BY MILK IMMUNE CELLS FROM CAMELS WITH SUBCLINICAL MASTITIS

Jamal Hussen, Mohammed Ali Al-Sukruwah and Khulud Bukhari
Department of Microbiology, College of Veterinary Medicine, King Faisal University, Al-Ahsa, Saudi Arabia

ABSTRACT

Subclinical mammary gland infections are within the most important infectious diseases in dromedary camels with high impact on milk production and animal health. Using flow cytometry, the present study analysed the capacity of milk phagocytes to form neutrophil extracellular traps (NETs) and to produce reactive oxygen species (ROS) *in vitro*. Based on the California mastitis test, clinically healthy camels were divided into animals with subclinical mastitis (n = 5) and camels with healthy mammary gland (n = 5). The *ex vivo* ROS production and the NETs formation activity of milk phagocytes were compared between healthy and affected animals. A basic fraction of phagocytes (10.0 ± 1.7% of total cells) with positive staining with the NETs-sensitive dye SYTOX™ Green was detected in milk samples from healthy camels. The NETs-positive fraction was significantly lower in milk from camels with subclinical mastitis (4.8 ± 1.5 % of total cells) compared to milk samples from healthy camels. Stimulation of milk cells with the gram-negative bacteria *E. coli* resulted in enhanced ROS production in milk phagocytes from both healthy and affected camels. The two groups, however, did not differ in the ROS level in their unstimulated or stimulated phagocytes. In conclusion, the present study identified basic levels of NETs formation by milk phagocytes separated from healthy camels. The reduced NETs formation by cells from infected camels may play a role in the pathogenesis of subclinical mammary gland infections in camels.

Key words: Camel, flow cytometry, immune cells, milk, Neutrophils NETosis, ROS

Neutrophil extracellular traps (NETs) are structures composed of DNA, histones, and antimicrobial proteins that are released extracellularly by neutrophils and other immune cells as a means for trapping and killing invading pathogens. Pisanu *et al* (2015) reported the formation of NETs in mammary alveoli of sheep suffering bacterial mastitis, providing detailed information for understanding pathogenic mechanisms enacted by bacteria to survive the action of the innate immune system in the mammary gland. Xie *et al* (2022) carried out research on the neutrophil extracellular traps (NETs) and reactive oxygen species (ROS) formation capacity of polymorphonuclear cells (PMN) during different lactational stages to Holstein cows and found it an excellent model to mimic inflammation and study fundamental aspects of the production of NETs and ROS *in vitro*.

Camels may be affected by all types of mastitis similar to other dairy animals (Al-Ashqar *et al,* 2015; Alebie *et al,* 2021; Geresu *et al,* 2021; Ranjan *et al,* 2021). Bovine milk somatic cells are typically represented by epithelial cells, neutrophils, macrophages, and lymphocytes as the major cell types (Riollet *et al*, 2000). Kaskous *et al* (2021) suggested that 150 x 10^3 cells/ml in milk is a limit value for healthy camel milk. If the somatic cell count (SCC) exceeds this limit, subclinical or clinical mastitis of the udder may occur and the milk may be contaminated with microbes. Aljumaah *et al* (2020) found that the objective SCC test possesses considerable diagnostic merit for early detection of subclinical mastitis in camels. Subclinical mastitis is associated with huge economic losses due to the reduced milk yield and quality and high treatment costs. In addition, it is a public health concern for camel milk consumers (Osman *et al,* 2014).

Milk phagocytes, including macrophages and neutrophils, are the primary effector cells of the mammary gland innate immune system with a key role during mammary gland infections (Alhussien *et al,* 2021). They contribute to the early elimination of bacterial pathogens by several antimicrobial functions, including phagocytosis, production of

SEND REPRINT REQUEST TO JAMAL HUSSEN email: jhussen@kfu.edu.sa

reactive oxygen and nitrogen species, and formation of cellular traps (Lippolis *et al,* 2006; Aulik *et al,* 2010; Swain *et al,* 2014). The aim of the present study was to investigate NETs formation and ROS production capacity by milk phagocytes from healthy camels and camels with subclinical mastitis.

Materials and Methods

Animals

Ten clinically healthy Majaheem dromedary she camels reared on a private camel farm at the Al-Ahsa camel market in eastern Saudi Arabia were included in the study. After discarding the first few milk jets, teat ends were cleaned and disinfected and 10 ml milk sample was collected for the California Mastitis Test (CMT) into sterile glass tubes. Another 50 ml of freshly milked sample was taken into sterile plastic tubes for cell separation and flow cytometry. Milk of all studied animals underwent CMT (Schalm and Noorlander, 1957; Seligsohn *et al,* 2020). For this, 3 ml of each quarter milk were added to an equal amount of CMT fluid and the mixture was rotated by circular movement. The reactions were graded according to the Scandinavian scoring system (Seligsohn *et al,* 2020). Animals with milk samples of a test score equal to or more than score 3 in the absence of clinical signs of mastitis were classified as subclinical mastitis animals. For healthy she-camels (n = 5 animals) with a test score of less than 3 and without clinical signs of mastitis, pooled composite milk samples representing all 4 quarters were prepared for flow cytometry. In the affected group (n = 5 animals), milk samples collected from affected quarters were further processed for flow cytometry.

Cell separation for flow cytometry

Milk samples were diluted with cold PBS (20 ml milk and 20 ml PBS) in conical 50 ml polypropylene tubes and the tubes were centrifuged at 1000×g and 4 °C for 20 min without brake. After removing the fat layer using a spatula, the supernatant was discarded. The cell pellet was resuspended with 30 ml cold PBS and washed twice at 600×g and 4°C for 10 min. Milk cell pellets were suspended in 1 ml cell culture medium (RPMI 1640) at a concentration of 5×10^6 cells/ml.

Analysis of the formation of neutrophil extracellular traps (NETs) by flow cytometry

Cell labeling was performed in a round-bottomed 96-well microtitre plate. For this, 100 µl of the cell suspension (5×10^5 cells per well) of each sample were pipetted into the well of a microtitre plate. To each well of the microtitre plate, one drop of the DNA-sensitive dye SytoxGreen (Invitrogen, Germany) and 10 µl of the cell viability dye propidium iodide (PI; 2 µg/ml, BD Biosciences, Germany) were added. After 15 min incubation at room temperature, the labeled cells were analysed on a FACS Calibur (BD Biosciences) by the acquisition of at least 50000 total cells. Collected flow cytometric data were analysed using the FCS Expres Software (V3; BD Biosciences).

Flow cytometric analysis of reactive oxygen species (ROS)

ROS generation was measured in 96-well round-bottom microtitre plates (Corning, NY, USA) as previously described (Hussen, 2021). Separated milk cells (5×10^5/well in RPMI medium) were incubated for 30 min (37°C, 5% CO_2) with heat-killed *E. coli* (50 bacteria/cell). After 15 min of incubation the ROS-sensitive dye dihydrorhodamine (DHR)-123 (1µg/mL final, Mobitec, Goettingen, Germany) was added to the wells. After incubation, labeled cells were washed with PBS and the relative amount of generated ROS was determined by flow cytometry.

Statistical Analyses

Data were processed with the Microsoft office Excel® program (version 2016 Microsoft) and statistical analysis was performed using the software program Prism (GraphPad software version 5, GraphPad Software, San Diego, USA). The unpaired student's t-test was used to compare the mean of the two groups. The results for each analysed parameter were presented graphically as means ± standard error of the mean (SEM). Results were considered statistically significant if the p-value was less than 0.05.

Results and Discussion

The mammary gland immune response to mastitic pathogens has been investigated for several animal species (Guiguen *et al,* 1996; Winnicka *et al,* 1999; Leitner *et al,* 2012; Blagitz *et al,* 2013; De and Mukherjee, 2013; Zecconi *et al,* 2020). Studies on the functional capacities of immune cells in the camel mammary gland are limited. The present study compared some antibacterial functions of milk leukocytes between healthy camels and camels with subclinical mastitis. Based on the results of California Mastitis Test (CMT), camels with a CMT test score of ≥ 3 in the absence of signs of clinical mastitis were considered as subclinical mastitis animals (Seligsohn *et al,* 2020).

Macrophages and neutrophils are key effector innate immune cells of the mammary gland with an essential role during mammary gland infections (Swain *et al*, 2014; Alhussien *et al*, 2021). In present study, antimicrobial function of milk phagocytes (granulocytes and macrophages) was analysed by evaluation of ROS production. The basal and stimulation-induced ROS production by milk phagocytes were analysed using dehydrohodamin-123 (Fig 1A). Basal ROS values of phagocytes were comparable ($p > 0.05$) between SCM and healthy milk samples. In addition, stimulation with *E. coli* induced similar response ($p > 0.05$) in phagocytes from SCM and healthy milk samples (Fig 1B).

The formation of neutrophil extracellular traps (NETs or NETosis) is a key antibacterial effector function of cells of myeloid lineage including neutrophils and macrophages (Ciliberti *et al*, 2021). Using NETosis, the pathogens are killed after trapping it into an extracellular network of processed chromatin or DNA decorated with histones in addition to cytoplasmic proteins from neutrophilic granules (Lippolis *et al*, 2006; Aulik *et al*, 2010; Remijsen *et al*, 2011).

Neutrophil extracellular traps (NETs) also function as critical cytotoxins at infection site to promote "neutrophil apoptosis" through process of "NETosis" to achieve extracellular entrapment of pathogens (Bryzek *et al*, 2019).

In present study, NET-formation was analysed by flow cytometry using green fluorescence dye SYTOX™ Green (Invitrogen, Germany). NET formation by milk phagocytes (neutrophils and macrophages) was compared between healthy camels and camels with subclinical mastitis. The

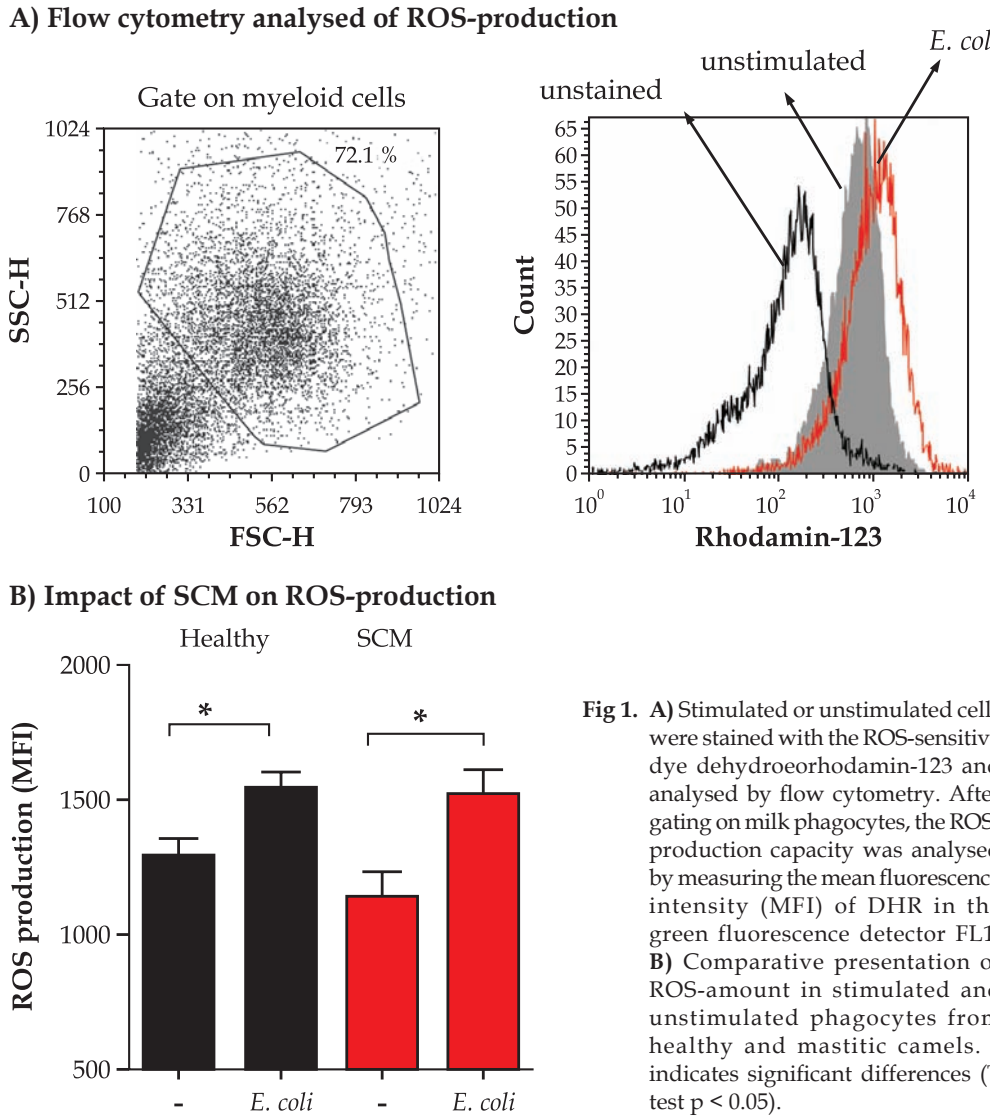

Fig 1. **A)** Stimulated or unstimulated cells were stained with the ROS-sensitive dye dehydroeorhodamin-123 and analysed by flow cytometry. After gating on milk phagocytes, the ROS-production capacity was analysed by measuring the mean fluorescence intensity (MFI) of DHR in the green fluorescence detector FL1. **B)** Comparative presentation of ROS-amount in stimulated and unstimulated phagocytes from healthy and mastitic camels. * indicates significant differences (T test $p < 0.05$).

A) Flow cytometric analysis of netosis in milk phagocytes

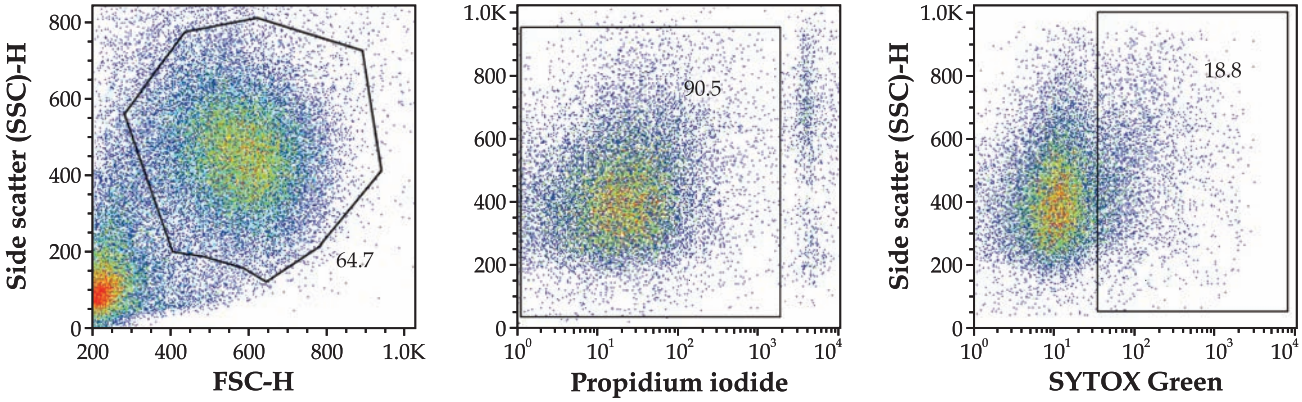

B) Net formation in phagocytes from healthy and mastitic camels

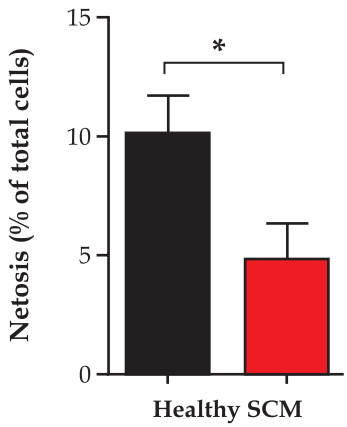

Fig 2. **A)** Flow cytometric analysis of NET-formation. Milk cells separated from healthy camels and camels with subclinical mastitis were stained with the DNA-sensitive dye SYTOX™ Green and analysed by flow cytometry. After gating on milk phagocytes, NET-formation was estimated as the percentage of SYTOX™ Green-positive cells with enhanced green fluorescence. **B)** Comparative presentation of net formation in phagocytes from healthy and mastitic camels. * indicates significant differences (T test $p < 0.05$).

percentage of milk phagocytes that formed NETs was significantly lower in milk from camels with subclinical mastitis (4.8 ± 1.5 % of total phagocytes) compared to healthy camels (10.0 ± 1.7) (Fig 2).

In conclusion, the present study identified basic levels of NETs formation by milk phagocytes separated from healthy camels. The reduced NETs formation by cells from infected camels may play a role in pathogenesis of subclinical mammary gland infections in camels.

Acknowledgement

This work was supported through the Annual Funding track by the Deanship of Scientific Research, Vice Presidency for Graduate Studies and Scientific Research, King Faisal University, Saudi Arabia (Project No. Grant46).

References

Al-Ashqar RA, Al-Mohammad Salem KM, Al Herz AKM, Al-Haroon AI and Alluwaimi AM. The CD markers of camel (*Camelus dromedarius*) milk cells during mastitis: the LPAM-1 expression is an indication of possible mucosal nature of the cellular trafficking. Research in Veterinary Science. 2015; 99:77-81 DOI: 10.1016/j.rvsc.2015.01.011.

Alebie A, Molla A, Adugna W, Tesfaye A and Ejo M. Prevalence, isolation, identification and risk factors of major bacterial cause of camel subclinical mastitis. BioMed Research International. 2021; 5522331 DOI: 10.1155/2021/5522331.

Alhussien MN, Panda BSK and Dang AK. A comparative study on changes in total and differential milk cell counts, activity, and expression of milk phagocytes of healthy and mastitic indigenous sahiwal cows. Frontiers in Veterinary Science. 2021; 8:670811 DOI: 10.3389/fvets.2021.670811.

Aljumaah, Riyadh Saleh, Almutairi Fares, Ayadi Moez, Alshaikh Mohammed Abdulrahman, Al-HaidaryAhmed Abrahim and Samara Emad Mohammed. Practicability of somatic cell count and electrical conductivity as subclinical mastitis diagnostic tests in camels (*Camelus dromedarius*). Scientia Agricola [online]. 2020, v. 77, n. 4 [Accessed 29 April 2022] , e202180373. Available from: <https://doi.org/10.1590/1678-992X-2018-0373>

Aulik NA, Hellenbrand KM, Klos H, *et al*. *Mannheimia haemolytica* and its leukotoxin cause neutrophil extracellular trap formation by bovine neutrophils. Infection and Immunity. 2010; 7811:4454-66 DOI: 10.1128/IAI.00840-10.

Blagitz MG, Souza FN, Santos BP, Batista CF, Parra AC, Azevedo LF, Melville PA, Benites NR and Della Libera AMMP. Function of milk polymorphonuclear neutrophil leukocytes in bovine mammary glands infected with *Corynebacterium bovis*. Journal of Dairy Science. 2013; 966:3750-7 DOI: 10.3168/jds.2012-6370.

Bryzek D, Ciaston I, Dobosz E, Gasiorek A, Makarska A, Sarna

M, Eick S, Puklo M, Lech M, Potempa B, Potempa J, Koziel J: Triggering NETosis *via* protease-activated receptor (PAR)-2 signaling as a mechanism of hijacking neutrophils function for pathogen benefits. Plos Pathog. (2019); 15(5):e1007773. DOI: 10.1371/journal.ppat.1007773

Ciliberti MG, Albenzio M, Claps S, Santillo A, Marino R and Caroprese M. NETosis of peripheral neutrophils isolated from dairy cows fed olive pomace. Frontiers in Veterinary Science. 2021; 8:626314 DOI: 10.3389/fvets.2021.626314.

De UK and Mukherjee R. Dynamics of milk leukocytes in response to a biological response modifier during bovine subclinical mastitis. Research in Veterinary Science. 2013; 952:352-7 DOI: 10.1016/j.rvsc.2013.06.010.

Geresu MA, Abera Leliso S and Liben GW. Camel mastitis: prevalence, risk factors, and isolation of major bacterial pathogens in Gomole District of Borena Zone, Southern Ethiopia. Veterinary Medicine International. 2021; 9993571 DOI: 10.1155/2021/9993571.

Guiguen F, Greenland T, Pardo E, Panaye G and Mornex JF. Flow cytometric analysis of goat milk lymphocytes: subpopulations and adhesion molecule expression. Veterinary Immunology and Immunopathology. 1996; 531-2:173-8 DOI: 10.1016/0165-2427(96)05553-5.

Hussen J. Bacterial species-specific modulatory effects on phenotype and function of camel blood leukocytes. BMC Veterinary Research. 2021; 171:241 DOI: 10.1186/s12917-021-02939-1.

Kaskous S, Al-Momani AQ, Al-Yacoub AN, Al-Najjar KA. Physiological perspective of milk somatic cell count in lactating camels. Journal of Camel Practice and Research. 2021; 28:319-325. 10.5958/2277-8934.2021.00049.7.

Leitner G, Merin U, Krifucks O, Blum S, Rivas AL and Silanikove N. Effects of intra-mammary bacterial infection with coagulase negative *Staphylococc*i and stage of lactation on shedding of epithelial cells and infiltration of leukocytes into milk: comparison among cows, goats and sheep. Veterinary Immunology and Immunopathology. 2012; 1473-4:202-10 DOI: 10.1016/j.vetimm.2012.04.019.

Lippolis JD, Reinhardt TA, Reinhardt TA, Goff JP and Horst RL. Neutrophil extracellular trap formation by bovine neutrophils is not inhibited by milk. Veterinary Immunology and Immunopathology. 2006; 1131-2:248-55 DOI: 10.1016/j.vetimm.2006.05.004.

Pisanu S, Cubeddu T, Pagnozzi D, Rocca S, Cacciotto C, Alberti A, Marogna G, Uzzau S and Addis MF. Neutrophil extracellular traps in sheep mastitis. Veterinary Research. 2015; 46(1):59. https://doi.org/10.1186/s13567-015-0196-x

Osman KM, Samir A, Orabi A and Zolnikov TR. Confirmed low prevalence of *Listeria* mastitis in she-camel milk delivers a safe, alternative milk for human consumption. Acta Tropica. 2014; 130:1-6 DOI: 10.1016/j.actatropica.2013.10.001.

Ranjan R, Narnaware SD and Prakash V. Incidence, risk factors and economic impact of clinical mastitis in dromedary camel (*Camelus dromedarius*). Tropical Animal Health and Production. 2021; 541:31 DOI: 10.1007/s11250-021-03035-0.

Remijsen Q, Kuijpers TW, Wirawan E, Lippens S, Vandenabeele P and Berghe TV. Dying for a cause: NETosis, mechanisms behind an antimicrobial cell death modality. Cell Death and Differentiation. 2011; 18:581-8 DOI: 10.1038/cdd.2011.1.

Riollet C, Rainard P and Poutrel B. Cells and cytokines in inflammatory secretions of bovine mammary gland. Advances in Experimental Medicine and Biology. 2000; 480:247-158.

Schalm OW and Noorlander DO. Experiments and observations leading to development of the California mastitis test. American Veterinary Medical Association. 1957; 1305:199-204.

Seligsohn D, Nyman AK, Younan M, Sake W, Persson Y, Bornstein S, Maichomo M, de Verdier K, Morrell JM and Chenais E. Subclinical mastitis in pastoralist dairy camel herds in Isiolo, Kenya: Prevalence, risk factors, and antimicrobial susceptibility. Journal of Dairy Science. 2020; 103:4717-31 DOI: 10.3168/jds.2019-17701.

Swain DK, Kushwah MS, Kaur M, Patbandha TK, Mohanty AK and Dang AK. Formation of NET, phagocytic activity, surface architecture, apoptosis and expression of toll like receptors 2 and 4 (TLR2 and TLR4) in neutrophils of mastitic cows. Veterinary Research Communications. 2014; 38:209-19 DOI: 10.1007/s11259-014-9606-1.

Winnicka A, Klucinski W, Hoser G, Sikora J and Kawiakv J. Flow cytometry analysis of milk and peripheral blood cells from goats during lactation. Zentralbl Veterinarmed A. 1999; 468:459-64 DOI: 10.1046/j.1439-0442.1999.00234.x.

Xie L, Pascottini OB, Zhi J, Yang H, Opsomer G, Dong Q. *In vitro* production of neutrophils extracellular traps is affected by the lactational stage of dairy cows. Animals. 2022; 12:564. https:// doi.org/10.3390/ani12050564.

Zecconi A, Zanini L, Cipolla M and Stefanon B. Factors affecting the patterns of total amount and proportions of leukocytes in bovine milk. Animals (Basel). 2020; 106 DOI: 10.3390/ani10060992.

SELECTED RESEARCH ON
CAMELID PARASITOLOGY

Hard bound, 291 pages, few figures coloured

New research and experience always broaden our knowledge, and help us adopting new diagnostic methods and treatments. Camel Publishing House has taken a step forward to compile this knowledge in form of a book and this Herculian task was accomplished with the help of dedicated editors. viz. Drs. T.K. Gahlot and M.B. Chhabra. ***Selected Research on Camelid Parasitology*** is most comprehensive guide to Camelid Parasitology. The classic reference book serves as a one stop resource for scientific information on major aspects of Camelid Parasitology. Featuring abundant photographs, illustrations, and data, the text covers camelid protozoa, helminths, and arthropods of dromedary and New World camelids. This hard bound book of 304 pages contains seroepidemiological studies, immunological and other diagnostic procedures, and new treatments of parasitic diseases. There are at least 17 countries involved in camelid parasitology research, viz. Ethiopia, France, India, Iran, Jordan, Kenya, Libya, Mauritania, Nigeria, Sultanate of Oman, Pakistan, Saudi Arabia, Sudan, Sweden, United Arab Emirates, Uganda and U.S.A. As per published papers in Journal of Camel Practice and Research (JCPR), 173 authors have contributed 72 manuscripts which are appropriately placed in 5 sections. The text of each manuscript published previously in JCPR remains the same except the pattern of numbering the references in the body of text. This book indicates a swing of camelid research during period 1994-2008 and will help identifying the missing links of research in this subject.

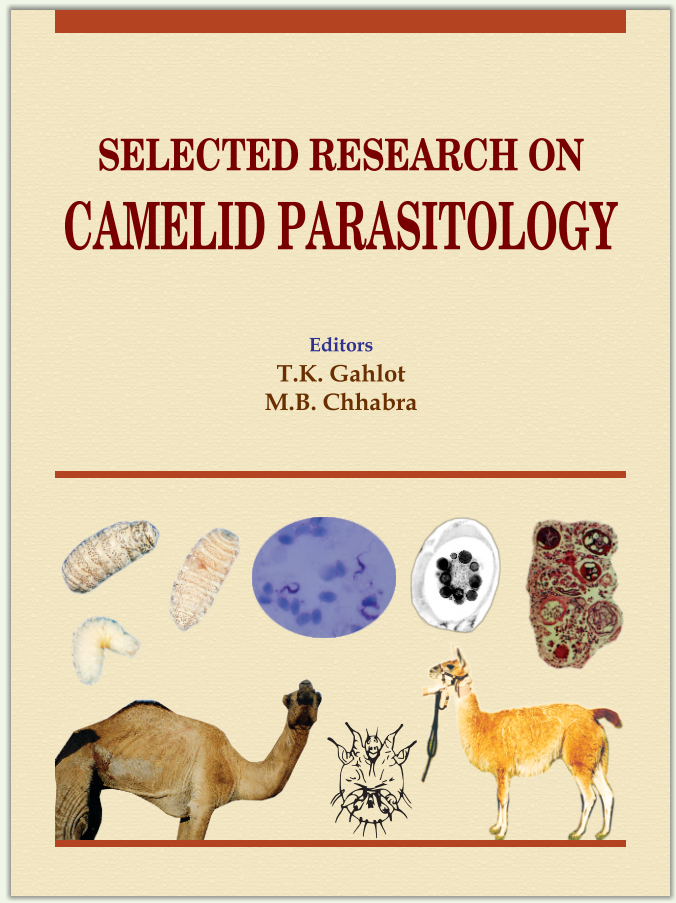

Editors:
T.K. Gahlot and M.B. Chhabra

Edition: 2009

Publisher: **Camel Publishing House**
67, Gandhi Nagar West,
Near Lalgarh Palace
Bikaner 334001 Rajasthan,
India
email: tkcamelvet@yahoo.com
website: www.camelsandcamelids.com

Price: US$ 200 (Abroad)
INR 3000 (India)

ISBN: 81-903140-0-9

DOI : 10.5958/2277-8934.2022.00022.4 Vol 29 No 2, p 161-167

PARASITOLOGICAL AND MOLECULAR INCIDENCE OF *Trypanosoma evansi* IN DROMEDARY CAMELS OF GUJARAT, INDIA

Bhupendrakumar J. Thakre[1], Binod Kumar[1], Nilima N. Brahmbhatt[2] and Krishna Gamit[3]

[1]Department of Veterinary Parasitology, [2]Animal Diseases Diagnosis Laboratory, Veterinary Clinical Complex; [3]Department of Livestock Production Management, College of Veterinary Science and Animal Husbandry, Kamdhenu University, Junagadh-362001, Gujarat, India

ABSTRACT

The present study was aimed to assess the incidence of *T. evansi* infections in camel in Saurashtra region of Gujarat, India, through microscopy and polymerase chain reaction (PCR) methods. Blood samples were collected from 192 camels, randomly. The diagnostic sensitivity and specificity of Field's stain, Giemsa stain and RoTat1.2 polymerase chain reaction (PCR) assays for detection of *T. evansi* in blood samples was evaluated. *T. evansi* infection recorded in camels based on Field's stain, Giemsa stain and RoTat1.2 PCR assays was 3.23%, 8.85% and 22.39%, respectively. Sensitivity of Field's stain was 35.29% while PCR test had 100% sensitivity in comparison to Giemsa stain for the detection of *T. evansi* in blood samples. The analytical sensitivity of newly developed RoTat1.2 PCR assay was determined as 1.07 pg of purified whole blood genomic DNA. Epidemiologically, *T. evansi* was an important pathogen in camels of all age groups but more prevalent in adult animals and in monsoon season.

Key words: Camels, Field's Stain, Giemsa stain, Polymerase chain reaction (PCR), RoTat1.2 VSG gene, Trypanosomosis

T. evansi infection is widely prevalent in different parts of India and is of significant economic importance in livestock production (Mahran, 2004; Juyal *et al,* 2007). The disease has been reported from almost all states of India viz., Haryana, Punjab, Uttar Pradesh and Jammu and Kashmir in northern India; Rajasthan, Gujarat and Maharashtra towards west andra Pradesh, Karnataka, Tamil Nadu towards south and Bihar and West Bengal in eastern India (Juyal *et al,* 2007; Ravindran *et al,* 2008; Kumar *et al,* 2015; Maharana *et al,* 2016). Though, the disease has been studied for the past many decades, the definite diagnosis still suffers from low sensitivity and specificity and as a result, the epidemiology of the disease is far from completely understood. The parasitological examinations frequently fail to detect patent infections because parasitemia is scanty in peripheral blood in chronic forms (Killick- Kendrick, 1968; Abdel-Rady, 2008). Antibody detection based serological diagnosis has limitations of differentiation between current and past infections, persistent titres and the occurrence of false-positive results (Bhutto *et al,* 2010). Accordinly, very high rate of prevalence of *T. evansi* in camels was recorded through various serological tests such as CATT/*T. evansi*, formol gel test, ELISA/VSG RoTat1.2, immune trypanolysis compared to PCR and standard trypanosome detection methods (STDM) (Tehseen *et al,* 2015; Hassan-Kadle *et al,* 2019).

Alternatively, polymerase chain reaction (PCR) has been developed for detection of trypanosomes (Masiga *et al,*1992; Claes *et al,* 2004; Aradaib and Magid, 2006; Konnai *et al,* 2009; Ghorui *et al,* 2012; Elhaig *et al,* 2013). PCR assays have been designed to target different genome sequences and there exists a consensus regarding the difference of sensitivity and specificity between the different PCR methods (Taylor *et al,* 2008; Pruvot *et al,* 2010; Sengupta *et al,* 2010; Tehseen *et al,* 2015). However, the sensitivity of the specificity of different available primers is varying (Pruvot *et al,* 2010; Padmaja, 2012). Based upon Rode Trypanozoon antigen type (RoTat) 1.2., a variable surface glycoprotein (VSG) gene, the *T. evansi* is classified as Type A (presence of RoTat1.2 gene) and Type B (absence of RoTat1.2 gene). *T. evansi* Type A is commonly found while Type B is rare and only reported from some part of Africa (Li *et al,* 2020). Based on the specificity of the targeted gene (Urakawa *et al,* 2001) and wide spread nature of *T. evansi* type A, the present study was aimed to identify *T. evansi*

SEND REPRINT REQUEST TO BINOD KUMAR email: drkumarbinod@gmail.com

infection in camels and to compare the parasitological techniques with RoTat1.2 PCR assay.

Materials and Methods

Study area and sample collection

A total of 192 blood samples were collected from camels at Veterinary Clinical Complex, Veterinary College, Junagadh and animal health camps organised by the institute during year 2017-20. The common clinical signs were loss of appetite, a decrease in productivity and weight loss of animals. A detailed clinical history and animal parameters like age, sex and breed were recorded. Blood samples were collected from the jugular vein into blood collection vials containing an anticoagulant (EDTA) for laboratory examination. *Trypanosoma* parasites were identified through microscopic examination and further confirmation was done by polymerase chain reaction (PCR) assay. To study the seasonal influence on infection rate, three distinct seasons were recognised in a year like rainy/monsoon season between July and October while the other two dry seasons prevail from November to February (winter) and from March to June (summer). For epidemiological study, animals were also grouped age wise, i.e. less the 5 years, 5-10 years and more than 10 years.

Parasitological examination of samples

Thin blood smears were subjected to Giemsa and Field's stains for parasitological examination. The parasites were identified according to the characters described by Soulsby (1982). Each slide was labeled on the smear indicating the animal breed, animal age, sex and date of collection. The remaining blood samples were preserved at -20°C for isolation of whole blood genomic DNA to test *T. evansi* infection through the PCR technique.

DNA extraction and RoTat1.2 PCR

Whole blood genomic DNA was isolated from 200 µl whole blood samples of camels using commercial GeneJET Whole Blood Genomic DNA Purification Mini Kit (Thermo Scientific, Lithuania). The manufacturer's protocol was followed for the DNA purification and DNA was eluted in 200 µl elution buffer. The DNA was stored at -20°C immediate after isolation until further use.

For molecular confirmation of *T. evansi* infection in camel, a set of primers specific to *T. evansi* RoTat 1.2 VSG gene were designed based on sequence available in NCBI (Accession No. AF317914) using online Primer3 web tools (http://primer3.ut.ee/). The primers were picked as LtF3: Forward primer 5'-CCA GGA GAC AGC TAC CTA GA-3' and LtB3: Reverse primer 5'-TGG CTG GTC GTC AAC TTT G-3' which amplify 219 bp fragment of RoTat1.2 gene of *T. evansi*. The designed primers were checked in-silicon for its specificity using the Primer-BLAST programme of NCBI (https://www.ncbi.nlm.nih.gov/tools/primer blast/index.cgi? LINK_LOC= BlastHome). The amplification of the targeted DNA sequence was done in a thermal cycler (Applied Biosystem, USA) in a 200 µL tubes holding a volume of 25 µL reaction mixture. The master mix consisted of 2.5 µL of DreamTaq Green buffer (Thermo Scientific, Lithuania), 0.5 µL of 10 mM dNTP mix (Thermo Scientific, Lithuania), 1 µL each (10 pmol) of the primers, 0.2 µL of DreamTaq DNA Polymerase (Thermo Scientific, Lithuania) and 4 µL of template DNA isolated from camel blood found microscopically positive for *T. evansi*. The nuclease-free water was used in place of DNA as a negative control. The volume was made up to 25 µL with nuclease-free water. The PCR reaction was done at laboratory optimised condition viz., initial denaturation at 95°C for 3 min followed by 35 cycles of denaturing at 96°C for 15 s, primer annealing at 60°C for 20 s and primer extension at 72°C for 25 s. This was followed by the last cycle of extension at 72°C for 5 min and hold at 4°C for an indefinite time. The amplified products were resolved in 1.2% agarose containing 0.5 µg/ml ethidium bromide and visualised by UV transillumination and photographs were taken.

Amplified products from a positive sample were purified using Gene JET Gel Extraction Kit (Thermo Scientific, Lithuania) following the manufacturer's protocol and 10 µl was submitted alogwith forward and reverse primes for Sanger sequencing to commercial service provider (Eurofins Genomics India Pvt. Ltd., Bengaluru, India). Obtained sequences were aligned and checked using BioEdit programme and BLASTn (NCBI, USA). Finally, sequence was submitted to GenBank (NCBI, USA).

All 192 samples tested through microscopic test were also tested using currently optimised RoTat1.2 PCR assay as discussed above.

Specificity and sensitivity of the PCR primers

To assess the specificity of the RoTat1.2 PCR assay, the total genomic DNA extracted from whole blood of different animals infected with other common haemoparasites viz., *Babesia bigemina, Theileria annulata, T. orientalis, B. canis vogeli, B. gibsoni, B. equi, B. cabali, Ehrlichia canis, Anaplasma marginale*

and Hepatozoon canis present in the laboratory were included in PCR assay and reactions were noted after resolving the PCR products on 1.2% agarose gel.

The analytical sensitivity of the PCR assay was assessed by the use of different concentrations of DNA diluted in nuclease-free water (NFW). The concentration of whole blood genomic DNA isolated from a microscopically positive blood sample was determined through Qubit®dsDNA BR assay kit in Qubit™ 4 Fluorometer (Thermo Scientific, Singapore) as per the manufacturer's instructions. To assess the threshold limit of PCR assay, DNA was diluted in five fold serial dilutions with NFW and the reaction was performed with each dilution as a template (1 µl) at optimised conditions. The amplification of the DNA sequence was confirmed by agarose gel (1.2%) electrophoresis containing ethidium bromide.

Statistical analysis

Chi square (χ^2) test was used for comparing the diagnostic methods and different epidemiological parameters and $p<0.05$ was considered as a significant difference between the tests. Using Giemsa stain as gold standard, the sensitivity and specificity of RoTat1.2 PCR and Field's stain microscopy were determined using Fischer's extract test at a 95% confidence interval (CI).

Results and Discussion

The microscopic examinations of thin blood smears revealed 3.23% and 8.85% infections of *Trypanosoma evansi* with Field's and Giemsa stains, respectively in camels. The difference between the two staining methods was statistically significant ($p<0.05$). When Giemsa stain was taken as gold standard, the sensitivity of Field's stain was found 35.29% with a range of 14.21 to 61.67%, specificity was 100% with a range of 97.91 to 100.00% Positive Predictive Value (PPV) was 100.00% and Negative Predictive Value (NPV) was 94.09% with a range of 91.80% to 95.76 at 95% confidence interval (CI). The present finding was in aggrement with results of Mendiratta *et al* (2006) where 34.57% sensitivity, 100% specificity and PPV and 87.23% NPV of Field's stain was observed in comparison to Leishman's stain for the detection of *Plasmodium falciparum* in human blood smear. However, higher sensitivity (97.72%) of Field's stain was recorded by Gaikwad and Chaya (2016). Though, Field's staining was low cost and rapid method but due to its lower sensitivity, Giemsa stain was preferred over it (Monzón *et al,* 1990).

Selection of most suitable target genes/nucleic acid fragments and designing of oligo-primers were the prerequisite for development of specific PCR assay. In present study, we targeted 219 bp fragments of very specific RoTat1.2 VSG genes of *T. evansi*. It was successfully amplified and optimised without any non-specific reactions (Fig 1A). To confirm the amplified product of targeted gene, sequence was generated from purified PCR product and submitted to GenBank (NCBI, USA) and accession was obtained (MZ032003). Upon BLASTn analysis (NCBI, USA), the newly generated sequence was aligned with 22 sequences of VSG gene of *T. evansi* available in GenBank. They showed 100% identities with maximum sequences (n=17; 10 sequences were having 100% query coverage) and 99.02% identities with 4 sequences (only 46% query coverage). Only one sequence (MT501210) which was having 100% query coverage shows 98.63% identities. This confirmed that the amplified product was from targeted organism. Moreover, the assay was found highly specific to detect the targeted organism as the primers pair did not react to the DNA of other commonly available haemoprotozoans in this region like *Babesia bigemina*, *Theileria annulata*, *T. orientalis*, *B. canis vogeli*, *B. gibsoni*, *B. equi*, *B. cabali*, *Ehrlichia canis*, *Anaplasma marginale* and *Hepatozoon canis* or host DNA at the optimised PCR conditions (Fig 1B).

RoTat1.2 VSG gene was targeted by many researchers for the specific diagnosis of *T. evansi* in animals including camels. Recently, Kumar *et al* (2021) targeted 200 bp fragment of RoTat1.2 gene to develop loop-mediated isothermal amplification (LAMP) assay for detection of *T. evansi* in domestic animals. Similarly, Li *et al* (2020) targeted RoTat1.2 gene fragment to develop recombinase polymerase amplification (RPA) lateral flow assay for detection of active *T. evansi* infection. Boushaki *et al* (2019) targeted 488 bp fragment of RoTat1.2 VSG and reported 11.2% prevelance of *T. evansi* in camels in Algeria compared to only 2.4% prevelance of *T. evansi* through Giemsa stained thin blood smear examination. However, Tehseen *et al* (2015) has compared the RoTat1.2 PCR with TBR1/2 PCR for the diagnosis of *T. evansi* in camels and they found almost comparable results. Though, *T. evansi* without RoTat1.2 VSG (called *T. evansi* Type B) was also recorded in certain part of Africa and Saudi Arabia (Ngaira *et al,* 2005; Salim *et al,* 2011; Alanazi *et al,* 2018) but in India it was not recorded till now.

Another important feature to be studied for a good primer was its higher analytical sensitivities.

Here, the analytical sensitivity of the assay was found upto1.07 pg of DNA (Fig 1A) which was comparable to the other PCR assay for diagnosis of *T. evansi* (Omanwar *et al*, 1999; Fernández *et al*, 2008; Sengupta *et al*, 2010; Pruvot *et al*, 2010).

In the present study, 22.39% samples were found positive for *T. evansi* using PCR assay (Fig 2) which is siginificantly ($p<0.05$) higher as compared to microscopy (Table 1). While considering the Giemsa staining technique as a gold standard, the sensitivity of PCR test was found 100% with a range of 80.49% to 100.00%, specificity was 85.14% with a range of 78.99 – 90.06%, PPV 39.53% (31.44% to 48.25%) and NPV 100% at 95% CI. PPV indicate the probability that the disease was present when the test was positive and NPV indicated about the probability that the disease was not present when the test was negative. Having 100% sensitivity and NPV for a test are good indicatiors for its utility in epidemiological studies as well as diagnosis of infected animals without any false negative results. Lower specificity and PPV of PCR was just because of inherent low sensitivity of microscopy. Similarly, Ereqat *et al* (2020) recorded 14.3% more positivity to *T. evansi* in animals in Palestine through 18S rRNA PCR (17%) compared to wet mount microscopy (2.7%). They recorded highest prevalence of *T. evansi* in camel (about one-third) compared to other domestic animals. Likewise, Ravindran *et al* (2008) also recorded significantly higher positivity of *T. evansi* infection through PCR (19.84%) comapared to Giemsa stained thin blood smear examination (1.5%). Among the different animals studied by him, the higest incidence of *T. evansi* was recorded in camels (~ 81% of total positive case) followed by donkeys and least in dogs. The low sensitivity of microscopy using thin blood smear may be related to low parasitaemia which might be due to early and/or chronic infection, visual mistakes made during the examination of slides, destruction of red blood cells due to hemolysis, the thickness, dirtiness or unsuitable blood smear staining compared to PCR (El-Naga and Barghash, 2016). Blood smear examination proved to be of limited value in diagnosis of subacute or chronic cases (Herbert and Lumsden, 1976; Desquesnes, 2004). In contrast, a high sensitivity of PCR with purified whole blood DNA was confirmed and was successful in diagnosis of infectious diseases as compared to

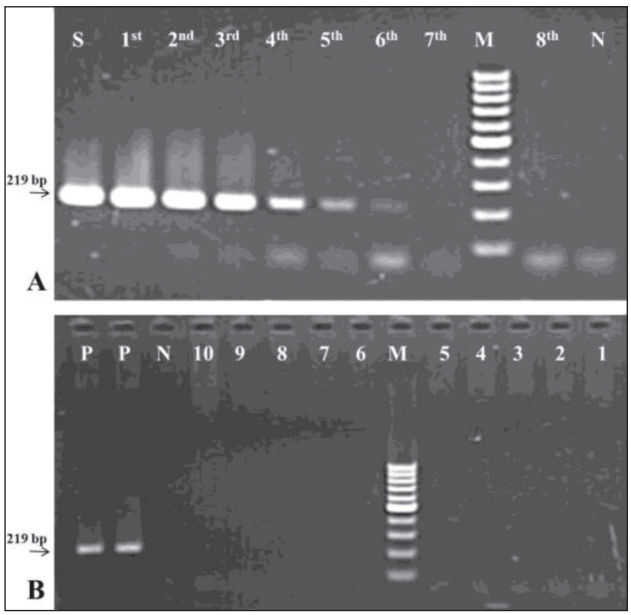

Fig 1. Analytical sensitivity and specificity of RoTat1.2 PCR for identification of *T. evansi* in camels. A. Determination of sentisivity on *T. evansi* positive samples [S- PCR on undiluted DNA, 1st to 8th - PCR on serial five-fold diluted DNA, N- no template control (negative); M- DNA ladder (100 bp DNA ladder, ready-to-use, Thermo scientific, Lithuania)]. **B.** Assessment of specificity of RoTat1.2 PCR [1. *Babesia bigemina*, 2. *Theileria annulata*, 3. *T. orientalis*, 4. *B. canis vogeli*, 5. *B. gibsoni*, 6. *B. equi*, 7. *B. cabali*, 8. *Ehrlichia canis*, 9. *Anaplasma marginale*, 10. *Hepatozoon canis*, N- Negative control (host DNA), P- positive control].

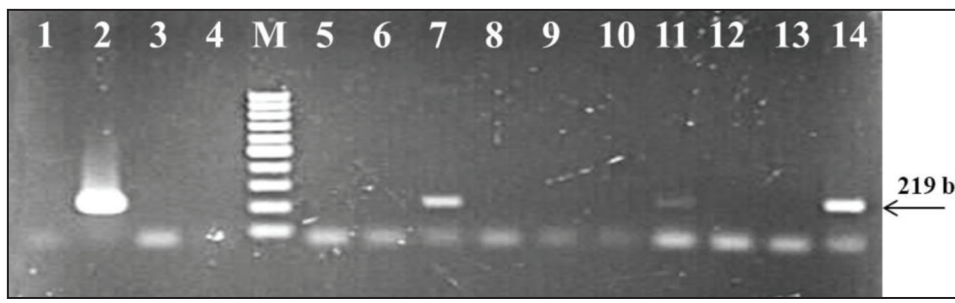

Fig 2. Identification of *T. evansi* infection in camels using RoTat1.2 PCR [1- negative control, 2- positive control, 3 to 14- field samples and M- 100 bp DNA ladder (100 bp DNA ladder, ready-to-use, Thermo Scientific, Lithuania)]. **Here,** samples 7, 11 and 14 showing positive reaction for *T. evansi* infection while, only sample no. 14 found positive through microscopy (Giemsa stain).

parasitological method (Gonzales *et al,* 2003; Abdel-Rady, 2006; Baticados *et al,* 2011).

Considering the PCR assay as an epidemiological tools to identify the *T. evansi* infection in camels, the highest incidence of infection was recorded in monsoon followed by summer and lowest in winter (Table 2). This might be due to the good environmental conditions for the fly to breed thus led to higher occurrence of disease (Rayulu *et al,* 2007; Maharana *et al,* 2016; Barghash, 2016).

Age wise incidence of *T. evansi* infection in camels was determined where significantly lower incidence of infection was noted in less than 5 years age groups compared to more than 5 years aged animals (Table 2). Similarly, Giro and Kula Jilo (2020) reported higher incidence of *T. evansi* infection in >4 years (18.12%) aged followed by 3-4 years (6.98%) and lowest in <3 years old camels (4.67%). Contrarily, some other scientists reported higher incidence of the disease in young camel of less than 5 years of age (Njiru *et al,* 2004; Singh *et al,* 2004). The incidence of infection varied with geographic area which may be correlated with the presence of vectors population. However, stress, inadequate nutrition, inadequate exercise, close confinement, transportation and managemental negligence might have played a vital role for predisposing the disease in young and adult group (Gutierrez *et al,* 2000; Njiru *et al,* 2002; Njiru *et al,* 2004; Moghaddar and Diantpor, 2009; Tadesse *et al,* 2012).

Table 1. Detection of *T. evansi* infections in camels (n=192) through microscopy and RoTat1.2 PCR assay.

	Giemsa stain	Field's stain	PCR assay
Positive	17	6	43
Negative	175	186	149
Percentage positive	8.85%	3.23%	22.39%

Table 2. Sex wise, age wise and seasonal incidence of *T. evansi* in camels through RoTat1.2 PCR assay.

Parameters	Total samples	Incidence (%)
Sex wise incidence		
Male	88	16 (18.18%)
Female	104	27 (25.96%)
Age wise incidence		
< 5 years	77	11 (14.28%)
5-10 year	90	26 (28.88%)
>10 years	25	06 (24.00%)
Seasonal incidence		
Summer	74	16 (21.62%)
Monsoon	91	23 (25.27%)
Winter	27	04 (14.81)

Trypanosomosis, which is a vector-borne disease, has little difference between the sex, however, in animals of present study a higher incidence of *T. evansi* was recorded in females (25.96%) compared to males (18.18%) (Table 2). This could be due to successive pregnancies and stress of lactations in females. Similarly, Rayulu *et al* (2007) and Padmaja (2012) reported higher incidence in females whereas it was lower in geldings. This might be due to prevailing managemental practices and population ratio of male to female (Njiru *et al,* 2002; Singh *et al,* 2004; Barghash *et al,* 2014; El-Naga and Barghash, 2016).

In conclusion, the *T. evansi* was more prevalent in adult animals during monsoon season in Saurashtra region of India. Though, microscopy was still considered as gold standards, the molecular test like PCR based on RoTat1.2 gene may be the method of choice for epidemiological studies of *T. evansi* with significantly higher sensitivity along with 100% NPV.

Acknowledgement

Authors are highly thankful to the Director of Research, Junagadh Agricultural University, Junagadh for providing funds and facilities at department. We are also thankful to Principal and Dean of College of Veterinary Science and Animal Husbandry for providing support in the research work.

References

Abdel-Rady A. Comparison of card agglutination test and parasitological methods for the diagnosis of camel trypanosomosis in Egypt: In Proceedings of the 2004 International Science Conference on Camels. Qassim, Saudi Arabia. 2006; pp 571-576.

Abdel-Rady A. Epidemiological studies (parasitological, serological and molecular techniques) of *Trypanosoma evansi* infection in camels (*Camelus dromedarius*) in Egypt. Veterinary World. 2008; 1(11):325-328.

Alanazi AD, Puschendorf R, Salim B, Alyousif MS, Alanazi IO and Al-Shehri HR. Molecular detection of equine trypanosomosis in the Riyadh Province of Saudi Arabia. Journal of Veterinary Diagnostic Investigation 2018; 30(6):942-945.

Aradaib IE and Magid AA. A simple and rapid method for detection of *T. evansi* in dromedary camel using a nested Polymerase Chain Reaction. Kinetoplastid Biology and Disease. 2006; 5:2.

Barghash SM. Evaluation of *in vitro* and *in vivo* activities of some medicinal plants against trypanosomosis. International Journal of Advanced Research. 2016; 4:1169-1178.

Barghash SM, Abou El-Naga TR, El-Sherbeny EA and Darwish AM. Prevalence of *Trypanosoma evansi* in Maghrabi Camels (*Camelus dromedarius*) in Northern-West Coast, Egypt using Molecular and Parasitological Methods. Acta Parasitologica. 2014; 5(2):125-132.

Baticados WN, Fernandez CP and Baticados AM (2011). Molecular detection of *Trypanosoma evansi* in cattle from Quirino province, Philippines. Veterinarski Archive 81(5):635-646.

Bhutto B, Gadahi J, Shah G, Dewani P and Arijo A. Field investigation on the prevalence of trypanosomosis in camels in relation to sex, age, breed and herd size. Pakistan Veterinary Journal. 2010; 30:175-177.

Boushaki D, Adel A, Dia ML, Büscherf P, Madani H, Brihoum BA, Sadaoui H, Bouayed NG and Issad NK. Epidemiological investigations on *Trypanosoma evansi* infection in dromedary camels in the South of Algeria. Heliyon. 2019; 5:e02086.

Claes F, Radwanska M, Urakawa T, Majiwa PA, Goddeeris BM and Buscher P. Variable surface glycoprotein RoTat 1.2 PCR as aspecific diagnostic tool for the detection of *Trypanosoma evansi* infections. Kinetoplastid Biology and Disease. 2004; 3:3.

Desquesnes M. Livestock Trypanosomoses and Their vectors in Latin America, CIRAD-EMVT publication, OIE, Paris, France. 2004.

Elhaig MM, Youssef AI and El-Gayar AK. Molecular and parasitological detection of *Trypanosoma evansi* in camels in Ismailia, Egypt. Veterinary Parasitology. 2013; 198(1):214-218.

El-Naga TRA and Barghash SM. Blood parasites in camels (*Camelus dromedarius*) in northern west coast of Egypt. Journal of Bacteriology and Parasitology. 2016; 7(1):1-7.

Ereqat S, Nasereddin A, Al-Jawabreh A, Al-Jawabreh H, Al-Laham N and Abdeen Z. Prevalence of *Trypanosoma evansi* in livestock in Palestine. Parasites & Vectors. 2020; 13:21. https://doi.org/10.1186/s13071-020-3894-9.

Fernades D, Gonzale B, Eleizalde M, Gonzale, EM, Prronr T and Alfonzo MEM. *Trypanosoma evansi*: A comparison of PCR and Parasitological diagnostic tests in experimentally infected mice. Experimental Parasitology. 2008; 121(1):1-7.

Gaikwad D and Chaya AK. Comparative staining methods for microscopic diagnosis of malaria. Indian Journal of Research. 2016; 5(8):236-237.

Ghorui SK, Kumar S and Patil NV. Nucleotide sequence of variable surface glycoprotein (VSG) gene from genomic DNA of *Trypanosoma evansi* isolated from camel, direct submission to GenBank with accession number JX134605. 2012.

Giro A and Jilo K. Prevalence of camel trypanosomosis and associated risk factors in Arero district, Borena Zone, Southern Ethiopia. International Journal of Veterinary Sciences Research. 2020; 6(1):014-022.

Gonzales JL, Jones TW, Picozzi K and Cuellar HR. Evaluation of a polymerase chain reaction assay for the diagnosis of bovine trypanosomosis and epidemiological surveillance in Bolivia. Kinetoplastid Biology and Disease. 2003; 2:8.

Gutierrez C, Juste MC, Corbera JA, Magnus E, Verloo D and Montoya JA. Camel trypanosomosis in the Canary Islands: Assessment of seroprevalence and infection rates using the card agglutination test (CATT/*T. evansi*) and parasite detection tests. Veterinary Parasitology. 2000; 90(1):155-159

Hassan-Kadle AA, Ibrahim AM, Nyingilili HS, Yusuf AA, Vieira TSWJ and Vieira RFC. Parasitological, serological and molecular survey of camel trypanosomosis in Somalia. Parasites and Vectors. 2019; 12:598. https://doi.org/10.1186/s13071-019-3853-5.

Herbert WJ and Lumsden WH. *Trypanosoma brucei*: a rapid match-ing methods for estimating the host's parasitemia. Experimental Parasitology. 1976; 40:427-431.

Juyal PD, Kaur P and Singh NK. Control strategies against trypanosomosis (Surra) due to *Trypanosoma evansi* in India. In: Proceedings of the National Seminar on "Recent diagnostic trends and control strategies for haemoprotozoan infections in livestock", Feb, 9-11, 2007, held at S.D. Agricultural University, Sardar Krushinagar, Gujarat. 2007; pp 4-7.

Killick-Kendrick R (1968).The diagnosis of trypanosomosis of livestock. A review of current techniques. Veterinary Bulletin 38:191-197.

Konnai S, Mekata H, Mingala CN, Abes NS, Gutierrez CA, Herrera RV, Dargantes AP, Witola WH, Cruz LC, Inoue N, Onuma M and Ohashi K. Development and application of a quantitative real-time PCR for the diagnosis of Surra in water buffaloes. Infection, Genetics and Evolution. 2009; 9:449-452.

Kumar Binod, Maharana Biswa, Brahmbhatt Nilima, Thakre B and Parmar Vijay. Development of a loop-mediated isothermal amplification assay based on RoTat1.2 gene for detection of Trypanosoma evansi in domesticated animals. Parasitology Research. 2021; 120. 10.1007/s00436-021-07118-7.

Kumar R, Kumar S, Virmani N and Yadav SC. Transplacental transmission of *Trypanosoma evansi* from experimentally infected donkey mare to neonatal foal. Journal of Equine Veterinary Science. 2015; 35:337-341.

Li Z, Pinto Torres JE, Goossens J, Stijlemans B, Sterckx YG and Magez S. Development of a recombinase polymerase amplification lateral flow assay for the detection of active *Trypanosoma evansi* infections. PLoS Neglected Tropical Diseases. 2020; 14(2):e0008044.

Maharana BR, Tewari AK, Saravanan BC and Sudhakar NR. Important haemoprotozoan diseases of livestock: Challenges in current diagnostics and therapeutics: An update. Veterinary World. 2016; 9(5):487-95.

Mahran OM. Some studies on blood parasites in camels (*Camelus dromedarius*) at Shalatin City, Red Sea Governorate. Assiut Veterinary Medical Journal. 2004; v59:102.

Masiga DK, Smyth AJ, Hayes P, Bromidge TJ and Gibson WC. Sensitive detection of trypanosomes in tsetse flies by DNA amplification. International Journal for Parasitology. 1992; 22:909-918.

Mendiratta DK, Bhutada K, Narang R and Narang P. Evaluation of different methods for diagnosis of

Plasmodium falciparum malaria. Indian Journal of Medical Microbiology. 2006; 24(1):49-51.

Moghaddar N and Diantpour V. Distribution pattern of *Trypanosoma evansi* in camels (*Camelus dromedarius*) in Iran. Journal of Camel Practice and Research. 2009; 16:73-75

Monzon CM and Villavicencio VI. Serum proteins in guinea-pigs and horses infected with *Trypanosoma evansi* (Steel, 1885). Veterinary Parasitology. 1990; 36(3-4):295-301.

Ngaira JM, Olembo NK, Njagi EN and Ngeranwa JJ. The detection of non-RoTat 1.2 *Trypanosoma evansi*. Experimental Parasitology. 2005; 110(1):30-8.

Njiru ZK, Bett IM, OLE-Mapeny JB, Githiori JM and Ndung UO. Trypanosomosis and helminthosis in camels: comparison of ranch and traditional camel management systems in Kenya. Journal of Camel Practice and Research. 2002; 34:183-186.

Njiru ZK, Constantine CC, Ndung'u JM, Robertson I, Okaye S, Thompson RCA and Reid SA. Detection of *Trypanosoma evansi* in camels using PCR and CATT/*T. evansi* tests in Kenya. Veterinary Parasitology. 2004; 124:187-199.

Omanwar S, Rao JR, Basagoudanavar SH, Singh RK and Butchaiah G. Direct and sensitive detection of *Trypanosoma evansi* by polymerase chain reaction. Acta Veterinaria Hungarica. 1999; 47:351-59.

Padmaja K. Haemato-biochemical studies of camels infested with trypanosomosis. Veterinary World. 2012; 5:356-358.

Pruvot M, Kamyingkird K, Desquesnes M, Sarataphan N and Jittapalapong S. A comparison of six primer sets for detection of *Trypanosoma evansi* by polymerase chain reaction in rodents and Thai livestock. Veterinary Parasitology. 2010; 171:185-193.

Ravindran R, Rao JR, Mishra AK, Pathak KML, Babu N, Satheesh CC and Rahul S. *Trypanosoma evansi* in camels, donkeys and dogs in India: comparison of PCR and light microscopy for detection. Veterinarski Arhiv. 2008; 78(1):89-94.

Rayulu VC, Singh A and Chaudhri SS. Monoclonal antibody based immunoassays for detection of circulating antigens of *Trypanosoma evansi* in buffaloes. Italian Journal of Animal Science. 2007; 6:907-910.

Salim B, Bakheit MA, Kamau J, Nakamura I and Sugimoto C. Molecular epidemiology of camel trypanosomosis based on ITS1 rDNA and RoTat 1.2 VSG genes in the Sudan. Parasites and Vectors. 2011; 4:31-36.

Sengupta PP, Balumahendirana M, Suryanaryanab W, Raghavendra AG, Shomea BR, Gajendragada MR and Prabhudas K. PCR-based diagnosis of surra-targeting VSG gene: experimental stud-ies in small laboratory rodents and buffalo. Veterinary Parasitology. 2010; 171:22-31.

Singh N, Pathak KML and Kumar R. A comparative evaluation of parasitological, serological and DNA amplification methods for diagnosis of natural *Trypanosoma evansi* infection in camels.Veterinary Parasitology. 2004 126:365-373.

Soulsby EJL. Helminths, Arthropods and Protozoa of Domesticated Animals, 7th edn. Baillier Tindall and Cassel Ltd, London. 1982.

Tadesse A, Omar A, Aragaw K, Mekbib B and Sheferaw D. A study on camel trypanosomosis in Jijiga zone, Eastern Ethiopia. Journal of Advanced Veterinary and Animal Research. 2012; 2:216-219.

Taylor TK, Boyle DB and Bingham J. Development of a TaqMan PCRassay for the detection of *Trypanosoma evansi*, the agent of surra. Veterinary Parasitology. 2008; 153(3-4):255-264.

Tehseen S, Jahan N, Qamar MF, Desquesnes M, Shahzad MI, Deborggraeve S and Büscher P. Parasitological, serological and molecular survey of *Trypanosoma evansi* infection in dromedary camels from Cholistan Desert, Pakistan. Parasites and Vectors. 2015; 8:415 DOI 10.1186/s13071-015-1002-3

Urakawa T, Verloo D, Moens L, Büscher P and Majiwa PA. *Trypanosoma evansi*: cloning and expression in *Spodoptera fugiperda* insect cells of the diagnostic antigen RoTat1. 2 Experimental Parasitology. 2001; 99:181-189.

BACK ISSUES OF JCPR AVAILABLE

ISSN 0971-6777 (Print)
ISSN 2277-8934 (Online)

JOURNAL OF CAMEL PRACTICE AND RESEARCH

www.camelsandcamelids.com • www.indianjournals.com

Volume 24 December 2017 Number 3

In This Issue

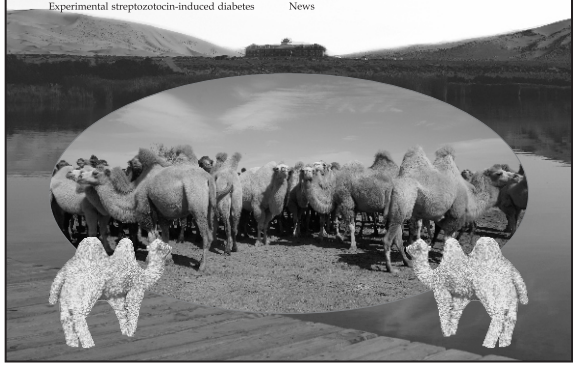

ISSN 0971-6777 (Print)
ISSN 2277-8934 (Online)

JOURNAL OF CAMEL PRACTICE AND RESEARCH

www.camelsandcamelids.com • www.indianjournals.com

Volume 25 April 2018 Number 1

In This Issue

ISSN 0971-6777 (Print)
ISSN 2277-8934 (Online)

JOURNAL OF CAMEL PRACTICE AND RESEARCH

www.camelsandcamelids.com • www.indianjournals.com

Volume 25 August 2018 Number 2

In This Issue

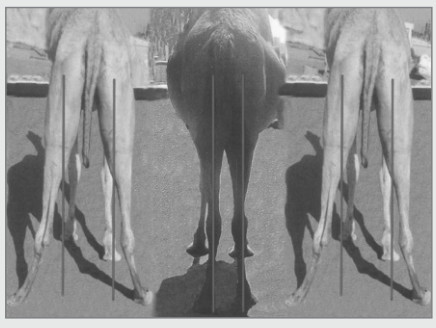

ISSN 0971-6777 (Print)
ISSN 2277-8934 (Online)

JOURNAL OF CAMEL PRACTICE AND RESEARCH

www.camelsandcamelids.com • www.indianjournals.com

Volume 25 December 2018 Number 3

In This Issue

See the details of list of contents of all previous issues of JCPR on our website
www.camelsandcamelids.com

Kindly refer querries to: Dr. T.K. GAHLOT, Editor, JCPR
email: tkcamelver@yahoo.com

DOI : 10.5958/2277-8934.2022.00023.6 Vol 29 No 2, p 169-176

BABESIOSIS AND ANAPLASMOSIS IN CAMELS (*Camelus dromedarius*) OF SAUDI ARABIA

Jamila S. Al Malki[1], Nahed Ahmed Hussien[1], Ehab M. Tantawy[2], Muataz A. Abdalla[3] and Malek A. Al Jawbrah

[1]Department of Biology, College of Science, Taif University, P.O. Box 11099, Taif 21944, Saudi Arabia
[2]Research and Development Sector, EGYVAC, VACSERA, Giza 12311, Egypt
[3]Department of Biology, University College of Al-Khurmmah, Taif University, P.O. Box 11099, Saudi Arabia

ABSTRACT

An epidemiological study was conducted on the occurrence of babesiosis and anaplasmosis infection in camels (*Camelus dromedarius*) in the Taif region of Saudi Arabia. A total of 102 blood samples were collected from apparently healthy camels, of varying ages and sex, from three different areas of the Taif region. The blood samples were investigated using Giemsa-stained blood smears and species-specific Polymerase chain reaction (PCR) (targeting 18S rRNA and the major surface protein–1β encoding genes for *Babesia* and *A. marginale*, respectively). The overall prevalence was 64.70% with a higher infection rate of *Anaplasma* (46.10%) than *Babesia* sp. (18.62%). In addition, there is a co-infection of both pathogens with prevalence rate 19.70%. According to age: the infection rate was highly significant in the younger animals (≤5 years) (33.33% and 58.97%) than older animals (>5 years) (9.52% and 38.09%) for *Babesia* and *Anaplasma*, respectively at p> 0.05. On the other hand, according to gender, the infection rate in males (29.73% and 72.97%) was higher than in females (12.31% and 30.77%) for *Babesia* and *Anaplasma* sp., respectively at p> 0.05. In conclusion, the present study adds insight into the epidemiology of babesiosis and anaplasmosis in the Taif region, Makkah Province of Saudi Arabia that needs control strategies to focus on the livestock.

Key words: *Anaplasma*; *Babesia*; *Camelus dromedarius*; prevalence; Saudi Arabia

Babesia and *Anaplasma* species are the most important tick-borne haemoparasites that may cause a serious threat to livestock, pets, and wildlife throughout the world (Guglielmone *et al*, 2015). Babesiosis and anaplasmosis are two separate diseases that often present in the same animal together (Kocan *et al*, 2010). *Babesia* species are transmitted by ixodid ticks to the vertebrate host, where they replicate in the red blood cells (Homer *et al*, 2000). Anaplasmosis is caused by *A. marginale*, which is worldwide spread and endemic in various regions in Africa and Asia (Kocan *et al*, 2003; 2010). Anaplasmosis is transmitted by at least 20 tick species (Stiller and Marchette, 1982) and disease causes serious health problems leading to reductions in animal productivity and substantial economic losses (El-Ashker *et al*, 2015).

Tick and tick-borne diseases remain a major threat to animals, causing serious economic losses in tropical and subtropical countries, including Saudi Arabia (Al-Nabati *et al*, 2022). These infections are regarded as a serious health problem, as they affect animal health, productivity, and performance including *Babesia* and *Anaplasma* infections (Megersa, 2010). Recently, it was reported a low prevalence of *Anaplasma platys* (5.3%) in local camels, however all samples (170 camels) tested negative for *Babesia* spp. and *Theileria* spp. in Riyadh Province of Saudi Arabia (Alanazi *et al*, 2020). In Asir Province, another study carried out in camels found that the overall prevalence was 2% with *Anaplasma* sp., while all the blood samples were free from *Babesia* sp. (Alshahrani *et al*, 2020). According to Al-Nabati *et al* (2022) the estimated overall prevalence of *Anaplasma* infection in camels was 44.99% in Riyadh and Eastern Region of Saudi Arabia. While *Babesia* sp. infection was not observed in any blood samples in the same study.

However, the prevalence of *Babesia* and *Anaplasma* species in Saudi Arabian camels, especially in the western region is least studied. Therefore, this study contributes to understanding the epidemiology of Babesiosis and Anaplasmosis infections in local camels in the Taif region of Makkah Province of Saudi Arabia.

Materials and Methods

Study area and blood sample collection

A total of 102 blood samples of apparently healthy camels (females (n=65), aged 3-12 years;

SEND REPRINT REQUEST TO JAMILA S. Al MALKI (j.ali@tu.edu.sa) and NAHED AHMED HUSSIEN (n.nahed@tu.edu.sa)

males (n=37), aged 1-7 years) were collected from three different areas of the Taif region (21°5668571N 40°7019237E, 21°25732N 40°50762E, and 21°2606711N 40°510672E). Data about camels such as age, gender was also recorded for each camel. About 2ml of blood samples (from ear veins) of camels were collected in EDTA coated tubes and obtained through veterinarians as per their periodic examination from the period December 2020 to February 2021.

Microscopic examination

Smears were made for all samples and stained with 10% buffered Giemsa, and examined under a light microscope for *Babesia* sp. and *Anaplasma* sp. diagnoses (Schalm, 1971).

DNA extraction

DNA was extracted manually by using low TKM1 (100mM Tris-HC1, pH 7.4, 250mM sucrose, 10mM EDTA) and high TKM2 (Tris HCl 10 mM pH 7.6, 10 mM KCl, 10 mM $MgCl_2$, 0.4 M NaCl, and 2mM EDTA) salt buffer according to Ahmad *et al* (2007). DNA was finally dissolved in 100 µl autoclaved Milli-Q water for further evaluation.

PCR amplification

Two different polymerase chain reactions were performed on the extracted DNA for *Babesia* sp. and *A. marginale* detection. Forward Bab-sp-F and reverse Bab-sp-R primers were used to amplify a 428 bp of small 18S rRNA gene fragment targeting *Babesia* sp. While MAR1bB2F and MAR1bB2R primers were used to amplify a 265 bp of the major surface protein–1β encoding gene (MAR1bB2) targeting *A. marginale* (Table 1).

PCR amplification was done in a total reaction volume of 20 µl: 7 µl H_2O, 1 µl (20 pmole) of each forward and reverse primers, 1 µl extracted DNA, and finally 10µl of 2× master mix. For both reactions: PCR amplification was done in a total reaction volume of 20 µl: 7 µl H_2O, 1 µl (20 pmole) of each forward and reverse primers, 1 µl extracted DNA, and finally 10µl of 2× master mix. The PCR reaction was set up with initial denaturation at 94°C (5 mins), 40 cycles of denaturation at 94°C (30 s), annealing at 61°C or 57 °C (30 s), and then extension at 72°C (45 s) for *Babesia* sp. and *A. marginale*, respectively. The final extension at 72°C (10 mins) was necessarily done for complete amplification. PCR products were separated on 1.5 % agarose gel (at 100V, 60 min), visualised, and then photographed by a gel documentation system. A low molecular weight DNA marker (50-1500 bp) was used in the agarose gel to confirm the amplified amplicon sizes.

Sequencing and phylogenetic evaluation

PCR products of *Babesia* sp. and *A. marginale* was subjected to sequencing using an ABI Prism 3730 Genetic Analyser automated sequencer. Sequences were aligned with others in the Genbank using online NCBI BLAST, phylogenetically estimated, and finally viewed as rectangular cladogram in the phylogenetic Tree View (Kuznetsov and Bollin, 2021).

Statistical analysis

The significant differences regarding the prevalence of *Babesia* and *Anaplasma* and their risk factors, such as age, gender, and source of the camels were calculated by c2 tests using a program in Statistical Package for the Social Sciences (SPSS), version 20.0, at $P< 0.05$.

Results

Babesia and *Anaplasma* sp. were detected microscopically from Giemsa's-stained blood films as shown in Fig 1. The overall infection of haemoparasites in camels was 64.70%, where 66 animals out of 102 were infected. There was a significant higher infection rate for *Anaplasma* sp. (46.10%) in comparison to *Babesia* sp. (18.62%) in camels at $p < 0.05$ (Table 2). There was a co-infection of *Babesia* and *Anaplasma* in 13 out of 102 (19.70%) camels of the total samples. PCR evaluation detected more positive samples than the parasitological assay as shown in Table 2.

According to the age the maximum infection rate was found in the younger animals (≤5 years) for

Table 1. Oligonucleotide sequences of primers used for PCR and sequencing in the present study.

Targeted Parasite	Targeted gene	Primers' name	Primers' sequences	PCR product (bp)	Reference
Babesia sp.	18S rRNA	Bab-F	5′-GTTTCTGCCCCATCAGCTTGAC-3′	428	Hilpertshauser *et al*, 2006
		Bab-R	5′-CAAGACAAAAGTCTGCTTGAAAC -3′		
A. marginale	major surface protein–1β encoding gene	MAR1bB2F	5′-GCTCTAGCAGGTTATGCGTC-3′	265	El-Naga and Barghash, 2016.
		MAR1bB2R	5′-CTGCTTGGGAGAATGCACCT-3′		

Babesia (33.33%) and *Anaplasma* (58.97%) (Table 3). On the other hand, this rate was significantly decreased in older animals (>5 years) for *Babesia* (9.52%) and *Anaplasma* (38.09%) at $p < 0.05$. The prevalence in camels concerning gender was significantly different at $p < 0.05$. The infection rate in males (29.73% and 72.97%) was higher than in females (12.31% and 30.77%) for *Babesia* sp. and *Anaplasma* sp., respectively. According to source the imported camels (80%) are highly infected than the local ones (44.33%) for *Anaplasma* sp., but this was contrary to *Babesia* sp. prevalence in local (16.49%) and imported (15.80%) animals as shown in Table 3.

Extracted DNA was used to amplify two separate genes' loci, 18S rRNA and major surface protein–1β encoding gene, for both *Babesia* sp. and *A. marginale*, to yield amplicons of 428 bp, and 265 bp, respectively. The present results report the success of PCR amplification for both selected portions as shown in Fig 2. However, the presence of other lower or higher bands, than the expected size of amplicons is non-specific.

Randomly selected PCR products from both loci were sequenced by using their forward/reverse primers and were blasted with other related sequences in different countries. Phylogenetic trees were constructed from those sequences according to higher percentage identity and query coverage range (Fig 3).

The BLAST analysis showed that the present sequence of the major surface protein–1β encoding gene related to *A. marginale* was found in

Table 2. Prevalence of *Babesia* and *Anaplasma* sp. infection detected microscopically and by PCR in camels of the present study.

Parasite	Prevalence in total 102 samples		
	PCR =*n* (%)	**Blood smear and PCR** =*n* (%)	**Total** =*n* (%)
***Babesia* (+ve)**	11 (10.78%)	8 (7.84%)	19 (18.62%)
***Anaplasma* (+ve)**	13 (12.74%)	34 (33.33%)	47 (46.10%)
Total	24 (23.53%)	42 (41.18%)	66 (64.70%)
X2	5.345		
P-value	0.020		

The chi-square statistic is 5.345. the *P-value* is 0.020 significant at $p < 0.05$.

Table 3. Risk factors associated with *Babesia* and *Anaplasma* sp. infections detected in camels of the present study.

Factor		Total samples	Babesia (+ ve)	Anaplasma (+ve)
		=n (%)	=n (%)	=n (%)
Age (years)	≤5	39/102 (38.2%)	13/39 (33.33%)	23/39 (58.97%)
	>5	63/102 (61.8%)	6/63 (9.52%)	24/63 (38.09%)
Total		102/102 (100%)	19/102 (18.62%)	47/102 (46.07%)
X2	6.392			
P-value	0.041			
The chi-square statistic is 6.392. the *P-value* is 0.041 significant at $p < 0.05$				
Gender	**Male**	37/102 (36.3%)	11/37 (29.73%)	27/37 (72.97%)
	Female	65/102 (63.8%)	8/65 (12.31%)	20/65 (30.77%)
Total		102/102 (100%)	19/102 (18.62%)	47/102 (46.07%)
X2	7.358			
P-value	0.025			
The chi-square statistic is 7.358. the *P-value* is 0.025 significant at $p < 0.05$				
Source	**Local**	97 (95.10%)	16/97 (16.49%)	43/97 (44.33%)
	Imported	5 (5%)	3/5 (15.80%)	4/5 (80%)
Total		102/102 (100%)	19/102 (18.62%)	47/102 (46.07%)
X2	3.046			
P-value	0.218			
The chi-square statistic is 3.046. the *P-value* is 0.218 non-significant at $p < 0.05$.				

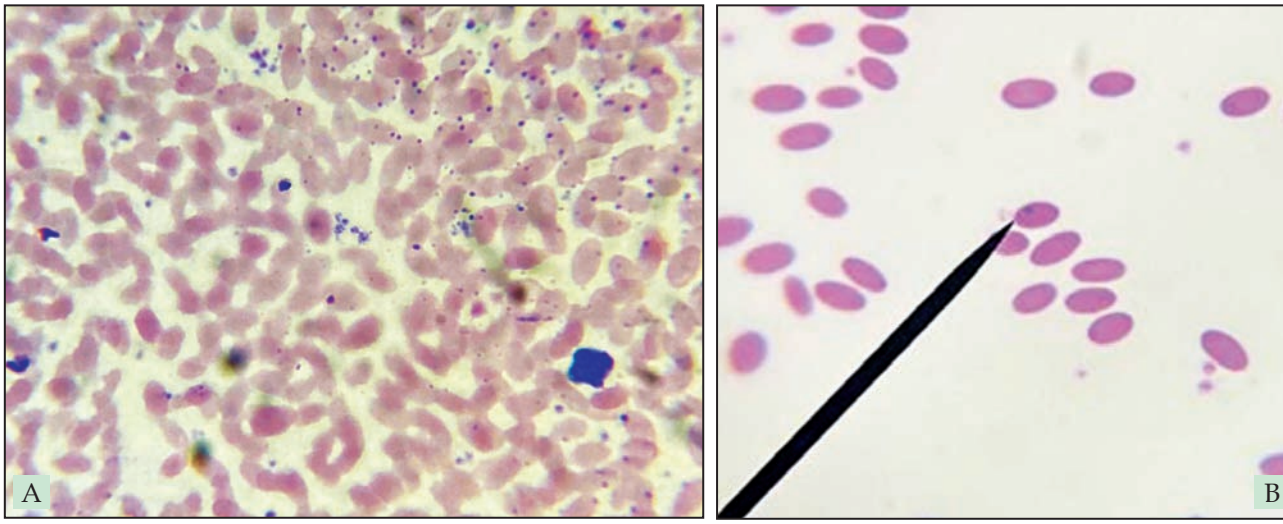

Fig 1. Light micrograph of camels' blood smear showing *Babesia* sp. (**A**) and *Anaplasma* sp. (**B**) of an infected erythrocyte. (100x)

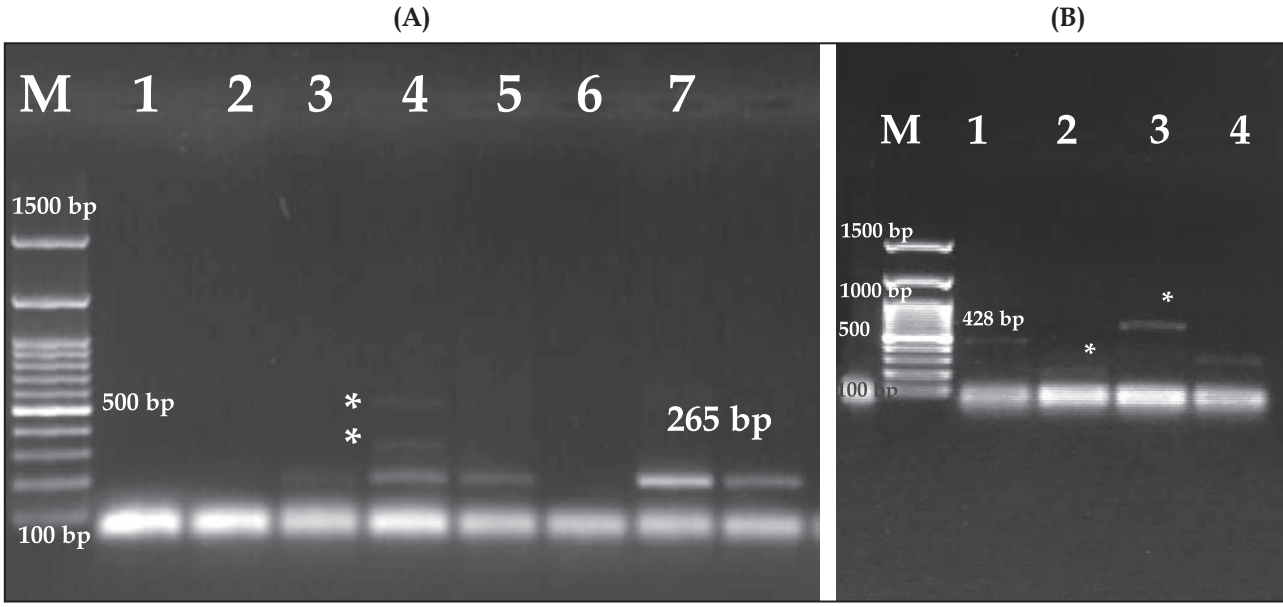

Fig 2. A 1.5% Agarose gel stained with ethidium bromide showing PCR product (265 bp) (**A**) and (428 bp) (**B**) of MAR1bB2R of *A. marginale* and small 18S rRNA gene fragment targeting *Babesia* sp., respectively. * Lower and higher bands are non-specific. Lane M: Low molecular weight marker (50-1500 bp).

blood samples from other countries, i.e. Pakistan (MK792346.1, MK792345.1, MK792344.1) (equine), South Africa (KU647720.1, KU647719.1) (cattle), Mexico (AF112480.1, AF111197.1, AF111195.1) USA (AF110808.1, AF348137.1, AF221693.1) and India (*Bos taurus*) MH476205.1. Sequence relationship with other most related neighboured sequences was constructed in rectangular cladogram as shown in Fig 3 A & B. On the other hand, the blast analysis of the present selected sequence of *Babesia* sp. was in relation to the same species found in blood samples from other countries, such as isolates in Goat-KAK13 in Turkey (MT498196.1), *Homo sapiens* (KY052789.1, KY052788.1, KX590752.1), cattle (MN901958.1, MN901956.1, MN900525.1, MN900524.1) and *Rhipicephalus microplus* (MH208614.1, MH208613.1) in China (Fig 3 C & D).

Discussion

Despite the efforts made to reduce the transmission of tick-borne diseases in animals, haemopathogens are still prevalent throughout the world. Babesiosis and Anaplasmosis are distributed throughout the world affecting the livestock population (Berggoetz *et al*, 2014; De La Fuente, 2017). There is insufficient data on tick-borne diseases especially *Babesia* and *Anaplasma* sp. in the Taif region in Saudi Arabia. Most of the previous studies investigated their prevalence in cattle and other

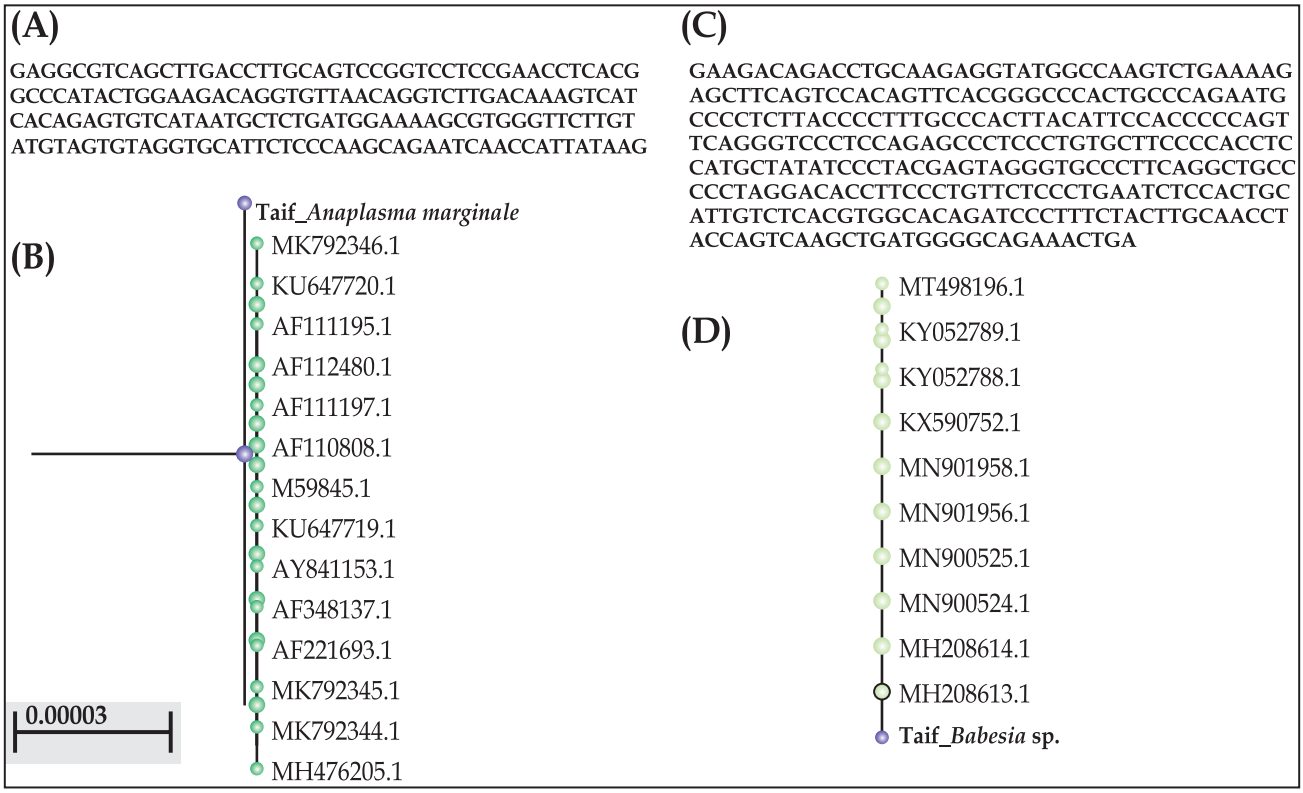

Fig 3. FASTA sequence of part of major surface protein–1β encoding gene and small 18S rRNA gene of *A marginale* (**A**) and *Babesia* sp. (**C**), respectively. Their relationship with other reference sequences from NCBI GenBank using a phylogenetic tree of A. marginale (**B**) and *Babesia* sp. (**D**). GenBank sequences were shown by their accession numbers. Bar scale represents 0.00003 nucleotide substitution per site.

species, but very few studies have investigated the prevalence of these parasites in camels.

The cumulative infection rate of Babesiosis and Anaplasmosis was found to be 18.62% and 46.10%, respectively as estimated from the examination of 102 camels in the present study area. The present results were consistent with previous studies in Egypt, in which they have recorded infection rates of *Babesia* (11.8%) and *Anaplasma* sp. (47.4%) (El-Naga and Barghash, 2016). On the contrary, another study in Somalia have recorded the overall prevalence of *Babesia* (52.2%) and *Anaplasma* sp. (13.2%) (Abdalla *et al*, 2017) that is not in agreement with the findings of present study. This may be explained by the husbandry practices in desert areas where all livestock share common inhabitancy and wandering in pasture lands with continuous migration.

Other studies in Saudi Arabia have reported prevalence of *Babesia* sp. in the Riyadh region (13.17%) (Swelum *et al*, 2014) and *Anaplasma marginale*, *Candidatus Anaplasma camelii* in Riyadh and Makkah regions and Asir Province as 40.50 and 2%, respectively (Ismael *et al*, 2016; Alshahrani *et al*, 2020). Yet, another study didn't record any *Babesia* infection in all camels they had tested in Riyadh (Alanazi *et al*, 2020) and Asir provinces (Alshahrani *et al*, 2020). This may be due to the isolation of the locality from *Babesia* infection or to the animals having been treated against *Babesia*. However, Ghafar and Shobrak (2014) have reported high prevalence of *Anaplasma* sp. closely related to *A. marginale* (99% identity) in camels, cattle, sheep, foxes, and Dabb lizards in the Taif region.

It was clear from the results that polymerase chain reaction gave better findings of the DNA of the pathogens than microscopic method, hene it was a more accurate and sensitive method than microscopy. It was paralleled with many studies that have used molecular tools to screen and identify *Babesia* and/or *Anaplasma* worldwide in camel hosts and their tick vectors as a more sensitive technique for the diagnosis of haemoparasitic infection (Belkahia *et al*, 2015; Abdalla *et al*, 2017; Ibrahim *et al*, 2017; Sharifiyazdi *et al*, 2017; Azeem *et al*, 2019; Selmi *et al*, 2019; Mirahmadi *et al*, 2022). In the present study, 18S rRNA and major surface protein–1β encoding genes were targeted for *Babesia* and *A. marginale* detection. The 18S rRNA gene is widely used in *Babesia* research for better identification and comparison (Bahrami *et*

al, 2017; Yue *et al*, 2020). The major surface proteins are considered as useful markers in *A. marginale* molecular epidemiology (Molad *et al*, 2009). There are six major surface proteins of *A. marginale* that are well characterised and are antigenically responsible for antibodies production in infected animals (Wei *et al*, 2020).

The present study has reported a high prevalence of *Babesia* (18.62%) and *A. marginale* (46.10%) in dromedaries of Saudi Arabia based on PCR evaluation. These findings are consistent with result of Junsiri *et al* (2020) who have recorded a high prevalence of *A. marginale* in cattle blood samples (10.30%) in Thailand based on PCR of the major surface proteins–4 gene. Moreover, they have observed a high degree of genetic diversity in the analysed *A. marginale* population according to their major surface proteins 2, 4, and 5 clones.

The short amplicons size (428 bp) of the 18S rRNA gene and (265 bp) of major surface protein–1β of *Babesia* and *A. marginale* obtained in PCR screening limits their deposition in GenBank. Also, in our previous studies, we have detected that those selected samples harbour other pathogens such as *Trypanosoma* (Al Malki and Hussien, 2022a), *Theileria* (Al Malki and Hussien, 2022b), and *Toxoplasma* (Al-Malki, 2022), making it more interfering in recovering targeted genes of near full-length using nested PCR (Wei *et al*, 2020).

Isolates of 18S rRNA and major surface protein–1β genes have shown phylogenic relationships with other isolates of *Babesia* and *A. marginale* in different hosts of other countries, as previously reported (Junsiri *et al*, 2020; Morikawa *et al*, 2021 and Wei *et al*, 2020). However, sequencing more isolates with larger amplicon sizes could be useful for the relationship assessment of those selected pathogens in the blood of camels found in Taif governorate, Saudi Arabia.

The present study showed a significantly higher percentage of *Babesia* (33.33%) and *Anaplasma* sp. (58.97%) infection among young camels (≤5 years) than older animals 9.52% and 38.09%, respectively. Recently, we have detected *Theileria* sp. in the same samples with higher prevalence in young camels than older animals (Al Malki and Hussien, 2022b). There is a co-infection of tick-borne pathogens (Anaplasmosis, Babesiosis and Theileriosis) in the same animal, because pathogens can share the same route of tick transmission (Lee *et al*, 2020). This could be due to poorly developed immune system to combat pathogen infection (Ahmed *et al*, 2008) or higher care for adult animals by the owner. Moreover, a lower infection prevalence in older animals may be due to the development of concomitant immunity due to their recurrent infections throughout their lifetime (Ilhan *et al*, 1998; Gharbi and Darghouth, 2014). On the other hand, there is a significant increase of *Babesia* (29.73%) and *Anaplasma* sp. (72.97%) infection in males than female camels 12.31% and 30.77%, respectively. This was in agreement with the result of Alanazi *et al* (2020), who reported a non-significant increase of *Babesia* (3.48%) and *Anaplasma* sp. (7.96%) infection in male cattle than female samples (1.24% and 3.11%) in four regions (Riyadh, Al-Kharj, Al-Hasa and Al-Qassim) of Saudi Arabia. The lower prevalence rate in female camels than males could be attributed to more care from their owners as female camel are source of milk during lactation and caring for their young ones.

In conclusion, the present study confirmed the prevalence of babesiosis and anaplasmosis in *Camelus dromedarius* of the Taif region, Saudi Arabia.

Acknowledgements

This work was supported by Taif University Researchers Supporting Project number (TURSP-2020/299), Taif University, Taif, Saudi Arabia. The authors would like to thank the Ministry of Environment, Water and Agriculture in Taif governorate (KSA) for facilitating data and sample collections.

Declarations

Ethics approval and consent to participate

Data and samples were collected from veterinarians as per their periodic examination according to ministerial recommendation. We obtained a permission letter from the Ministry of Environment, Water and Agriculture (KSA) to collect cattle and camel samples from different locations in Taif for our research study with the number 106082/1074/1442, date 21-02-1442H. Sample collection and all experimental procedures were performed in accordance with a national ethical requirement. National Committee of Bioethics (NCBE) at King Abdulaziz City for Science and Technology (KACST) with number: 10023117, valid till 01 October 2023.

Availability of data and materials

All data generated or analysed during this study are included in this published article.

Competing interests

The authors declare that they have no competing interests.

Funding

Taif University Researchers Supporting Project number (TURSP-2020/299), Taif University, Taif, Saudi Arabia.

References

Abdalla MI, Ahmed AHK and Hamisi SN. Microscopic and molecular detection of camel anaplasomosis and piroplasmaosis in Banadir region, Somalia. Open Access Journal of Veterinary Science and Research. 2017; 2(1):000127.

Ahmad S, Ghosh A, Nair DL and Seshadri M. Simultaneous extraction of nuclear and mitochondrial DNA from human blood. Genes and Genetic Systems. 2007; 82: 429-432.

Ahmed JS, Glass EJ, Salih DA and Seitzer U. Innate immunity to tropical theileriosis. Innate Immunty. 2008; 14(1):5-12.

Al Malki JS. Serological and molecular surveillance of *Toxoplasma gondii* of camels in Taif, Saudi Arabia. Egyptian Journal of Veterinary Sciences. 2022; 53(2):219-227.

Al Malki JS and Hussien NA. Molecular characterization of *Trypanosoma evansi*, *T. vivax* and *T. congolense* in camels (*Camelus dromedarius*) of KSA. BMC Veterinary Research. 2022a; 18, 45.

Al Malki JS and Hussien NA. Microscopic, serological, and molecular screening of *Theileria* annulata in camels (*Camelus dromedarius*) of Saudi Arabia. Journal of Camel Practice and Research. (2022b); 29(1):61-66.

Alanazi AD, Nguyen VL, Alyousif MS, Manoj R, Alouffi AS, Donato R, Sazmand A, Mendoza-Roldan JA, Dantas-Torres F and Otranto D. Ticks and associated pathogens in camels (*Camelus dromedarius*) from Riyadh Province, Saudi Arabia. Parasites and Vectors. 2020; 13:110

Al-Nabati E, Alajmi R, Metwally DM, Al-Turaiki IM, Tellez-Isaias G and Abdel-Gaber R. Molecular detection of tick-borne rickettsial pathogens associated with the Arabian camel (*Camelus dromedarius*) in Riyadh and the eastern region, Saudi Arabia. Acta Parasit. 2022.

Alshahrani MY, Alanazi AD, Alouffi AS, Abdullah HHAM, Allam AM, Mahmoud MS, Abdel-Shafy S, Alfaifi MH and Alkhathami AG. Molecular detection of Candidatus *Anaplasma camelii* in camels (*Camelus dromedarius*) from Asir Province, Saudi Arabia. Tropical Biomedicine. 2020; 37(3):587-598.

Azeem T, Tipu MY, Aslam A, Ahmed S, Abid SA, Iqbal A, Akhtar N, Saleem M, Mushtaq A and Umar S. Haematobiochemical disorder in camels suffering from different haemoparasites. Pakistan Journal of Zoology. 2019; 51(2):591-596.

Bahrami S, Tabandeh MR and Tafreshi ARG. Prevalence and molecular identification of piroplasmids in Iranian dromedaries (*Camelus dromedarius*). Journal of Zoo and Wildlife Medicine. 2017; 48(4):1026-1030.

Belkahia H, Said MB, Sayahi L, Alberti A and Messadi L. Detection of novel strains genetically related to *Anaplasma platys* in Tunisian one-humped camels (*Camelus dromedarius*). Journal of Infection in Developing Countries. 2015; (10):1117-1125.

Berggoetz M, Schmid M, Ston D, Smith V, Chevillon C, Pretorius AM, *et al*. Tick-borne pathogens in the blood of wild and domestic ungulates in South Africa: Interplay of game and livestock. Ticks Tick-borne Diseases. 2014; 5:166-175.

De La Fuente J, Antunes S, Bonnet S, Cabezas-Cruz A, Domingos AG, Estrada-Peña A, Johnson N, Kocan KM, Mansfield KL and Nijhof AM. Tick-pathogen interactions and vector competence: identification of molecular drivers for tick-borne diseases. Frontiers in Cellular and Infection Microbiology. 2017; 7:114.

El-Ashker M, Salama M, El-Sebaei M, Risha E, Abdelhamid F, El-Diasty M and El-Fadl E. Significance of clinical variables and selected biochemical markers in predicting the outcome of bovine anaplasmosis. Veterinary Medicine. 2015; 60(6):301-308.

El-Naga TRA and Barghash SM. Blood parasites in camels (*Camelus dromedarius*) in northern west coast of Egypt. Journal of Bacteriology and Parasitology. 2016; 7:258.

Ghafar M and Shobrak M. Molecular detection and characterization of *Anaplasma phagocytophilum*, the causative agent of human granulocytic anaplasmosis, in some animals suspected to be competent reservoirs in Taif district, Kingdom of Saudi Arabia. Life Science Journal. 2014; 11(6).

Gharbi M and Darghouth MA. A review of Hyalomma scupense (*Acari, Ixodidae*) in the Maghreb region: from biology to control. Parasite. 2014; 21:12-18.

Guglielmone AA, Robbins RG, Apanaskevich DA, Petney TN, Estrada-Peña A and Horak IG. The hard ticks of the world. Dordrecht: Springer. 2015; pp 738.

Hilpertshauser H, Deplazes P, Schnyder M, Gern L and Mathis A. *Babesia* spp. identified by PCR in ticks collected from domestic and wild ruminants in southern Switzerland. Applied and Environmental Microbiology. 2006; 72:6503-6507.

Homer MJ, Aguilar-Delfin I, Telford SR, Krause PJ and Persing DH. Babesiosis. Clinical Microbiology Reviews. 2000; 13(3):451-469.

Ibrahim AM, Kadle AA and Nyingilili HS. Microscopic and molecular detection of camel piroplasmosis in Gadarif State, Sudan. Veterinary Medicine International. 2017; 9345231.

Ilhan T, Williamson S, Kirvar E, Shiels B and Brown C. *Theileria annulata*: Carrier State and Immunity a. Annals of the New York Academy of Sciences. 1998; 849(1):109-25.

Ismael A, Swelum A, Khalaf A and Alowimer A. First evidence of natural anaplasmososis in *Camelus dromedarius* in Saudi Arabia. Journal of Camel Practice and Research. 2016; 23(1):95-100.

Junsiri W, Watthanadirek A, Poolsawat N, Kaewmongkol S, Jittapalapong S, Chawengkirttikul R and Anuracpreeda P. Molecular detection and genetic diversity of

Anaplasma marginale based on the major surface protein genes in Thailand. Acta Tropica. 2020; 205:105338.

Kocan KM, de la Fuente J, Blouin EF, Coetzee JF and Ewing SA. The natural history of *Anaplasma marginale*. Veterinary Parasitology. 2010; 167(2-4):95-107.

Kocan KM, Guglielmone AA and Mele RD. Antigens and alternatives for control of *Anaplasma marginale* infection in cattle. Society. 2003; 16(4):698-712.

Kuznetsov A and Bollin CJ. NCBI Genome Workbench: Desktop Software for Comparative Genomics, Visualisation, and GenBank Data Submission. Methods in Molecular Biology. 2021; 2231:261-295.

Lee S, Lee H, Park JW, Yoon SS, Seo HJ, Noh J, Yoo MS, Kim KH, Park Y, Cho YS and So BJ. Prevalence of antibodies against *Anaplasma* spp., Borrelia burgdorferi sensu lato, *Babesia* gibsoni, and Ehrlichia spp. in dogs in the Republic of Korea. Ticks and Tick-borne Diseases. 2020; 11(4):101412.

Megersa B. An epidemiological study of major camel diseases in the Borana lowland, southern Ethiopia. Oslo: Drylands Coordination Group. 2010.

Mirahmadi H, Ghaderi A, Barani S, Alijani E, Mehravaran A and Shafiei R. Prevalence of camel babesiosis in southeast of Iran. Veterinary Medicine and Science. 2022; 8:343-348.

Molad T, Fleidrovich L, Mazuz M, Fish L, Leibovitz B, Krigel Y and Shkap V. Genetic diversity of major surface protein 1a of *Anaplasma marginale* in beef cattle. Veterinary Microbiology. 2009; 136:54-60.

Morikawa M, Mitarai S, Kojima I, Okajima M, Hatai H, Takano A, Shimoda H, Maeda K, Matsuu A, Yoshida A, Hayashi K, Ozawa M and Masatani T. Detection and molecular characterisation of *Babesia* sp. in wild boar (*Sus scrofa*) from western Japan. Ticks Tick Borne Diseases. 2021; 12(4):101695.

Schalm OW. Veterinary Hematology. 2nd ed. Philadelphia: Lea and Febiger. 1971.

Selmi R, Dhibi M, Ben Said M, Ben Yahia H, Abdelaali H, Ameur H, Baccouche S, Gritli A and Mhadhbi M. Evidence of natural infections with *Trypanosoma*, *Anaplasma* and *Babesia* spp. in military livestock from Tunisia. Tropical Biomedicine. 2019; 36(3):742-757.

Sharifiyazdi H, Jafari S, Ghane M, Nazifi S and Sanati A. Molecular investigation of *Anaplasma* and Ehrlichia natural infections in the dromedary camel (*Camelus dromedarius*) in Iran. Comparative Clinical Pathology. 2017; 26(1):99-103.

Stiller D and Marchette N. The *Anaplasma*taceae, Bartonellaceae, and Rochalimaea quintana. In: Marchette, N.J. (Ed.), Ecological Relationships and Evolution in the Rickettsiae. CRC Press, Boca Raton, Florida, USA. 1982; pp 98-106.

Swelum AA, Ismael AB, Khalaf AF and Abouheif MA. Clinical and laboratory findings associated with naturally occurring babesiosis in dromedary camels. Bulletin-Veterinary Institute in Pulawy. 2014; 58:299-233.

Wei CY, Wang XM, Wang ZS, Wang ZH, Guan ZZ, Zhang LH, *et al*.. High prevalence of *Babesia* microti in small mammals in Beijing. Infectious Diseases of Poverty. 2020; 9:155.

Yue C, Deng Z, Qi D, Li Y, Bi W, Ma R, Yang G, Luo X, Hou R and Liu S. First detection and molecular identification of *Babesia* sp. from the giant panda, *Ailuropoda melanoleuca*, in China. Parasites Vectors. 2020; 13:537.

DOI : 10.5958/2277-8934.2022.00024.8 Vol 29 No 2, p 177-182

COMPARATIVE ANATOMY OF THE OPHTHALMIC DIVISION OF THE TRIGEMINAL NERVE IN CAMEL AND SHEEP WITH SPECIAL REFERENCE TO ITS CLINICAL IMPORTANCE

Eman A. Eshrah[1], Ahmed I. Abo-Ahmed[1] and Fatgzim Latifi*[2]

[1]Assistant professor of Anatomy and Embryology, Department of Anatomy and Embryology, Faculty of Veterinary Medicine, Benha University, Egypt

[2]Department of Veterinary Medicine, Faculty of Agriculture and Veterinary, University of Prishtina "Hasan Prishtina", Bul. "Bill Clinton" p.n, 10000 Prishtina, Kosovo

ABSTRACT

The aim of this study was to describe the topographic anatomy and the distribution pattern of ophthalmic division of the trigeminal nerve in 5 dromedary camels and 3 sheep. In both species, the origin and the primary branches of the ophthalmic nerve were similar, but they differed in the pattern of distribution. The primary branches included were zygomaticotemporal nerve, frontal nerve, fronal sinus branch and nasociliary nerve. The study would help deciding the sites of this nerve block in these species.

Key words: Camel, cornual nerve, frontal nerve, infratrochlear nerve, ophthalmic nerve, sheep, supraorbital nerve

The ophthalmic branch is the smallest of the three divisions of the trigeminal nerve, purely sensory and innervates the cilliary body, the cornea and the iris; to the lacrimal gland and conjunctiva (Shankland, 2001). Anaesthesia of these nerves is sometimes necessary for eyelid and conjunctival biopsies and other minor surgeries (Michau, 2005). Furthermore, this nerve blockade is preferred for some minor ophthalmic operation in the eye and/or the upper eyelid (Badawy and Eshra, 2015). The cornual nerves are involved in the analgesic preferred technique for dehorning in ruminants (Hall *et al,* 2001).

The ophthalmic division of the trigeminal nerve is well described in other species, namely, equine, bovine and canines (Levine *et al,* 2008) but the clinical anatomy of this nerve in dromedaries and ovine is scarcely reported.

This study was aimed to describe the topographic anatomy and distribution pattern of ophthalmic division of the trigeminal nerve in dromedary camel (*Camelus dromedarius*) and sheep (*Ovis aries*).

Materials and Methods

This study was performed in accordance with the ethical guidelines approved by the Institutional Animal Care and Use Committee of the Faculty of Veterinary Medicine, Benha University, Egypt. The study was conducted on 10 heads from apparently healthy mature males (5 camels, 3 sheep) which were obtained immediately after slaughter from Toukh and Qalioube abattoir, Egypt. One camel skull was used for demonstrating the foramina of the nerve exit in this species. Each head was frozen at -18° C, until these were used for this study. Nomenclature used in this study was written according to the Illustrated Nomina Anatomica Veterinaria (Schaller, 2011) and Smuts and Benzuidenhout (1987).

Results

Ophthalmic nerve

Origin and distribution: In camels and sheep, the ophthalmic nerve originated intracranially (at level of foramen lacerum) from the trigeminal ganglion in a common trunk with the maxillary nerve (Fig 1a, b). It exited the cranium through the orbitorotundum foramen (Fig 1a, b). In camels, it was divided immediately after its origin within the cranial cavity to give its primary branches (Fig 1a). However, in sheep, the division occurred just at the foramen of exit (orbitorotundum) (Fig 1b). In the two species, the ophthalmic nerve gave off the

SEND REPRINT REQUEST TO CORRESPONDING AUTHOR* FATGZIM LATIFI email: fatgzim.latifi@uni-pr.edu

following branches, from the lateral to the medial: the zygomaticotemporal nerve, which was the most lateral branch, the frontal nerve, the fronal sinus branch and the nasociliary nerve, which was the most medial branch (Fig 1a, b).

Frontal sinus branch: In camel, it arose either from the ophthalmic or the frontal nerve (Fig 1a, b). In sheep, it originated from the ophthalmic nerve in close association to the frontal nerve. In the two species, it coursed along the upper border of the dorsal rectus muscle, until it left the orbit through a small foramen, which led into the frontal sinus.

Zygomaticotemporal nerve: In camels, it detached the lacrimal nerve just as it emerged from the orbitorotundum foramen. It then coursed rostral on the dorsolateral part of the orbit, along the medial border of the lateral rectus muscle. It pierced the periorbital fat pad until it reached the angle of junction between the zygomatic process of the frontal bone and the zygomatic process of the temporal bone (Fig 2a). At this junction, it ended by division into medial and lateral branches. The medial branches ran under the frontoscutularis muscle, where it gave branches to the skin of the temporal region. The lateral branches ended in malaris muscle and the skin of this facial region.

In sheep, the course and distribution of the zygomaticotemporal nerve were similar to those in camels, except for its terminal branches. The division into medial and lateral branches was not clear in sheep; however, ventral to the lacrimal gland the nerve left the periorbita accompanied with the cornual vein. It then turned caudomedially to run under the frontoscutularis muscle, where it gave off branches to the skin of the temporal region, and finally divided giving the cornual nerves (Fig 2b). The latter distributed at the lateral and caudal sides of the base of the horn (Fig 2b).

Frontal nerve: In the camel, it was divided into two branches, i.e. the supraorbital and the infratrochlear nerves. The latter left the orbit through the orbital fissure, while, the supraorbital nerve continued the course of the frontal nerve and proceeded rostrodorsally within the periorbita until it reached the orbital rim, namely at the level of the supraorbital notch, where it pierced the skin of the upper eye lid (Fig 2a). In sheep, the supraorbital nerve exited the skull through the supraorbital foramen, and distributed within the skin of the upper eyelid, whereas the infratrochlear nerve arose from the nasociliary nerve.

Nasociliary nerve: In camel, after it emerged from the the orbitorotundum foramen, it coursed between the dorsal oblique and the medial rectus muscles (Fig 3a). During its course, it gave muscular branches to these muscles and the levator palpebrea superiorus, the long cilliary nerve and the communicating branch to the cilliary ganglion. It then terminated by giving the ethmoidal and the frontal nerve. The latter was the continuation of the nasociliary nerve in camel.

The nasociliary nerve had similar origin and course in sheep (Fig 3b). However, it gave two to three long cilliary nerves, instead of the single branch found in camels (Fig 3c). In addition, the infratrochlear nerve was the continuation of the nasociliary nerve in sheep.

In camel and sheep, the infratrochlear nerve as its name implies, passed below the pulley (the trochlea) of the obliques dorsalis muscle. In camel only it left the orbit through the orbital fissure. In both species, the infratrochlear coursed caudomedially under the frontalis muscles to give cutaneous branches to the frontal region. In sheep, it also gave cornual branches, which supply the lateral and the rostral sides of the base of the horn.

In the two species, the ethmoidal nerve was the smaller branch of the nasociliary nerve. It penetrated the ethmoidal foramen to gain access the nasal cavity, where it coursed on the dorsolateral border of the nasal septum. Finally, the ethmoidal nerve terminated in the mucous membrane covering the cranial part of nasal septum and the dorsal nasal concha.

Clinical importance:

In the camel the site of needle insertion for supraorbital nerve block was at the level of the supraorbital notch, where the nerve exited the skull (Fig 4 a, b, c). However, in sheep, the needle was inserted at the foramen of exit, i.e., the supraorbital foramen (Fig 5 a, b).

To achieve local anaesthesia of the horn in sheep, the cornual nerves of the zygomaticotemporal nerve and the infratrochlear nerve must be desensitised. For the blockade of the cornual branches of the zygomaticotemporal nerve, the needle was inserted just caudal to the frontal process of the zygomatic bone, closer to the root of the supraorbital process (Fig 5 a, b). However, for blocking the cornual branches of the infratrochlear nerve the needle was inserted dorsomedially close to the orbital margin (Fig 5 a, b).

Discussion

The present study demonstrated the branching pattern of the ophthalmic division of the trigeminal

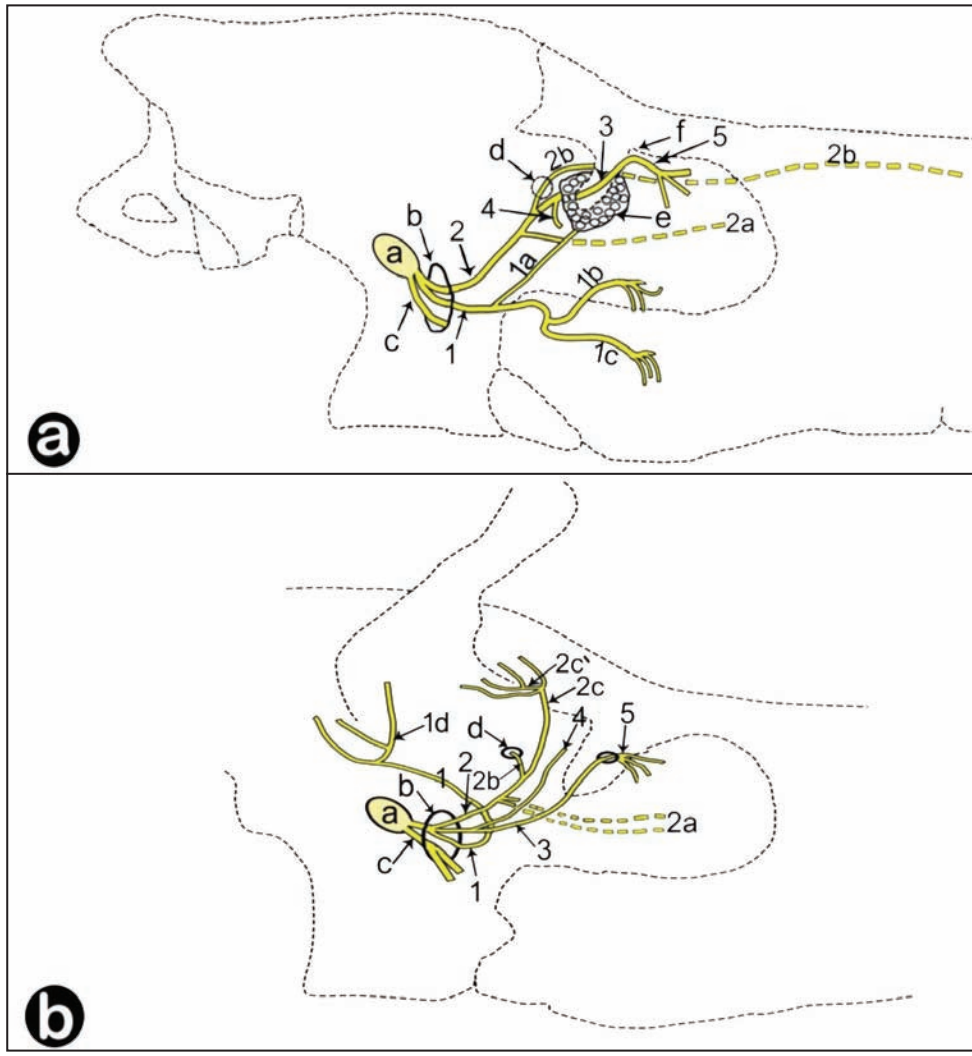

Fig 1. An illustration showing branching of the ophthalmic nerve in camel (a) and sheep (b), showing: Trigeminal ganglia (a), orbitorotundum foramen (b), maxillary nerve (c), ethmoidal foramen (d), lacrimal gland (e), supra orbital notch (f), zygomaticotemporal n. (1), lacrimal n. (1a), medial branch of zygomaticotemporal nerve (1b), lateral branch of zygomaticotemporal nerve (1c), cornual branches of zygomaticotemporal nerve (1d), nasociliary nerve (2), long cilliary nerve (2a), ethmoidal nerve (2b), infratrochlear nerve in sheep (2c), cornual branches of infratrochlear nerve (2c), frontal nerve (3), frontal sinus branch (4), supraorbital nerve (5).

nerve in camels and sheep with special reference to the clinical importance. The origin and the primary branches of the ophthalmic nerve are similar, but the primary division occurs intracranial in the camel (Ahmed, 1979), and not at the foramen of exit as in sheep and the other ruminants (Sisson and Grossman, 1975). They also differ in the pattern of distribution of these branches. The zygomaticotemporal nerve in camels ended by division into medial and lateral branches. However, in sheep these medial and lateral branches were not clear and instead the zygomaticotemporal nerve left the periorbita and finally, divided giving the cornual nerves. The infratrochlear nerve arose from the frontal nerve in camels, while in sheep it arose from the nasociliary nerve. The frontal sinus branch usually arose from the frontal nerve in camels, but in sheep it arose from the ophthalmic nerve itself. The nasociliary nerve continued as the frontal nerve in camel, whereas in sheep it continued as the infratrochlear nerve. It also gave off a single long cilliary nerve in the camels, but in sheep as well as other small ruminants it gave two-three long cilliary nerves. The above-mentioned anatomical differences were similar to those described in camels (Ahmed, 1979; Smuts and Benzuidenhout, 1987) and in small ruminants (Sisson and Grossman, 1975; Dyce *et al*, 1996).

Comparing with other ruminants, the camel orbit had special anatomical features (Badawy and Eshra, 2018), this may explain the difference of

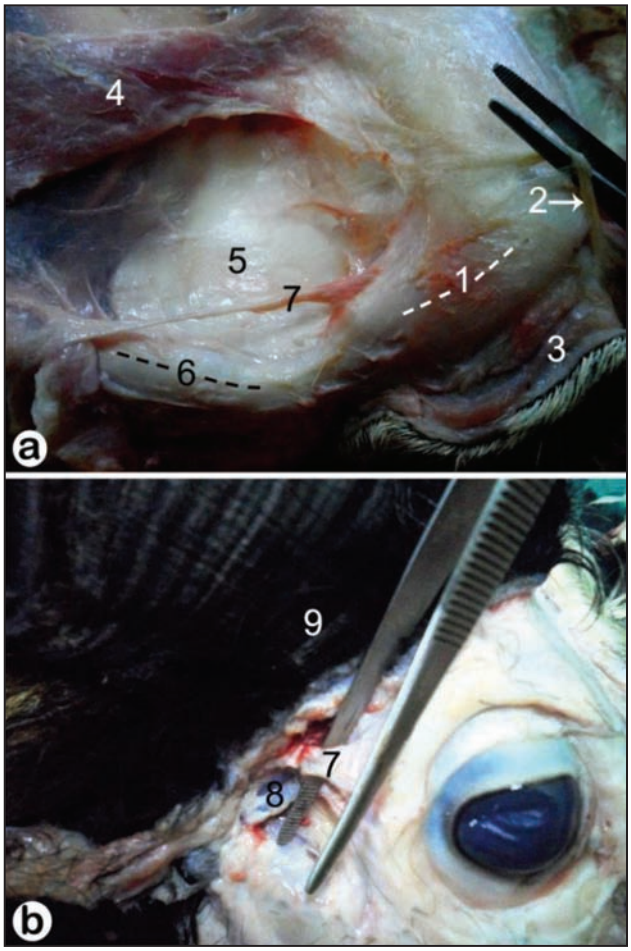

Fig 2. Camel (a) and sheep (b) heads (dissected), showing: supraorbital process (1), supraorbital nerve (2), upper eyelid reflected (3), notice that the supraorbital nerve terminates in the subcut. Of the upper eyelid, Frontoscutularis muscle (4), temporal fossa (5), zygomatic arch (6), zygomaticotemporal nerve (7), cornual vein (8), base of the horn (9).

foramina of exits between camel and other ruminants. In camels, the supraorbital foramen was absent and instead there was a supraorbital notch, at which the supraorbital nerve left the orbit. On the other hand, the infratrochlear nerve exited the camel skull through the orbital fissure, while in sheep it directly pierced the periorbita and gave the cornual branches. These observations in camels cause in agreement with those described by Ahmed (1979) and Smuts and Benzuidenhout (1987) in camel, and disagreed with Shahid and Kausar (2005), Monfared (2013) and Almayahi (2014) who reported that the infratrochlear fissures (orbital fissures) were the exit of the supraorbital nerve.

Regarding the clinical importance, the sites used in this study for needle insertion cause in agreements with those used for nerve blockade in sheep (Hall *et al*, 2001), and camel (Badawy and Eshra, 2015). For cornual nerve block in sheep, palpation of the nerves is done by rolling the skin and subcutaneous muscles

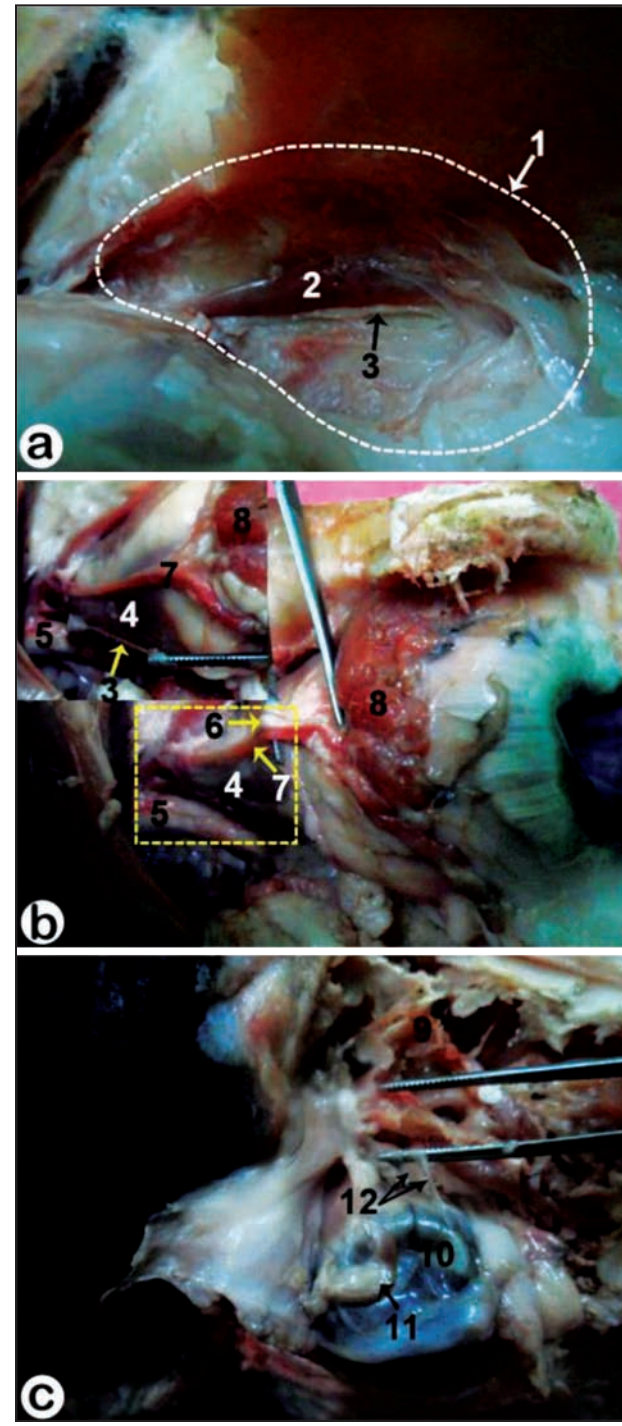

Fig 3. Camel (a) and sheep (b) heads (dissected), showing: camel orbit (eyeball removed) (1), medial rectus muscle (2), nasociliary nerve (3), retractor bulbi (4), maxillary nerve (5), lacrimal nerve (6), lacrimal artery (7), lacrimal gland (8), supraorbital process (excised) (9), eyeball (10), obliqus dorsalis muscle (11), long cilliary nerves (two nerves) (12).

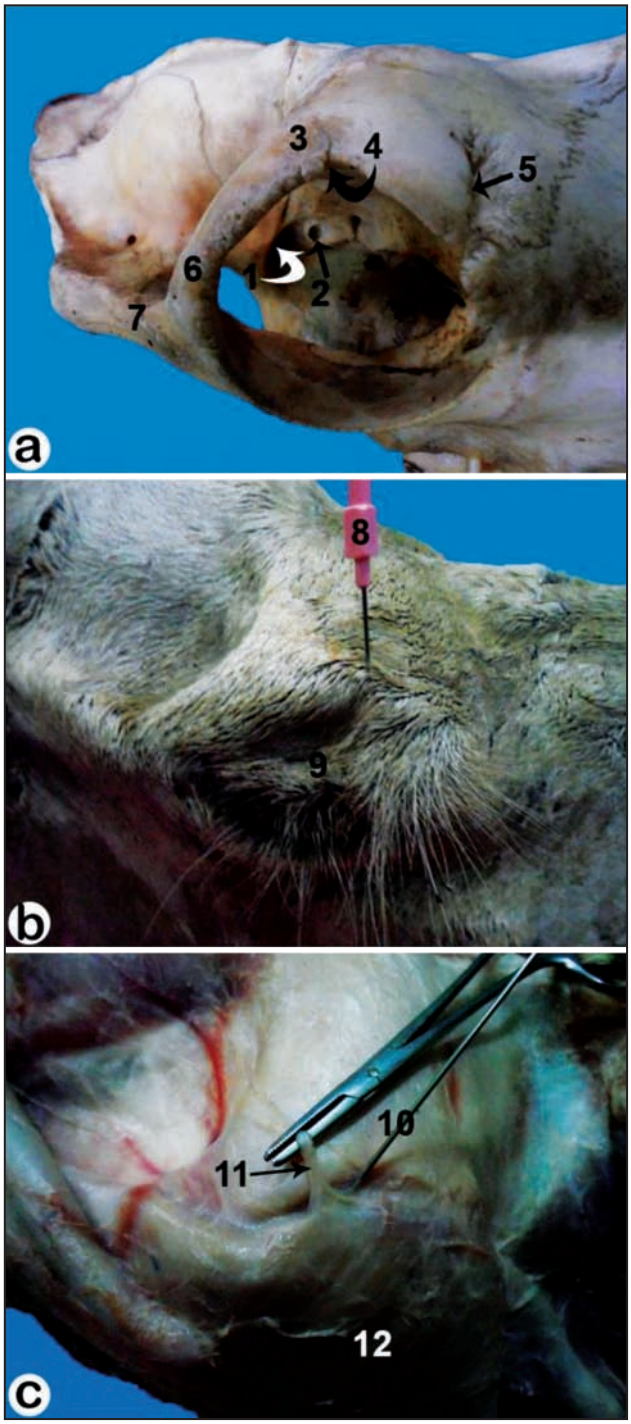

Fig 4. Site of needle insertion for supraorbital nerve block in the camel: camel bony orbit (skull) (a), camel head (b), dissection at sites of the needle insertion (c): orbitorotundum foramen (1), optic foramen (2), supraorbital process (3), supraorbital notch (4), orbital fissure (exit of infratrochlear nerve) (5), zygomatic process of frontal bone (6), zygomatic process of temporal bone (7), site of needle placement of supraorbital nerve, at level of supraorbital notch (8), upper eyelid (9), site of needle placement of supraorbital nerve (dissected) (10), supraorbital nerve located just at the level of supraorbital notch (11), upper eyelid reflected (12).

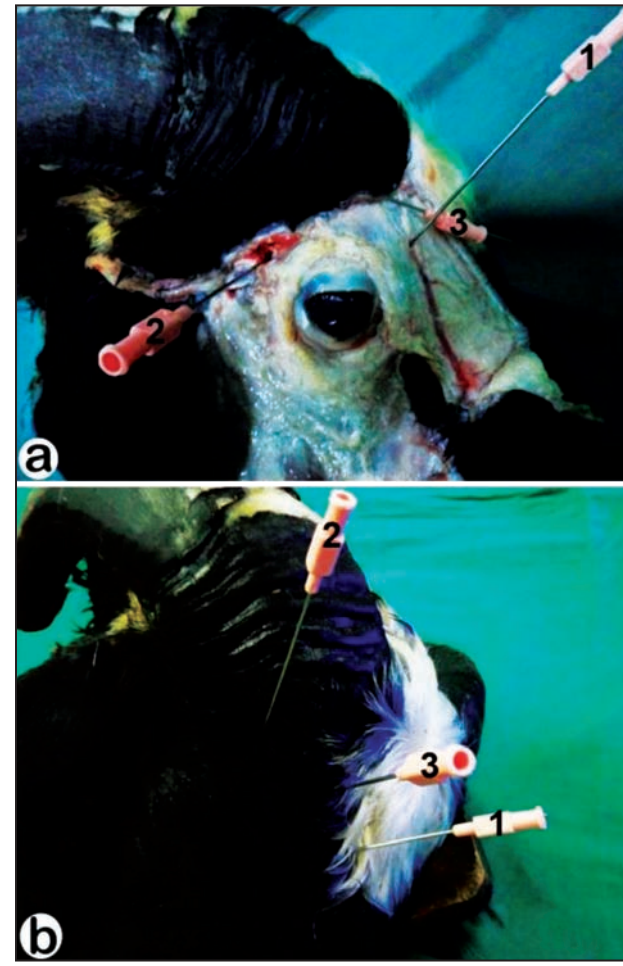

Fig 5. Sheep head showing: Site of needle placement of supraorbital nerve, at supraorbital foramen (1), site of needle placement of cornual branch of zygomaticotemporal nerve (2), site of needle placement of cornual branch of infratrochlear nerve (3).

over them before inserting the needle. Similarly, the supraorbital nerve can easily be located at the level of supraorbital foramen in sheep, and at the supraorbital notch in camels.

Conclusion

The origin and primary branches of ophthalmic nerve were similar; however, the secondary branches and pattern of distribution were different. The clinically important nerves described in the study were the supraorbital nerve in camel and sheep, and the cornual nerves of the zygomaticotemporal nerve and the infratrochlear nerve. The sites of nerve block for these nerves were demonstrated.

References

Ahmed KZS. Some anatomical studies of the trigeminal nerve (N. trigeminus) of the one humped camel (*Camelus dromedarius*). M.V.Sc thesis. Faculty of Veterinary Medicine, Zagazig University. 1979.

Almayahi MS. Anatomical description of orbital region in one humbed camel (*Camelus dromedarius*). Basra Journal of Veterinary Research. 2014; 1(1):43-49.

Badawy AM and Eshra EA. Supra-orbital nerve block in dromedary camel (*Camelus dromedarius*). Journal of Camel Practice and Research. 2015; 22(2):285-288.

Badawy AM and Eshra EA. Development of an ultrasound-guided technique for retrobulbar nerve block in dromedary camels: a cadaveric study. Veterinary Anaesthesia and Analgesia. 2018; 45(2):175-182. doi: 10.1016/j.vaa.2017.09.039

Dyce KM, Sack WO and Wensing CJG. Textbook of Veterinary Anatomy. 2nd Ed. W.B. Saunders Company, Philadelphia, London, Toronto, Montreal, Sydney, Tokyo. 1996.

Hall, LW, Clarke KW and Trim CM. Anaesthesia of sheep, goats and other herbivores. Veterinary Anaesthesia. 2001; 341–366. doi:10.1016/b978-070202035-3.50014-0

Levine JM, Levine GJ, Hoffman AG and Bratton G. Comparative anatomy of the horse, ox, and dog: The brain and associated vessels. Compendium Equine: Continuing Education for Veterinarians. 2008; 3:153-164.

Michau TM. Equine Ocular Examination: Basic and Advanced Diagnostic Techniques. Equine Ophthalmology. 2005; v1–62. doi:10.1016/b0-72-160522-2/50004-2

Monfared AL. Applied anatomy of the head regions of the one-humped camel (*Camelus dromedarius*) and its clinical implications during regional anaesthesia. Global Veterinaria. 2013; 10(3):322-326. DOI:10.5829/idosi. gv.2013.10.3.72128.

Schaller O. Illustrated Veterinary Anatomical Nomenclature. 5th Ed. Ferdinand Enke Verlag Stuttgart, Germany. 2011.

Shahid RU and Kausar R. Comparative gross Anatomical studies of the skull of one-humped camel (*Camelus dromedarius*). Pakistan Veterinary Journal. 2005; 25(4):205-206.

Shankland WE. The trigeminal nerve Part II: the ophthalmic division. Cranio. 2001; 2001;19(1):8-12. doi:10.1080/08869634.2001.11746145

Sisson S and Grossman JD. Anatomy of the Domestic Animals, 5th Ed. W.B. Sounders Company, Philadelphia. U.S.A. 1975.

Smuts MM and Bezuidenhout AJ. Anatomy of the Dromedary. Oxford: Clarendon Press. 1987.

DOI : 10.5958/2277-8934.2022.00025.X Vol 29 No 2, p 183-190

COMPARISON OF SOME HORMONAL AND BIOCHEMICAL CONSTITUENTS IN FOLLICULAR FLUID OF PREDOMINANT FOLLICLE COEXIST WITH OVERSIZED FOLLICLE AND ITS COUNTERPART PRESENT IN THE ABSENCE OF OVERSIZED FOLLICLE IN CAMELS (*Camelus dromedarius*)

I.M. Ghoneim[1,2], M.M. Waheed[1,2] and A.M.A. Meligy[1,3]

[1]Department of Clinical Sciences, College of Veterinary Medicine, King Faisal University, Al-Ahsa 31982, Al-Hufof P.O. 400, Kingdom of Saudi Arabia

[2]Department of Theriogenology, Faculty of Veterinary Medicine, Cairo University, Giza 12515, Egypt

[3]Physiology Department, Plant Protection Research Institute (PPRI), Agricultural Research Centre (ARC), Giza, Egypt

ABSTRACT

This study was aimed to compare between some hormonal and metabolic constituents in follicular fluids and serum of predominant follicles coexisting with oversized follicles and its counterpart present in absence of oversized follicle in camels (*Camelus dromedarius*). Follicular fluids and sera were collected from animals who had follicles size 0.5–1.0 cm (small; n = 10), >1.0–1.6 cm (medium; n = 10) and >1.6–2.0 cm (large; n = 10) which were present in absence or presence of oversize follicles. Follicular fluids and sera were subjected to biochemical and hormonal analysis. Results revealed increased concentrations of oestradiol 17- β (E2) of follicular fluid from the various size antral predominant follicle which existed in the absence of oversize follicle. A significant (P<0.01) high concentration of P4 present in the follicular fluid of small size predominant follicle coexisted with the oversize follicle. A highly significant cortisone concentration was recorded in follicular fluid of small, medium and large predominate existing in absence of oversize follicles. The insulin like growth factor II (IGF-II) and general thyroxine in the follicular fluid from the small follicles that exist in the absence of the oversize follicles were significantly lower (P<0.0001) compared with that of the small follicles that coexisted with the oversize follicle. Ultra-sensitivity triiodothyronine concentrations were significantly high in follicular fluid collected from predominant small and medium size follicle (P<0.001and P<0.0001, respectively) existing in absence of oversize follicle. In conclusion, the presence of an oversize follicle alters hormonal and biochemical constituents of follicular fluid of predominant follicle coexist with it.

Key words: Camel, oestradiol 17-β, follicles, hormones, metabolites

Dromedary camels display a distinguishing reproductive pattern among different domestic animal species. The single hump camels have been classified as induced ovulatory animal (Wilson, 1984; Tibary and Anouassi, 1997). The ovulation mainly occurs in response to coitus (El-wishy, 1987; Ismail, 1987). The camels' oestrous cycle has no luteal activity (Musa and Abusineina, 1978; Skidmore *et al,* 1995). Accordingly, the dromedary oestrous cycle is described as a 'follicular wave pattern (Skidmore *et al,* 1996; Tibary and Anouassi, 1996; Tibary and Anouassi, 1997; Skidmore *et al,* 2013). Follicles mature in six days, maintain their size for 13 days and regress in 8 days (Musa and Abusineina, 1978). In absence of mating, the fate of the mature follicle follows one of two possible paths: atresia and vanishing in the ovarian stroma or cystic degeneration (Tibary and Anouassi, 1996). The ovarian cysts have been reported in the dromedary (El wishy, 1987), IIama and alpaca (Bravo *et al,* 1993). In dromedary camels, there is inconsistency about the incidence of ovarian cysts. If the female camel is not bred, 30 to 40% of them are predisposed to develop some forms of cystic ovaries (Tibary and Anouassi, 1996). Abattoir survey revealed that the incidence of the ovarian cyst was 6.9% (Al-Afaleq *et al,* 2012). Rectal examination indicated that the frequency of ovarian cyst in the camel is 4.7% (Ali *et al,* 2010). The effect of ovarian cysts on camel fertility is uncertain (Ghoneim *et al,* 2013). Some authors (Tibary and Anouassi, 1997) suggested that

SEND REPRINT REQUEST TO M.M. WAHEED email: mmwaheed@kfu.edu.sa

ovarian cysts are a physiologic variation of follicular dynamics and do not affect the fertility (Tinson and McKinnon, 1992). Based on the size, camel ovarian cysts were considered to be pathologic (Ali *et al,* 2010). Camels' oversized follicles are accompanied by infertility problems in the form of repeat breeding, nymphomania and anoestrus (Waheed *et al,* 2017). As the biochemical metabolites of follicular fluids are vital for the maturation and fertilisation of the oocyte, the changes in these metabolites may influence the growth and quality of the oocyte. The goal of the present study is, therefore, to compare some hormonal and biochemical composition of the predominant antral follicle coexisting with oversized with its counterpart present in absence of oversized follicle.

Materials and Methods

During the breeding season (October–April), 219 genitalia were recovered from clinically healthy adult (6–15 years of age) non-pregnant female camels (*Camelus dromedarius*) at a local abattoir in the eastern province of the Kingdom of Saudi Arabia. The reproductive history of those animals was unknown. A 10 mL blood sample was collected from each animal during exsanguinations into non-heparinised tubes. After slaughtering, the genitalia were macroscopically examined to confirm that these were clinically normal. Immediately after collection, selected ovarian pairs and blood samples were transported to the laboratory in an icebox within one-hour post-slaughter. In the laboratory, ovaries were washed twice in cooled 0.9% NaCl and blotted dry. Paired ovaries bearing functional corpus luteum were excluded from the investigation. Both predominant antral follicles coexisting with thin wall oversized follicle (>20 mm in diameter; Tibary and Anouassi, 1997) and from ovaries which have no oversized follicles were considered for measuring using a Vernier caliper. Based on follicle diameter, 3 follicle categories were considered for puncture: 0.5–1.0 cm (small; n = 10), >1–1.6 cm (medium; n = 10) and >1.6–2.0 cm (large; n=10). Follicular fluids of the predominant follicle were aspirated using sterilised 22-gauge hypodermic needles and syringes. The follicular fluid was centrifuged at 1250X g at 4°C for 10 minutes. The supernatant was harvested and stored at -20°C pending analysis. Blood sera from selected animals were separated and stored at -20°C until analysis.

Hormonal and biochemical analysis

Enzyme immune assay kits purchased from Mybiosource® (USA) were used for estimation of the concentrations of camel oestradiol 17-Beta-Dehydrogenase (E2; pg/mL; Catalog No. MBS9381137), camel progesterone (P4; ng/mL; Catalog No. MBS7606970), camel cortisone (ng/mL; Catalog No. MBS062065), camel insulin-like growth factor-II (IGF-II; ng/mL; Catalog No. MBS058122), camel ultra-sensitivity triiodothyronine (nmol/L; Catalog No. MBS056436), general thyroxine (ng/mL; Catalog No. MBS289276) and vit C (µg/ml; Catalog No. MBS2700398).

The laboratory reported intra- and inter-assay coefficient of variances of the studied hormonal and biochemical constituents were 4.4% and 5.1% for oestradiol, 2.3% and 4.8% for progesterone, 4.4% and 5.1% for cortisone, 3.1% and 3.9% for insulin-like growth factor-II, 2.3% and 4.1% for ultra-sensitivity triiodothyronine, 3.2% and 5.3% for general thyroxine, 3.9% and 7.4% for vitamin C, respectively. The kits did not validate before the use with camel follicular fluid or serum. The sensitivity of assays for oestradiol 17-Beta-dehydrogenase, progesterone, cortisone, insulin-like growth factor-II, ultra-sensitivity triiodothyronine, general thyroxine and vit C were 0.1 ng/ml, 0.188 ng/ml, 1.0 ng/ml, 1.0 ng/ml, 0.1 nmol/L, 0.0975 ng/ml and 173.5 µg/ml, respectively. All measurements were carried out according to the manufacturers' guidelines. The optical densities were measured using an ELISA reader (Absorbance Microplate Reader ELx800TM, BioTek®, Highland Park, VT, USA and Microplate Strip Washer (ELx800 TM, BioTek®, Highland Park, VT, USA).

Statistical analysis

The data of hormonal and biochemical constituents are presented as the means ± SEM. Analyses were conducted by Student's t-test (t)using INSTAT software 3.1 (2017).

Results

The mean concentrations of oestradiol, cortisone and vitamin C in follicular fluid from the small follicles that exist in the absence of the oversized follicles were found higher as compared with that of the small follicles that coexist with the oversized follicles ($P<0.0001$; Table 1). The concentrations of progesterone were lower in the follicular fluid harvested from the small follicles that exist in the absence of oversized follicles than that collected from the small follicles that coexist with oversized follicle ($P<0.01$). The IGF-II and general thyroxine in the follicular fluid from the small follicles that exist in the absence of the oversized follicles were lower

compared with that of the small follicles that coexisted with the oversized follicle (P<0.0001). There was no difference in the concentration of oestradiol and cortisone in the serum of camels bearing small follicle which exist in absence of oversized follicle and serum of camels bearing small follicle coexist with oversized follicle (P>0.05; Table 2). The mean concentration of progesterone in the serum of camels bearing small follicle exist in absence of oversized follicle was significantly lower than that bearing small follicle coexist with oversized follicle (P<0.0001; Table 2).

The IGF-II levels in the serum of camels bearing small follicle exist in absence of oversized follicle was significantly higher (P<0.0001) than that bearing small follicle coexist with oversized follicle. The serum of camels bearing small follicle exist in absence of oversized follicle had significantly lower (P<0.0.05) concentration of ultra-sensitivity triiodothyronine than that bearing small follicle coexist with oversized follicle. Likewise, the general thyroxine concentration was lower (P<0. 001) in the serum of camels bearing small follicle which existed in absence of oversized follicle than that bearing small follicle which coexisted with oversized follicle. However, the vitamin C concentration was significantly higher (P<0. 0.0.05) in the serum of camels bearing small follicle exist in absence of oversized follicle than that bearing small follicle coexist with oversized follicle.

Oestradiol, cortisone, IGF-II and ultra-sensitivity triiodothyronine concentrations were

Table 1. Concentrations of some hormonal and biochemical constituents (mean ± SEM) in the follicular fluid of predominant small follicle which coexisted with oversize follicle and its counterpart present in the absence of oversize follicle in camels.

Hormonal and biochemical constituents	Fluid from small follicle exist in absence of oversize follicle	Fluid from small follicle coexist with oversize follicle	P-value
Oestradiol 17- β (pg/ml)	703.0^{a} ± 51.96 C.I.* 585.48 – 820.52	24.9^{b} ± 1.12 C.I.* 22.37 – 27.43	P<0.0001
Progesterone (ng/ml)	0.07^{a} ± 0.02 C.I.* 0.035 – 0.105	0.014^{b} ± 0.002 C.I.* 0.009 – 0.019	P<0.01
Cortisone (ng/ml)	0.40^{a} ± 0.02 C.I.* 0.36 – 0.44	0.004^{b} ± 0.0004 C.I.* 0.003 – 0.005	P<0.0001
Insulin-like growth factor-II (ng/ml)	83.48^{a} ± 0.45 C.I.* 82.47 – 84.49	111.57^{b} ± 0.45 C.I.* 110.55 – 112.59	P<0.0001
Ultra-sensitivity triiodothyronine (nmol/L)	4.70^{a} ± 0.02 C.I.* 4.67 – 4.73	4.32^{b} ± 0.09 C.I.* 4.13 – 4.52	P<0.001
General thyroxine (ng/ml)	9.24^{a} ± 0.02 C.I.* 9.20 – 9.28	9.80^{b} ± 0.01 C.I.* 9.79 – 9.81	P<0.0001
Vitamin C (µg/ml)	15.54^{a} ± 0.32 C.I.* 14.81 – 16.27	11.95^{b} ± 0.63 C.I.* 10.52 – 13.38	P<0.0001

Means with dissimilar superscripts are significantly different; *Confidence Interval

Table 2. Concentrations of some hormonal and biochemical constituents (mean ± SEM) in the serum of the camels bearing predominant small follicle which coexisted with oversize follicle and its counterpart present in the absence of oversize follicle.

Hormonal and biochemical constituents	Serum of camels bearing small follicle exist in the absence of oversize follicle	Serum of camels bearing small follicle coexist with oversize follicle	P-value
Oestradiol 17- β (pg/ml)	1.51 ± 0.48 C.I.* 13.42 – 15.58	1.90 ± 0.60 C.I.* 13.04 – 15.76	0.8977
Progesterone (ng/ml)	0.041^{a} ± 0.002 C.I.* 0.037 – 0.045	0.069^{b} ± 0.005 C.I.* 0.057 – 0.081	P<0.0001
Cortisone (ng/ml)	0.002 ± 0.0003 C.I.* 0.002 – 0.003	0.002 ± 0.0003 C.I.* 0.001 – 0.003	0.2098
Insulin-like growth factor- II (ng/ml)	111.14^{a} ± 0.77 C.I.* 109.39 – 112.89	92.99^{b} ± 2.32 C.I.* 87.75 – 98.24	P<0.0001
Ultra-sensitivity triiodothyronine (nmol/L)	4.25^{a} ± 0.01 C.I.* 4.23 – 4.27	5.29^{b} ± 0.39 C.I.* 4.41 – 6.17	P<0.05
General thyroxine (ng/ml)	8.88^{a} ± 0.005 C.I.* 8.87 – 8.89	9.14^{b} ± 0.059 C.I.* 9.01 – 9.27	P<0.001
Vitamin C (µg/ml)	22.56^{a} ± 0.05 C.I.* 22.45 – 22.68	20.33^{b} ± 0.85 C.I.* 10.41 – 22.25	P<0.05

Means with dissimilar superscripts are significantly different; *Confidence Interval

higher in follicular fluid obtained from the medium follicles that existed in the absence of the oversized follicles compared with that of the medium follicles that coexisted with the oversized follicles (Table 3). Significant differences were not reported in the values of the progesterone and vitamin C between the follicular fluid harvested from the medium follicles that existed in the absence of oversized follicles and that collected from the medium follicles that coexisted with oversized follicle. The general thyroxine concentrations in follicular fluid from medium follicles that existed in the absence of the oversized follicles were higher (P<0.01) compared with that of the medium follicles that coexisted with the oversized follicles.

Oestradiol, cortisone and vitamin C didn't vary significantly between serum of camels bearing medium follicles which existed in the absence of oversized follicle and the serum of camels bearing medium follicles which coexisted with the oversized follicles (Tabel 4). Progesterone and general thyroxine concentrations were significantly higher (P<0.01) in the serum of the animals bearing medium follicles coexisted with the oversized follicle than in the serum of the animals bearing medium follicles exist in the absence of oversized follicle. The IGF-II concentrations were higher (P<0.0001) in the serum of the camels bearing medium follicles existed in the absence of oversized follicle than in the serum of the camels bearing medium follicles coexist with the oversized follicle. The ultrasensitive triiodothyronine values were significantly higher (P<0.0001) in the serum of the animals bearing medium follicles coexist with the oversized follicle than that serum of animals bearing medium follicles exist in absence of oversized follicle.

Oestradiol and cortisone were higher (P<0.0001) in the follicular fluid of large size predominant follicles which existed in the absence of oversized follicle than that in the follicular of large size predominant follicles fluid coexist with the oversized follicle (Table 5). There were no significant differences in the concentrations of the progesterone, IGF-II and ultra-sensitivity triiodothyronine between the follicular fluid of large size predominant follicles exist in the absence of oversized follicle and that fluid of large size predominant follicles which coexisted with the oversized follicle.

The concentrations of the general thyroxine and vitamin C were higher (P<0.001) in the follicular fluid of the large predominant follicles that coexist with oversized follicle than that of the follicular fluid of large size predominant follicles which exist in the absence of the oversized follicle (Table 5). There was no significant differences in the concentrations of the oestradiol, cortisone and general thyroxine between the serum of the camels bearing large size predominant follicles exist in the absence of oversized follicle and the serum of camels bearing large size predominant follicles which coexist with the oversized follicles (Table 6). The progesterone concentrations in the serum of the animals bearing large size predominant follicles coexisting with the oversized follicle were significantly higher than that detected in the serum

Table 3. Concentrations of some hormonal and biochemical constituents (mean ± SEM) in the follicular fluid of medium size predominant follicle which coexisted with oversize follicle and its counterpart present in the absence of oversize follicle in camels (*Camelus dromedarius*).

Hormonal and biochemical constituents	**Fluid from medium size predominant follicle exist in the absence of oversize follicle**	**Fluid from medium size predominant follicle coexist with oversize follicle**	***P-value***
Oestradiol 17- β (pg/ml)	531.10^{a} ± 25.38 C.I.* 473.69 – 588.51	10.90^{b} ± 0.82 C.I.* 9.04 – 12.76	P<0.0001
Progesterone (ng/ml)	0.016 ± 0.003 C.I.* 0.010 – 0.022	0.016 ± 0.003 C.I.* 0.008 – 0.024	0.9999
Cortisone (ng/ml)	0.28^{a} ± 0.02 C.I.* 0.24 – 0.33	0.004^{b} ± 0.0009 C.I.* 0.002 – 0.006	P<0.0001
Insulin-like growth factor-II (ng/ml)	100.19^{a} ± 1.84 C.I.* 96.02 – 104.36	88.98^{b} ± 1.35 C.I.* 85.93 – 92.03	P<0.0001
Ultra-sensitivity triiodothyronine (nmol/L)	4.67^{a} ± 0.02 C.I.* 4.63 – 4.71	3.20^{b} ± 0.03 C.I.* 3.14 – 3.25	P<0.0001
General thyroxine (ng/ml)	10.22^{a} ± 0.28 C.I.* 9.58 – 10.87	9.28^{b} ± 0.02 C.I.* 9.23 – 9.34	P<0.01
Vitamin C (µg/ml)	12.38 ± 0.08 C.I.* 12.21 – 12.55	12.28 ± 0.41 C.I.* 11.35 – 13.21	0.8150

Means with dissimilar superscripts are significantly different; *Confidence Interval

of the animals bearing large size predominant follicles whih exist in the absence of oversized follicle (P<0.01). The IGF-II was significantly elevated (P<0.001) in the serum of the animals bearing large size predominant follicles coexisting with the oversized follicle than those animals bearing large size predominant follicles exist in the absence of oversized follicles. The ultra-sensitive triiodothyronine concentrations were significantly raised in the serum of the camels bearing large size predominant follicles coexisting with the oversized follicle than those animals bearing large size predominant follicles which existed in the absence of oversized follicle (P<0.0001). The vitamin C concentrations were significantly higher in the serum of the camels bearing large size predominant follicles exist in the absence of oversized follicles than those animals bearing large size predominant follicles coexisting with the oversized follicles (P<0.0001).

Discussion

The assessment of some hormonal and biochemical composition of the predominant antral follicle coexisting with oversized with its counterpart present in absence of oversized follicle were the goals of this study. Follicular fluid holds different biochemical metabolites that are derived from serum or synthesised locally in the follicles and shared in the metabolic activities of follicular cells (Edwards, 1974; Gérard *et al,* 2002). The constituents of the follicular fluid change through the growth and development of each follicle (Wise, 1987). This study reported a significant increase in the concentrations of oestradiol of follicular fluid from the various size antral predominant follicle that exist in the absence of oversize follicle. The ability of antral follicles to produce large amounts of oestradiol is a distinctive sign of follicle health status (Kobayashi *et al,* 2006). The prsent study demonstrated no significant change in the level of oestradiol either in the serum of camels bearing large follicle existing in absence of oversize follicle or in serum of camels bearing large follicle coexisting with the oversize follicle. The presence of the oversize follicle does not associate with a significant increase in serum oestradiol (Ghoneim *et al,* 2013). The present study recorded a significant high progesterone in the follicular fluid of small size predominant antral follicle coexist with the oversize follicle. Granulosa and theca cells secret large amounts of progesterone which act as a precursor for androgen and subsequently estrogen production (McNatty *et al,* 1984). Progesterone promotes the production of proteolytic enzymes essential for the collapse of follicles at ovulation (Iwamasa *et al,* 1992). The source of the significant high peripheral progesterone concentrations reported in camels bearing different size predominant follicles which coexisted with oversized follicle may be the adrenal cortex (Asher *et al,*1989). Glucocorticoids in follicular fluid are derived from the general circulation (Lewicka *et al,* 2003). The glucocorticoid status of ovarian follicular fluid is prognostic to oocyte quality (Lewicka *et al,* 2003). The 11beta-hydroxysteroid dehydrogenases convert cortisol to its inactive metabolite cortisone and *vice versa* (Quinkler *et al,*

Table 4. Concentrations of some hormonal and biochemical constituents (mean ± SEM) in the serum of the camels bearing medium size predominant follicle which coexisted with oversize follicle and its counterpart present in the absence of oversize follicle.

Hormonal and biochemical constituents	Serum of camels bearing medium size predominant follicle exist in absence of oversize follicle	Serum of camels bearing medium size predominant follicle coexist with oversize follicle	*P-value*
Oestradiol 17-17- β (pg/ml)	2.51 ± 0.71 C.I.* 10.59 – 13.81	3.37 ± 1.07 C.I.* 7.89 – 12.71	0.1553
Progesterone (ng/ml) in serum	0.069^{a} ± 0.003 C.I.* 0.063 – 0.075	0.083^{b} ± 0.003 C.I.* 0.077 – 0.089	P<0.01
Cortisone (ng/ml) in serum	0.001 ± 0.0002 C.I.* 0.0009 – 0.002	0.002 ± 0.0002 C.I.* 0.002 – 0.003	0.0652
Insulin-like growth factor-II (ng/ml)	102.50^{a} ± 7.60 C.I.* 85.31 – 119.69	48.49^{b} ± 1.87 C.I.* 44.27 – 52.72	P<0.0001
Ultra-sensitivity triiodothyronine (nmol/L)	4.35^{a} ± 0.05 C.I.* 4.23 – 4.47	4.70^{b} ± 0.04 C.I.* 4.60 – 4.80	P<0.0001
General thyroxine (ng/ml)	9.17^{a} ± 0.02 C.I.* 9.13 – 9.21	10.35^{b} ± 0.34 C.I.* 9.59 – 11.11	P<0.01
Vitamin C (µg/ml)	24.16 ± 0.67 C.I.* 22.64 – 25.68	22.00 ± 1.13 C.I.* 19.45 – 24.55	0.1172

Means with dissimilar superscripts are significantly different; *Confidence Interval

2003). This study reported a high significant cortisone concentration in follicular fluid of small, medium and large predominate by existing in absence of oversize follicles wherever, there were no recorded significant changes in peripheral cortisone in animals that had or had not oversize follicles. Cortisol inhibits the ovarian steroidogenesis (Michael *et al,* 1993) and stimulate oocyte maturation (Fateh *et al,* 1989; Jimena *et al,* 1992). IGF-II concentrations in the follicular fluid of the predominant small follicles coexisting with the oversize follicle were significantly high. On the other hand, the follicular fluid of the predominant medium size follicle existing in the absence of an oversize follicle had significantly high concentration of IGF-II. IGF-II concentrations in the serum of camels bearing small, medium and large size predominant follicle which existed in absence of oversize follicle were significantly high. In primate species, IGFII is the predominant circulating and intraovarian form of IGFs (Giudice, 2001; Tkachenko *et al,* 2021). IGFII stimulates granulosa steroidogenesis (Giudice, 2001). Parallel with the results of Tabatabaei *et al* (2011), ultrasensitive triiodothyronine concentrations were significantly high in follicular fluid collected from predominant small and medium size follicle existing in absence of oversized follicle. General thyroxine concentrations were significantly high in the follicular fluid of predominant small and large

Table 5. Concentrations of some hormonal and biochemical constituents (mean ± SEM) in the follicular fluid of the camels bearing large size predominant follicle which coexisted with oversize follicle and its counterpart present in the absence of oversize follicle.

Hormonal and biochemical constituents	Fluid from large follicle exist in absence of oversize follicle	Fluid from large follicle coexist with oversize follicle	*P-value*
Oestradiol 17- β (pg/ml)	664.10^{a} ± 13.26 C.I.* 634.11 – 694.09	9.00^{b} ± 1.08 C.I.* 6.57 – 11.43	P<0.0001
Progesterone (ng/ml)	0.017 ± 0.003 C.I.* 0.009 – 0.025	0.017 ± 0.003 C.I.* 0.009 – 0.025	0.9999
Cortisone (ng/ml)	0.28^{a} ± 0.02 C.I.* 0.23 – 0.32	0.009^{b} ± 0.001 C.I.* 0.007 – 0.011	P<0.0001
Insulin-like growth factor-II (ng/ml)	93.28 ± 2.07 C.I.* 88.61 – 97.95	91.55 ± 2.10 C.I.* 86.81 – 96.29	0.5639
Ultra-sensitivity triiodothyronine (nmol/L)	3.66 ± 0.16 C.I.* 3.31 – 4.01	3.73 ± 0.08 C.I.* 3.55 – 3.92	0.6952
General thyroxine (ng/ml)	8.88^{a} ± 0.23 C.I.* 8.37 – 9.39	10.60^{b} ± 0.29 C.I.* 9.94 – 11.26	P<0.001
Vitamin C (µg/ml)	9.61^{a} ± 0.29 C.I.* 8.95 – 10.27	11.26^{b} ± 0.19 C.I.* 10.82 – 11.70	P<0. 001

Means with dissimilar superscripts are significantly different; *Confidence Interval

Table 6. Concentrations of some hormonal and biochemical constituents (mean ± SEM) in the serum of the camels bearing large size predominant follicle which coexisted with oversize follicle and its counterpart present in the absence of oversize follicle.

Hormonal and biochemical constituents	Serum of camels bearing large follicle exist in absence of oversize follicle	Serum of camels bearing large ollicle coexist with oversize follicle	*P-value*
Oestradiol 17- β (pg/ml)	17.60 ± 1.04 C.I.* 15.26 – 19.94	15.30 ± 0.92 C.I.* 13.22 – 17.38	0.1140
Progesterone (ng/ml)	0.059^{a} ± 0.001 C.I.* 0.057 – 0.061	0.069^{b} ± 0.002 C.I.* 0.064 – 0.074	P<0.01
Cortisone (ng/ml)	0.002 ± 0.0003 C.I.* 0.0008 – 0.002	0.002 ± 0.0003 C.I.* 0.0009 – 0.003	0.8364
Insulin-like growth factor-II (ng/ml)	55.84^{a} ± 1.93 C.I.* 51.47 – 60.21	73.98^{b} ± 3.61 C.I.* 65.82 – 82.14	P<0.001
Ultra-sensitivity triiodothyronine (nmol/L)	4.75^{a} ± 0.007 C.I.* 4.73 – 4.77	4.95^{b} ± 0.007 C.I.* 4.93 – 4.97	P<0.0001
General thyroxine (ng/ml)	8.55 ± 0.20 C.I.* 8.09 – 9.92	8.30 ± 0.077 C.I.* 8.13 – 8.47	0.2650
Vitamin C (µg/ml)	23.18 ± 0.22 C.I.* 22.68 – 23.68	15.49 ± 0.72 C.I.* 13.86 – 17.12	P<0.0001

Means with dissimilar superscripts are significantly different; *Confidence Interval

size follicles that coexist with the oversize follicle. The follicular fluid of predominant medium size follicle that exist in absence of oversize follicle had a significant high concentration of general thyroxine. The concentrations of general thyroxine in the serum of camels bearing small and medium size follicles coexist with oversized follicle were significantly high. The majority of thyroxine present in follicular fluid appear to be derived from peripheral blood and enter follicles through theca interna cells (Cai *et al,* 2019). Thyroid hormones control the growth, differentiation, and metabolism in almost all somatic tissues (Ingbar and Wieber, 1981). Moreover, thyroxine affects the folliculogenesis (Ashkar *et al,* 2010; Verga Falzacappa *et al,* 2012; Zhang *et al,* 2013; Fedail *et al,* 2014) and ovarian steroidogenesis (Cecconi *et al,* 1999). In this study, Vitamin C concentrations were significantly high in follicular fluid of small size predominant follicle exists in absence of oversized follicle and in follicular fluid of large size predominant follicle which coexisted with the oversized follicle. The serum of camels bearing small and large size predominant follicle exist in absence of oversized follicle had a significant high concentration of Vitamin C. The ovaries store high amounts of ascorbic acid within the granulosa, thecal, and luteal cells (Deane, 1952). Ascorbic acid endorses steroidogenesis (Sanyal and Datta, 1979), acts as an antioxidant (Goralczyk *et al,* 1992; Luck *et al,* 1995) and assets in remodeling the basement membrane during follicular growth (Murray *et al,* 2001).

The current study revealed significant differences in some hormonal and biochemical constituents between follicular fluids from predominant follicle which coexisted with the oversized follicle and its counterpart present in the absence of the oversized follicle. Relying on these outcomes we can hypothesise that the presence of an oversize follicle alters some hormonal and biochemical constituents of follicular fluid of predominant follicle which coexist with it.

Acknowledgements

The authors like to acknowledge the Deanship of Scientific Research at King Faisal University for their financial support (the annual support track grant no. 170110).

References

Al-Afaleq AI, Hegazy AA, Hussein MF and Dughaym AM. Pathological disorders of the female reproductive system in slaughtered camels (*Camelus dromedarius*) in Saudi Arabia. Comparative Clinical Pathology. 2012; 21:245-51.

Ali A, Tharwat M and Al-Sobayil FA. Hormonal, biochemical, and haematological profiles in female camels (*Camelus dromedarius*) affected with reproductive disorders. Animal Reproduction Science. 2010; 118:372-376.

Asher GW, Peterson AJ and Duganzich D. Adrenal and ovarian sources of progesterone secretion in young female fallow deer, *Dama dama*. Journal of Reproduction and Infertility. 1989; 85:667-675.

Ashkar FA, Bartlewski PM, Singh J, Malhi PS, Yates KM, Singh T and King WA. Thyroid hormone concentrations in systemic circulation and ovarian follicular fluid of cows. Experimental Biology and Medicine (Maywood). 2010; 235:215-221.

Bravo PW, Stabenfeldt GH, Fowler ME and Lasley BL. Ovarian and endocrine patterns associated with reproductive abnormalities in llamas and alpacas. Journal of the American Veterinary Medical Association. 1993; 202:268-272.

Cai YY, Lin N, Zhong LP, Duan HJ, Dong YH, Wu Z and Su H. Serum and follicular fluid thyroid hormone levels and assisted reproductive technology outcomes. Reproductive Biology and Endocrinology. 2019; 17:90-97.

Cecconi S, Rucci N, Scaldaferri ML, Masciulli MP, Rossi G, Moretti C, D'Armiento M and Ulisse S. Thyroid hormone effects on mouse oocyte maturation and granulosa cell aromatase activity. Endocrinology. 1999; 140:1783-1788.

Deane HW. Histochemical observation on the ovary and oviduct of the albino rat during the oestrus cycle. American Journal of Anatomy. 1952; 91:363-413.

Edwards RG. Follicular fluid. Journal of Reproduction and Infertility. 1974; 37:189-219.

El wishy AB. Reproduction in the female dromedary (*Camelus dromedarius*): a review. Animal Reproduction Science. 1987; 82:587-593.

Fedail JS, Zheng K, Wei Q, Kong L and Shi F. Roles of thyroid hormones in follicular development in the ovary of neonatal and immature rats. Endocrine. 2014; 46:594-604.

Fateh M, Ben-Rafael Z, Benadiva CA, Mastroianni L and Jr Flickinger GL. Cortisol levels in human follicular fluid. Fertility and Sterility. 1989; 51:538-541.

Gérard N, Loiseau S, Duchamp G and Seguin F. Analysis of the variations of follicular fluid composition during follicular growth and maturation in the mare using proton nuclear magnetic resonance (1HNMR). Reproduction. 2002; 124:241-248.

Ghoneim IM, Waheed MM, El-Bahr SM, Alhaider AK and Al-Eknah MM. Comparison of some biochemical and hormonal constituents of oversized follicles and preovulatory follicles in camels (*Camelus dromedarius*). Theriogenology. 2013; 79:647-52.

Giudice LC. Insulin-like growth factor family in Graafian follicle development and function. Journal of the Society for Gynecologic Investigation. 2001; 8:S26-9.

Goralczyk R, Moser UK, Matter U and Weiser H. Regulation of steroid hormone metabolism requires L-ascorbic acid. Annals of the New York Academy of Sciences. 1992; 669:349-951.

Ingbar SH and Wieber KA. The thyroid gland. In: Williams

RH, editor. Textbook of Endocrinology. Philadelphia: W.B. Sounders Company. 1981; pp 117-243.

INSTAT. INSTAT 3.1 General statistical package software. 2017.

Ismail ST. A review of reproduction in the female camel (*Camelus dromedarius*) Theriogenology. 1987; 28:363-371.

Iwamasa J, Shibata S, Tanaka N, Matsuura K and Okamura H. The relationship between ovarian progesterone and proteolytic enzyme activity during ovulation in the gonadotrophin-treated immature rat. Biology of Reproduction. 1992; 46:309-313.

Jimena P, Castilla JA, Peran F, Ramirez JP, Vergara F, Jr Molina R, Vergara F and Herruzo A. Adrenal hormones in human follicular fluid. Acta Endocrinology. (Copenh). 1992; 127:403-406.

Kobayashi Y, Jimenez-Krassel F, Ireland JJ and Smith GW. Evidence of a local negative role for cocaine and amphetamine regulated transcript (CART), inhibins and low molecular weight insulin like growth factor binding proteins in regulation of granulose cell oestradiol production during follicular waves in cattle. Reprod. Reproductive Biology and Endocrinology. 2006; 4:22-33.

Lewicka S, von Hagens C, Hettinger U, Grunwald K, Vecsei P, Runnebaum B and Rabe T. Cortisol and cortisone in human follicular fluid and serum and the outcome of IVF treatment. Human Reproduction. 2003; 18:1613-1617.

Luck MR, Jeyaseelan I and Scholes RA. Ascorbic acid and fertility. Biology of Reproduction. 1995; 52:262-266.

McNatty KP, Heath DA, Henderson KM, Lun S, Hurst PR, Ellis LM, Montgomery GW, Morrison L and Thurley DC. Some aspects of thecal and granulosa cell function during follicular development in the bovine ovary. Journal of Reproduction and Fertility. 1984; 72:39-53.

Michael AE, Pester LA, Curtis P, Shaw RW, Edwards CR and Cooke BA. Direct inhibition of ovarian steroidogenesis by cortisol and the modulatory role of 11 beta-hydroxysteroid dehydrogenase. Clinical Endocrinology. 1993; 38:641-644.

Murray AA, Molinek MD, Baker SJ, Kojima FN, Smith MF, Hillier SG and Spears N. Role of ascorbic acid in promoting follicle integrity and survival in intact mouse ovarian follicles *in vitro*. Journal of Reproduction and Infertility. 2001; 121:89-96.

Musa BE and Abusineina ME. The oestrous cycle of the camel (*Camelus dromedarius*). Veterinary Record. 1978; 103:556-557.

Quinkler M, Troeger H, Eigendorff E, Maser-Gluth C, Stiglic A, Oelkers W, Bähr V and Diederich S. Enhanced 11 beta-hydroxysteroid dehydrogenase type 1 activity in stress adaptation in the guinea pig. Journal of Endocrinology 2003; 176:185-92.

Sanyal S and Datta S. Effect of ascorbic acid in *in vitro* rat adrenal and ovarian steroidogenesis. Indian Journal of Experimental Biology. 1979; 17:86-88.

Skidmore JA, Billah M and Allen WR. The ovarian follicular wave pattern in the mated and non-mated dromedary camel (*Camelus dromedarius*). Journal of Reproduction and Fertility. Supplements. 1995; 49:545-548.

Skidmore JA, Billah M and Allen WR. The ovarian follicular wave pattern and induction of ovulation in the mated and non-mated one-humped camel (*Camelus dromedarius*). Journal of Reproduction and Fertility. 1996; 106:185-92.

Skidmore JA, Morton KM and Billah M. Artificial insemination in dromedary camels. Animal Reproduction Science. 2013; 136:178-186.

Tabatabaei S, Mamoei M and Aghaei A. Dynamics of ovarian follicular fluid in cattle. Comparative Clinical Pathology. 2011; 20:591-595.

Tibary A and Anouassi A. Ultrasonographic changes of the reproductive tract in the female camel (*Camelus dromedarius*) during the follicular cycle and pregnancy. Journal of Camel Practice and Research. 1996; 1:71-90.

Tibary A and Anouassi A. Reproductive physiology in female camelidae. In: Tibary, A. (Ed.), Theriogenology in Camelidae Anatomy, Physiology, Pathology and Artificial Breeding. Actes Editions, Institut Agronomique et Vétérinaire Hassan II. 1997; pp 169-241. Rabat.

Tinson AH and McKinnon AO. Ultrasonography of the reproductive tract of the female dromedary camel. Proceedings of the 1st International Camel Conference. Dubai (UAE). 1992; February 2-6, pp 129-135. (1992).

Tkachenko OY, Wolf S, Lawson MS, Ting AY, Rodrigues JK, Xu F, Bishop CV, Stouffer RL and Xu J. Insulin-like growth factor 2 is produced by antral follicles and promotes preantral follicle development in macaques. Biology of Reproduction. 2021; 104:602-610.

Verga Falzacappa C, Timperi E, Bucci B, Amendola D, Piergrossi P, D'Amico D, Santaguida MG, Centanni M and Misiti S. T(3) preserves ovarian granulosa cells from chemotherapy-induced apoptosis. Journal of Endocrinology. 2012; 215:281-289.

Waheed MM, Ghoneim IM, Hasseeb MM and Al-Muhasen FM. Behavioural, hormonal and histopathological changes accompanying the oversized follicles in camels (*Camelus dromedarius*). Journal of Camel Practice and Research. 2017; 24:27-34.

Wilson RT. The Camel. Longman, London/New York. 1984; pp 83-102.

Wise T. Biochemical analysis of bovine follicular fluid: albumin, total protein, lysosomal enzymes, ions, steroids and ascorbic acid content in relation to follicular size, rank, atresia classification and day of estrous cycle. Journal of Animal Science. 1987; 64:1153-1169.

Zhang C, Guo L, Zhu B, Feng Y, Yu S, An N and Wang X. Effects of 3, 5, 3′-triiodothyronine (t3) and follicle stimulating hormone on apoptosis and proliferation of rat ovarian granulosa cells. Chinese Journal of Physiology. 2013; 56:298-305.

DOI : 10.5958/2277-8934.2022.00026.1 Vol 29 No 2, p 191-196

PROTEIN PROFILE AND GLYCOSIDASE ACTIVITIES OF PROSTATE AND BULBOURETHRAL GLANDS SECRETION IN CAMELS (*Camelus dromedarius*)

Sabry M. El-Bahr[1,2], M.M. Waheed[3,4], I.M. Ghoneim[3,4], I.F. Albokhadaim[1], A.M.A. Meligy[5] and M.G. El Sebaei[1,6]

[1]Department of Biomedical Sciences, [3]Department of Clinical Sciences, [5]Central Diagnostic Lab., College of Veterinary Medicine, King Faisal University, Al-Ahsa 31982, P.O. 400, Saudi Arabia
[2]Department of Biochemistry, Faculty of Veterinary Medicine, Alexandria University, Alexandria 21523, Egypt
[4]Department of Theriogenology, Faculty of Veterinary Medicine, Cairo University, Giza 12515, Egypt
[6]Department of Biochemistry and Chemistry of Nutrition, Faculty of Veterinary Medicine, Mansoura University, Mansoura, 35516, Egypt

ABSTRACT

This study was aimed to investigate protein profiles and glycosidase activities of bulbourethral and prostate glands secretion in dromedary camels. Sixteen healthy male camels (5-13 years old) were slaughtered and both glands were collected. The obtained secretions of both glands were used for determination of protein profile by 7-20% gel electrophoresis. Activities of β-N-acetylglucosaminidase, α-N-acetylgalactosaminidase and α-L-fucosidase were also determined. The current findings showed 11 (175.7, 129.3, 126.8, 94.9, 77.8, 74.4, 71.1, 53.3, 21.8, 15.9 and 9 kDa) and 15 (124.6, 89.7, 81.1, 75.5, 72.1, 60, 54.4, 48.9, 43.3, 40, 32.5, 24, 17.8, 13.3 and 9 kDa) protein bands in secretion of bulbourethral and prostate gland, respectively. Three (77.8, 53.3 and 9 kDa) and 6 bands (81.1, 75.5, 48.9, 17.8, 13.3 and 9 kDa) showed higher staining intensities in bulbourethral and prostate secretion, respectively. Both secretions shared a band of 9 kDa with higher intensity in bulbourethral secretion. Activities of glycosidase in bulbourethral and prostate secretions were verified and were higher in bulbourethral than in prostate secretion. α-L-fucosidase showed higher activity in glands secretions compared to other enzymes. Conclusively, bulbourethral and prostate secretions may be involved in coagulation processes of dromedary semen due to their contents of secretory proteins and glycosidases.

Key words: Accessory sex glands, bulbourethral, camels, electrophoresis, glycosidases, prostate, proteins

Dromedary camels display a distinguishing anatomical and physiological pattern among different domestic animal species. Male dromedaries have two accessory sex glands, prostate and bulbourethral glands and they do not have seminal vesicles (Elwishy, 1988; Hafez and Hafez, 2001). Camel semen has been characterised as very viscous and forms coagulum directly after collection (Lichtenwalner *et al,* 1996; Bravo *et al,* 1997; Zeidan *et al,* 2000). The reproductive efficiency in camelids is low (Tibary, 1997; Skidmore, 2003). The viscosity in camel semen hinders the sperm motility (Tibary, 1997; Aminu and Sahani, 2000) and does not permit the semen to blend well with the diluents until it is completely liquefied (Wani, 2009). From the other side, glycosidases are a group of hydrolytic enzymes originate from lysosome and catalyse the hydrolysis of glycoproteins, glycolipids and glycosaminoglycans (Miller *et al,* 1993; Hahn *et al,* 2001; Jóźwik *et al,* 2003). Glycosidases play an important role in different reproductive events such as cumulus cells expansion (Takada *et al,* 1994), sperm capacitation (Taitzoglou *et al,* 2007), sperm oviductal epithelial cells interaction (Lefebvre *et al,* 1997), sperm zona pellucida binding (Miranda *et al,* 2000; Zitta *et al,* 2006), polyspermy block (Miller *et al,* 1993) and early embryos development (Tsiligianni, 2018). The present study was aimed to determine the protein profile and activities of some glycosidases (β-N-acetylglucosaminidase, α-N-acetylgalactosaminidase and α-L-fucosidase) of the bulbourethral and prostate glands secretions in dromedary camel.

Materials and Methods

Animals and samples

A total of 16 mature healthy male camels (5-13 years old) with unknown reproductive history were slaughtered in the local abattoir in Al-Ahsa

SEND REPRINT REQUEST TO SABRY M. EL-BAHR email: selbahar@kfu.edu.sa; sabryelbahr@hotmail.com

Governorate during the breeding season (November to March). After slaughtering, the prostate and bulbourethral glands were collected and transferred in an ice tank to the laboratory within half an hour. For each male the bulbourethral and prostate glands were dissected in a petri dish and squeezed using a metal squeezer to obtain their secretion. The collected fluid was centrifuged at 1500 g for 10 min and the supernatant were stored at -80ºC pending analysis.

Analysis of enzymes

Three enzymes were estimated in the bulbourethral and prostate secretion using ELISA reader (Absorbance Microplate Reader ELx 800TM BioTek®, USA; Microplate Strip Washer ELx 50TM BioTek®, USA) and commercial ELISA diagnostic kits (My Biosource®). These enzymes were camel β-N-acetylglucosaminidase (Catalog # MBS094638), camel α-N-acetylgalactosaminidase (Catalog # MBS053019) and camel α-L-fucosidase (Catalog # MBS092780). The procedures for analysis and calculation were adopted according to the manufacturer instruction.

Sodium dodecyl-sulfate polyacrylamide gel electrophoresis (SDS-PAGE) fractionation of proteins in glands secretion

Five samples of bulbourethral gland secretions each containing 100µg of protein were pooled. The same procedures were carried out with 5 samples of prostate gland secretion. The protein concentration in the pooled samples of each gland secretions was determined by using QuantiProTM BCA Assay kit (Sigma Chemical Company, UK) and stored at -20°C. The pooled samples of each gland secretion were subjected to one dimensional SDS-PAGE gradient gel electrophoresis (Laemmli, 1970) on 7–20% gradient gel as follow: 50µg protein of each pool was diluted with an equal volume of Bio-Rad Laemmli sample buffer, Cat. No. 161-0737 [62.5mM Tris-HCl (pH 6.8), 2% SDS, 0.01% Bromophenol blue, 25% glycerol, 5% β-mercaptoethanol], heated to 100°C for 5 min and loaded onto a 4% stacking polyacrylamide gel which was overlaid on top of a 7-20% resolving gel. A total of 5µl of pre-stained protein ladder of molecular weights ranged from 10-200 kDa (Cell Signaling Danvers, MA, USA) was loaded in a separate well. Gels were run at room temperature at 150V for one hour then at 100V until completion overnight. Coomassie Blue stain was used for visualisation of the gel protein-banding pattern. A calibration curve based on the molecular weight markers was constructed and used to calibrate the molecular weight of individual proteins in the secretion. For permanent records, the gel was rinsed in distilled water and photographed and documented using gel documentation system (Gel DocTMXR System, Bio-Rad).

Statistical analysis

Data are presented as means ± SEM for bulbourethral and prostate secretion, and compared by t-test using SPSS program, version 16.0 (Inc, 2007). Two-way analysis of variance (ANOVA) was used to compare the activities of the relevant enzyme activities in the same gland secretion.

Results

SDS-PAGE fractionation of bulbourethral and prostate gland secretion revealed a pattern of 11 and 15 protein bands, respectively when stained by Commassie blue stain (Fig 1 and 2) (Table 1 and 2). The molecular weight of these bands were 175.7, 129.3, 126.8, 94.9, 77.8, 74.4, 71.1, 53.3, 21.8, 15.9 and 9 kDa in bulbourethral gland secretion (Fig 1; Table 1). The molecular weight of protein bands of prostate gland secretion were 124.6, 89.7, 81.1, 75.5, 72.1, 60, 54.4, 48.9, 43.3, 40, 32.5, 24, 17.8, 13.3 and 9 kDa (Fig 2; Table 2). One band (9 kDa) was common in both glands secretion, however, this band showed higher intensity in bulbourethral gland secretion compared

Table 1. SDS-PAGE fractionation of bulbourethral gland secretion visualised by Coomassie blue stain.

No of band (from up to down)	Molecular weight (kDa)	No of band (from up to down)	Molecular weight (kDa)
1	175.7	7	71.1
2	129.3	8	53.3
3	126.8	9	21.8
4	94.9	10	15.9
5	77.8	11	9
6	74.4		

Table 2. SDS-PAGE fractionation of prostate gland secretion visualised by Coomassie blue stain.

No of band (from up to down)	Molecular weight (kDa)	No of band (from up to down)	Molecular weight (kDa)
1	124.6	9	43.3
2	89.7	10	40
3	81.1	11	32.5
4	75.5	12	24
5	72.1	13	17.8
6	60	14	13.3
7	54.4	15	9
8	48.9		

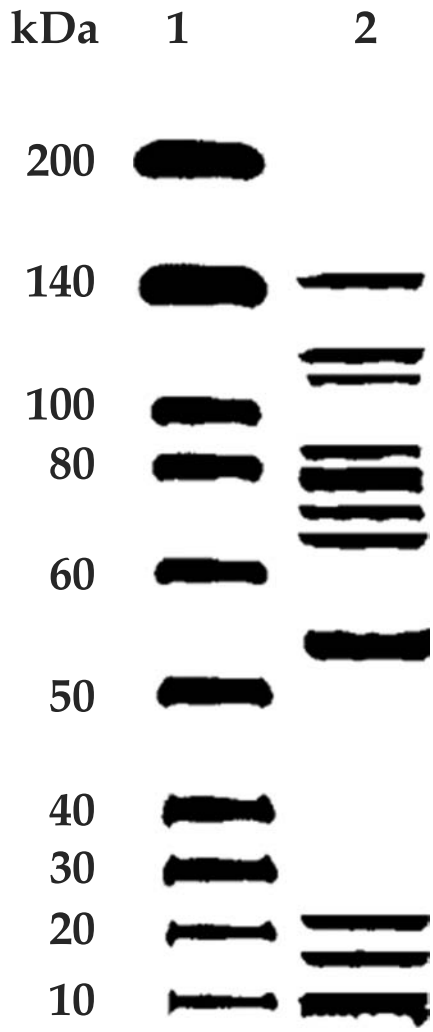

Fig 1. Protein profile of Bulbourethral gland secretion on 7-20% polyacrylamide gel stained by Coomassie blue. Lane 1- Molecular weight markers. Lane 2- Bulbourethral gland secretion.

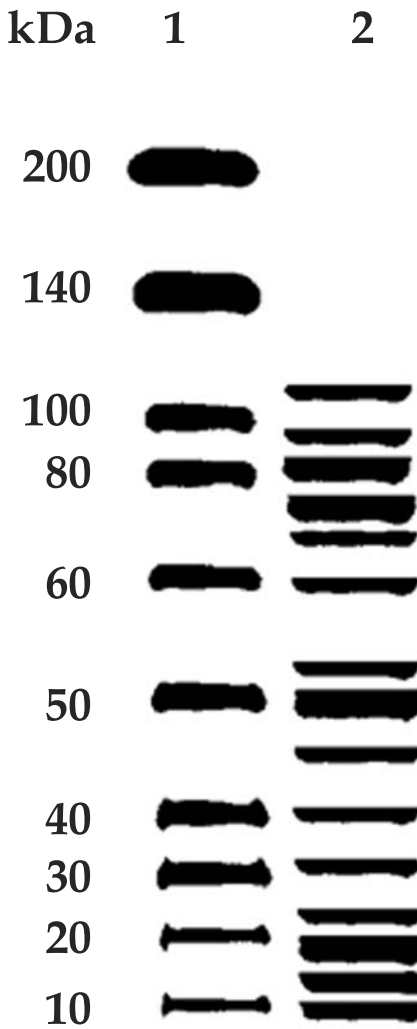

Fig 2. Protein profile of Prostate gland secretion on 7-20% polyacrylamide gel stained by Coomassie blue. Lane 1- Molecular weight markers. Lane 2- Prostate gland secretion.

to that of prostate gland (Fig 1 and 2, respectively) (Table 1 and 2, respectively). Three bands (77.8, 53.3 and 9kDa) showed the higher staining intensities in bulbourethral gland secretion (Fig 1). Six bands (81.1, 75.5, 48.9, 17.8, 13.3 and 9kDa) showed the higher staining intensities in prostate gland secretion (Fig 2). The activities of β-N-acetylglucosaminidase, α-N-acetylgalactosaminidase and α-L-fucosidase enzymes increased significantly ($P<0.05$) in bulbourethral compared to that of prostate gland secretion (Table 3). The activity of α-L-fucosidase was significantly higher than that of other studied glycosidases (β-N-acetylglucosaminidase, α-N-acetylgalactosaminidase) in both bulbourethral and prostate gland secretion (Table 3). The dominance of glycosidases activities was to α-L-fucosidase followed by β-N-acetylglucosaminidase and finally by α-N-acetylgalactosaminidase (Table 3).

Table 3. The activities of glycosidase enzymes in prostate and bulbourethral glands secretion of dromedary camels (mean ± SEM), (n=16).

Enzymes	Units	Bulbourethral	Prostate	P-value
Camel β-N-acetylglucosaminidase	ng/ml	2.18 ± 0.10^{Ya}	1.43 ± 0.07^{Yb}	0.000006
Camel α-N-acetylgalactosaminidase	ng/ml	2.35 ± 0.07^{Xa}	2.12 ± 0.08^{Xb}	0.021598
Camel α-L-fucosidase	ng/ml	13216.84 ± 10.92^{Wa}	9663.16 ± 6.56^{Wb}	0.000009

a–c within rows, means ± SEM with different superscripts differ significantly ($P < 0.05$).
w-y within columns, means ± SEM with different superscripts differ significantly ($P < 0.05$).

Discussion

As far as we know this is the first study that evidenced the role of proteins and glycosidases in the viscosity and coagulation process of semen of camels. Many proteins from seminal plasma had been related to either fertility, like in bull (Killian *et al,* 1993), boar (Flowers, 1998), stallion (Brandon *et al,* 1999) and buffalo (Harshan *et al,* 2009), freezability, as in bulls (Asadpour *et al,* 2007) or viability of spermatozoa, like in bulls and rams (Barrios *et al,* 2000). Addition of plasma proteins to semen probably improved the function of semen extenders and consequently, fertility. There is very little information available about the seminal plasma protein profile or its functions in camelids. The most notable feature in the anatomy of the internal genitalia of camelids was the absence of vesicular glands (Tibary and Anouassi, 1997); they only possessed a prostate and two bulbourethral glands. In most mammalians, secretion by the vesicular glands accounts for all the major seminal plasma proteins (Bergeron *et al,* 2005). Moreover, bovine seminal plasma proteins, secreted by vesicular glands, mediate sperm recognition and binding to the oviductal epithelium to form a reservoir (Gwathmey *et al,* 2006). During ejaculation, spermatozoa mixed with bovine seminal plasma proteins. These proteins removeed some cholesterol from the plasmatic membrane and subsequently bind to choline phospholipids. This replacement process did not allow free movement of phospholipids, and consequently stabilised the plasmatic membrane (Villemure *et al,* 2003). The current findings revealed the presence of 11 proteins bands in bulbouretheral gland secretion of male dromedary camels. The molecular weight of these bands were 175.7, 129.3, 126.8, 94.9, 77.8, 74.4, 71.1, 53.3, 21.8, 15.9 and 9 kDa. Previous study (Apichela *et al,* 2014) indicated the presence of 8 protein bands in bulbouretheral gland secretion of male llama by using one dimension 8-18% gradient SDS-PAGE and the molecular weight of these bands were 254, 231, 203, 169, 148, 130, 118 and 49 kDa. As displayed in the result study, the number and molecular weight of bands in dromedary camels were different from that detected in llama (Apichela *et al,* 2014). This difference mainly attributed to species difference, type of separated gel and/or the type of used molecular weight marker. The result study demonstrated that the bulbourethral and prostate glands secreted several proteins that may facilitate sperm adhesion to the oviduct in camelids. At least 11 or 15 protein bands had been found in bulbourethral and prostate glands secretion, respectively that were secreted by these glands. Some of them seem related to the ability of sperm to form an oviductal reservoir, and hence, they would prolong spermatozoa life in the female genital tract. This differed dromedary from other species, such as boar, in which bulbourethral secretions did not contain proteins (they were not detected electrophoretically or by gel filtration) (Schellpfeffer and Hunter, 1970). By means of mass spectrometry, four seminal plasma proteins have been identified in alpaca (Kershaw-Young and Maxwell, 2012). One of them, Mucin 5B, was a gel-forming protein produced by the bulbourethral glands and had been related to semen viscosity. Mucin 5B could be responsible for the laminar substance that entraps spermatozoa in the sperm reservoir following mating. This protein probably degraded by some mechanism of sperm release triggered by the oviduct, although allowing spermatozoa ascend to the site of fertilisation. The results indicated that the camels' bulbourethral and prostate glands seemed to produce protein molecules with particular functions and needed to be identified. The introduction of semen into the female tract orchestrated striking molecular and cellular changes that facilitated conception and pregnancy. Seminal plasma contained many molecules bind to cognate receptors on target cells in the female reproductive tract, activating changes in gene expression leading to modifications in the cellular composition, structure and function of local tissues and of tissues distal to the reproductive (Robertson, 2005). In the present study, 3 (77.8, 53.3 and 9kDa) and 6 bands (81.1, 75.5, 48.9, 17.8, 13.3 and 9kDa) showed higher staining intensities in bulbourethral and prostate gland secretion, respectively. In addition, both secretions shared a band of 9 kDa but higher intensity was recorded in bulbourethral secretion. Previously, Stelletta *et al* (2021) demonstrated that the concentration of 15-18 kDa molecular weight (MW) proteins showed a positive correlation with sperm concentration and foal rate in horses. They concluded that a strong positive correlation was found between sperm concentration and 23-28 kDa MW proteins (r=0.77). In addition, the volume of 19-22 kDa MW proteins was negatively correlated with pregnancy and foal rate. Similarly, the volume of high MW proteins (173-385 kDa) correlated negatively with sperm motility and foal rate (Stelletta *et al,* 2021). The current study may give explanation for relation between fertility and protein profile of bulbourethral and prostate glands secretions including the role of the shared band and the other bands of higher intensities in both bulbourethral and prostate gland secretion.

Glycosidases were engaged in several reproductive events such as cumulus cells expansion (Takada *et al,* 1994), sperm capacitation (Taitzoglou *et al,* 2007), sperm oviductal epithelial cells interaction (Lefebvre *et al,* 1997), sperm zona pellucida binding (Miranda *et al,* 2000; Zitta *et al,* 2006), polyspermy block (Miller *et al,* 1993) and early embryos development (Tsiligianni, 2018). The activity of glycosidases (β-N-acetylglucosaminidase, α -N-acetylgalactosaminidase and α-L-fucosidase) has been verified in the uterine luminal fluid of the dromedary camels (Ghoneim *et al,* 2021), cattle (Tsiligianni *et al,* 2007; Tsiligianni, 2018), sheep (Tsiligianni *et al,* 2003; Samartzi *et al,* 2020) and mares (Reilas *et al,* 2000).

Previous study of Jauhiainen and Vanha-Perttula (1986) demonstrated that in the fractionation with gel filtration on Sepharose 6B, the beta-N-acetylglucosaminidase (beta-NAG) activities derived from bull testis and caput epididymidis had smaller molecular weights than did the secretory enzymes in seminal plasma, seminal vesicle secretion and cauda epididymidis. Maximum activity of all beta-NAG isoenzymes was observed at pH 5.0 (Jauhiainen and Vanha-Perttula, 1986). This study explained the presence of glycosidase activities in bulbourethral and prostate glands secretions of dromedary camels. As indicated recently for uterine fluid (Ghoneim *et al,* 2021), the current findings explains that β-N-acetylglucosaminidase, α-N-acetylgalactosaminidase and α-L-fucosidase in bulbourethral and prostate glands secretions may play a role in carbohydrate-mediated events in the uterus of dromedary camels. Glycosidases played an important role in different reproductive events; one of them was sperm capacitation (Taitzoglou *et al,* 2007). Parallel to that, in the present study the activities of α-L-fucosidase were reported to be significantly higher than that of other studied glycosidases in both bulbourethral and prostate gland secretion. This may indicate the major role of this enzyme in sperm capacitation besides other studied enzymes. Presence of the glycosidases in uterine luminal fluid of the dromedary camel had also been documented (Ghoneim *et al,* 2021). However, the activities of α-L-fucosidase reported to be higher significantly than that of other studied glycosidases in the uterine fluid of dromedary camels (Ghoneim *et al,* 2021). The current study concluded that bulbourethral and prostate gland secretions may be involved in viscosity and coagulation processes of dromedary semen owing to their contents of secretory proteins and glycosidases.

Acknowledgement

The authors would like to acknowledge the Deanship of Scientific Research, King Faisal University for their financial support (The research groups track grant # 1811024). The authors thanks Vet. Abdulkareem Alshabiby due to his assistance during the collection of glands secretion.

References

Aminu D, Sahani M. Preliminary attempts to collect and cryopreserve camel semen. Journal of Camel Practice and Research. 2000; 7(2):181-186.

Apichela SA, Argañaraz ME, Giuliano S, Zampini R, Carretero I, Miragaya M and Miceli DC. Llama oviductal sperm reservoirs: involvement of bulbourethral glands. Andrologia. 2014; 46(3):290-295.

Asadpour R, Alavi-Shoushtari SM, Rezaii SA and Ansari MH. SDS-polyacrylamide gel electrophoresis of buffalo bulls seminal plasma proteins and their relation with semen freezability. Animal Reproduction Science. 2007; 102(3-4):308-313.

Barrios B, Pérez-Pé R, Gallego M, Tato A, Osada J, Muiño-Blanco T and Cebrián-Pérez JA. Seminal plasma proteins revert the cold-shock damage on ram sperm membrane. Biology of Reproduction. 2000; 63(5):1531-1537.

Bergeron A, Villemure M, Lazure C and Manjunath P. Isolation and characterisation of the major proteins of ram seminal plasma. Molecular Reproduction and Development. 2005; 71(4):461-470.

Brandon CI, Heusner GL, Caudle AB and Fayrer-Hosken RA. Two-dimensional polyacrylamide gel electrophoresis of equine seminal plasma proteins and their correlation with fertility. Theriogenology. 1999; 52(5):863-873.

Bravo PW, Flores D and Ordoñez C. Effect of repeated collection on semen characteristics of alpacas. Biology of Reproduction. 1997; 57(3):520-524.

Elwishy A. Reproduction in the male dromedary (*Camelus dromedarius*): a review. Animal Reproduction Science. 1988; 17(3-4):217-241.

Flowers W (1998). Boar fertility and artificial insemination. Proceedings: The 15th International Pig Veterinary Society Congress, Birmingham, England, July 5-9, 1998; pp 45-52.

Ghoneim I, Waheed M, Meligy A and El-Bahr S. The activity of glycosidases (β -N-acetylglucosaminidase, α-N-acetylgalactosaminidase and α l fucosidase) in the uterine luminal fluid and blood serum of the dromedary camel (*Camelus dromedarius*) during the follicular cycle. Journal of Camel Practice and Research. 2021; 28(2):131-135.

Gwathmey TM, Ignotz GG, Mueller JL, Manjunath P and Suarez SS. Bovine seminal plasma proteins PDC-109, BSP-A3, and BSP-30-kDa share functional roles in storing sperm in the oviduct. Biology of Reproduction. 2006; 75(4):501-507.

Hafez ES and Hafez B. Reproductive parameters of male dromedary and bactrian camels. Archives of Andrology. 2001; 46(2):85-98.

Hahn G, Malenica M, Müller W, Taubert E and Petrak T. Influence of postmortal glycolysis on meat quality and technological properties of turkey breast. Proc of the XV Europ Symp on the Quality of Pol Meat. 2001; pp. 9-12.

Harshan HM, Sankar S, Singh LP, Singh MK, Sudharani S, Ansari MR, Singh SK, Majumdar AC and Joshi P. Identification of PDC-109-like protein(s) in buffalo seminal plasma. Animal Reproduction Science. 2009; 115(1-4):306-311.

Inc S. SPSS 16.0 for Windows. 2007; SPSS Inc, Chicago.

Jauhiainen A and Vanha-Perttula T. beta-N-acetylglucosaminidase in the reproductive organs and seminal plasma of the bull. Journal of Reproduction and Fertility. 1986; 76(1):239-250.

Jóźwik A, Śliwa-Jóźwik A, Bagnicka E and KOŁąTAJ A. The influence of selection on reaction to stress in mice. IX. Effect of dietary protein level on activity of lysosomal enzymes in liver and kidney. Journal of Animal Breeding and Genetics. 2003; 120(2):124-131.

Kershaw-Young CM and Maxwell WM. Seminal plasma components in camelids and comparisons with other species. Reproduction in Domestic Animals. 2012; 47 (Suppl 4):369-375.

Killian GJ, Chapman DA and Rogowski LA. Fertility-associated proteins in Holstein bull seminal plasma. Biology of Reproduction. 1993; 49(6):1202-1207.

Laemmli UK. Cleavage of structural proteins during the assembly of the head of bacteriophage T4. Nature. 1970; 227(5259):680-685.

Lefebvre R, Lo MC and Suarez SS. Bovine sperm binding to oviductal epithelium involves fucose recognition. Biology of Reproduction. 1997; 56(5):1198-1204.

Lichtenwalner AB, Woods GL and Weber JA. Ejaculatory pattern of llamas during copulation. Theriogenology. 1996; 46(2):285-291.

Miller DJ, Gong X and Shur BD. Sperm require beta-N-acetylglucosaminidase to penetrate through the egg zona pellucida. Development (Cambridge, England). 1993; 118(4):1279-1289.

Miranda PV, González-Echeverría F, Blaquier JA, Mahuran DJ and Tezón JG. Evidence for the participation of beta-hexosaminidase in human sperm-zona pellucida interaction *in vitro*. Molecular Human Reproduction. 2000; 6(8):699-706.

Reilas T, Huhtinen M, Oksanen M, Katila T. Relationship between embryo recovery rate and uterine lavage fluid composition in postpartum mares. Reproduction, Nutrition, Development. 2000; 40(4):383-391.

Robertson SA. Seminal plasma and male factor signalling in the female reproductive tract. Cell and Tissue Research. 2005; 322(1):43-52.

Samartzi F, Theodosiadou EK, Rekkas CA, Saratsi A, Lymberopoulos AG, Vainas E *et al*. Effect of equine chorionic gonadotropin on glycosidase activity in the reproductive tract of ewes, in relation to ovarian response and embryo yield. Small Ruminant Research. 2020; 191:106186.

Schellpfeffer DA and Hunter AG. Electrophoretic and gel filtration behaviour of boar seminal plasma proteins before and after removal of accessory sex glands. Journal of Reproduction and Fertility. 1970; 23(2):291-298.

Skidmore JA. The main challenges facing camel reproduction research in the 21st century. Reproduction (Cambridge, England) Supplement. 2003; 61:37-47.

Stelletta C, Alberti S, Cil B, Tekin K, Tirpan MB, Arganaraz M, Akcay E and Daskin A. Use of biochemical and protein profiles of seminal plasma to prediction of semen quality and fertility in stallions. Polish Journal of Veterinary Sciences. 2021; 24(4):505-514.

Taitzoglou IA, Kokoli AN and Killian GJ. Modifications of surface carbohydrates on bovine spermatozoa mediated by oviductal fluid: a flow cytometric study using lectins. International Journal of Andrology. 2007; 30(2):108-114.

Takada M, Yonezawa N, Yoshizawa M, Noguchi S, Hatanaka Y, Nagai T, Kikuchi K, Aoki H and Nakano M. pH-sensitive dissociation and association of beta-N-acetylhexosaminidase from boar sperm acrosome. Biology of Reproduction. 1994; 50(4):860-868.

Tibary A and Anouassi A. Breeding soundness examination of the female camelidae. Theriogenology in Camelidae: Anatomy, Physiology, BSE, Pathology and Artificial Breeding Ed A Tibary Actes Editions, Institut Agronomique et Veterinaire Hassan II: 1997; 243-310.

Tibary A. Theriogenology in Camelidae. Male breeding soundness examination. Mina Abu Dhabi, UAE: Abu Dhabi Printing Press. 1997; pp 79-113.

Tsiligianni T. The possible role of certain glycosidase on cow reproduction. Theriogenology Insight-An International Journal of Reproduction in all Animals. 2018; 8(1):21-32.

Tsiligianni T, Amiridis GS and Vainas E. Activity of glycosidases (beta-N-acetyloglucosaminidase, alpha-mannosidase, and beta-galactosidase) in the uterine luminal fluid of cows after multiple ovulation. Canadian Journal of Veterinary Research. 2007; 71(4):300-304.

Tsiligianni T, Samartzi F, Amiridis G, Koronaki A, Liapouras C and Vainas E. Relationship between Glycosidases activity in the uterine luminal fluid and superovulatory response of Chios ewes. Reproduction in Domestic Animals. 2003; 38:364.

Villemure M, Lazure C and Manjunath P. Isolation and characterisation of gelatin-binding proteins from goat seminal plasma. Reproductive Biology and Endocrinology. 2003; 1:39-49.

Wani N. *In vitro* embryo production in camel (*Camelus dromedarius*) from *in vitro* matured oocytes fertilised with epididymal spermatozoa stored at 4 C. Animal Reproduction Science. 2009; 111(1):69-79.

Zeidan A, El-Darawany A, Absy G and Abdel-Ghaffar A. Testicular measurements, semen characteristics, blood components and penetrating ability of the dromedary camels spermatozoa into cervical mucus in different seasons of the year. Zagazig Veterinary Journal. 2000; 28:43-52.

Zitta K, Wertheimer EV and Miranda PV. Sperm N-acetylglucosaminidase is involved in primary binding to the zona pellucida. Molecular Human Reproduction. 2006; 12(9):557-563.

DOI : 10.5958/2277-8934.2022.00027.3 Vol 29 No 2, p 197-202

MAGNETIC RESONANCE IMAGING OF THE DROMEDARY CAMEL STIFLE

Z.A. Al Mohamad
Department of Clinical Sciences, College of Veterinary Medicine, King Faisal University,
PO Box 400, Al-Ahsa 31982, Kingdom Saudi Arabia

ABSTRACT

The objective of the present investigation was to develop a high-field magnetic resonance imaging (MRI) protocol for assessment of the dromedary camel stifle region and to describe normal MRI appearance of the stifle by comparing MRI images with their corresponding anatomic slices. Twelve cadaveric hind limbs were obtained from 6 clinically sound adult dromedary camels without hind limb lameness. Cadaveric stifles were scanned by 1.5 Tesla MRI system using T1-weighted, T2-weighted, proton density gradient echo and short Tau inversion recovery sequences in 3 planes. After imaging, stifles were frozen at – 18°C for 2 weeks, then sectioned in sagittal, dorsal or transverse planes. Optimal MRI images from different sequences and planes were evaluated and correlated to their corresponding gross anatomic slices. Descriptive findings of the articular cartilage, subchondral bone, cruciate ligaments, menisci, menisco-tibial and menisco-femoral ligaments, long digital extensor tendon, and patellar ligament were reported. The high-field MRI protocol described in this study provided high spatial and contrast resolution of the osseous and soft tissue structures of the dromedary camel stifle joint. Data obtained in this study could be used as normal reference standards for evaluation of the dromedary camel stifle in clinical situations.

Key words: Dromedary camel, imaging, MRI, stifle

Diagnosis of stifle injuries is routinely based on physical examination followed by radiography and/or ultrasonography (Bourzac *et al,* 2009; Beccati *et al,* 2013). Radiography is classically used to diagnose osteochondral injuries of the stifle joint of equines, although some osteochondral defects of the femoropatellar and femorotibial joints could not be detected radiographically (Barr *et al,* 2006; Nelson *et al,* 2016). Advanced imaging through of stifle joint in camels has been done by Sangwan and Gahlot (2015).

The stifle joint of dromedary is very important as many lameness imaging of hind quarter originate from this joint. Lameness of hind quarter involving stifle joint is well reported (Gahlot, 2007; Al–Juboori, 2013; Ramadan,1994) The anatomy of sifle joint is different than other large animals as it has absence of the medial patellar ligament in camels (Krishnamurthy *et al,* 1979). Lameness in stifle joint has been caused by upward fixation of patella (Gahlot *et al,* 1991; Krishnamurthy *et al,* 1992; Mistry *et al,* 1991), ruptured cranial cruciate ligament (Pearce and Hurtig, 1999) and arthritis (Shoieb and Sayed-Ahmed, 2016).

Magnetic resonance imaging (MRI) is a noninvasive modality that allows combined evaluation of articular cartilage, subchondral bone, and soft tissue structures associated to the joint in equines (Santos *et al,* 2015). Many researchers have done studies on Magnetic Resonance Image (MRI) of the digits (El-Shafey and Abd Al-Galil, 2012), tarsus (Al Mohamad *et al*, 2021), fetlock joint, pastern and coffin joints (Irahim *et al,* 2019 a,b), carpal joint (Ibrahium and Shaker, 2018), temporomandibular joint (Arencibia *et al,* 2012), cranioencephalic structures (Arencibia *et al,* 2005), head structures (Emam *et al,* 2020) and normal brain (Arencibia *et al,* 2004) of camels. However, MRI of stifle joint in camels has not been reported previously.

The purpose of the present study was, therefore, to carry out the normal magnetic resonance imaging of stifle in dromedary camel. A corroborative interpretation of MRI images was done by the sagittal, transverse and dorsal cryosections of hindlimbs used for MRI imaging.

Materials and Methods

Right and left stifles were collected from 6 adult camels (3 males and 3 non pregnant females; age range, 7-16 years; and weight, 450-625 kg) that were clinically sound and free from any pathology or lameness.

SEND REPRINT REQUEST TO Z.A. AL MOHAMAD email: zalmohammad@kfu.edu.sa

Immediately after death, limbs were disarticulated at the hip joint and maintained in normal position. The limbs were placed in the central bore of a 1.5 Tesla Ingenia MRI system (Philips Ingenia 1.5T MRI; Philips GmbH, Hamburg, Germany) with the lateral aspect as the dependent portion and the long axis of the limb parallel to the MRI table (to simulate the limb of a camel in lateral recumbency), then scanned in transverse, sagittal and dorsal planes. Sagittal images were produced by orienting slices parallel to the medial and lateral margins of the femur and tibia at the level of the medial collateral ligament. Dorsal images were produced by orienting slices parallel to the longitudinal axis of the femorotibial joint on sagittal images. The transverse plane was acquired by orienting slices perpendicular to the medial collateral ligament and parallel to menisci and joint space on sagittal images. The scanning sequences were T1-weighted (T1), T2-weighted (T2), Proton Density (PD) gradient echo and Short Tau Inversion Recovery (STIR). Acquisition settings were: repetition time, 3,160 milliseconds; echo time, 14 milliseconds; echo number, 1; excitation number, 1 matrix size, 512; and slice thickness, 4 mm. Representative images at various levels that best correlated with the gross anatomic slices were selected.

After imaging, the specimens were frozen at – 18 °C for 2 weeks. Frozen stifles were sectioned transversely, sagittally or dorsally by means of an electric band saw into 1 cm slice thickness. The cut surfaces of each section were rinsed, numbered and photographed. Anatomic slices were used to facilitate an accurate interpretation of the anatomical structures and were correlated to their corresponding MRI images for identification and confirmation of each anatomical structure and its signal intensity.

Results and Discussion

The MRI images acquired in this study accurately represented the gross specimen evaluation of all structures, including the menisci, meniscotibial and meniscofemoral ligaments, and the cruciate ligaments of the dromedary camel stifle joint (Smuts and Bezuidenhout, 1987). MRI images in stable joint of present study showed a differential and tomographic details of cartilage, cortical bone, subchondral bone, trabecular bone, cancellous bone, menisci, ligaments, tendons and muscles. The obtained results were in agreement with the previous reports in horses confirming that MRI offers the best evaluation technique of all anatomical structures of the stifle joint particularly the soft tissue structures (Peterfy *et al,* 1994; Widmer *et al,* 2000; Nagy and Dyson, 2011). Results of the present study showed that MRI enabled investigation of intra-articular structures of stifle joint that would facilitate detection and diagnosis of stifle injuries in dromedary camel.

In present study, representative anatomic structures were identified on MRI images and frozen sections (Figs 1, 2 and 3). The sagittal and dorsal plane images allowed evaluation of articular alignment, synovial fluid and synovial membrane while transverse plane images provided the most detailed evaluation of cruciate ligaments. Use of high-field 1.5 Tesla magnet and pulse sequences of a gradient echo in T1, T2, PD and STIR produced excellent anatomic delineation of the bony, articular, ligamentous, and tendinous structures of the dromedary camel stifle joint. T1 and PD sequences produced images with high definition and good signal intensity and provided high anatomical details. The T2 sequence demonstrated the synovial structures and had a good contrast between synovial fluid, soft tissues, bones and cartilaginous structures. STIR sequence was valuable for identification of areas with high fat content. The MRI protocol and sequences used in this study were in general accordance with reports in horses (Tucker and Sampson, 2007; Daglish *et al,* 2018). However, MRI of the equine stifle was difficult depending on patient size (Holcombe *et al,* 1995; Judy, 2011).

Soft tissue structures comprising the stifle joint were consistently identified including medial collateral ligament, cranial and caudal cruciate ligaments, patellar ligament, medial and lateral cranial meniscotibial ligaments, meniscofemoral ligament, popliteal tendon, joint capsule and synovial fluid. Similar data were reported in horses (Holcombe *et al,* 1995; Tucker and Sampson, 2007), except that lateral collateral ligament and medial and lateral patellar ligaments are absent in camels (Smuts and Bezuidenhout, 1987).

The medial collateral ligament appeared more lobulated and generally was well-defined, had low signal intensity on all image sequences and surrounding by higher signal intensity fat-containing soft tissues that was evident on STIR images. The cranial and caudal cruciate ligaments had homogeneous very low signal intensity on PD, T2 and STIR images. The medial and lateral menisci had moderate signal intensity on T1 and PD sequences, and low signal intensity on STIR and T2 images. On

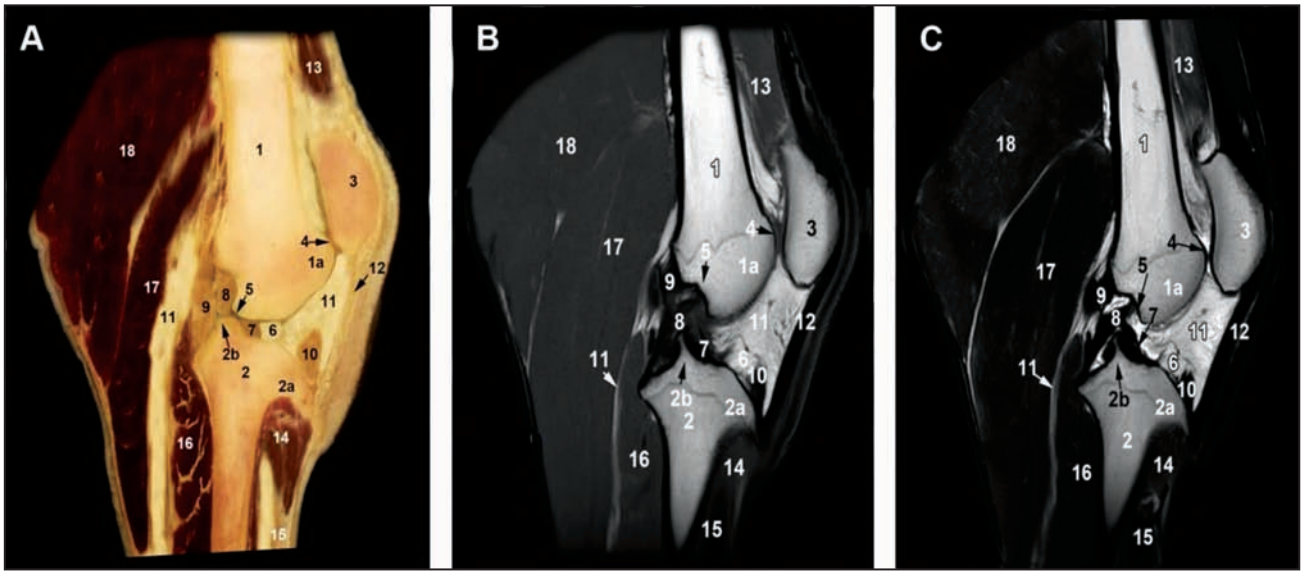

Fig 1. Midline sagittal cryosection (A) and T1 weighted (B) and T2 weighted (C) MRI images at the level of the tibial intercondylar eminence. Cranial is to the right, proximal to the top. 1, femur; 1a, lateral femoral condyle; 2, tibia; 2a, tibial tuberosity; 2b, intercondylar eminence of tibia; 3, patella; 4, femoropatellar articulation; 5, femorotibial articulation; 6, lateral meniscus; 7, meniscofemoral ligament; 8, caudolateral bundle of cranial cruciate; 9, caudal cruciate ligament; 10, patellar ligament; 11, fat; 12, lateral patellar retinaculum; 13, rectus femoris muscle; 14, fibularis longus muscle 15, common tendon of the long digital extensor and fibularis tertius muscles; 16, long digital flexor muscle; 17, lateral head of gastrocnemius muscle; 18, semimembranosus muscle.

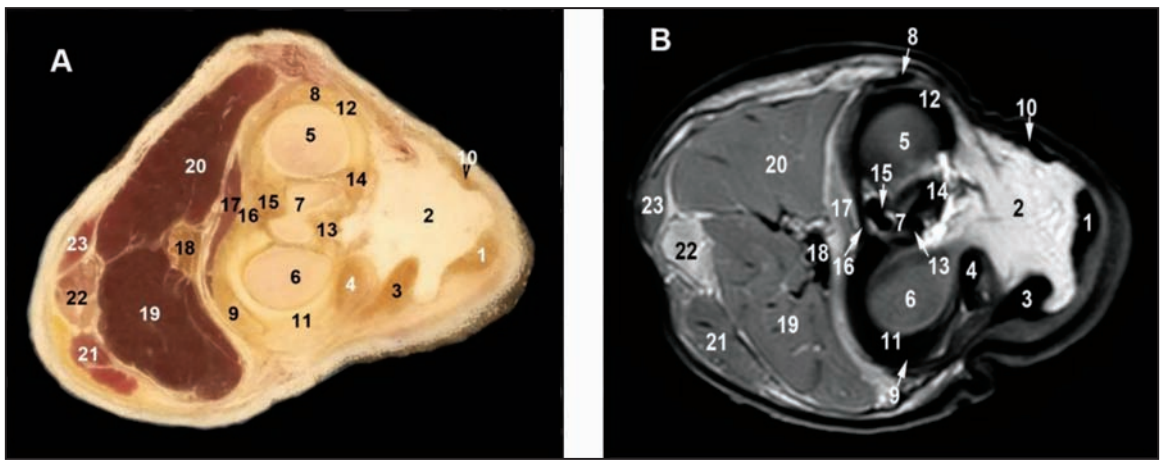

Fig 2. Transverse cryosection (A) PD MRI image at the level of the menisci and tibial intercondylar eminence. Cranial is to the right, medial to the top. 1, patellar ligament; 2, fat; 3, insertion tendon of gluteobiceps muscle; 4,; combined tendons of long digital extensor and fibularis tertius muscles 5, medial femoral condyle; 6, lateral femoral condyle; 7, tibial intercondylar eminence; 8, medial collateral ligament; 9, origin of popliteus muscle; 10, medial patellar retinaculum; 11, lateral meniscus; 12 medial meniscus; 13, cranial lateral meniscotibial ligament; 14, cranial medial meniscotibial ligament; 15, caudal cruciate ligament; 16, intermeniscial ligament; 17, popliteus muscle; 18, superficial digital flexor muscle; 19, lateral head of gastrocnemius muscle; 20, medial head of gastrocnemius muscle; 21, gluteobiceps muscle; 22, semitendinosus muscle; 23, semimembranosus muscle.

T1 - weighted images, signal intensity was similar to articular cartilage, but on other images they have lower signal than cartilage. Tendons and ligaments of the stifle joint had homogenous low signal intensity on all sequences. Synovial fluid in the surrounding sheaths and in the joint had high signal intensity on PD and T2 sequences and low signal intensity on T1 images. The muscles supporting the stifle joint had intermediate to high signal intensity on PD images and moderately low signal intensity on T1, T2 and STIR images. The boundaries of muscles were seen with slightly higher signal intensity on T1 and STIR images, slightly lower signal intensity on PD images. The same was reported in horses (Santos *et al,* 2015) and dogs (Przeworski *et al,* 2016). In camels, femoropatellar and medial and lateral

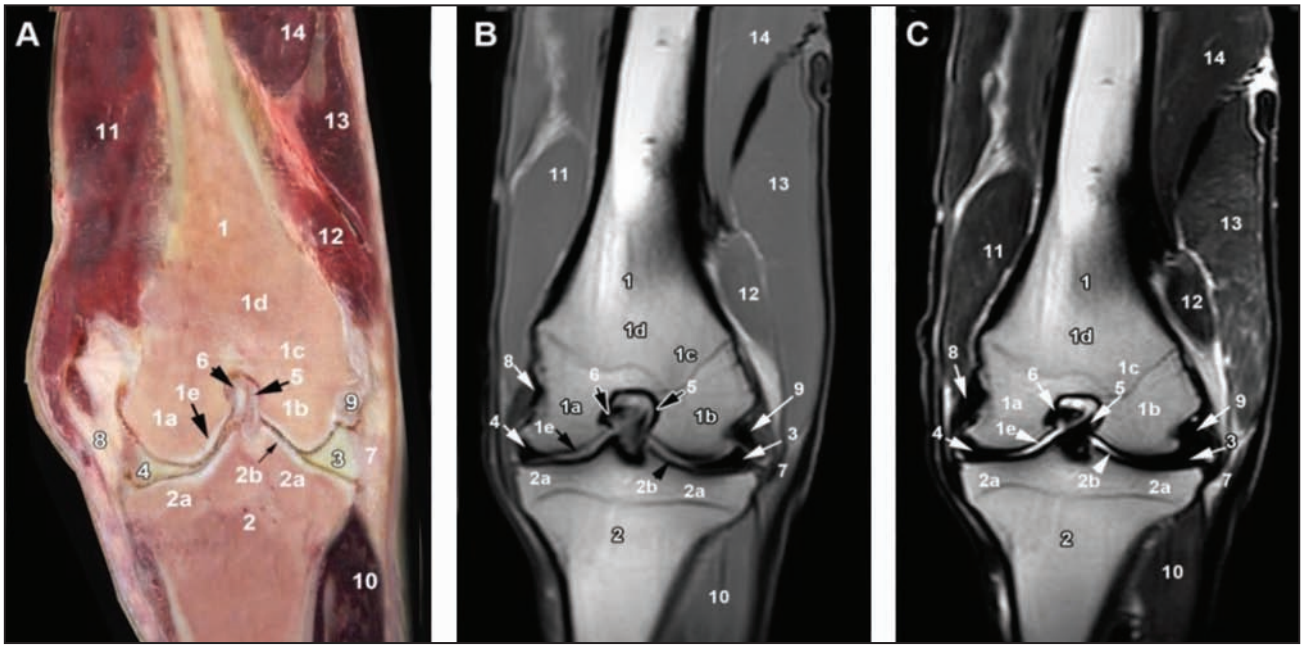

Fig 3. Middle dorsal cryosection (A) and T1 weighted and T2 weighted MRI images at the level of the medial collateral ligament. Medial is to the left and proximal to the top. 1, femur; 1a, medial femoral condyle; 1b, lateral femoral condyle; 1c, femur cancellous bone; 1d, femur trabecular bone; 1e, articular cartilage of femur; 2, tibia; 2a, tibial plateau; 2b, articular cartilage of tibia; 3, lateral meniscus; 4, medial meniscus; 5, caudal cruciate ligament; 6, cranial cruciate ligament; 7, tendon of the popliteal muscle; 8, medial collateral ligament; 9, common origin of fibularis tertius and lateral digital extensor muscles; 10, cranial tibial muscle; 11, medial head of gastrocnemius muscle; 12, lateral head of gastrocnemius muscle; 13, vastus lateralis muscle; 14, rectus femoris muscle.

femorotibial compartments are communicated (Smuts and Bezuidenhout, 1987), while in horses the medial and lateral femorotibial compartments are separated by a synovial membrane (Budras *et al,* 2011).

In all sequences, the articular cartilage, subchondral bone, cortical bone, cancellous bone with its trabercular structure was consistently visualised. On T2 and PD images, articular cartilage was recognised as a layer of homogenous intermediate to high signal intensity with a smooth osteochondral junction and was clearly defined from the bone underneath it in all joints by the differences in signal intensity. On T1, PD and T2 images, cancellous bone had intermediate to high signal intensity, representing the fat content of the bone. Subchondral bone had homogenous low signal intensity with regular osteochondral junction. Cancellous bone had heterogeneous signal intensity with a well-defined trabecular pattern. On STIR images, cancellous bone had homogeneous low signal intensity, there was no distinct definition between the cortical and cancellous bones as both had low signal intensity, articular cartilage was barely visible and was recognised as a very thin layer of intermediate signal intensity. Our protocol allowed MRI examinations of all stifles and anatomical structures as well as signal intensities of each individual structure were completely delineated in accordance with reports for human knees (Chien *et al,* 2020) and equine stifle joint (Santos *et al,* 2015).

The present study provided a depiction of the normal MRI features of dromedary camel stifle joint associated with its corresponding gross anatomical sections. In this study, freezing of limbs in the same position as the MRI examination allowed exact matching between gross anatomical sections and MRI images which facilitated evaluation and identification of various structures of the stifle joint. This study provided an anatomic and MRI reference for the dromedary camel stifle joint, which can be used as a guide for interpretation of clinical cases and as a reference for other research projects.

Acknowledgements

This work was supported by the Deanship of Scientific Research, Vice Presidency for Graduate Studies and Scientific Research, King Faisal University, Saudi Arabia [Project No. GRANT315].

References

Abedellaah BA, Awaad AS, Elhawari SF and Sharshar AM. Normal brain of one-humped camel: a study with magnetic resonance imaging and gross dissection

anatomy. Indian Journal of Veterinary Surgery. (2015); 36(1):46-50.

Al Mohamad ZA, Hagag U, Tawfiek MG and El Nahas A. Magnetic resonance imaging of the normal dromedary camel tarsus. BMC Veterinary Research. (2021); 17:101-110.

Al–Juboori A. Prevalence and etiology of lameness in racing camels (*Camelus dromedarius*) in Abu Dhabi Emirate. Journal of Camelid Science. 2013; 6:116-121.

Arencibia A, Blanco D, González N, Rivero MA. Computed tomography and magnetic resonance imaging features of the temporomandibular joint in two normal camels. Anatomy Research International. (2012); pp 1-6.

Arencibia A, Rivero MA, Gil F, Ramirez JA, Corbera JA, Ramirez G and Vasquez JM. Anatomy of the cranioencephalic structures of the camel (*Camelus dromedarius*) by imaging techniques: a magnetic resonance imaging study. Anatomia Histolologia Embryologia. (2005); 34(1):52-55.

Atef Abd Al-Galil and El-Shafey AA. Magnetic resonance imaging of the one-humped camel (*Camelus dromedarius*) digits. Journal of American Science. 2012; 8:549-556.

Barr ED, Pinchbeck GL, Clegg PD and Singer ER. Accuracy of diagnostic techniques used in investigation of stifle lameness in horses: 40 cases. Equine Veterinary Education. (2006); 18:326-331.

Beccati F, Chalmers HJ, Dante S, Lotto E and Pepe M. Diagnostic sensitivity and interobserver agreement of radiography and ultrasonography for detecting trochlear ridge osteochondrosis lesions in the equine stifle. Veterinary Radiology and Ultrasound. (2013); 54:176-184.

Bourzac C, Alexander K, Rossier Y and Laverty S. Comparison of radiography and ultrasonography for the diagnosis of osteochondrosis dissecans in the equine femoropatellar joint. Equine Veterinary Journal. (2009); 41:685-692.

Budras K, Sack W and Rock S. Anatomy of the Horse, 5th edn. Schlütersche Verlagsgesellschaft mbH & Co. KG., Hannover, Germany. (2011); pp 16-31.

Chien A, Weaver JS, Kinne E and Omar I. Magnetic resonance imaging of the knee. Polish Journal of Radiology. (2020); 85:509-531.

Daglish J, Frisbie DD, Selberg KT and Barrett MF. High field magnetic resonance imaging is comparable with gross anatomy for description of the normal appearance of soft tissues in the equine stifle. Veterinary Radiology and Ultrasound. (2018); 59:721-736.

El-Shafey AA and Abd Al-Galil ASA. Magnetic resonance imaging of the one-humped camel (*Camelus dromedarius*) digits. Journal of American Science. (2012); 8(9):549-556.

Emam H, Aref M, Ismail AA, Abdelaal A, Gouda S, and Gomaa M. Description of normal head structures of the one-humped camel (*Camelus dromedarius*) by magnetic resonance imaging, computed tomography, and cross-sectional anatomy. Veterinary World. (2020); 13(8):1581-1587.

Gahlot TK, Chouhan DS and Choudhary RJ. Treatment of upward fixation of patella in camels (*Camelus dromedarius*). Indian Veterinary Journal. 1991; 68(12):1178-1179

Gahlot TK. Lameness in camels. Proceedings of the International Camel Conference "Recent trends in Camelids Research and Future Strategies for Saving Camels", Rajasthan, India. (2007; pp 158-165.

Holcombe SJ, Bertone AL, Biller DS and Haider V. Magnetic resonance imaging of the equine stifle. Veterinary Radiology and Ultrasound. (1995); 36:119-125.

Ibrahim AH, Adam ZE and Tawfiek MG. Normal cross-sectional anatomy and magnetic resonance imaging of pastern and coffin joints in camel. Journal of Veterinary Medical Research. (2019a); 26(2):271-279.

Ibrahium AM and Shaker NA. Gross anatomical structure and magnetic resonance images of the carpal joint in one humped camel (*Camelus dromedarius*) and its arterial blood supply. International Journal of Veterinary Science. 2018; 7(1):12-17.

Ibrahim AH, Adam ZE and Tawfiek MG. Cross-sectional anatomy, magnetic resonance imaging and computed tomography of fetlock joint in camel. Journal of Veterinary Medical Research. (2019b); 26(2):258-270.

Judy CE. Magnetic resonance imaging of the equine stifle. Veterinary Radiology and Ultrasound. (2011); 52:479-484.

Krishnamurthy D, Tyagi RP, Sharma DN. Absence of the medial patellar ligament in camels. Indian Veterinary Journal. 1979; 56(3):243-5. PMID: 478616.

Krishnamurthy D, Tyagi RPS and Sharma DN. Upward fixation of the patella in camels. Proceedings of the First International Camel Conference, Dubai, 2nd 6th February. 1992; 357-359.

Mistry JN, Chandel BS, Suthar BN and Tadkod DM. Upward fixation of patella in camel case reports. Indian Veterinary Journal. 1991; 68(5):469-470

Nagy A and Dyson S. Magnetic resonance anatomy of the carpus of the horse described from images acquired from low-field and high-field magnets. Veterinary Radiology and Ultrasound. (2011); 52(3):273-283.

Nelson BB, Kawcak CE, Goodrich LR, Werpy NM, Valdés-Martínez A and McIlwraith CW. Comparison between computed tomographic arthrography, radiography, ultrasonography, and arthroscopy for the diagnosis of femorotibial joint disease in western performance horses. Veterinary Radiology and Ultrasound. (2016); 57:387-402.

Pearce SG and Hurtig MB. Surgical repair of a ruptured cranial cruciate ligament in a dromedary camel. Journal of American Veterinary Medical Association. 1999; 215(9):1325-7, 1282. PMID: 10553447.

Peterfy CG, Linares R and Steinbach LS. Recent advances in magnetic resonance imaging of the musculoskeletal system. Radiologic Clinics of North America. (1994); 32(2):291-311.

Ramadan RO. Surgery and Radiology of the Dromedary Camel. Ist edn. Al-Jawab Printing Press. Kingdom of Saudi Arabia. 1994.

Sangwan A and Gahlot TK. Advanced imaging studies on normal stifle joint of camel (*Camelus dromedarius*). Journal of Camel Practice and Research. (2015); 22(1):133.

Santos MP, Gutierrez-Nibeyro SD, Mcknight AL and Singh K. Gross and histopathologic correlation of low-field magnetic resonance imaging findings in the stifle of asymptomatic horses. Veterinary Radiology and Ultrasound. (2015); 56(4):407-416.

Shoieb SM and Sayed-Ahmed M. Clinical and clinico-pathological findings of arthritic camel calf associated with mycoplasma infection (*Camelus dromedarius*). Journal of Dairy, Veterinary and Animal Research. 2016; 3(1):26-30. DOI: 10.15406/jdvar.2016.03.0006

Smuts MS and Bezuidenhout AJ. Anatomy of the Dromedary. Oxford, Clarendon Press. (1987); pp 54-104.

Tucker RL and Sampson SN. Magnetic resonance imaging protocols for the horse. Clinical Techniques in Equine Practice. (2007); 6:2-15.

Widmer WR, Buckwalter KA, Fessler JF, Hill MA, VanSickle DC and Ivancevich S. Use of radiography, computed tomography and magnetic resonance imaging for evaluation of navicular syndrome in the horse. Veterinary Radiology and Ultrasound. (2000); 41(2):108-116.

DOI : 10.5958/2277-8934.2022.00028.5 Vol 29 No 2, p 203-206

ECHOBIOMETRY OF EYES OF DROMEDARY CAMELS (*Camelus dromedarius*)

Subith C., S.K. Jhirwal, P. Bishnoi and T.K. Gahlot
Department of Veterinary Surgery and Radiology, College of Veterinary and Animal Science, Rajasthan University of Veterinary and Animal Sciences, Bikaner-334001, Rajasthan, India

ABSTRACT

Transcorneal ultrasonographic scanning of 12 adult healthy camels of both sex were performed using linear array transducer on B-mode. The ultrasonographic appearance of the eye was described and ocular dimensions were recorded. The echo-biometric studies on four parameters i.e. anterior chamber depth (ACD), lens thickness (LT), vitreous chamber depth (VCD) and axial length (AL) were recorded. The ultrasonography showed that the eyes of camels were appeared as slightly ovoid structures with anechoic contents such as anterior chamber, vitreous chamber and lens. The cornea, anterior and posterior lens capsule, iris, granula iridica/corpora nigra and sclera-retinal rim appeared as hyperechoic. Non-significant differences were found in all parameters when compared between right and left eyes of male and female camels. However, the anterior chamber depth in male camels were significantly higher than female camels $P \leq 0.05$. The present study provides echo-morphometric view of the intra-ocular structure in adult healthy eyes of camels.

Key words: Camel eye, Echobiometry, Ultrasonography

The ophthalmic ultrasonography is a reliable tool to quantify the ocular dimensions and it is safe and non-invasive procedure (Dudea, 2011). Ocular ultrasound biometry was used in different animals, i.e. cat (Mirshahi *et al*, 2014), goat (Ribeiro *et al*, 2009), horse (Gialletti *et al*, 2018; Sorouri *et al*, 2009) and dromedary camel (Kelawala *et al*, 2015). Ultrasonographic measurements of the Bulbous oculi of the camel were done in terms of corneal thickness, anterior chamber depth, lens thickness, vitreous chamber depth, axial length and optical axis (Khan and Türker, 2021). Echobiometry of eye usually provides direct dimensions (Kelawala *et al*, 2015; Osuobeni and Hamidzada, 1999; Yadegari *et al*, 2013) but indices are more reliable than diameters because they are independent of the size (Kara *et al*, 2011).

Camels are vulnerable to a variety of ophthalmic problems, including corneal and eyelid laceration, panophthalmos, corneal opacity, and descematocele etc (Bishnoi and Gahlot, 2001). Ocular ultrasonography of camel eye is well studied previously (Tharwat and El-Omar, 2021; Yadegari *et al,* 2013). Ultrasonography of the eye provides a detailed examination of the interior of the eye.

Echobiometry of the eyes of dromedary camels is least studied, hence present study was undertaken to perform echobiometry of eye of camels by transcorneal ultrasonographic scanning.

Materials and Methods

Twelve live healthy adult camels with the clear cornea and without any ocular pathology were selected (6 male and 6 female) for ocular ultrasonography. Camels were restrained in sternal recumbency and mild sedation was given by xylazine hydrochloride[1] (at the dose rate of 0.2 mg/Kg body weight) by intravenous route. B- mode transcorneal ultrasonography (Edan U2 prime edition) was done by using a linear array transducer of frequency 8-13 MHz. Coupling gel was applied over the transducer and probe was placed gently over the corneal surface perpendicular to the centre of the cornea (vertical plane, Fig 1). Ocular echobiometric measurements were recorded in the vertical plane image. After the procedure excess coupling gel was wiped off with cotton, and the eye was rinsed with normal saline.

Diverse ocular echobiometric parameters measured in both left and right eyes of all the camels were - anterior chamber depth (ACD), lens thickness (LT), vitreous chamber depth (VCD) and Axial length (AL). Statistical analysis, student's t test was used for comparing the left and right eyes and between male and female camels under the study.

1. XYLAXINE, Indian Immunologicals Ltd,Telangana, India

SEND REPRINT REQUEST TO SUBITH C. email: subith001@gmail.com

Results

On B-mode ultrasonography camel eye appeared as slightly ovoid in structure. Cornea, anterior chamber, lens, iris, ciliary body, vitreous chamber and sclera-retinal rim were well visualised ultrasonographically (Fig 2). Corneal stroma, anterior chamber, vitreous chamber, lens cortex and nucleus appeared as an anechoic area and anterior and posterior corneal layer, iris, ciliary body, anterior and posterior lens capsules and sclera-retinal rim appeared as hyperechoic images. The cornea appeared as three-layered, two hyperechoic convex lines with an anechoic area in between. Iris was located adjacent to the anterior lens capsule and ciliary body. Granula iridica/ corpora nigra appeared as a hyperechoic structure in the anterior chamber from the dorsal side of the iris which was well visualised sonographically in all the camels. The sclero-retinal rim appeared as a concave hyperechoic line in the posterior globe wall and its 3 layers could not be differentiated ultrasonographically. The optic disc was not a consistent finding in the study and it appeared as raised or depressed hyperechoic structure in the posterior wall. The nerve tract showed mixed echogenic shadow, which started from the posterior margin of the sclero-retinal layer.

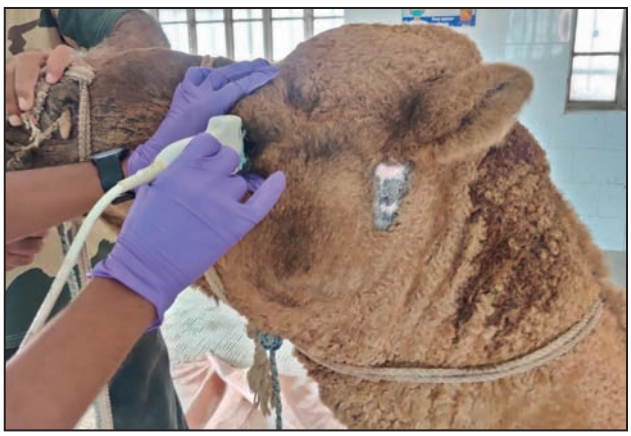

Fig 1. Vertical plane ultrasonography in camel eye will a linear array transducer.

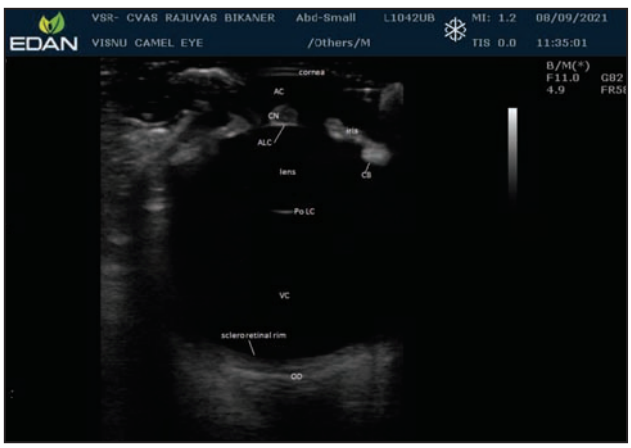

Fig 2. Sonogram of camel eye (AC-anterior chamber, CN-corpora nigra, CB- ciliary body, ALC- anterior lens capsule, Po LC-posterior lens capsule, VC-vitreous chamber, OD-optic disc).

The various echobiometric parameters recorded are summarised in table 1 and table 2. There was no significant difference noted in any of the ocular components between the left and right eyes of male and female camels. However, the overall values of ACD were significantly higher in male camels than female camels ($P \leq 0.05$).

Table 1. Ultrasonographic measurements (Mean ± SE) of the ocular structures of the left and right eye of dromedary camels (n-=12).

Ocular structures	Left eye (in mm)	Right eye (in mm)
ACD	5.65±0.31	5.8±0.41
LT	10.53±0.45	10.21±0.41
VCD	17.84±0.57	17.72±0.51
AL	34.33±0.59	34.07±0.66

Table 2. Ultrasonographic measurements (Mean ± SE) of the ocular structures of the male (n-=6) and female (n=6) adult camels (* indicate $P \leq 0.05$).

Ocular structures	Sex (Mean ± SE) in mm	
	Male	Female
ACD	6.15*±0.33	5.3*±0.39
LT	10.07±0.6	10.68±0.26
VCD	18.12±0.5	17.43±0.58
AL	34.78±0.3	33.62±0.95

Discussion

Ocular sonography is an easy, non-invasive diagnostic procedure used to identify ocular pathology. An early diagnosis of eye disease is crucial for the success of the treatment.

In present study the ultrasonography of camel eye was done by B mode using linear array transducer. Khan and Türker (2021) also used ultrasound B-mode technique for ocular measurements of the hybrid camel and it showed amplitude of returned echoes as dots (Mirshahi *et al*, 2014). A probe of the B-scan can also generate charismatic image of the eye as it transmits multiple sound waves (Solarte and Shaikh, 2007). Another crucial component of these devices is transducer and generally, linear transducers having 7.5 to 10 MHz frequency are used for ocular measurements (Dudea, 2011). The assessment of ocular dimensions is crucial for ophthalmic surgeons and must be determined before any ophthalmic interference (Grinninger *et al*, 2010).

Ultrasonography was performed under xylazine sedation in the current study and other researchers also did it under xylazine sedation (El-Tookhy *et al*, 2012 and Abedellaah *et al,* 2017). A standoff pad is usually required to visualise the cornea (Hager *et al,* 1987). However, standoff pad was not used in the present study instead a copious amount of coupling gel was used, which obviate the use of a standoff pad. The ultrasonographic appearances of ocular structures were similar to previous observations in camel eyes (El-Tookhy *et al,* 2012; Yadegari *et al,* 2013; Kelawala *et al,* 2015; Abedellaah *et al,* 2017).

The ocular components of camel eyes were identical to buffalo (Assadnassab and Fartashvand, 2013), horse (Reef, 1998; Tripathi *et al,* 2018), cattle (El-Maghraby *et al,* 1995; Potter *et al,* 2008; Tripathi *et al,* 2018), goat (Ribeiro *et al,* 2009; Athar *et al,* 2021a), sheep (Athar *et al,* 2021b) and dog (Kumawat and Jhirwal, 2021). The structure resembling granula iridica described in the equine eye (Diaz, 2004; Valentini *et al,* 2010) was also well developed and observed in camels in this study and similar observations were made by other researchers also (El-Tookhy *et al,* 2012; Kelawala *et al,* 2015). These structures help them of case of direct exposure to sunlight into the eye (Samuelson, 2007). Khan and Türker (2021) recorded ultrasonographic details of eyeballs of hybrid camels and these showed 95% confidence intervals for measurements as corneal thickness (CT) (1.56-1.87), ACD (2.33-4.27), LT (6.81-10.00), VCD (23.01-24.44), AL (35.13-38.60) and Optical axis (OA) (34.89-37.24). The value of ACD/AL was found bigger while VCD/AL of adult one-humped camel were found smaller in size by Kassab (2012), Kelawala *et al* (2015) and Yadegari *et al* (2013) as compared to the hybrid camel (Khan and Türker, 2021). Transcorneal method of ocular sonography was used in this study and a similar method was also used by others (Kassab, 2012; EL-Tookhy *et al*, 2012; Yadegari *et al,* 2013 and Kelawala *et al,* 2015). Parrot has higher values for ACD/AL and LT/AL but very much smaller optical axis index (OA/AL) (Lehmkuhl *et al*, 2010) than the camel (Khan and Türker, 2021).

Good quality US images were obtained in vertical plane (longitudinal) positioning of the probe in the present study which was in agreement with others researchers (El-Magharaby *et al,* 1995; Ribeiro *et al,* 2010). No significant difference was detected between left and right eyes echobiometry in dromedary as also reported by others (Yadegari *et al,* 2013 and Kelawala *et al,* 2015). However a significant difference was noted between male and female camels ACD. A higher ACD was noted in male camels than females, and the higher mean values may be attributed to the small sample size and difference in breed and age of the animal under the present study.

References

Abedellaah B, Sharshar A, Shoghy K and Rashed R. Normal ocular structure of dromedary camel (*Camelus dromedarius*): Gross, ultrasonographic and computed tomographic study. Assiut Veterinary Medical Journal. 2017; 63(153):231-236.

Assadnassab G and Fartashvand M. Ultrasonographic evaluation of buffalo eyes. Turkish Journal of Veterinary and Animal Sciences. 2013; 37(4):395-398. doi:10.3906/vet-1104-9

Athar H, Parrah JD, Mir AQ, Moulvi BA, Makhdoomi DM, Dar MU and Handoo N. Ocular Ultrasonography and Echobiometry in Goats of Different Age and Breed. Indian Journal of Animal Research. 2021a; 1:5.

Athar H, Parrah JU, Handoo N, Mir AQ, Dar MU and Qureshi B. Ocular ultrasonography and echobiometry in sheep. Turkish Journal of Veterinary and Animal Sciences. 2021b; 45(2):221-228.doi:10.3906/vet-2004-102

Bishnoi P and Gahlot TK. A note on incidence and occurrence of diverse ophthalmic affections in camels (*Camelus dromedarius*). Journal of Camel Practice and Research. 2001; 8:73-75.

Diaz OS. Ultrasound of the equine eye and adnexa and clinical applications. Clinical Techniques in Equine Practice. 2004; 3(3):317-325.https://doi.org/10.1053/j.ctep.2005.02.009

Dudea SM. Ultrasonography of the eye and orbit. Medical Ultrasonography. 2011; 13(2):171-174.

El-Maghraby HM, Nyland TG and Bellhorn RW. Ultrasonographic and biometric evaluation of sheep and cattle eyes. Veterinary Radiology and Ultrasound. 1995; 36(2):148-151.https://doi.org/10.1111/j.1740-8261.1995.tb00236.x

El-Tookhy O, Al-Sobayil FA and Ahmed AF. Normal ocular ecobiometry of the dromedary camels. Journal of Camel Practice and Research. 2012; 19(1):13-17.

Gialletti R, Marchegiani A, Valeriani T, Nannarone S, Beccati F, Fruganti A and Laus F. A survey of ocular ultrasound abnormalities in horse: 145 cases. Journal of Ultrasound. 2018; 21(1):53-59. https://doi.org/10.1007/s40477- 018-0284-7

Grinninger P, Skalicky M and Nell B. Evaluation of healthy equine eyes by use of retinoscopy, keratometry, and ultrasonographic biometry. American Journal of Veterinary Research. 2010; 71(6):677-681.https://doi.org/10.2460/ajvr.71.6.677

Hager DA, Dziezyc J and Millchamp NJ. Two-dimensional real-time ocular ultrasonography in the dog. Veterinary Radiology. 1987; 28(2):60-66.https://doi.org/10.1111/j.1740-8261.1987.tb01726.x

Kara ME, Sevil Kilimci F, Yildirim IG, Onar V and Pazvant G. The intercondylar fossa indices of male and female dog

femora. Veterinary and Comparative Orthopaedics and Traumatology : V.C.O.T. 2011; 24(3):211–214. https:// doi. org/10.3415/VCOT-10-04-0058

Kassab A. Ultrasonographic and macroscopic anatomy of the enucleated eyes of the buffalo (*Bos bubalis*) and the one-humped camel (*Camelus dromedarius*) of different ages. Anatomia, Histologia, Embryologia. 2012; 41(1):7-11. https://doi.org/10.1111/j.1439-0264.2011.01097.x

Kelawala DN, Patil DB, Parikh PV, Sini KR, Parulekar EA, Amin NR and Rajput PK. Normal Ocular Ultrasonographic Biometry and Fundus Imaging of Indian Camel (*Camelus dromedarius*). Journal of Camel Practice and Research. 2015; 22(2):181-185.DOI: 10.5958/2277-8934.2015.00028.4

Khan K and Türker F. Ultrasonographic measurements of the Bulbous oculi of the camel. Animal Health Production and Hygiene. 2021; 10(1):23-26.

Kumawat NK and Jhirwal SK. B-mode ultrasonographic appearance of the globe and intraocular structures of eye in dogs. The Pharma Innovation Journal. 2021; 10(2):68-71.

Lehmkuhl RC, Almeida MF, Mamprim MJ and Vulcano LC. B-mode ultrasonography biometry of the Amazon Parrot (*Amazona aestiva*) eye. Veterinary Ophthalmology. 2010; 13 Suppl, 26–28. https://doi. org/10.1111/ j.1463-5224.2010.00797.x

Mirshahi A, Shafigh SH and Azizzadeh M. Ultrasonographic biometry of the normal eye of the Persian cat. Australian Veterinary Journal. 2014; 92(7):246-249. https:// doi.org/10.1111/avj.12189

Osuobeni EP and Hamidzada WA. Ultrasonographic determination of the dimensions of ocular components in enucleated eyes of the one-humped camel (*Camelus dromedarius*). Research in Veterinary Science. 1999; 67(2),125– 129. https://doi.org/10.1053/rvsc.1998.0288

Potter T J, Hallowell GD and Bowen I M. Ultrasonographic anatomy of the bovine eye. Veterinary Radiology & Ultrasound. 2008; 49(2), 172–175. https:// doi. org/10.1111/j.1740-8261.2008.00345.x

Reef VB. Equine Diagnostic Ultrasound: WB Saunders Company, Philadelphia. 1998; pp 480-547.

Ribeiro AP, Silva ML, Rosa JP, Souza SF, Teixeira IA and Laus JL. Ultrasonographic and echobiometric findings in the eyes of Saanen goats of different ages. Veterinary Ophthalmology. 2009; 12(5):313-317.https://doi. org/10.1111/j.1463-5224.2009.00719.x

Ribeiro AP, Santos NL, Silva VC, Campos AF, Teixeira A and Laus JL. Ultrasonographic and ecobiometric findings in the eyes of adult goats. Ciência Rural. 2010; 40(3):568-573.https://doi.org/10.1590/S0103-84782010005000019

Samuelson D. Ophthalmic anatomy. Veterinary Ophthalmology. Ames: Blackwell. 2007; 37-148.

Solarte CE and Shaikh A. Ultrasound techniques in ophthalmology. Ophthalmology investigation and examination techniques. Butterworth-Heinemann, Philadelphia. 2007; 137-149. DOI: 10.1016/B978-0-7506-7586- 4.50017-9.

Sorouri S, Masoudifard M, Raoufi A and Aghazadeh M. Ultrasonographic findings of some ocular structures in Caspian miniature horse. 2009; https://doi.org /10.22099/ IJVR.2009.1716

Tharwat M and El-Omar T. Ocular ultrasonography in camels (*Camelus dromedarius*): review. Journal of Camel Practice and Research. 2021; 28(2):185-190.DOI: 10.5958/2277-8934.2021.00031.X

Tripathi DM, Malik V and Pandey RP. Transcorneal intraocular ultrasonographic and echo-biometric evaluation of bovine and equine eyes. Indian Journal of Veterinary Surgery. 2018; 39(1):7-12.

Valentini S, Tamburro R, Spadari AJM and Spinella G. Ultrasonographic evaluation of equine ocular diseases. A retrospective study of 38 eyes. Journal of Equine Veterinary Science. 2010; 30(3):150-154.https://doi. org/10.1016/j.jevs.2010.01.058

Yadegari M, Salehi A, Ashtari A and Ashtari MS. B-mode ultrasound biometry of intraocular structures in dromedary camels (*Camelus dromedarius*). Global Veterinaria. 2013; 10(1):71-74. DOI: 10.5829/idosi. gv.2013.10.1.71148

DOI : 10.5958/2277-8934.2022.00029.7 Vol 29 No 2, p 207-213

INTRAVITREAL INJECTION OF GENTAMICIN IN DROMEDARY CAMEL WITH UVEITIS

Turke Shawaf
Department of Clinical Sciences, College of Veterinary Medicine and Animal Resources, King Faisal University, Al Hasa, Saudi Arabia

ABSTRACT

This study was aimed to evaluate intravitreal injection of gentamicin in cases of uveitis in camels. Eighteen camels that suffered from anterior, posterior or panuveitis were included in the present study. Complete ophthalmic examinations were performed before and following the treatments and these were treated with a 4 mg gentamicin which was injected intravitreally together with topical antibiotics for one week, and topical nonsteroidal anti-inflammatory drugs over the course of 2-6 weeks based on each camel's individual response to therapy. One third camels (33%) affected with uveitis had poor vision before the treatments, while vision was not improved by 10% after six months improvement of vision was seen from 41-75% after one year of intraocular injection of gentamicin. The results of this study showed that the intravitreal gentamlcin injection in camel affected with anterior uveitis, posterior uveitis and panuveitis help in healing and improved the vision.

Key words: Camel, gentamicin, intravitreal, ophthalmology, uveitis

Ocular affections in camels, like in most other livestock, can cause a debilitating condition that can severely affect animal productivity (Bishnoi and Gahlot, 2004; Fahmy *et al,* 2003; Kumar *et al,* 2016). However, camels are prone to eye injuries while browsing from trees and thorny weeds and it results into corneal wounds and injuries to the outer parts of the eye (Abdella *et al,* 2018; Bishnoi and Gahlot, 2004). Moreover, camels suffer from a wide range of ophthalmic affections, which causes anterior and posterior eyes infection (Abdella *et al,* 2018; Fahmy *et al,* 2003; Gebreyohanes and Assen, 2017). Occasionally, damage to the eye can be severe enough and may lead to blindness (Abdella *et al,* 2018).

Uveitis is characterised by exceptionally wide heterogeneity, regarding both oetiology and symptoms (Laven and Lawrence, 2006; Malalana *et al,* 2017). The pathophysiology and course of the disease are complex and multifactorial associated with various symptoms (Rojas-Carabali *et al,* 2021). The classic signs of uveitis are episcleral congestion, epiphora, corneal oedema, blepharospasm, aqueous flare and fibrin in the anterior chamber (Fingerhut *et al,* 2019; Rojas-Carabali *et al,* 2021). The chronic from of uveitis may lead to irreversible complications (Fischer *et al,* 2019; Rojas-Carabali *et al,* 2021). Few reports described uveitis in camels (Abdella *et al,* 2018; Fahmy *et al,* 2003; Gahlot, 2000; Madany *et al,* 2006) and there are no specific treatments reported for uveitis in camels except local and systemic anti-inflammatory treatment (Bishnoi and Gahlot, 2004; Madany *et al,* 2006). Recently, uveitis is being treated in veterinary medicine in many surgical procedures like pars plana vitrectomy in horses, dogs and non-human primates (Fingerhut *et al,* 2019; Fruhauf *et al,* 1998; Hirashima *et al,* 2022; Hopster *et al,* 2013; Tshilenge *et al,* 2016). However, intravitreal injection of gentamicin in horses (Fischer *et al,* 2019), suprachoroidal injection of triamcinolone in horses (Gagnon *et al,* 2021) and cidofovir injection in dogs with chromic glaucoma (Low *et al,* 2014) has been reported.

Several recent studies indicated the good efficacy of gentamicin in equine recurrent uveitis (ERU) (Fischer *et al,* 2019; Kleinpeter *et al,* 2019; Launois *et al,* 2019).

This study was, therefore, aimed to evaluate the efficacy of single-dose intravitreal injections of gentamicin in cases of uveitis of camels.

Materials and Methods

Ethical approval

The study was approved for research purposes by the Ethics Committee at King Faisal University in Saudi Arabia (Approval number: KFU-REC-2021-OCT-EA00010).

SEND REPRINT REQUEST TO TURKE SHAWAF email: tshawaf@kfu.edu.sa

Animals

Camels (aged 2-18 years) with uveitis (n=18; male=7, females=11) brought to the Veterinary Teaching Hospital, College of Veterinary Medicine, King Faisal University were selected. The uveitis was unilateral (n=9) and bilateral (n=9). Further clinical examination revealed panuveitis (n=12), anterior uveitis (n=2) and posterior uveitis (n=4). Complete history, clinical examination, ocular examinations using ophthalmoscope and ultrasound were performed in Veterinary Teaching Hospital. The clinical signs of uveitis were conjunctival congestion, miosis, epiphora, blepharoedema or blepharospasm, aqueous flare, photophobia, fibrin in the anterior chamber, equatorial vesicular cataracts, capsule adhesions, lens vitreous body opacifications, and retinal detachment. This study was conducted from March 2020 to January 2022.

Ocular examination

After history and clinical examination, complete ophthalmic examinations were performed to differentiate between anterior (Fig 1B) and posterior and panuveitis (Fig 1A) by evaluation (dazzle, and pupillary light reflexes (PLR)), slit-lamp biomicroscope (Kowa SL-15) (Kowa Company Ltd., Tokyo, Japan) and a subjective clinical vision assessment (menace response) and neuro-ophthalmic indirect ophthalmoscopy (Heine Beta 200 and Heine Omega 500; Heine Optotechnik, Herrsching, Germany). Aqueous flare was graded as follows: 0 (none), 1 (faint), 2 (moderate), 3 (severe) or 4 (blood

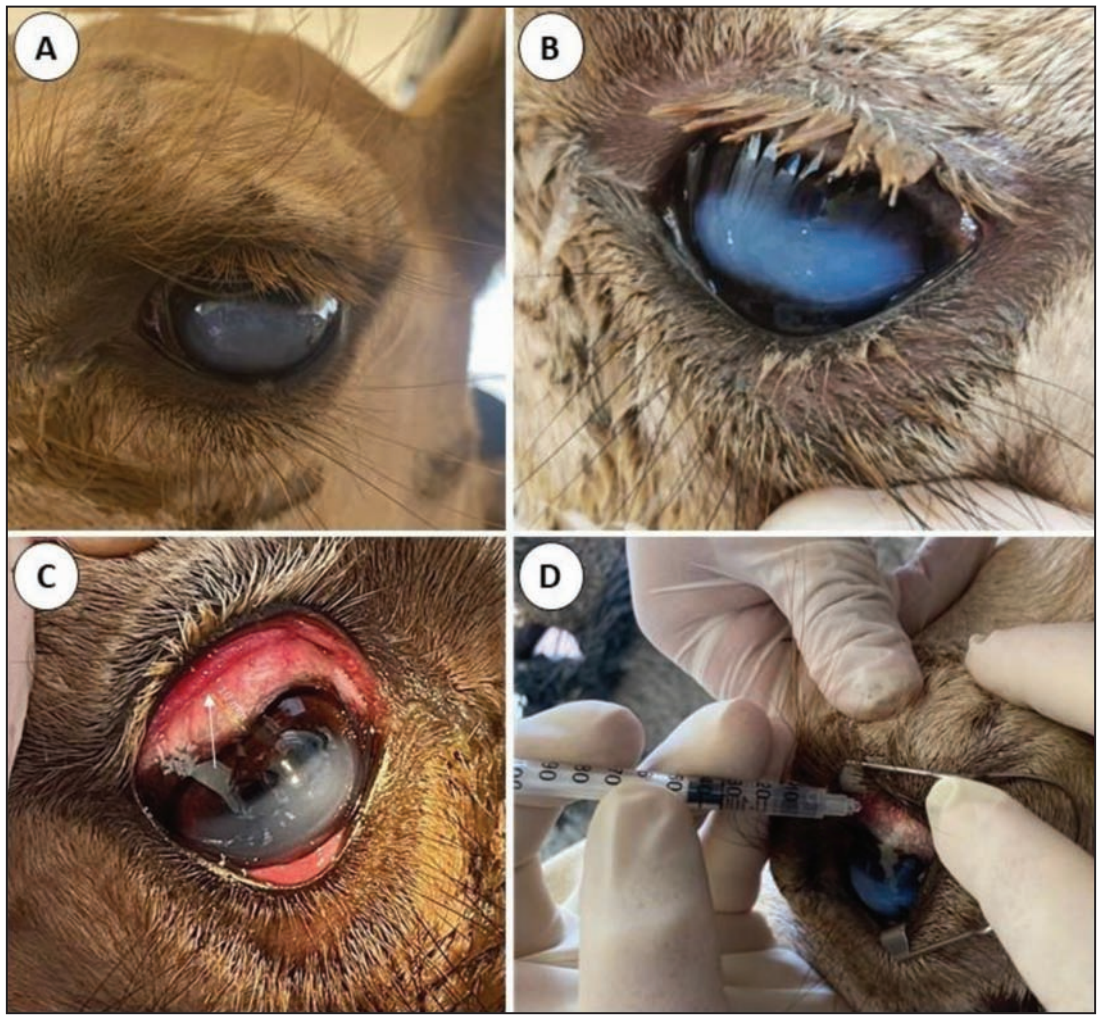

Fig 1. (**A**) Five-year old camel presented for a persistent chronic panuveitis of the left eye with an accumulation of fibrin in the anterior and posterior chamber, blepharospasm and miosis were present. (**B**) Twelve-year old camel affected with anterior uveitis with epiphora, corneal oedema, and blepharospasm. (**C**) This image shows the place of intravitreal injection, where the yellow dashed line indicates the distance between the upper part of the cornea and the place of injection (10 mm); the white arrow showed the position of injection. (**D**) This image shows the intravitreal injection after opening the eye using a Barraquer eyelid speculum; the injection is done using a 30-gauge needle/syringe combination.

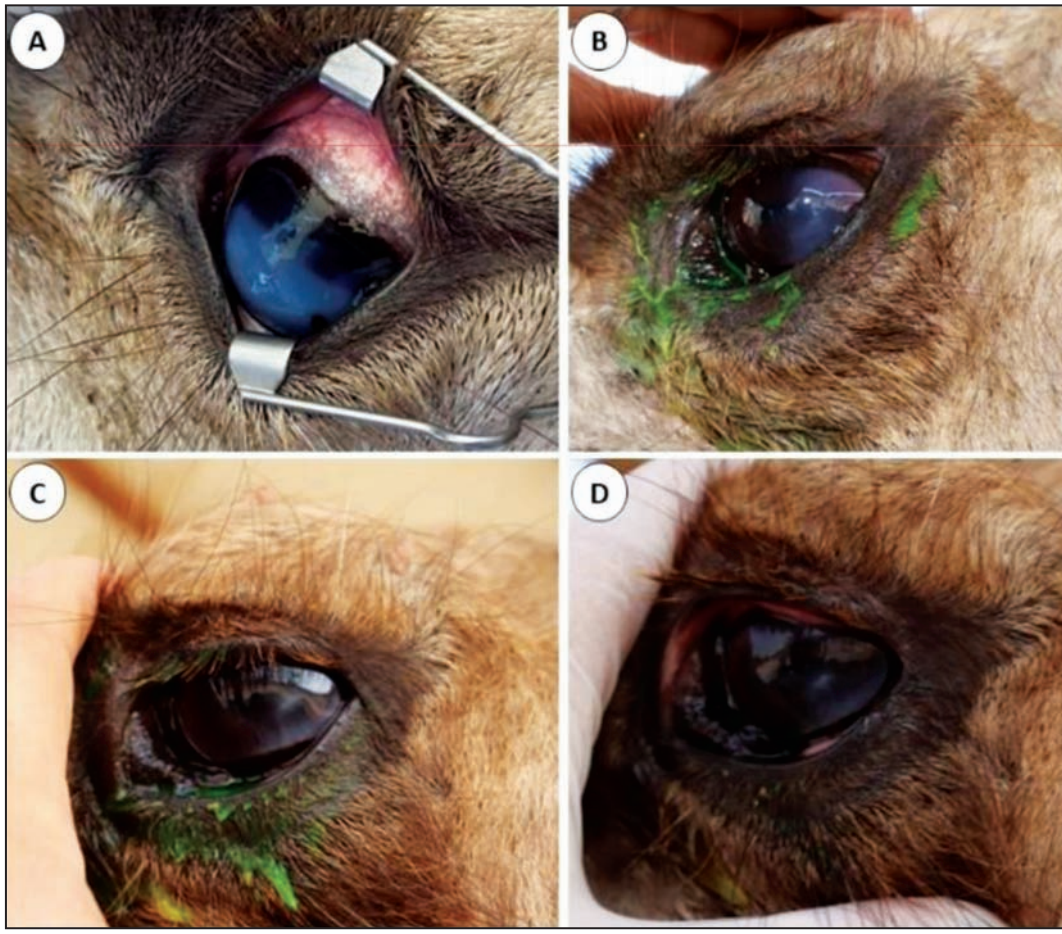

Fig 2. (**A**) Twelve-year old camel before the intravitreal injection presented with anterior uveitis with corneal oedema and overall cloudiness. (**B**) Four weeks after injection: Slight reduction in cloudiness and fibrin in the anterior chamber. (**C**) Six months after injection: reduced corneal oedema (by 50%), cloudiness with improved vision. (**D**) One year after injection: more reduced cloudiness than six months ago; the vision was restored to a moderate degree.

or fibrin present in the anterior chamber) (Lam *et al,* 2015). Fundus images were obtained by Kowa Genesis (Kowa Company Ltd., Tokyo, Japan) in camels with posterior segment abnormalities, whenever possible.

Sedation and intravitreal gentamicin injection

Each camel was sedated with intravenous injection of xylazine 2% (0.1 mg/kg bodyweight; Rompun, Bayer Health Care), and an auriculopalpebral nerve block (1.5 mL lidocaine SC, 2% Lidocain inj., Teva) was performed on the respective eye. Topical oxybuprocaine (Novesine 0.4% eyedrops, OmniVision) was used for topical corneal analgesia. However, eyelids were held open manually. The ocular surface was first irrigated with 0.5% povidone-iodine solution (Betadine, Egis) and then rinsed with saline. Following sedation, the camel's head was positioned atop a pair of pads placed on a ground to increase stability. The conjunctival fornices were irrigated with 1.0 ml of baby shampoo solution (0.1% dilute in saline solution), 1.0 ml of a 1.0% dilute iodine solution, and 1.0 ml of balanced saline solution (Brooks *et al,* 2017). Dorsal globe exposure was facilitated with prototype eyelid retractor, and further enhanced by rotating the camel's head away from the examiner to exaggerate ventral globe rotation. Camels were treated with a 4 mg injectable gentamicin solution containing preservatives (Genta80; 80 mg/ml) which was drawn up in a 30- gauge needle/syringe combination (12mm length, 1.0 ml insulin syringe) (Fig 1D). The injection site was 10 mm posterior to the limbus at 12 o'clock (Fig 1C). Due to the difficulty of accurately measuring and determining the injection point with calipers, the injection point was roughly estimated by the examiner immediately before the injection. The injection was facilitated by applying gentle but steady pressure while slowly and deliberately rotating the needle in a clockwise manner with the needle directed toward the optic nerve head to avoid inadvertent contact

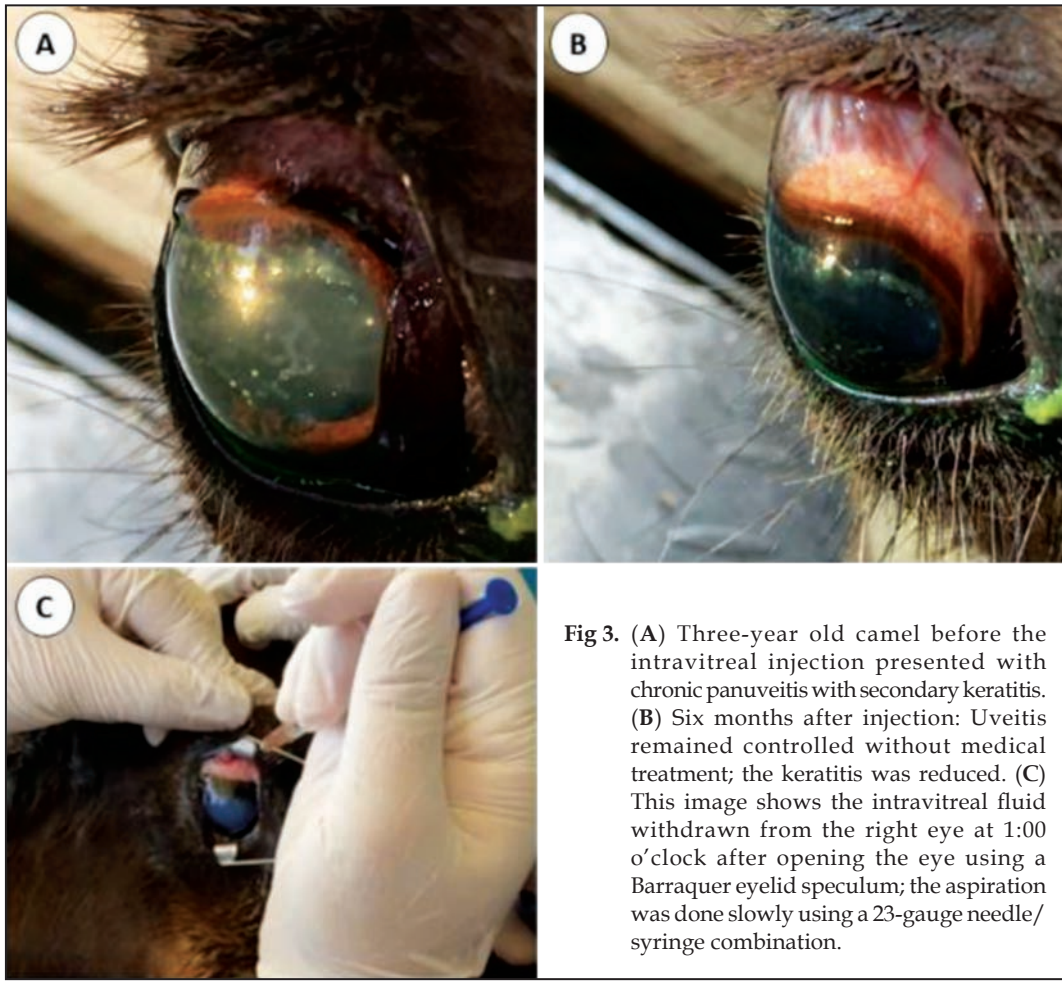

Fig 3. (**A**) Three-year old camel before the intravitreal injection presented with chronic panuveitis with secondary keratitis. (**B**) Six months after injection: Uveitis remained controlled without medical treatment; the keratitis was reduced. (**C**) This image shows the intravitreal fluid withdrawn from the right eye at 1:00 o'clock after opening the eye using a Barraquer eyelid speculum; the aspiration was done slowly using a 23-gauge needle/ syringe combination.

with the lens. Same fluid quantity from vitreous was withdrawn using a second insulin syringe with 23-gauge needle at either the 11:00 o'clock (left eye) or 1:00 o'clock (right eye) positions in order to keep the same fluid pressure in the ocular and this fluid was used for more investigations (Fig 3C).

Post-injection therapy and Follow-up examination

Post intravitreal injection, a medical therapy consisting of topical antibiotics (Oxytetracyclin) q12h for one week, and topical nonsteroidal anti-inflammatory drugs (NSAIDs) that were gradually tapered over the course of 2-6 weeks based on each camel's individual response to therapy. Systemic Flunixin-meglumine @ 1.1mg/kg, q24h was also administered intravenously for 7 days. Camels were monitored weekly for the first month. Subsequent follow-up examinations were spaced further apart based on the camel's individual response to treatment. Inflammation was markedly reduced which was evident by absence of signs of uveitis (Fig 2A, B, C, D and Fig 3A, B).

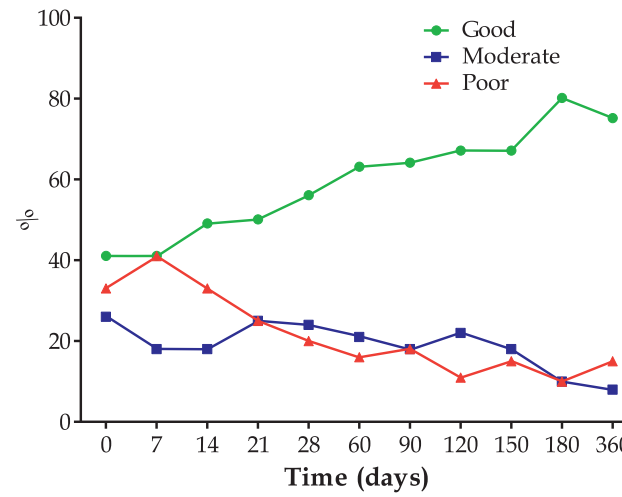

Fig 4. Changes in vision after intravitreal gentamlcin injection.

Statistical analysis

The obtained data was recorded in Excel spreadsheets and imported into Graph Pad Prism 7 (GraphPad Software, San Diego, CA, USA) software for further analysis. Graphs, calculations, and

Table 1. Subjective visual assessment pre- and post-intravitreal gentamicin injection (days).

Time (days)	Camels	Eyes	Unilateral/ bilateral	Improvements eyes (%)		
				Good	*Moderate*	*Poor*
Pre-injection (0 days)	18	27	9/9	11 (41%)	7 (26%)	9 (33%)
Post-injection (7 days)	18	27	9/9	11 (41%)	5 (18%)	11 (41%)
Post-injection (14 days)	18	27	9/9	13 (49%)	5 (18%)	9 (33%)
Post-injection (21days)	18	27	9/9	13 (50%)	7 (25%)	7 (25%)
Post-injection (28 days)	18	25	9/8	14 (56%)	6 (24%)	5 (20%)
Post-injection (60 days)	16	24	8/8	15 (63%)	5 (21%)	4 (16%)
Post-injection (90 days)	15	22	8/7	14 (64%)	4 (18%)	4 (18%)
Post-injection (120 days)	15	22	8/7	15 (67%)	5 (22%)	2 (11%)
Post-injection (150 days)	15	22	8/7	15 (67%)	4 (18%)	3 (15%)
Post-injection (180 days)	14	20	8/6	16 (80%)	(10%)2	2 (10%)
Post-injection (360 days)	8	12	4/4	9 (75%)	1 (8%)	2 (15%)

statistical analyses were performed using GraphPad Prism software.

Results and Discussion

The information is limited about treatment of uveitis in camels; therefore. the main goal of this study was to conduct clinical trial of the intravitreal injection of gentamicin to treat the uveitis by minimising ocular inflammation and restoration of vision to a varying degree (Fischer *et al,* 2019; Gerding and Gilger, 2016; Wollanke *et al,* 2022). However, the pharmacodynamics of gentamicin in the all types or stages of uveitis remains enigmatic (Fischer *et al,* 2019; Gan *et al,* 2001; Kleinpeter *et al,* 2019; Wollanke *et al,* 2022). Romeike *et al* (1998) reported that the primary mechanism of action of gentamicin could suppress or block the activation of specific T-cell that are identified to play a significant role in autoimmune uveitis. While, many studies in recent years reported successful treatments of equine recurrent uveitis affected with Leptospira using intraocular gentamicin injection due to the direct effect of gentamicin on gram-negative bacteria and improvement was noticed within days of starting treatment (Fischer *et al,* 2019; Voelter *et al,* 2020; Wollanke *et al,* 2022).

In present study, no difficulties were found in intraocular injection in camels under sedation and local anesthesia except the posterior movement of the eye, which was more than described in horses or humans (Ganapathy *et al,* 2018; Jose-Vieira *et al,* 2021; Yi *et al,* 2008). In animals of present study, the eye was pushed and fixed it in the anterior part of the orbital cavity directly before the injection by applying pressure in medial side of the zygomatic process to expose the eye in order to facilitate the injection process. A difficulty was noticed in withdrawing the vitreous humor samples using the 30-gauge needle but fluid withdrawal was easy and safe with 23-gauge needle as in equine (Ackermann *et al,* 2021). One of the limitations of this study was the difficulty in follow up of the treatment with the owners, especially keeping the camel in the shade during the first days after treatment, which may have an impact on the results of the treatment.

In present study, 62% of eyes of affected camels had panuveitis, while the incidence of posterior and anterior uveitis were 27% and 11%, respectively. However, studies are scarce about the type of uveitis in camels (Kumar *et al,* 2016; Madany *et al,* 2006). A similar increased percentage of panuveitis type was recorded in horses (Ackermann *et al,* 2021; Fischer *et al,* 2019; Wollanke *et al,* 2022), while a higher percentage for anterior uveitis was reported in humans (Roche *et al,* 2021; Silvestri *et al,* 2020). The results of this study showed that the intravitreal gentamicin injection in camel affected with anterior uveitis, posterior uveitis and panuveitis helped in healing and improved the vision (Fig 2 and 3). On the other hand, three eyes in two camels developed cataracts, retinal degeneration and loss of vision after intraocular injection. Therefore, the risks of injection cannot be ignored, and must be discussed in detail with the owner before starting the treatment options (Fischer *et al,* 2019; Launois *et al,* 2019). In this study, nine eyes (Table 1 and Fig 5) (33%) affected with uveitis had poor vision before the treatments, while the vision decreased to 10% after six months of intraocular injection of gentamicin which was in agreement with result of Fischer *et al* (2019) and Kleinpeter *et al* (2019) for treatments of equine recurrent uveitis. The increased percentage of good vision improvement of eyes was from 41% to 75%

after one year of treatment indicated the effectiveness of intravitreal injections of gentamicin in animals of present study (Fig 2D). The stability of equine recurrent uveitis with reduction of ophthalmological symptoms and an improvement in vision after intravitreal injection with a single low dose of gentamicin was seen (Fischer *et al,* 2019; Kleinpeter *et al,* 2019; Wollanke *et al,* 2022). However, two camels of present study suffering from unilateral panuveitis continued to have poor vision even after one year of the treatment (Table 1).

In conclusion, intravitreal injection in camels affected with uveitis can be treated by intervitseal injection of gentamicin. However treatment and after care protocol needs more attention.

Acknowledgements

This work was supported through the Annual Funding track by the Deanship of Scientific Research, Vice Presidency for Graduate Studies and Scientific Research, King Faisal University, Saudi Arabia [Project No. GRANT684].

References

Abdella ME, Habeeballa HA, Mohamed MS, Babiker MY and and Abakar AD. Preliminary report on the occurrence of ocular disorders among one-humped camel (*Camelus dromedarius*) Raised at Al Butana Plain, Sudan. Journal of Camel Research and Production. 2018; 2:28-39.

Ackermann K, Kenngott R, Settles M, Gerhards H, Maierl J and Wollanke B. *In vivo* biofilm formation of pathogenic Leptospira spp. in the vitreous humor of horses with recurrent uveitis. Microorganisms. 2021; 9:1-14.

Baath J, Ells AL, Crichton A, Kherani A and Williams RG. Safety profile of intravitreal triamcinolone acetonide. Journal of Ocular Pharmacology and Therapeutics. 2007; 23:304-310.

Bishnoi P and Gahlot T. Ophthalmic affections in camels (*Camelus dromedarius*). Veterinary Practitioner. 2004; 5:89-93.

Fahmy LS, Hegazy AA, Abdelhamid MA, Hatem ME and Shamaa AA. Studies on eye affections among camels in Egypt: Clinical and bacteriological studies. Scientefic Journal of King Faisal Univ. 2003; 4:159-176.

Fingerhut L, Ohnesorge B, von Borstel M, Schumski A, Strutzberg-Minder K, Morgelin M, Deeg CA, Haagsman HP, Beineke A, von Kockritz-Blickwede M and de Buhr N. Neutrophil Extracellular Traps in the Pathogenesis of Equine Recurrent Uveitis (ERU). 2019; Cells 8:1528

Fischer BM, McMullen RJ, Jr., Reese S and Brehm W. Intravitreal injection of low-dose gentamicin for the treatment of recurrent or persistent uveitis in horses: Preliminary results. BMC Veterinary Research. 2019; 15:29.

Fruhauf B, Ohnesorge B, Deegen E and Boeve M. Surgical management of equine recurrent uveitis with single port pars plana vitrectomy. Veterinary Ophthalmology. 1998; 1:137-151.

Gagnon NA, Hartley C and Gilger BC. Efficacy and safety of suprachoroidal triamcinolone injection in horses with poorly responsive equine recurrent uveitis. Veterinary Ophthalmology. 2021; 24:308-312.

Gahlot T. Selected Topics on Camelids. The Camelid Publishers., India. 2000.

Gan IM, van Dissel JT, Beekhuis WH, Swart W and van Meurs JC. Intravitreal vancomycin and gentamicin concentrations in patients with postoperative endophthalmitis. British Journal of Ophthalmology. 2001; 85:1289-1293.

Ganapathy PS, Lowder CY, Arepalli S, Baynes K, Li M, Bena J and Srivastava SK. Treatment duration and side effect profile of long-term use of intravitreal preservative-free triamcinolone acetonide in uveitis. American Journal of Ophthalmology. 2018; 194:63-71.

Gebreyohanes MG and Assen AM. Adaptation mechanisms of camels (*Camelus dromedarius*) for desert environment. Journal of Veterinary Science and Technology. 2017; 8:1-5.

Gerding JC and Gilger BC. Prognosis and impact of equine recurrent uveitis. Equine Veterinary Journal. 2016; 48:290-298.

Hirashima S, Takiyama N and Umeda Y. Outcome of 25-gauge pars plana vitrectomy via a lateral approach without proptosis of the globe: A retrospective study in 72 dogs (78 eyes). Veterinary Ophthalmology. 2022; 25:23-30.

Hopster K, Ohnesorge B, von Borstel M, Rohn K and Kastner S. Influence of atracurium on cardiovascular parameters in horses undergoing vitrectomy during general anaesthesia, and on recovery duration and quality. Tierarztlische Praxis Ausg G Grosstiere Nutztiere. 2013; 41:371-377.

Jose-Vieira R, Ferreira A, Meneres P, Sousa-Pinto B and Figueira L. Efficacy and safety of intravitreal and periocular injection of corticosteroids in noninfectious uveitis: a systematic review. Survive Ophthalmology. 2021; 12.002.

Kleinpeter A, Gopfert A, Kohler E and Brehm W. Intravitreal injection of low-dose gentamicin for the treatment of ERU-affected horses. Tierarztl Prax Ausg G Grosstiere Nutztiere. 2019; 47:25-34.

Kumar P, Purohit N and Gahlot T. Retrospective analysis of ocular affections in dromedary camels. Journal of Camel Practice and Research. 2016; 23:247-250.

Launois T, Gonzalez Hilarion LM, Barbe F, Leurquin C, Bihin B, Hontoir F, Dugdale A and Vandeweerd JM. Use of intravitreal injection of gentamicin in 71 horses with equine recurrent uveitis. Journal of Equine Veterinary Science. 2019; 77:93-97.

Laven RA and Lawrence KR. An outbreak of iritis and uveitis in dairy cattle at pasture associated with the supplementary feeding of baleage. New Zealand Veterinary Journal. 2006; 54:151-152.

Low MC, Landis ML and Peiffer RL. Intravitreal cidofovir injection for the management of chronic glaucoma in dogs. Veterinary Ophthalmology. 2014; 17:201-206.

Madany J, Nowakowski H, Pępiak A and Paśko S. Uveitis anterior in a camel – A clinical case. Bulletin of the Veterinary Institute in Pulawy. 2006; 50:131-135.

Malalana F, Blundell RJ, Pinchbeck GL and McGowan CM. The role of *Leptospira* spp. in horses affected with recurrent uveitis in the UK. Equine Veterinary Journal. 2017; 49:706-709.

Roche D, Badard M, Boyer L, Lafforgue P and Pham T. Incidence of anterior uveitis in patients with axial spondyloarthritis treated with anti-TNF or anti-IL17A: a systematic review, a pairwise and network meta-analysis of randomized controlled trials. Arthritis Research Therapeutic. 2021; 23:192.

Rojas-Carabali W, Reyes-Guanes J, Villabona-Martinez V, Fonseca-Mora MA and de-la-Torre A. Intermediate Uveitis Etiology, Complications, Treatment, and Outcomes in a Colombian Uveitis Referral Center. Clinical Ophthalmology Journal. 2021; 15:2597-2605.

Romeike A, Brugmann M and Drommer W. Immuno-histochemical studies in equine recurrent uveitis (ERU). Veterinary Pathology Journal. 1998; 35:515-526.

Silvestri E, Bitossi A, Bettiol A, Emmi G, Urban ML, Mattioli I, Di Scala G, Bacherini D, Lopalco G, Venerito V, Iannone F, Vitale A, Tosi GM, Rizzo S, Fabiani C, Cantarini L, Virgili G, Vannozzi L and Prisco D. Adalimumab effectively controls both anterior and posterior noninfectious uveitis associated with systemic inflammatory diseases: focus on Behcet's syndrome. Inflammopharmacology. 2020; 28:711-718.

Tshilenge KT, Ameline B, Weber M, Mendes-Madeira A, Nedellec S, Biget M, Provost N, Libeau L, Blouin V, Deschamps JY, Le Meur G, Colle MA, Moullier P, Pichard V and Rolling F. Vitrectomy Before Intravitreal Injection of AAV2/2 Vector Promotes Efficient Transduction of Retinal Ganglion Cells in Dogs and Nonhuman Primates. Hum Gene Therapeutic Methods. 2016; 27:122-134.

Voelter K, Vial Z, Pot SA and Spiess BM. Leptospiral antibody prevalence and surgical treatment outcome in horses with Equine Recurrent Uveitis (ERU) in Switzerland. Veterinary Ophthalmology. (2020) 23:327 648-658.

Wollanke B, Gerhards H and Ackermann K. Infectious Uveitis in Horses and New Insights in Its Leptospiral Biofilm-Related Pathogenesis. Microorganisms. 2022; 10:1-14

Yi NY, Davis JL, Salmon JH and Gilger BC. Ocular distribution and toxicity of intravitreal injection of triamcinolone acetonide in normal equine eyes. Veterinary Ophthalmology. 2008; 1:15-19.

SELECTED RESEARCH ON CAMELID IMMUNOLOGY

(Hard Bound, 392 pages, few figs coloured, Edition 2016)

In 1989 a group of biologists led by Raymond Hamers at the Free University Brussels investigated the immune system of dromedaries. This discovery was published in Nature in 1993. Based on their structure, these peculiar camelid antibodies have been named Heavy Chain Antibodies (HCAb), as they are composed of heavy chains only and are devoid of light chains. Sera of camelids contain both conventional heterotetrameric antibodies and unique functional heavy (H)-chain antibodies (HCAbs). The smaller size and monomeric single domain nature make these antibodies easier to transform into bacterial cells for bulk production, making them ideal for research purposes. Camelid scientists world over were greatly fascinated by a new field of research called "Camelid Immunology". Significant research has been done on camelid immunology in recent decade. In order to benefit future camelid immunology researchers, this book was planned in the series of "Selected Topics" by Camel Publishing House with a title- "Selected Research on Camelid Immunology" edited by T.K. Gahlot, U. Wernery and Serge Muyldermans. This book is a unique compilation of research papers based on "Camelid Immunology" and published in Journal of Camel Practice and Research between 1994-2015. Research on this subject was done in 93 laboratories or institutions of 30 countries involving about 248 scientists. In terms of number of published papers in JCPR on the immunology the following countries remain in order of merit (in parenthesis), i.e. Iran (1), India and UAE (2), China and Saudi Arabia (3), Sudan (4), Kenya and Belgium (5), USA (6), Germany (7) and so on. The book contains 11 sections and is spread in 384 pages. The diverse sections are named as overview of camel immune system; determinates of innate immunity, cells, organs and tissues of immune system; antibodies; immunomodulation; histocompatibility; seroprevalence, diagnosis and immunity against bacteria, viruses, parasites and combination of other infections; application of camel immunoglobulins and applications of immune mechanisms in physiological processes. The camelid immunology has to go a long way in its future research, therefore, this reference book may prove quite useful for those interested in this subject. Book can be seen on www.camelsandcamelids.com.

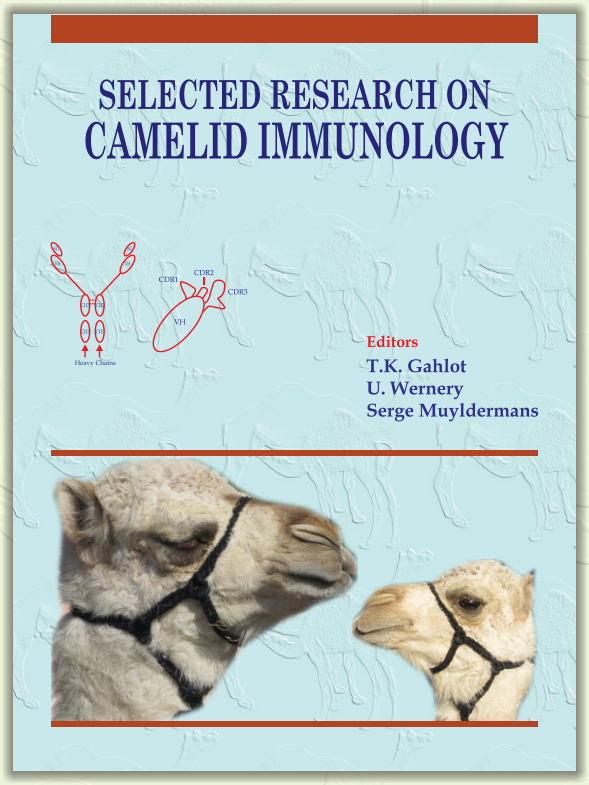

Editor:
T.K. Gahlot
U. Wernery
Serge Muyldermans

Edition: 2016

Publisher:
Camel Publishing House
67, Gandhi Nagar West, Near Lalgarh Palace,
Bikaner-334001 Rajasthan, India
email: tkcamelvet@yahoo.com

Website:
www.camelsandcamelids.com
www.tkgahlotcamelvet.com

Price: US $ 475
INR 12500

ISBN 81-903140-4-1

DOI : 10.5958/2277-8934.2022.00030.3 Vol 29 No 2, p 215-222

INVESTIGATION OF LAMENESS IN RACING DROMEDARY CAMELS (*Camelus dromedarius*) AND ASSOCIATED OXIDATIVE STRESS BIOMARKERS

Wael El-Deeb[1,2] and Mohammed A. Abdelghani[1,3]

[1]Department of Clinical Sciences, College of Veterinary Medicine, King Faisal University, Al-Ahsa, Saudi Arabia
[2]Department of Internal Medicine, Infectious Diseases, and Fish Diseases, Faculty of Veterinary Medicine, Mansoura University, Mansoura, Egypt
[3]Department of Theriogenology, Faculty of Veterinary Medicine, Assuit University, Assuit, 71526, Egypt

ABSTRACT

In racing camels, lameness is measured to be a major health issue and an economically important problem for many camel owners. This study aimed to investigate different oxidative stress and antioxidant biomarkers in the blood of racing lamed dromedary camels. Moreover, to highlight their role in lameness diagnosis, pathogenesis and to emphasise its role to monitor treatment response. Thirty five out of 315 racing camels exhibited clinical lameness. The serum levels of malondialdehyde (MDA) and nitric oxide (NO) in lame dromedary camels with different perceived causes of lameness (punctured foot, traumatic injury) were remarkably over than those detected in the control healthy dromedary camels. However, lame dromedary camels had significantly lower levels of serum superoxide dismutase (SOD), reduced glutathione (GSH), catalase (CAT), and total antioxidant capacity (TAC) when compared with the control healthy camels. The serum levels of MDA, NO, SOD, GSH, CAT, and TAC markers in lame dromedary camels pre-and post-treatment were measured in this study. An obvious decline was detected in serum levels of MDA and NO of lame camels after 10 days of treatment, whereas, the levels of antioxidant markers (SOD, GSH, CAT, and TAC) were significantly increased toward normal values. The ROC curves were created. The AUCs were assessed to evaluate the accuracy of each variable to distinguish diseased and healthy camels. Based on the ROC curves and AUCs; MDA, SOD, GSH, CAT, TAC, and NO were considered highly diagnostic and predictive biomarkers of lame dromedary camels. Moreover, the addition of antioxidants to the treatment protocol of lameness may enhance the treatment response in camels.

Key words: Camel, catalase, glutathione, lameness, malondialdehyde, super oxide dismutase

A variety of factors and widely varied causes can lead to camel lameness, including direct trauma, nutritional problems, punctured foot, abnormal limb conformation, and infectious disease (Gahlot and Chouhan, 1992; Ramadan, 1994; Gahlot, 2007; Al- Juboori, 2011a; Al-Juboori, 2011b; Al-Juboori, 2010; Mostafa and Khalil, 2018; Mostafa, 2020). Lameness in camels is characterised by partial or non-weight bearing by one or more limbs, swelling of the joints, pain upon palpation, protruding toes, shivering while sitting, and an asymmetrical pelvis (Gahlot, 2007). In addition to decreased milk production, decreased reproductive performance, growth retardation, and culling from farms or competition, lame camels also suffer from diminished physiological vitality and need additional treatment and care costs (Manefield and Tinson, 1997; Al-Ani, 2004 and Al-Juboori, 2010). Camel lameness differs from that of cattle and horses owing to its unique anatomy, biomechanics, geoclimatic adaptations, and use (Gahlot, 2000). There is increasing evidence that oxidative damage contributes to many diseases, such as atherosclerosis, cancer, liver damage, rheumatoid arthritis, immunological incompetence, neurodegenerative disorders, and aging (Dalle-Donne *et al,* 2003; Habif *et al,* 2001). Oxidative stress (OS) is defined as RONS (Reactive Oxygen/Nitrogen species) that exceed the body's antioxidant capacity (Finaud *et al,* 2006).

The body produces RONS as a result of its normal metabolic processes and through exposure to an array of environmental and physiological stressors. The tissue's specific antioxidant defenses and the specific macromolecules targeted by RONS will determine the degree of damage and disease generation that may accompany OS. The total antioxidant capacity of the body provides protection against the excessive production of reactive oxygen

SEND REPRINT REQUEST TO WAEL EL-DEEB email: weldeeb@kfu.edu.sa

and nitrogen species (RONS) by cells (Bloomer and Fisher-Wellman, 2008). Endogenous and exogenous compounds contribute to antioxidant capacity (Halliwell and Gutteridge, 1999; Possamai *et al,* 2007). The former recognised antioxidant compounds include uric acid, superoxide dismutase, catalase, and glutathione peroxidase. Over the last decade, various tests for the measurement of OS have been developed to assess the oxidative status of an individual under normal or pathological conditions or after any kind of intervention. By measuring the levels of markers for ongoing oxidative damage in serum and plasma samples, we can get a complete picture of the OS state in the body (Argqelles *et al,* 2004).

There have only been a few studies comparing antioxidant capacity and OS in domestic animals, particularly in racing dromedary camels (Mousa *et al,* 2006). Our study measured (malondialdehyde) MDA as well as nitric oxide (NO) (as markers of OS), super oxide dismutase (SOD), reduced glutathione (GSH), catalase (CAT), and total antioxidant capacity (TAC) levels (as markers of antioxidant status) in lame racing dromedary camels and healthy ones. Moreover, the study monitored the oxidant-antioxidant status in lame dromedary camels after 10 days of treatment.

Materials and Methods

Camels' selection and sampling protocol

A total of 315 racing dromedary camels, aged 5.5–8.1 years, were investigated between January and September 2019 in one camel herd in the eastern region of Saudi Arabia. A total of 35 out of 315 racing camels exhibited clinical lameness. Punctured feet and traumatic injuries were diagnosed as lesions responsible for clinical lameness in these racing camels. Bovine hoof testers and walking on sandy, pebbled or hard tracks were used to diagnose lame camels (Gahlot, 2000 and 2007). Moreover, 20 clinically healthy racing dromedary camels were carefully chosen as a control group.

Whole blood samples were collected from clinically lame dromedary camels (N = 35) and the control healthy group (N = 20) for further biochemical analysis. Lame dromedary camels were subjected to a treatment protocol which included the use of non-steroidal anti-inflammatory drugs (NSAIDS) (2.2 mg flunixin per kg of camel body weight, IV injection), cleaning, and disinfection of lesions for five consecutive days, with complete rest of the affected camels.

Evaluation of oxidative stress and antioxidant biomarkers

With the help of commercial ELISA kits (Cayman, USA), malondialdehyde, reduced glutathione, catalase, and superoxide dismutase activities were determined in serum. After nitrate has been reduced to nitrite by the Griess reagent, nitric oxide (NO) is determined as the nitrite concentration in serum. Using sodium nitrite as a standard, the reaction was measured at nm (Ding *et al,* 1988). A commercial test kit (Bayer diagnostics) was used to measure total serum protein concentration. The NO concentration in serum was measured using a Nmol/mg protein unit. Beers and Sizer (1952) method, CAT activity was measured in the RBC hemolysate. CAT activity was measured by measuring the difference in absorbance per min/mg Hb following the decomposition of H_2O_2. Spectrophotometric analysis of TAC was conducted using kits supplied by Biodiagnostic®, Egypt.

Data Analysis

All parameters were expressed as mean ± SD. Comparisons in mean were performed by Kruskal–Wallis ANOVA on Ranks followed by Dunn's multiple comparisons. The different means were significant at $P<0.05$. Statistical analysis was performed using JMP software version 11.0.0 (SAS Institute, Cary, NC, USA). Spearman's rank correlation test was used to investigate the correlation between parameters. Each assay's diagnostic accuracy was evaluated by creating the ROC (receiver operator characteristics) curve and determining the area under the curve (AUC). An AUC of 0.7 to 0.9 was considered moderately accurate, an AUC of >0.9 highly accurate, and an AUC of 1 perfect.

Results

The serum levels of MDA and NO in lame dromedary camels with different causes were remarkably (P 0.0001) higher than those detected in the control healthy dromedary camels (Fig 1). However, we found that lame dromedary camels had significantly lower levels of serum SOD, GSH, CAT, and TAC when compared with the control healthy camels. (Fig 1). The serum levels of MDA, NO, SOD, GSH, CAT, and TAC markers in lame dromedary camels pre-and post-treatment were measured in this study. A significant decline was detected in serum levels of MDA and NO of lame camels after ten days of treatment, whereas the levels of antioxidant markers (SOD, GSH, CAT, and TAC) were significantly increased towards normal values (Fig 2). Spearman's correlation was estimated for

the study biomarkers in clinically lame camels and healthy ones and in lame camels before and after 10-days of treatment (Table 1). There was a significant appositive correlation between TAC, SOD, GSH, and CAT. However, significant negative correlations were observed between OS markers (MDA and NO) and all tested antioxidants (TAC, SOD, GSH, and CAT) in camels under investigation.1

The diagnostic test characteristics of OS and parameters in racing dromedary camels with clinical lameness were explored in table 2. The ROC curves were created. The AUCs were assessed (Fig. 3) to evaluate the accuracy of each variable in distinguishing diseased and healthy camels. Based on the ROC curves and AUCs, MDA (AUC = 0.910), SOD (AUC = 0.922), GSH (AUC = 0.901), TAC (AUC = 1), and NO (AUC = 0.994) were similarly highly diagnostic and predictive for treatment response in lame dromedary racing camels.

Table 1. Correlation matrix using spearman test among different oxidative stress biomarkers in racing dromedary camels with clinical lameness.

	sMDA	CAT	GSH	SOD	NO	TAC
sMDA	1					
CAT	-0.557	1				
GSH	-0.527	0.524	1			
SOD	-0.542	0.497	0.556	1		
NO	0.589	-0.613	-0.515	-0.558	1	
TAC	-0.557	0.633	0.518	0.64	-0.597	1

Serum malondialdehyde (sMDA), catalase (CAT), reduced glutathione (GSH), super oxide dismutase (SOD)

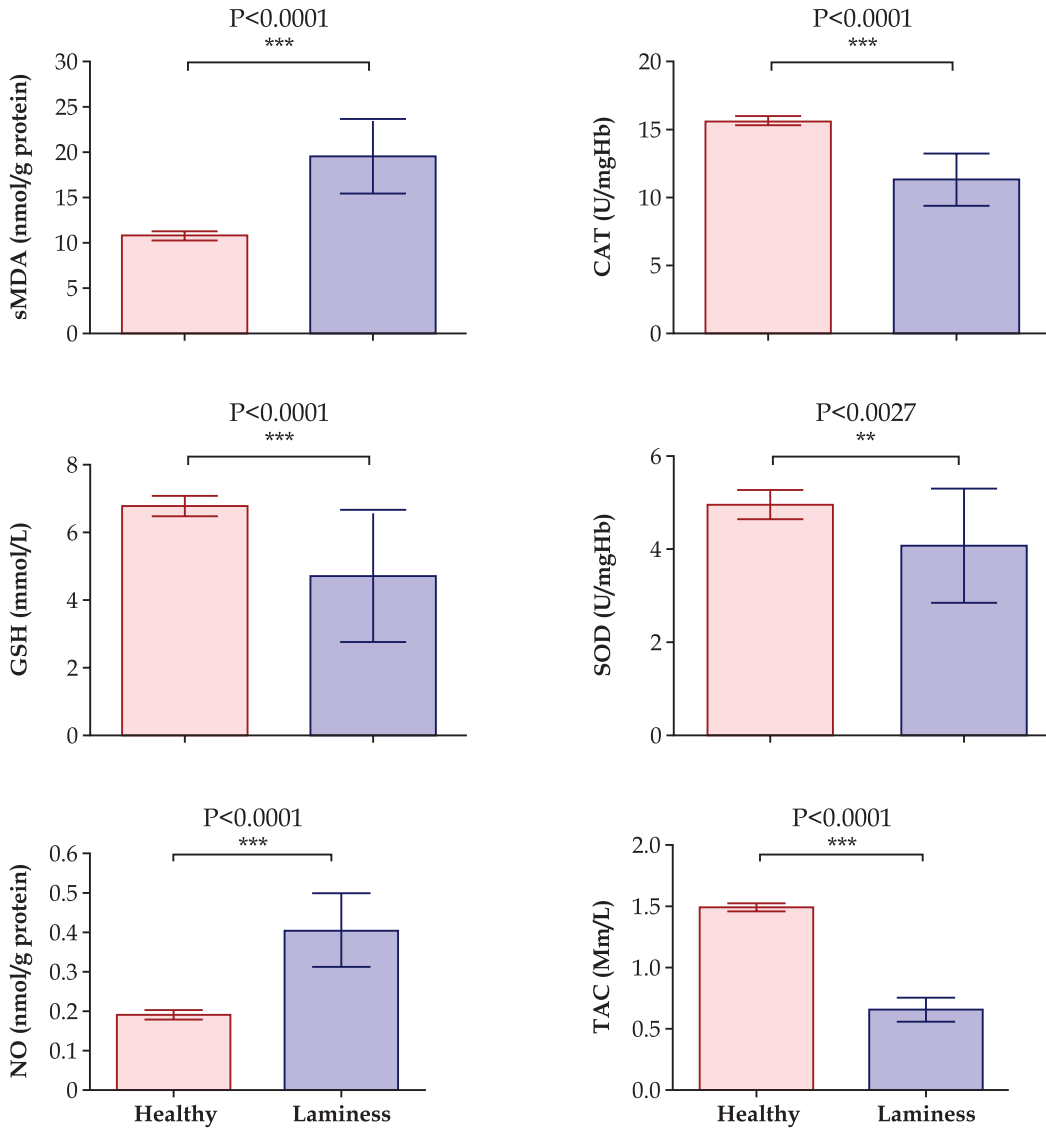

Fig 1. Box plots displaying variability of malondialdehyde (MDA); catalase (CAT), reduced glutathione (GSH); super oxide dismutase (SOD), nitric oxide (No) and total antioxidant capacity (TAC) in healthy and lame dromedary racing camels.

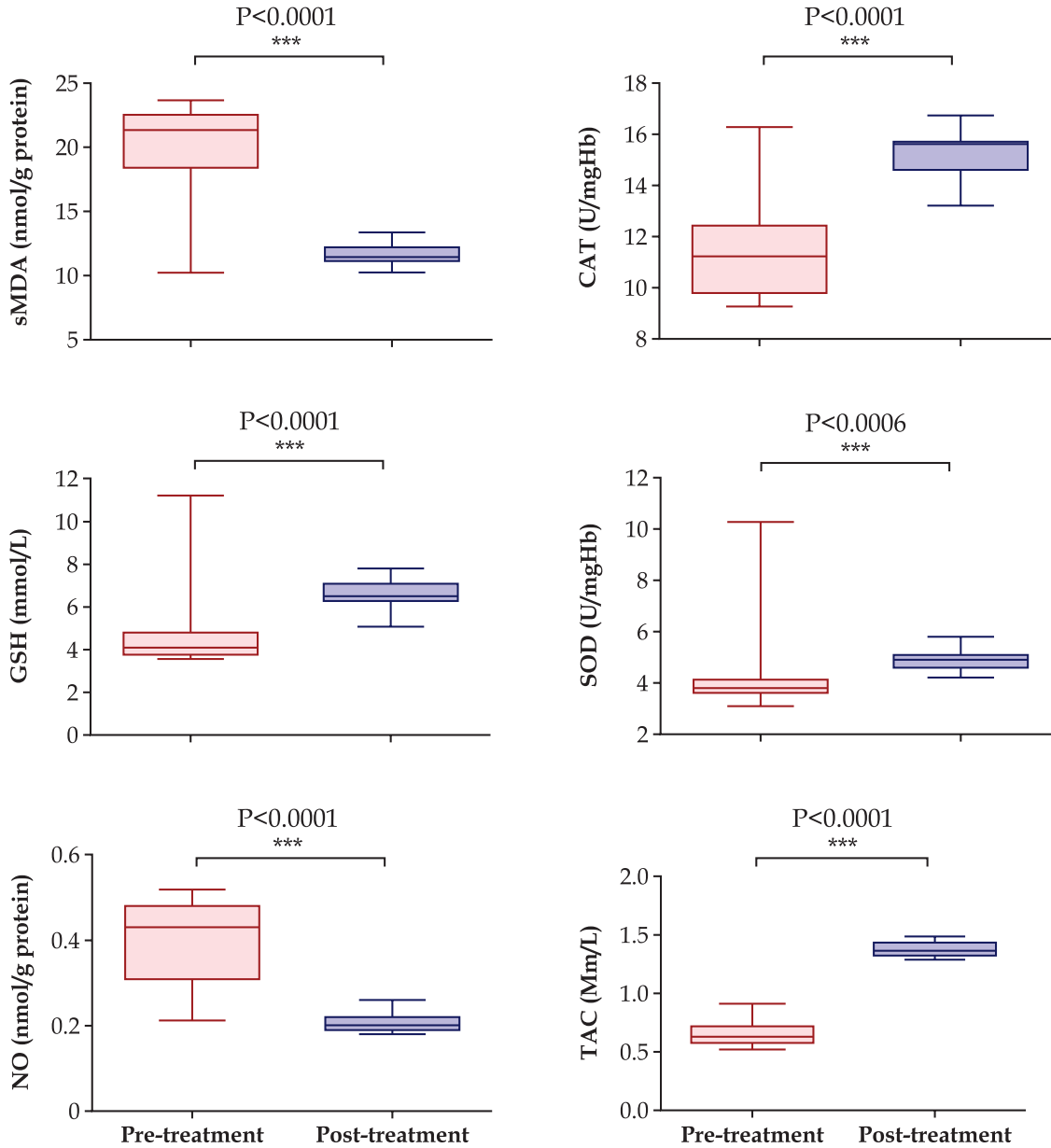

Fig 2. Box plots elucidating changeability of malondialdehyde (MDA); catalase (CAT), reduced glutathione (GSH); super oxide dismutase (SOD), nitric oxide (NO) and total antioxidant capacity (TAC) in lame dromedary racing camels before and after treatment.

Table 2. Diagnostic test characteristics of oxidative stress parameters in racing dromedary camels with clinical lameness.

Parameters	Threshold	AUC
sMDA (nmol /g protein)	≥ 13.48	0.910
CAT (U/mg Hb)	≤ 14.40	0.958
GSH (mmol /L)	≤ 6.05	0.901
SOD (U/mg Hb)	≤ 4.35	0.922
NO (nmol/g protein)	≥ 0.24	0.994
TAC (Mm/L)	≤ 1.15	1.00

Serum malondialdehyde (sMDA), catalase (CAT), reduced glutathione (GSH), super oxide dismutase (SOD).

Discussion

The clinical signs of lame camels in this study are in concurrence with the clinical picture of lame camels reported in other studies (Gahlot, 2007; Al-Juboori, 2011a and Al-Juboori, 2011b; Al-Juboori, 2013; Mostafa and Khalil, 2018; Mostafa, 2020).

There are several types of stress that athletes of all species encounter, including OS. According to the results presented in this study, circulating OS is generated by increased free radical generation (increased NO levels), lipid peroxidation enhancements (increased MDA levels), combined

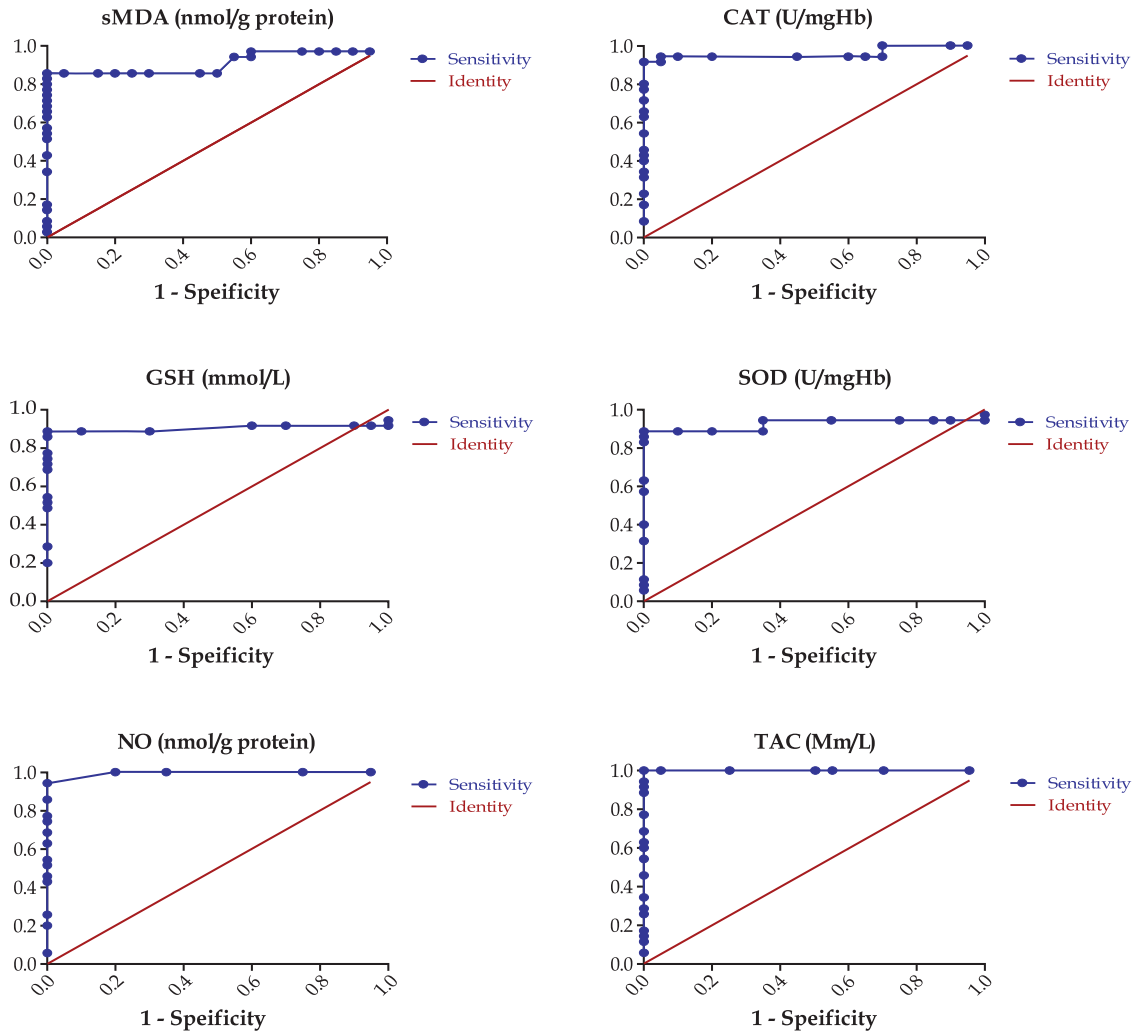

Fig 3. Receiver operating characteristic (ROC) curve analysis of malondialdehyde (MDA); catalase (CAT), reduced glutathione (GSH); super oxide dismutase (SOD), nitric oxide (NO) and total antioxidant capacity (TAC) in healthy and lame dromedary racing camels.

with abnormalities of antioxidant status (reduced GSH, SOD, CAT, and TAC) in racing dromedary camels clinically affected by lameness. As far as we know, this study is the first to describe OS status in lame dromedary racing camels. It is known that OS is involved in the pathogenesis of lameness in dairy cows (Al-Qudah and Ismail, 2012; Zhao *et al,* 2015).

In particular, polyunsaturated lipids are prone to oxidation. Biomarkers of lipid peroxidation are considered the best indicators of OS since lipids are one of the most vulnerable substrates to free radical damage (Georgieva, 2005).

During the radical-induced breakdown of polyunsaturated fatty acids, MDA forms. The reaction between MDA and thiobarbituric acid produces thiobarbituric acid reactive substances (TBARS), which facilitates the measurement of these substances by spectrophotometry (Janero, 1990). In this study, increased levels of serum MDA and NO in lame racing dromedary camels under the same environment, diet, training management, and feeding regimen proved that OS influences lameness in dromedary racing camels. In addition, significantly reduced levels of tested antioxidants (SOD, GSH, CAT, and TAC) markers were observed in lame racing dromedary camels, providing yet another support for the notion that oxidative damage may be involved in lameness pathogenesis.

OS is any disturbance in the normal redox state of cells that will cause veritably bad effects due to the yield of peroxides, and free radicals, leading to damage of all factors in the cell, including proteins, lipids, and DNA (Kowaltowski and Vercesi, 1999). Accordingly, OS can cause disturbances in normal mechanisms of the cellular capability to detoxify the reactive interceders or to repair the cell

damage (Kowaltowski and Vercesi, 1999). As proved previously and verified in this study, a complex association exists between OS and inflammation. Moreover, OS is a consequence of the imbalance between reactive oxygen species (ROS) and product and antioxidant capacity. This can be because of either heightened ROS generation detected, a disturbed antioxidant system, or a combination of both (as perceived in this study). In the presence of OS, uncontained ROS attacks modify and denature functional and structural molecules, leading to cell injury (Vaziri, 2008).

Comparable to our findings, it was reported that MDA levels were increased in varieties of inflammatory conditions in dromedary camels like acute, and chronic cystitis (Abd Ellah, *et al,* 2012; El-Deeb and Buczinski, 2015), liver abscess (El-Deeb *et al,* 2014), *Coxiella burnetii* infection (El-Deeb *et al,* 2019) and *Trypanosoma evansi* infection (Saleh *et al,* 2009; El-Deeb and Elmoslemany, 2015; El-Bahr and El-Deeb, 2016).

The NO levels in lame dromedary racing camels' cases compared to those in the control group, a statistically highly significant increase ($P<0.0001$) was observed. NO and peroxynitrite are free nitrogen derivatives among the reactive nitrogen species (RNS) (Tabakoglu and Durgut, 2013). Yarim *et al* (2006) described NO as a free radical that mediates both physiological and pathological events in the body. Despite its primary role in defending against bacteria, viruses, and parasites, NO has been reported to suppress the immune system. Accordingly, NO may protect or damage tissues depending on its concentration (Bozukluhan *et al,* 2013). In the presence of bacterial infections, macrophages produce large amounts of nitric oxide and exhibit antibacterial properties (Bozukluhan *et al,* 2016). A different viewpoint suggests that nitric oxide has anti-inflammatory property (Miranda *et al,* 2001). A major component of inflammatory diseases is peroxynitrite, a strong oxidising agent in tissues and organs. Sezer and Keskin (2014) described peroxynitrite as a highly toxic form of nitric oxide. According to a other research study, neutrophils released from diseased animals produce high levels of NO and myeloperoxidase, which ultimately leads to nitrotyrosine formation (i.e., protein damage) (Wessely-Szponder *et al,* 2004).

As detected in this study, increased NO production was also reported in humans with other inflammatory skin diseases and cutaneous infections (Serarslan *et al,* 2005; Bickers and Athar, 2006). In harmony with our findings, synovial fluid NO levels were significantly higher in 20 arthritic calves than in the control group (Yurdakul and Sartas, 2013). According to Yarim *et al* (2006) and Bozukluhan *et al* (2013) serum NO levels were higher in cattle with foot-and-mouth disease than in the control group, which was attributed to NO release and immune system stimulation.Conclusively, the increase in NO levels in this study suggests that it contributes actively to the development of racing dromedary camel lameness.

Since SOD catalyses the dismutation of superoxide to hydrogen peroxide (Halliwel *et al,* 1993), it is an important first line of defense against pro-oxidants. In this study, the levels of SOD, GSH, CAT, and TAC were significantly decreased in lame camels when compared with controls. Observed reductions in SOD, and CAT activities in the serum of lame racing camels in our study correlate with lower glutathione levels in the serum. The levels of tested antioxidants significantly increased toward normal values following the lameness treatment protocol. The present study provides evidence that levels of examined antioxidants can be used to evaluate the state of OS in lame camels, and to guide the treatment response.

Several methods have been developed to determine total antioxidant capacity (TAC) because it is difficult to measure each antioxidant component separately and their interaction within the plasma. The antioxidant capacity is based on the cumulative effect of all antioxidants present in plasma, and body fluids (Ghiselli *et al,* 2000). In this study, we detected that TAC is significantly decreased in lame dromedary camels and that it positively correlates significantly with all tested antioxidants, which gives a new and easy tool to evaluate the antioxidant status in lame camels, and to monitor treatment response.

The antioxidant state is the product of numerous distinct chemicals and systemic metabolic interactions interacting together (Ghiselli *et al,* 2000). TAC, as a single metric, provides useful information about the dynamic equilibrium between pro-oxidants and antioxidants in the plasma compartment (Ghiselli *et al,* 2000; Cao and Prior, 1998). Comparable to our results, TAC is an effective method for assessing stress in transported calves (Pregel *et al,* 2005). To conclude, evaluating TAC in camels may be a more precise and efficient indicator of camel lameness than measuring a single metric, which may reveal individual variances.

Present investigation has established a link between OS and lameness. Compared with our

results, OS biomarkers were similarly higher in sheep with hoof disorders (Talukder *et al,* 2015). Several inflammatory pathways are known to be activated by changes in the redox state of cattle (Sordillo and Aitken, 2009; Shi *et al,* 2015).

In present investigation it was revealed that the levels of MDA (AUC = 0.910) and antioxidant biomarkers (AUCs ranged from 0.901–1) were considered sensitive and specific biomarkers for differentiating lame camels from healthy ones and this might help monitoring the progress of treatment. This study found that lame camels have higher levels of MDA and NO biomarkers and lower serum levels of SOD, GSH, CAT, and TAC than healthy camels. The results of this study suggest that the measurement of MDA, NO, and antioxidant biomarkers in addition to physical examinations of camels with lameness may be a putative diagnostic and predictive tool for lameness in racing dromedary camels. Moreover, the addition of antioxidants to the treatment protocol may enhance the treatment progress in lame camels.

Acknowledgement

This work was supported through the Annual Funding track by the Deanship of Scientific Research, Vice Presidency for Graduate Studies and Scientific Research, King Faisal University, Saudi Arabia [Project No. AN000583].

References

Abd Ellah MR, Khamis F and Elnisr NA. Serum lipoproteins, antioxidants and urine biochemical constituents in camel cystitis. Comparative Clinical Pathology. 2012 21:515-519. DOI: 10.1007/s00580-010-1121-3

Al Juboori A. Lameness of camels in United Arab Emirates. Proceedings of the 16th Symposium and 8th Conference of Lameness in Ruminants, 28 February-3rd March, Rotorua, New Zealand. 2011a; pp 71.

Al Juboori A. Studies on common diseases of racing camels in UAE. Proceedings of the European Buiatrics Forum organised by the French Buiatrics Association, November 16-18, Marseille, France. 2011b; pp 171.

Al Juboori A, Naseer A, JiJi K. Management and healthcare of racing camels. XXVI World Buiatrics Congress 2010, Santiago, Chile, November 2010; 14-18, 521, pp 32.

Al-Ani FK. Camels: Management and Diseases. First Edition. Dar Ammar Book Publisher. 2004.

Al-Qudah KM, Ismail ZB. The relationship between serum biotin and oxidant/antioxidant activities in bovine lameness. Research in Veterinary Science. 2012; 92:138-141.

Argqelles S, Garcia S, Maldonado M, Machado A, Ayala A. Do the serum oxidative stress biomarkers provide a reasonable index of the general oxidative stress status? Biochimica et Biophysica Acta. 2004; 1674:251-259.

Bickers DR and Athar M. Oxidative Stress in the Pathogenesis of Skin Disease. Journal of Investigative Dermatology. 2006; 126:2565-2575. doi:10.1038/sj.jid.5700340

Bloomer RJ and Fisher–Wellman KH. Blood Oxidative Stress Biomarkers: Influence of Sex, Training Status, and Dietary Intake. Gender Medicine. 2008; 5:218-228.

Bozukluhan K, Atakisi E and Atakisi O. Nitric oxide levels, total antioxidant and oxidant capacity in cattle with foot-and-mouth-disease. The journal of the Faculty of Veterinary Medicine, University of Kafkas. 2013; 19(1): 179-181.

Bozukluhan K, Merhan O, Ogun M, Cihan M and Gokce G. Determination of the levels of some oxidative stress parameters in calves with omphalitis. Fırat Üniversitesi Sağlık Bilimleri Veteriner Dergisi. 2016; 30(2):79-81.

Cao G and Prior RL. Comparison of different analytical methods for assessing total antioxidant capacity of human serum. Clinical Chemistry. 1998; 44:1309-1315.

Dalle-Donne I, Rossi R, Giustarini D, Milzani A and Colombo R. Protein carbonyl groups as biomarkers of oxidative stress, Clinica Chimica Acta. 2003; 329:23-38.

E-Deeb WM, Fouda TA and El-Bahr SM. Clinicobiochemical investigations of partuberclosis of camels in Saudi Arabia: proinflammatory cytokines and oxidative stress markers. Pakistan Veterinary Journal. 2014; 34(4):484-488.

El-Bahr SM and El-Deeb WM. Acute phase proteins, oxidative stress markers in camels with *Trypanosoma evansi*. Parasitology. 2016; 143:518-522.

El-Deeb W and Buczinski S. The diagnostic and prognostic importance of oxidative stress biomarkers and acute phase proteins in urinary tract infection (UTI) in camels, PeerJ. 2015; 3:e1363.

El-Deeb W and Elmoslemany A. Cardiac and oxidative stress biomarkers in *Trypanosoma evansi* infected camels: diagnostic and prognostic prominence. Parasitology. 2015; 142(6):767-772.

El-Deeb W, Ghoneim I, Fayez M, Elsohaby I, Alhaidera A and El Gioushy M. Acute phase proteins, proinflammatory cytokines and oxidative stress biomarkers in sheep, goats and she-camels with *Coxiella burnetii* infection induced abortion. Comparative Immunology, Microbiology and Infectious Disease. 2019; 67:101352.

Finaud J, Lac G and Filaire E. Oxidative stress: Relationship with exercise and training. Sports Medicine. 2006; 36:327-358.

Gahlot TK and Chouhan DS. Camel Surgery. 1st Edn. Gyan Prakashan Mandir, Bikaner, India. 1992.

Gahlot TK. Lameness in camels. Proceedings of the International Camel Conference "Recent Trends in Camelids Research and Future Strategies for Saving Camels", Rajasthan, India. 2007; pp 158-165.

Gahlot TK. Selected Topics on Camelids. First Ed. 2000. pp 378.

Georgieva NV. Oxidative stress as a factor of disrupted

ecological oxidative balance in biological systems – a review. Bulgarian Journal of Veterinary Medicine. 2005; 8:1-11.

Ghiselli A, Serafini M, Natella F and Scaccini C. Total antioxidant capacity as a tool to assess redox status: critical view and experimental data. Free Radical Biology and Medicine. 2000; 29:1106-1114.

Habif S, Mutaf I, Turgan N, Onur E, Duman C, Özmen D and Bayindir O. Age and gender dependent alterations in the activities of glutathione related enzymes in healthy subjects. Clinical Biochemistry. 2001; 34:667-671.

Halliwell B and Gutteridge JMC. Free Radical in Biology and Medicine New York: Oxford University Press. 1999; 529-534.

Janero DR. Malondialdehyde and thiobarbituric acid-reactivity as diagnostic indices of lipid peroxidation and peroxidative tissue injury. Free Radical Biology and Medicine. 1990; 9:515-540.

Kowaltowski AJ and Vercesi AE. Mitochondrial damage induced by conditions of oxidative stress. Free Radical Biology and Medicine. 1999; 26(3-4):463-71. DOI: 10.1016/s0891-5849(98)00216-0

Manefield GW and Tinson AH. Camels- a compendium. University of Sydney Post Graduate Foundation in Veterinary Science, Australia. 1997.

Miranda KM, Espey MG and Wink DA. A rapid, simple spectrophotometric method for simultaneous detection of nitrate and nitrite. Nitric Oxide. 2001; 5(1):62-71.

Mostafa MB. Distal limb lameness in draught dromedary camels. Journal of Camel Practice and Research. 2020; 27(3):359-366.

Mostafa MB and Khalil AH. Linear and angular biometric measurements of limbs of camels (*Camelus dromedarius*). Journal of Camel Practice and Research. 2018; 25(2):153-162.

Mousa HM, Omer OH, Ali BH, Al-Wabel N, Ahmed SM. Antioxidant levels in tissues of young and adult camels (*Camelus dromedarius*). Journal of Physiology and Biochemistry. 2006; 62:213-218.

Possamai FP, Fortunato JJ, Feier G, Agostinho FR, Quevedo J, Wilhelm FD and Dal-Pizzol F. Oxidative stress after acute and sub-chronic malathion intoxication in Wistar rats. Environmental Toxicology ad Pharmacology. 2007; 23:198-204.

Pregel P, Bollo E, Cannizzo FT, Biolatti B, Contato E and Biolatti PG. Antioxidant capacity as a reliable marker of stress in dairy calves transported by road. Veterinary Record. 2005; 156:53-54.

Ramadan RO. Surgery and Radiology of the Dromedary Camel. Ist Edn. Al-Jawab Printing Press. Kingdom of Saudi Arabia. 1994; pp 68, 74, 210-213, 217, 246.

Saleh MA, Al-Salahy MB and Sanousi SA. Oxidative stress in blood of camels (*Camelus dromedarius*) naturally infected with *Trypanosoma evansi*. Veterinary Parasitology 2009; 162:192-199.

Serarslan G, Yilmaz HR and Söğüt S. Serum antioxidant activities, malondialdehyde and nitric oxide levels in human cutaneous leishmaniasis. Clinical and Experimental Dermatology. 2005; 30(3):267-71. DOI: 10.1111/j.1365-2230.2005.01758.x

Sezer K and Keskin M. Role of the free oxygen radicals on the pathogenesis of the diseases. Fırat Üniversitesi Sağlık Bilimleri Veteriner Dergisi. 2014; 28(1):149-156.

Shi X, D Li, Q Deng, Y Li, G Sun, X Yuan, Y Song, Z Wang, X Li, X Li and G Liu. NEFAs activate the oxidative stress mediated NF-kappaB signaling pathway to induce inflammatory response in calf hepatocytes. Journal of Steroid Biochemistry and Molecular Biology. 2015; 145:103–112. http://dx.doi.org/10.1016/j.jsbmb.2014.10.014.

Sordillo LM and Aitken SL. Impact of oxidative stress on the health and immune function of dairy cattle. Vet. Immunol. Immunopathol. 2009; 128:104-109. http://dx.doi.org/10.1016/j. vetimm.2008.10.305.

Tabakoglu E and Durgut R.Oxidatıve stress in veterinary medicine and effects in some important diseases. Adana Veteriner Kontrol Enstitüsü Müdürlüğü Dergisi. 2013; 3(1):69-75.

Talukder S, Gabai G and Celi P. The use of digital infrared thermography and measurement of oxidative stress biomarkers as tools to diagnose foot lesions in sheep. Small Ruminant Research. 2015; 127:80-85. http://dx.doi.org/10.1016/j.smallrumres.2015.04.006.

Vaziri ND. Causal link between oxidative stress, inflammation and hypertension. Iranian Journal of Kidney Diseases. 2008; 2(1):1-10.

Wessely-Szponder J, Bobowiec R, Martelli F, Wojcik M and Kosior-Korzecka U. Assessment of neutrophil components as markers of lung injury in the course of bovine respiratory tract infections. Polish Journal of Veterinary Sciences. 2004; 7:157-161.

Yarim GF, Nisbet C, Cenesiz S and Coskuner A. The investigation of the effect of foot and mouth disease on nitric oxide levels and adenosine deaminase activity in sheep. Veterinary Journal of Ankara University. 2006; 53(2):161-164.

Yurdakul G and Sarıtas ZK. Evaluation of clinic, radiographic and some biochemical blood serum and synovial fluid parameters of arthritis cases in calves. Kocatepe Veterinary Journal. 2013; 6(2):13-22.

Zhao XJ, Wang XY, Wang ZY, Wang L and Wang ZH. Oxidative stress and imbalance of mineral metabolism contribute to lameness in dairy cows. Biological Trace Element Research. 2015; 164:43-49. DOI 10.1007/s12011-014-0207-1

DOI : 10.5958/2277-8934.2022.00031.5 *Vol 29 No 2, p 223-228*

PATHOLOGICAL STUDY OF VARIOUS LIVER LESIONS PREVALENT IN CAMELS OF RAJASTHAN

Shesh Asopa[1], I. Vyas[2], H. Dadhich[2] and A. Joshi[3]

[1]Assistant Professor, [2]Professor, Department of Veterinary Pathology, College of Veterinary and Animal Science, RAJUVAS, Bikaner, India

[3]Veterinary Officer, Department of Animal Husbandry, Bikaner, Rajasthan

ABSTRACT

Tissue samples of liver (n=80) were examined from carcasses of camels of either sex, irrespective of age groups and breeds during post-mortem examination from July 2017 to June 2018. Out of these, 36 samples showed gross lesions were processed for subsequent histopathological examination. An overall incidence of liver lesions in camel recorded was and these 45 per cent (36 out of 80). Diverse pathological lesions in liver were abscess, cirrhosis, fatty changes, haemorrhages, haemosiderosis, hepatitis, hydatidosis, hydropic degeneration and necrosis showing occurrence as 2.50, 8.75, 5.00, 6.25, 1.25, 5.00, 5.00, 3.75 and 7.50 per cent, respectively. Cirrhosis (8.75 per cent) and haemosiderosis (1.25 per cent) were reported as the most prevalent and least prevalent pathological conditions, respectively, affecting liver of camels during the study period.

Key words: Camel, liver, lesions, pathology

The Camel is generally considered resistant animal and suffers only few diseases compared to other livestock species (Narnaware *et al,* 2021). Hepatocellular injury is one of the pathologic condition affecting domestic animals including camels (Belina *et al,* 2015). The causes of liver lesions in camel are numerous but primarily liver is affected by toxic substances, infectious diseases, parasitic hepatitis, tumours etc. which contribute to hepatobiliary disease, such as hepatic insufficiency (Kitila, 2016). Mehta *et al* (2012) reported maximum mortality (41.39%) in camel due to involvement of digestive system. Björklund (2014) and Tornquist *et al* (1991) reported hepatitis and hepatic lipidosis is common pathological findings in camelids. Tharwat *et al* (2012) performed ultrasound guided hepatic biopsy to diagnose liver pathology in camels.

Various types of pathological lesions found in liver of camel included hepatitis, cirrhosis (El-Mahdy *et al,* 2013; Thrwat, 2020), fibrosis (Hegazy *et al*, 2010) necrosis (Abu Damir *et al*, 1993), non specific hepatic degeneration and fibrosis (Hegazy *et al,* 2010), liver abscess (Aljameel *et al,* 2014) and haemosiderosis. Miscellaneous conditions like degenerative changes as fatty changes, hydropic degeneration and various circulatory disturbances as hyperaemia, oedema and haemorrhages are also common. The frequent pathological findings in various diseases of camel comprise of the involvement of liver. In many instances, such lesions in liver are of great value in diagnosis of camel diseases. The pathological conditions of liver in camel have not so far been studied extensively. Thus study was undertaken to find out gross and histopathology of various liver lesions of camels prevalent in Rajasthan.

Materials and Methods

For the present study, 80 tissue samples of liver were examined from carcasses of camels of either sex, irrespective of age groups and breeds during post-mortem examination from July 2017 to June 2018. Out of these, 36 samples of liver showed gross lesions these were further processed for histopathological examination. All the representative tissue samples were collected in 10% buffered formalin for histopathological examination. The tissues were processed mechanically for paraffin embedding by acetone and benzene technique (Lillie, 1965). The tissue sections of 4-5 microns or micrometer thickness were cut and stained with haematoxylin and eosin staining method as a routine. Van Gieson's special staining method was used for demonstration of collagen fibres (Culling, 1974). The detailed histopathological observations were recorded.

SEND REPRINT REQUEST TO SHESH ASOPA email: asopa.shesh27@gmail.com

Results and Discussion

Various liver lesions recorded in present study are placed in Table 1. An overall incidence of various pathological conditions affecting liver was recorded as 45 per cent (36 out of 80) which corresponded well with the findings of Hamza *et al* (2017) which was 45.7 per cent. Liver showed higher incidence of inflammatory conditions, degenerative changes, circulatory disturbances and parasitic infestation.

Table 1. Incidence of various liver lesions recorded in present study.

S. No.	Type of condition	No. of samples	Percentage
1.	Abscess	2	2.50
2.	Cirrhosis	7	8.75
3.	Fatty changes	4	5.00
4.	Haemorrhages	5	6.25
5.	Haemosiderosis	1	1.25
6.	Hepatitis	4	5.00
7.	Hydatidosis	4	5.00
8.	Hydropic degeneration	3	3.75
9.	Necrosis	6	7.50
	Total	**36**	**45.00**

Abscess

This condition was recorded in 2.50 per cent cases in present study. A higher incidence was reported by Aljameel *et al* (2014) as 13.5 per cent. Grossly, multiple small white foci containing whitish caseous pus along with congestion and haemorrhages were observed. Microscopically, focal area of necrosis enclosed by thick capsule along with polymorphonuclear leucocytic infiltration (Fig 1) was seen. These changes were in agreement with earlier findings of El-Mahdy *et al* (2013), Belina *et al* (2015) and Terab *et al* (2021).

This condition might be due to pyogenic bacterial infections or fascioliasis and secondary bacterial complication (Belina *et al,* 2015). Liver abscesses are found in CLA or pseudotuberculosis infection (Terab *et al,* 2021).

Cirrhosis

The occurrence of cirrhosis was 8.75 per cent in present study whereas Jamshidi and Zahedi (2014) found it as 10 per cent.

Grossly, affected liver was reduced in size and was firm and difficult to cut. Microscopically, presence of chronic fibrosed inflammation confined to the areas extending only a short distance beneath the capsule (Fig 2), presence of fibrous bands running in between parenchyma along with little lymphocytic infiltration and perivascular fibrosis mainly in portal area was observed. These findings were in close approximation to the observations reported by Singh (1998) and Ibrahim *et al* (2021).

Cirrhosis was frequently noticed concomitant with parasitic condition, however, in many cases contributory factors could not be incriminated. Ibrahim *et al* (2021) reported severe fibrosis in hepatic torsion in camels.

Fatty Changes

This condition was recorded in 5.00 per cent cases. A higher incidence was (20%) observed by El-Mahdy *et al* (2013). Grossly, liver appeared pale, soft and greasy with rounded edges. Histopathologically, the hepatic cells showed fatty changes with presence of fat droplets as clear round spaces and granular cytoplasm (Fig 3) were in agreement with earlier findings of Singh *et al* (2006) and Zakian *et al* (2016).

Ketosis may be one of the possible causes of fatty changes. Other factors involved copper sulphate poisoning (Damir *et al,* 1993) or PPR infection (Zakian *et al,* 2016) or Brucellosis (Abdirahman, 2020).

Haemorrhages

This condition was recorded in 6.25 per cent cases. A lower incidence (2.91%) was reported by Singh (1998). Grossly, large and irregular superficial areas and pin-point haemorrhagic areas of variable sizes were seen on liver. Microscopically, severe haemorrhages replaced the hepatic parenchyma along with congestion, necrosis and presence of inflammatory infiltration in adjacent parenchyma were in agreement with observations of Singh (1998) and Ibrahim *et al* (2021).

This condition might be due to trauma or Aflatoxin B1 residues (Al-Gabri, 2013) or hepatic torsion (Ibrahim *et al,* 2021).

Haemosiderosis

This condition was recorded in 1.25 per cent cases which corresponded well with the findings of Singh (1998) who found it 1.45 per cent. Grossly, the liver showed brownish tinge due to the presence of haemosiderin in hepatic cells. Microscopically, haemosiderin as golden coloured pigment filled in phagocytes (Fig 4) was in agreement with Singh (1998) and Ibrahim *et al* (2021).

This condition might be observed in scars, in areas where haemorrhages had occurred or in chronic

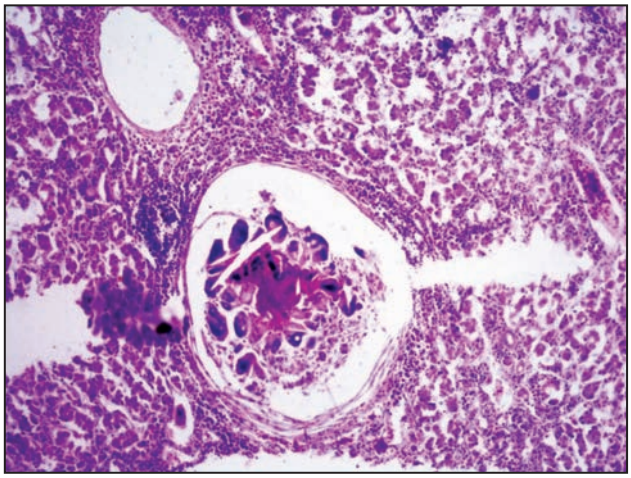

Fig 1. Microphotograph of liver abscess showing focal area of necrosis enclosed by thick capsule along with polymorphonuclear leucocytic infiltration. H&E 100X.

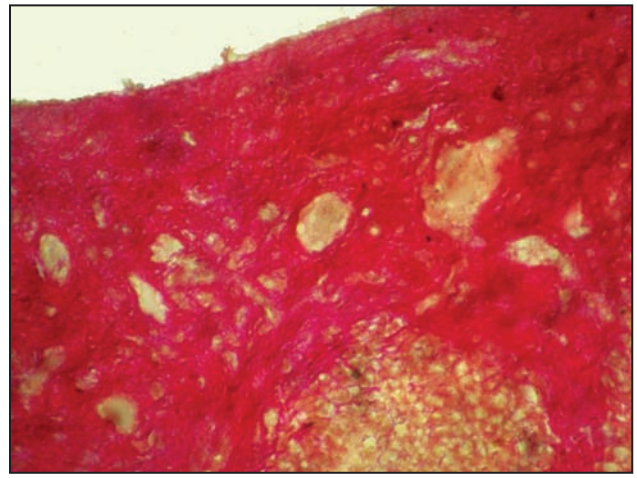

Fig 2. Microphotograph of liver showing red coloured fibrous tissue along with thickened glisson's capsule. Van Gieson's 100X.

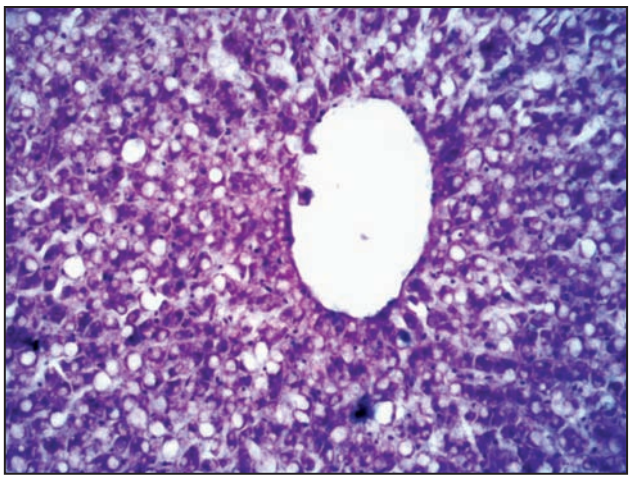

Fig 3. Microphotograph of liver showing fatty changes indicating fat droplets as clear round spaces. H&E 200X.

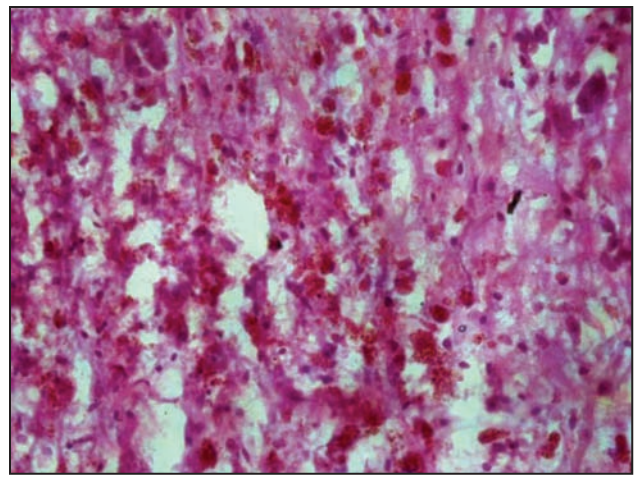

Fig 4. Microphotograph of liver showing haemosiderin as golden coloured pigment filled in phagocytes. H&E 400X.

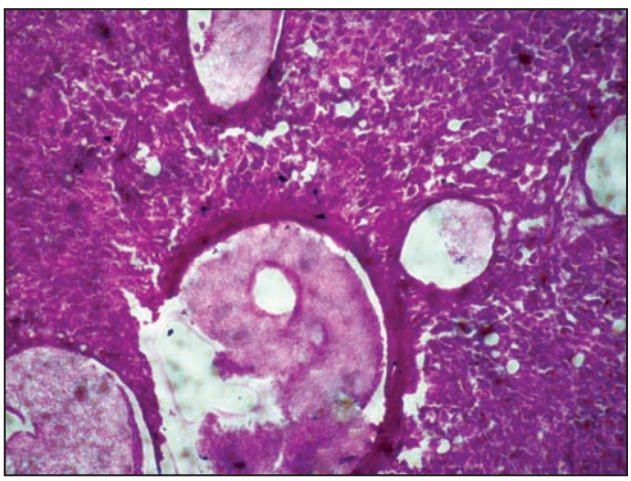

Fig 5. Microphotograph of liver showing multiple cysts with eosinophilic lamellated wall and presence of faint pink homogenous substance along with hepatocellular degeneration. H&E 100X.

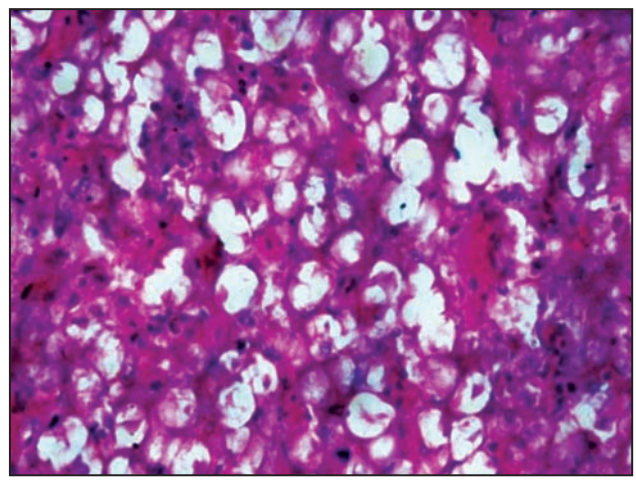

Fig 6. Microphotograph of liver showing hydropic degeneration as small clear vacuoles along with cellular infiltration. H&E 200X.

passive hyperaemia (Runnels *et al,* 1976). Ibrahim *et al* (2021) reported this condition in hepatic torsion in camel.

Hepatitis

This condition was recorded in 5.00 per cent cases. A higher incidence (20%) was reported by El-Mahdy *et al* (2013). Grossly, the liver was markedly enlarged and centres of lobules were opaque, grayish or yellowish. Microscopically, infiltration of lymphocytes and few neutrophils along with areas of hepatocellular degeneration was seen. These changes were in agreement with earlier findings of Seboussi *et al* (2009), El-Mahdy *et al* (2013) and Tavella *et al* (2018).

The inflammation of liver might be caused by various conditions including toxicity of diminazene aceturate (Homeida *et al,* 1981) or selenium toxicity (Seboussi *et al,* 2009).

Hydatidosis

This condition was recorded in 5.00 per cent cases. Almost similar findings were reported by Mirzaei *et al* (2016) as 4.54 per cent. Grossly, grayish white detectable hydatid cysts of variable sizes were located either single or multiple on the surface and embedded in the hepatic parenchyma which was in agreement with earlier report of Osman (2008). Microscopically, cyst wall appeared as outer eosinophilic lamellated layer with presence of faint pink homogenous substance within the lumen (Fig 5) was in harmony with those mentioned by Tantawy (1992) and Borai *et al* (2013).

Hydatidosis in liver might be due to the fact that liver possesses great capillaries site encountered by the parasite, which adopt the portal vein route and primarily hepatic filtering system sequentially (Kebede *et al,* 2009). Nourani and Salimi (2013) reported hydatid cyst as the most common hepatic lesion in liver of camels.

Hydropic degeneration

This condition was recorded in 3.75 per cent cases. A higher incidence (18.67%) was recorded by El-Mahdy *et al* (2013). Microscopically, the liver cells increased in size due to accumulation of fluid. Small clear vacuoles seen within the cytoplasm along with hepatocellular degeneration and cellular infiltration (Fig 6) which were in agreement with Singh *et al* (2006), El-Mahdy *et al* (2013) and Tavella *et al* (2018).

This condition might occur due to pathogenic infections such as Hepatitis E virus 8 infection (Wang *et al*, 2018) or toxic conditions such as closantel toxicity (Raval *et al,* 2018).

Necrosis

This condition was recorded in 7.50 per cent cases and a higher incidence (18.1%) was reported by Salem and Azza (2011). The gross findings were presence of grayish necrotic foci on surface. The involved hepatocytes showed dense, granular and opaque cytoplasm with coagulative necrosis. Similar findings were reported by Borai *et al* (2013) and Zakian *et al* (2016).

This presumably may be due to involvement of some toxins in feed possibility fungal, bacterial or plant toxins or chemicals playing some role in causing the condition.

Groom *et al* (1995) reported hepatic-necrosis in an alpaca which was associated with halothane anaesthesia possibly due to hepatotoxic effect of halothane on liver.

In present study the tumours of liver were not seen. However, intrahepatic cholangiocarcinoma in an 18-year-old male camel has been reported and it was composed of gland-like structures and/or solitary islands of neoplastic cells in the tumoural stroma (Birincioglu *et al,* 2008).

Most of the pathological conditions of liver in camels are diagnosed during postmortem examination. However, a more detailed study of liver lesions is required to identify these pathological conditions during clinical examination through modern diagnostic tools.

References

Abdirahman DB. Camel Brucellosis: Sero-prevalence and Pathological Lesions at Slaughterhouses in Garissa County, Kenya. Doctoral dissertation, University of Nairobi, Kenya. 2020.

Abu Damir H, Eldirdiri NI, Adam SEI, Howarth JA, Salih YM and Idris OF. Experimental copper poisoning in the camel (*Camelus dromedarius*). 1993; Journal of Comparative Pathology 108(2):191-208. https://doi.org/10.1016/S0021-9975(08)80221-6.

Al-Gabri NA. Pathological Studies on the effect of aflatoxins in camel liver. Masters Thesis (MVSc), Thamar University, Yemen. 2013.

Aljameel MA, Halima MO, El Tigani-Asil AE, Abdalla SA and Abdellatif MM. Liver abscesses in dromedary camels: Pathological characteristics and aerobic bacterial aetiology. Open Veterinary Journal. 2014; 4(2):118-123.

Belina D, Giro B, Ashenafi H, Demissie T and Muktar Y. Review on camel liver pathology and its major diagnostic approaches. Global Journal of Veterinary Medicine and Research. 2015; 3(1):068-079.

Birincioglu S, Avci H and Aydogan A. Seminoma and cholangio carcinoma in 18-year-old male camel. Journal of Veterinary and Animal Sciences. 2008; 32(2):141-44.

Björklund C. Book on diseases and causes of death among camelids in Sweden - A retrospective study of necropsy cases 2001-2013. ISSN: 1652-8697. Swedish University of Agricultural Sciences. 2014.

Borai MG, Nagi ARA, Gab-Allah MS, El-Mashad ABI and Mustafa SA. Comparative pathological studies on bacterial affections of liver in Farm Animals. Doctoral Dissertation, Benha University, Egypt. 2013.

Culling CFA. Histopathological and histochemical techniques. Butterworths, London, Bosten. 1974.

Damir HA, Eldirdiri NI, Adam SEI, Howarth JA, Salih YM and Idris OF. Experimental copper poisoning in the camel (*Camelus dromedarius*). Journal of Comparative Pathology. 1993; 108(2):191-208. doi= {10.1016/ S0021-9975(08)80221-6}

El-Mahdy MM, Bakeer AM and Wazzan AAA. Pathological Studies on Liver affections in Saudi Arabia camels. Egyptian Journal of Comparative Pathology and Clinical Pathology. 2013; 26(1):85-108.

Groom S, Checkley S and Crawford B. Hepatic-necrosis associated with halothane anaesthesia in an alpaca. Canadian Veterinary Journal. 1995; 36(1):39-41.

Hamza II, Shuaib YA, Suliman SE, Abdalla MA. Aerobic bacteria isolated from internal lesions of camels at Tambool slaughter house. Journal of Advanced Veterinary and Animal Research. 2017; 4(1):22-31. doi= {10.5455/javar.2017.d185}

Hegazy AA, Altabari G, Gameel AA, Hussein YA and Hatem ME. Non specific hepatic degeneration and fibrosis in camels (*Camelus dromedarius*). 2010; Mansoura Veterinary Medical Journal. XII, 25-35.

Homeida AM, El Amin EA, Adam SEI and Mahmoud MM. Toxicity of diminazene aceturate (Berenil) to camels. Journal of Comparative Pathology. 1981; 91(3):355-360. doi= {10.1016/0021-9975(81)90005-0}

Ibrahim A, El-Ghareeb WR, Aljazzar A, Al-Hizab FA and Porter BF. Hepatic lobe torsion in 3 dromedary camels. Journal of Veterinary Diagnostic Investigation. 2021; 33(1):136-139. doi={10.1177/ 1040638720971813}

Jamshidi K and Zahedi A. An abbattoir-based study on relative prevalence of histopathologic patterns of hepatic lesions in one-humped camels (*Camelus dromedarius*), Semnan, Iran. Camel: An International Journal of Veterinary Sciences. 2014; 2(2):1-10. doi={10.5958/2321-709X.2014.00001.3}

Kebede M, Mitiku A and Tilahun G. Hydatidosis of slaughtered animals in Bahir Dar Abattoir, North-western Ethiopia. Tropical Animal Health and Production. 2009; 41:43-50.

Kitila Dinaol. Review on camel liver pathology and Its major diagnostic approaches. 2016; 10.13140/RG.2.1.4379.8646.

Lillie RD. Histopathological Technique and Practical Histochemistry. Mc Graw Hill Book Company. New York and London. 1965.

Mehta SC, Bissa UK, Chirania BL and Patil NV. Mortality analysis and herd growth in Indian dromedary breeds. Journal of Camel Practice and Research. 2012; 19(1):37-44.

Mirzaei M, Rezaei H, Nematollahi A and Ashrafihelan J. Survey of hydatidosis infection in slaughtered camel (*Camelus dromedarius*) in Tabriz area, Northwest Iran. Journal of Parasitic Diseases. 2016; 40(2):444–447.

Narnaware SD, Ranjan R, Dahiya SS, Panchbuddhe A, Bajpai D, Tuteja FC and Sawal RK. Pathological and molecular investigations of systemic form of camelpox in naturally infected adult male dromedary camels in India. Heliyon. 2021; 7(2):e06186. doi= {10.1016/j.heliyon.2021.e06186}

Nourani H and Salimi M. Pathological study on liver of dromedary camels. Journal of Camel Practice and Research. 2013; 20(1):97-100.

Osman AMA. Pathological and Biomolecular Study on Hydatid Disease in Camels, Cattle and Sheep. Masters Thesis (MVSc), University of Khartoum, Sudan. 2008.

Raval SH, Parmar RS, Chhatpar KD, Patel JG, Patel BJ and Joshi DV. Accidental closantel toxicosis in camels. Indian Journal of Veterinary Pathology. 2018; 42(1):15-18. doi= {10.5958/0973-970X.2018.00003.2}

Runnels RA, William SM and Andrew WM. Principles of Veterinary Pathology. 7th edn. Scientific Book Agency, Calcutta. 1976.

Salem SI and Azza HM. Clinicopathological, cytological and histopathological studies on liver and kidney affections in camels. Global Veterinaria. 2011; 7:557–571.

Seboussi R, Faye B, Alhadrami G, Askar M, Bengoumi M and Elkhouly A. Chronic selenosis in camels. Journal of Camel Practice and Research. 2009; 16(1):1-14.

Singh T (1998). Incidence and classification of liver lesions in camel (*Camelus dromedarius*). Masters Thesis (MVSc), Rajasthan Agricultural University, Bikaner, Rajasthan, India. 1998.

Singh T, Sharma GD, Singh AP, Dadhich R and Surender S. Incidence and pathology of degenerative changes in liver of camels. Veterinary Practitioner. 2006; 7(1):35-36.

Tantawy AA (1992). Clinicopathological and histopathological studies on relation between pancreatic lesion and affection in liver of camel. Masters Thesis (MVSc), Zagazig University, Benha, Egypt. 1992.

Tavella A, Bettini A, Cocchi M, Idrizi I, Colorio S, Viel L, Zanardello C and Zanolari P. Isolation of *Streptococcus agalactiae* in a female llama (*Lama glama*) in South Tyrol (Italy). BMC Veterinary Research. 2018; 14(1):343.

Terab AMA, Abdel Wahab GED, Ishag HZA, Khalil NAH, El Tigani-Asil ETA, Hashem FM, Khalafalla AI, Shah AAM and Al Muhairi SSM. Pathology, bacteriology and molecular studies on caseous lymphadenitis in *Camelus dromedarius* in the Emirate of Abu Dhabi, UAE, 2015-2020. Plos one. 2021; 16(6):e0252893. doi= {10.1371/journal.pone.0252893}

Tharwat M. Ultrasonography of the liver in healthy and diseased camels (*Camelus dromedarius*). Journal of Veterinary Medical Science. 2020; 82(4):399-407. doi={10.1292/jvms.19-0690}

Tharwat M, Al-Sobayil F and Buczinski S. Ultrasound-guided hepatic and renal biopsy in camels (*Camelus dromedarius*): technique development and assessment of the safety. Small Ruminant Research. 2012; 103(2-3):211-219. doi= {10.1016/ j.smallrumres.2011.09.006}

Tornquist SJ, Van Saun RJ, Smith BB, Cebra CK, Snyder SP. Hepatic lipdidosis in llama and alpacas: 31 cases. Journal of the American Veterinary Medical Association. 1991; 214(9):1368-72.

Wang L, Zhuang H and Wang L. Prevalence, pathogenesis and cross-species transmission of a novel hepatitis E virus from bactrian camels. Journal of Hepatology. 2018; 68:784-785.

Zakian A, Nouri M, Kahroba H, Mohammadian B and Mokhber-Dezfouli MR. The first report of peste des petits ruminants (PPR) in camels (*Camelus dromedarius*) in Iran. Tropical Animal Health and Production. 2016; 48(6):1215-1219.

DOI : 10.5958/2277-8934.2022.00032.7 Vol 29 No 2, p 229-235

EPIDEMIOLOGICAL INVESTIGATION ON GENITAL MYIASIS OF BACTRIAN CAMELS IN PARTS OF INNER MONGOLIA, CHINA

Jin Liu, Bin Hou, Jiya Wuen, Nan Jiang, Tian Gao and Surong Hasi[1]

College of Veterinary Medicine, Inner Mongolia Agricultural University; Key Laboratory of Clinical Diagnosis and Treatment Technology in Animal Disease, Ministry of Agriculture and Rural Affairs, Hohhot, Inner Mongolia 010018, China

[1]Inner Mongolia Institute of Camel Research, Badain Jaran 737300, China

ABSTRACT

The incidence and prevalence of Bactrian camel genital myiasis seriously endanger the health of camels and hinder the healthy development of Bactrian camel industry. In order to further understand the epidemic situation of the disease in main production areas of Bactrian camels in Inner Mongolia, China, from May to October 2021, 3 areas with severe incidences in Alxa Left Banner, Urad North Banner and Durbed Banner were selected for epidemiological investigation. Total of 2038 female camels in 21 camel herds were investigated. The results showed that the overall prevalence rate was 26.6%, the highest incidence group reached 82.6%, while the lowest group was only 1.4%. The prevalence rates of Bactrian camel genital myiasis in Alxa Left Banner, Urad North Banner and Durbed Banner was 28.0%, 23.8% and 23.7%, respectively. The pathogen of Bactrian camel genital myiasis is *Wohlfahrtia magnifica*, and the highest prevalence often occurs in July to August in each year. The prevalence rate in female camels under 5 year-old was lower than that of in adult camels, and it was highest in female camels between 5-15 years old and give birth 2-4 times and no deaths were found. The prevalence rate in free-range female camels was higher than that in half-house-raised camels, and the morbidity was lowest in fully-housed female camels. Camels grazing on pastures near the lakes and riverbanks had higher morbidity than that of in camels grazing on other pastures. Therefore, the morbidity of genital myiasis in Bactrian camels is significantly affected by age, number of deliveries, feeding method, different regions and pasture types.

Key words: Bactrian camel, epidemiology, genital myiasis

Genital myiasis in Bactrian camels is caused by larva of *Wohlfahrtia magnifica* in the external reproductive organs of female camels. *Wohlfahrtia magnifica* (Diptera: Sarcophagidae) is mainly found in Southeastern Europe, southern Russia, Asia, the Middle East and northern Africa (Pirali Kheirabadi *et al,* 2014). *W. magnifica* infests a wide range of animals, infects their genital tract and other open wounds. Six flocks of sheep infested with genital myiasis have been reported in China, and the identified pathogens were all *W. magnifica* (Li *et al,* 2019). Three cases of genital myiasis in a goat, a ram and a dog have been reported in Italy (Gaglio *et al,* 2011). In Fars province of Iran, 61% of all animal wound myiasis were caused by larvae of *W. magnifica* (Rafinejad *et al,* 2014). A case of gingival myiasis was reported in Xinjiang, China, and the pathogen was identified as *W. magnifica* (Zhang, 2005).

The present study investigated the prevalence of Bactrian vaginal myiasis in some areas of Inner Mongolia, China.

Materials and Methods

Survey area

The grassland types in Alxa Left Banner, Urad North Banner and Durbed Banner are mainly desert and semi-desert steppe, with scarce water resources and sparse vegetation. The present investigations was carried out in above 3 comparable regions with similar landscape and different soil conditions and water sources.

Epidemiological survey

According to the life cycle of flies, comprehensive investigation was carried out by visiting farmers, distributing standardised questionnaires and electronic questionnaires on May to October in 2021. The content of the questionnaires include the basic information of the herdsman, the number and age of infected she-camels, and the rearing environment. All survey data was summarised and statistically analysed.

SEND REPRINT REQUEST TO SURONG HASI email: surong@imau.edu.cn, baohaas@163.com

Symptom assessment

All of the investigated camel herds were clinically examined visually, then the infected camels were subsequently restrained using ropes one by one and careful inspection was carried out to the swelling and damage of vulva, surrounding blood stains and presence of larvae in the wound and their number.

Sample collection

Five infected camels were randomly selected from each of 3 regions. Ten larvae at different stages were collected from each camel, and put them into formalin, respectively. Then, 10 third-stage larvae were collected from each of the 5 infected camel, and put them into a foam box with a length of 20 cm and a width of 10 cm that has been pre-installed with local sand, and spray a small amount of water on the surface of the sand to make the surface sand slightly wet. Finally, the box was covered with gauze, took them back to the laboratory, and cultivated it at room temperature (about 26°C), until the larvae emerged into flies.

Morphological observation

Stereo Discovery.V20 microscope was used to observe the morphology of the 1st, 2nd and 3rd stage larvae (Fig 2) and the artificially hatched adult flies from 3 different regions.

Results

Morphological observation of larva

Clinical examination showed that the larva of 3 developmental stages existed at the wound site of most infected camels. The length of 1st instar larvae was 1-3 mm, 2nd instar larvae was 3-12 mm, and 3rd instar larva was 12-20 mm (Fig 1).

The larvae had 1 pseudoscolex, 3 thoracic segments, 8-10 abdominal segments, anus and other structures. The 9th and 10th abdominal segment were located on the ventral surface of the 8th abdominal segment, which was usually not obvious, and the 10th segment was the anal plate. The pseudoscolex had a pair of downwardly curved and sharp mouth hooks, and there was a long labrum between the two mouth hooks of the first stage larvae, but the labrum of the second stage larvae has disappeared. This was consistent with the observations of An *et al* (2019). Ring spines were covered on the dorsal and ventral sides of the larvae at each stage, and the number of spines were decreased significantly from the 7th abdominal segment. A deep cup-shaped depression was observed on the posterior surface of the 8th abdominal segment with several pairs of conical fleshy processes at the edge of the depression.

Morphological observation of adult flies

The 3rd instars were successfully eclosioned after 15-20 days in laboratory, and their morphological characteristics were observed by Stereo Discovery.V20 stereomicroscope (Fig 3).

The adult fly was 9-13 mm in length, with naked compound eyes and dense silvery powder on parafrontalia, parafacialia and posterior eyes. When viewed from the top of the head, the width of the frons was about half that of the head, and when viewed from the side, the height of the bucca was about half that of the eye. Occiput expanded backwardly. Antennae were slightly shorter, the length of the third section was about 1.5 times that of the second section, and there were arista at the base of the third section. Thoracic segment had black background and grey powder, 3 black vertical stripes on the tergite. Lower squama was about 2 times of the upper squama. The abdomen was long and oval, with distinct black patches, and spots like water drop. The central black patches on the 3rd and 4th tergites were large and were connected to the 1st and 2nd syntergite forward, and the 5th tergite had smaller black patch. According to the characteristics of the adult fly, and its larvae were obligate parasitic warm-blooded vertebrates (Fan, 1994). The adult flies were identified as *W. magnifica*. The pathogen of genital myiasis of Bactrian camels in these 3 areas was *W. magnifica*.

Clinical manifestation

According to the local lesions of affected camels, these were grouped into lightly, moderately and heavily infected camels (Fig 4). In lightly affected camels, the vulva was slightly swollen, a small amount of blood stains could be seen in the tail and hind legs, lesions caused by larvae can be seen at or near the inner margin of the vulva mucosa, with a diameter between 1-3 cm, and no secondary infection was seen. Usually less than 100 larvae were counted per camel, and no repeated infection appeared after application of pesticide.

In moderately infected camels, the vulva was significantly swollen, accompanied by bloody and fibrinous excretion, lesions and septic wounds can be seen at the vulva, with a diameter between 3-8 cm. There were 100-200 larvae in perineal area and vaginal tissue. The camels had pain response, continuous rubbing of wound area, and partial anorexia. A small number of camels had recurrence of infection after treatment with pesticide.

First instar Second instar Third instar

Fig 1. The body length of larvae at each stage.

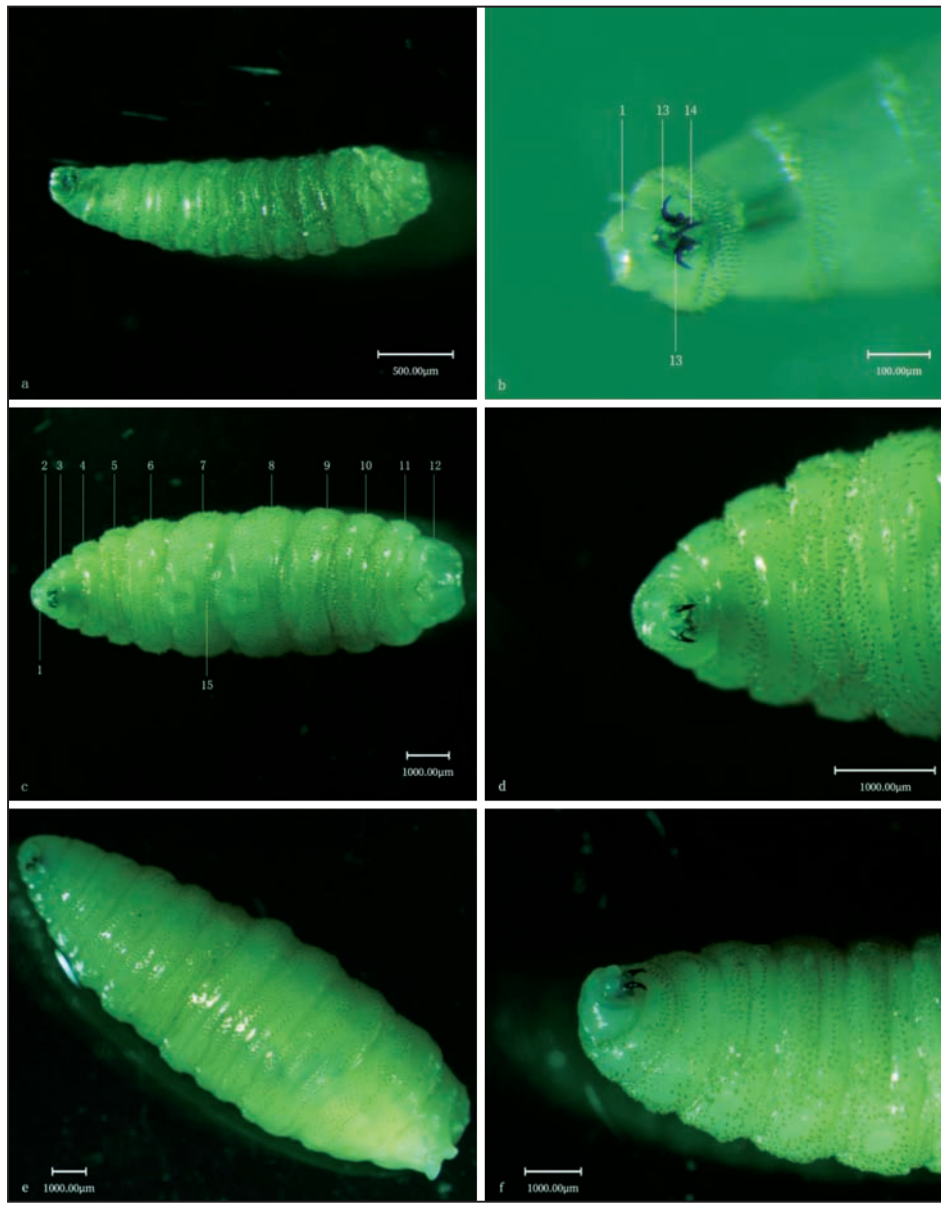

Fig 2. The larvae of each stage were observed under stereoscope.

(a) First instar, (b) Head of first instar, (c) Second instar, (d) Head of second instar, (e) Third instar, (f) Head of third instar. 1 is pseudoscolex, 2-4 is thoracic segment (usually 3 segments), 5-12 is abdominal segment (usually 8~10 segments), 13 is mouth hooks, 14 is Labrum, and 15 is Spine.

In heavily infected camels, the vulva was severely swollen, accompanied by bloody and purulent excretion, severe lesions and septic wounds were seen at the vulva, with a diameter greater than 8 cm. Usually, more than 200 larvae were found in multiple larger wounds. The genital area appeared strongly deformed and swollen. All infected camels showed obvious restlessness, loss of appetite, malnutrition, prolonged disease course, and repeated infection after treatment. Among infected camels, about 30% were lightly infected and rest of them were moderately or heavily infected camels, and most of heavily infected camels remained infected whole year.

Epidemiological Statistics

Total of 2038 she-camels were investigated in 21 camel herds, with a minimum of 23 camels, a maximum of 300 camels per herd examined. Among

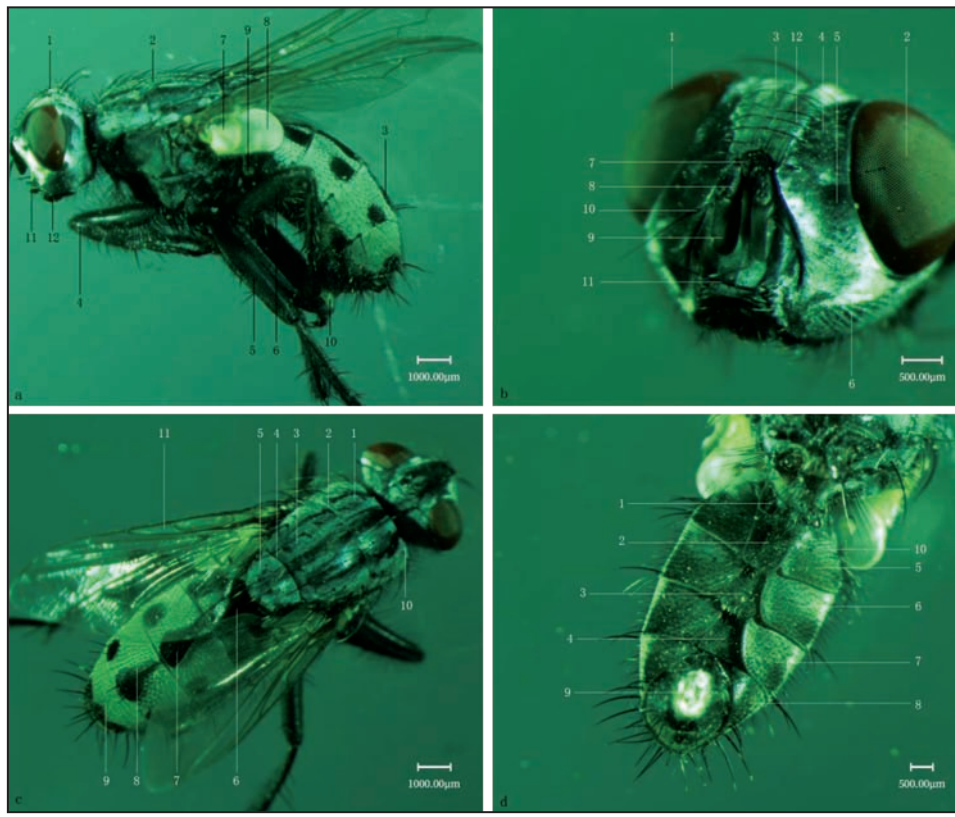

Fig 3. Stereoscopic observation of artificially eclosioned fly **(a)** Side view, **(b)** Head, **(c)** Dorsal view, **(d)** Ventral view of the abdomen. **(a):** 1. Head, 2. Thoracic, 3. Abdomen, 4. Front legs, 5. Middle legs, 6. Hind legs, 7. Upper squama, 8. Lower squama, 9. Halter, 10. Terminalia, 11. Palpi, 12. Proboscis. **(b):** 1. Compound eyes, 2. Ommatidia, 3. Interfrontalia, 4. Parafrontalia, 5. Parafacialia, 6. Bucca, 7. The first section of the antenna, 8. The second section of the antenna, 9. The third section of the antenna, 10. Arista, 11. Vibrissae, 12. Inter-frontal bristles. **(c):** 1. Mesothorax prescutum, 2. Scutal sulcus, 3. Mesothorax postscutum, 4. Scutellar suture, 5. Scutellum, 6. 1st and 2nd abdominal segment, 7. 3rd abdominal segment, 8. 4th abdominal segment, 9. 5th abdominal segment, 10. Humeral callus, 11. Wing. **(d):** 1. 1st sternite, 2. 2nd sternite, 3. 3rd sternite, 4. 4th sternite, 5. 1st and 2nd abdominal segment, 6. 3rd abdominal segment, 7. 4th abdominal segment, 8. 5th abdominal segment, 9. Anus, 10. Spiracles.

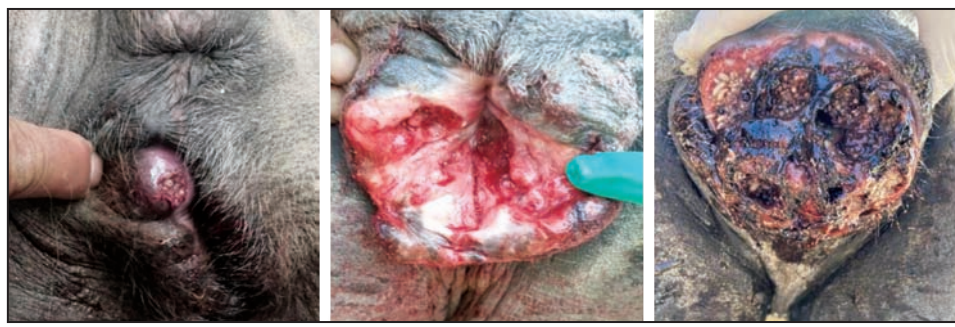

Light Moderate Severe

Fig 4. Clinical manifestations of lesions with different degrees of infection

them, a total of 491 camels were infected, and the prevalence rate found was 26.6% (Table 1). No deaths occurred. A total of 1151 she-camels from 14 camel herds were investigated in Alxa Left Banner, and 280 were infected, with a prevalence rate of 28.0%. A total of 747 she-camels were investigated from 4 camel herds in Durbed Banner, and 181 were infected, with a prevalence rate of 23.7%. A total of 140 she-camels were investigated from 3 camel herds. In Urad North Banner 30 were infected, with a prevalence rate of 23.8%. Therefore, the prevalence rate was similar in the 3 regions, and the earliest cases appeared in mid-May, then gradually increased in June and July, peaked in July and August, then gradually decreased in September and almost ended in mid-October.

Among the 21 camel herds surveyed, 15 were free-range camel herds on natural pastures, 5 were semi-free-range camel herds, and 1 was a completely house-raised camel herd. The highest incidence rate reached 82.6%, which was one of the free-range camel group; and the lowest incidence rate was only 1.4%, which was a semi grazing camel group. The average prevalence rate of grazing camels, semi grazing camels and completely house-raised camels

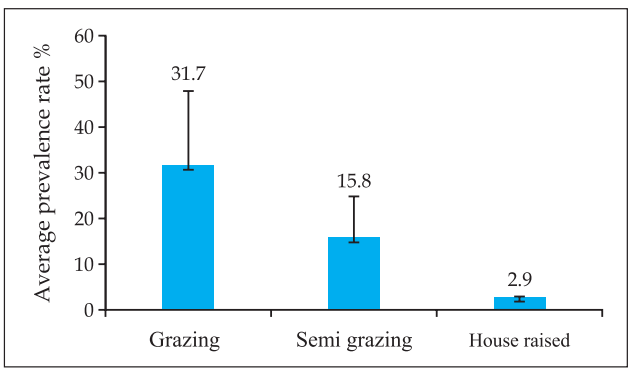

Fig 5. Average prevalence rate of female camels in different feeding methods.

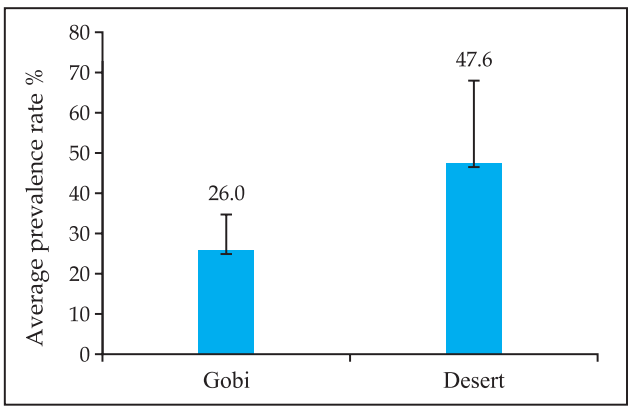

Fig 6. Average prevalence rate of female camel in different grassland types.

was 31.7%±16.2%, 15.8%±9.0% and 2.9%, respectively (Fig 5).

Among the 15 free-range camel herds, 11 camel herds were distributed in the arid grasslands of the Gobi, drinking well water; 4 camel herds were distributed in desert grasslands, with plenty of natural water sources such as lakes and river beaches. The prevalence of camels distributed in desert grasslands with lakes and river beaches was generally higher than that of camels in the Gobi steppe (Fig 6).

We further analysed 277 infected camels and found that the youngest camel infected was 7 months old and the oldest was 20 years old. Three infected camels were 1 year age, 25 camels were between 1 and 5 years and 249 camels were over 5 years of age.

We further analysed the parity of 52 infected camels and found that there were 6 camels that had not produced calves, the rest were multiparous female camels, and the female camels who had given birth to 2 calves had the highest prevalence rate (Table 2).

Discussion

After artificial eclosioned and morphological observation, the maggots collected in this survey were identified as *W. magnifica*. This was similar with the epidemiological investigated results of vaginal myiasis of Bactrian camels by Huhe *et al* (1994) in Alxa Left Banner. This indicates that vaginal myiasis of Bactrian camels caused by the larva of the *W. magnifica* has been prevalent in these areas for a long time. A case of genital myiasis of Bactrian camel caused by *Wohlfahrtia magnifica* was reported in southwest of Iran (Sazmand and Joachim, 2017). An outbreak of genital myiasis was reported in 13 Bactrian camel herds in Mongolia, and the pathogen was identified as *W. magnifica* (Schumann *et al,* 1976). In 2009, Schnur *et al* (2009) investigated the myiasis of livestock in Israel and speculated that the pathogen of 2 cases of camels genital myiasis may be the *W. magnifica*.

The clinical symptoms observed in this investigation were similar to those described by Jiang (2016) who also found swollen vulva, constant discharge of blod and channels formed by fly maggots in inner wall of vagina. In this investigation, only 3 cases were found with serious genital tract infection extending to the anus, and no infection was found in male camels.

In Alxa Left Banner, a total of 1151 female camels were investigated and the average prevalence rate was 28.0%, which was about 20% lower than the result of ErD *et al* (2012).

Table 1. Statistics on genital myiasis of Bactrian camels in part areas of Inner Mongolia.

Areas	No. of herds	Total No. of investigated	No. of infected	Average prevalence rate (%)
Alxa Left Banner	14	1151	280	28.0±19.2
Durbed Banner	4	747	181	23.7±5.2
Urad North Banner	3	140	30	23.8±13.5
Total	21	2038	491	26.6±16.7

Table 2. Relationship between the number of produced calves and prevalence rate.

Number of produced calves	0	1	2	3	4	5	6	7
prevalence rate (%)	11.5	15.4	30.8	17.3	15.4	5.8	3.8	0

The occurrence and development of myiasis are closely related to the life history of *W. magnifica*. It has been reported that the *W. magnifica* are in the form of pupae in winters and temperature is the key to their successful eclosion (Li, 2020). Hot weather from July to August and increased rainfall is ideal for the reproduction of flies, resulting in a rapid increase in the prevalence rate of genital myiasis. The average prevalence rate was higher in camels distributed near river shoals, hills and lake basins in present study. The prevalence rate of grazing female camels (31.7%) was significantly higher than that of semi grazing camels (15.8%), and this was again obviously higher than that of house raised camels (2.9%). This was mainly due to house raised camels have a small range of activities, access to clean food and water. In addition, the pens were regularly cleaned, hence there was lack of breeding conditions for flies, and the chance of camels contacting with flies was greatly reduced, thus occurrence of the disease was less.

It has been reported that the *W. magnifica* chooses to larviposition in the vagina of a female camel, which may be related to its antennae sensing surrounding chemical signals (Wang, 2019). Local farmers also said that camels with energy imbalance or postpartum vaginal inflammation were more susceptible to genital myiasis. Infection rates in juvenile camels are lower than in adult camels in most camel herds, and only 3 juvenile camels were found be infected during this investigation. This survey found that the prevalence rate of female camels over 5 years and with 2~4 parities was significantly higher than other camels.

Much attention should be paid to the prevention and control of this disease. Huhe *et al* (1994) used fly maggots powder to treat vaginal myiasis in Bactrian camels. Strengthening farmer's awareness of the disease and rational use of drugs are also helpful to control the disease and this would promote the healthy development of camel husbandry and impart economic benefits to the camel farmers.

Reference

An XW, ErD MT, Cu AW, Buren BY, Sarina, Zhi LK, Wang C and Baoshan. Morphological observation of the larva of the Alxa bactrian camel vaginal myiasis. Progress in Veterinary Medicine. 2019; 40(1):47-52.

ErD MT, Danengtai, Danengtai, Wang LH, Hubisihalatu and Zhao W. Investigation on the incidence of vaginal myiasis in Alxa Bactrian camels. Chinese Journal of Veterinary Medicine. 2012; 48(3):46-47.

Fu LH and Liu AH. China statistical yearbook-2021. China Statistical Press 2021:404.

Fan ZD. Key to the Common Flies of China. (2nd edition). Science Press. 1994; pp 456-621.

Gaglio G, Brianti E, Abbene S and Giannetto S. Genital myiasis by *Wohlfahrtia magnifica* (Diptera, Sarcophagidae) in Sicily (Italy). Parasitology Research. 2011; 109(5):1471-1474.

Huhe BT, Baiyin BT and Du YF. Epidemiological investigation of bactrian camel vaginal myiasis. Journal of Inner Mongolia Agricultural and Animal Husbandry College. 1994; 04:59-62.

Huhe BT, Baiyin BT, Ba YG, Guo YH and Du YF. Experimental observation of Fly maggots powder in treating vagina myiasis of camels. Animal Husbandry and Feed Science. 1995; 02:31-32.

Jiang JQ. Study on cytokines of Alxa Bactrian camels artificially infected vaginal myiasis and morphological observation on vaginal tissue. Master's thesis. Inner Mongolia Agricultural University. 2016.

Li YQ, Li X, Liu JL, Liu AH, Guo PF, Han Y, Shang YJ, Guan GQ, Liu ZJ, Liu GY, Luo JX and Yin H. Molecular identification and detection of *Wohlfahrtia magnifica* in ovine vulvar myiasis in Gansu, China. Tropical Animal Health and Production. 2019; 51(8):2629-2634.

Li HB. Study on overwintering behaviors of *Wohlfahrtia magnifica* pupae and heat shock protein genes. Master's thesis. Inner Mongolia Agricultural University. 2020.

Pirali Kheirabadi K, Dehghani Samani A and Rajabi Vardanjani H. A report on the genital myiasis by *Wohlfahrtia magnifica* in camel herds in southwest of Iran. Veterinary Research Forum. 2014; 5(4):329-332.

Rafinejad J, Akbarzadeh K, Rassi Y, Nozari J, Sedaghat MM, Hosseini M, Alipour H, Ranjbar A and Zeinali D. Traumatic myiasis agents in Iran with introducing

of new dominant species, *Wohlfahrtia magnifica* (Diptera:Sarcophagidae). Asian Pacific Journal of Tropical Biomedicine. 2014; 4(6):451-455.

Sazmand A and Joachim A. Parasitic diseases of camels in Iran (1931-2017) - a literature review. Parasite. 2017; 24:21.

Schumann H, Ribbeck R and Beulig W. *Wohlfahrtia magnifica* (Schiner, 1862 Diptera: Sacrophagidae) causing a vaginal myiasis in domesticated two-humped camels in the Mongolian People's Republic. Arch Exp Veterinarmed. 1976; 30(6):799-806.

Schnur HJ, Zivotofsky D and Wilamowski A. Myiasis in domestic animals in Israel. Veterinary Parasitology. 2009; 161(3-4):352-355.

Wang C. Morphological observation of *Wohlfahrtia magnifica* pupae and its transcriptional group at each developmental stage. Master's thesis. Inner Mongolia Agricultural University. 2019.

Zhang PL. The larvae of *Wohlfahrtia magnifica* were detected in the gingiva. Journal of Clinical Laboratory Science. 2005; 06:442.

BACK ISSUES OF JCPR AVAILABLE

ISSN 0971-6777 (Print)
ISSN 2277-8934 (Online)

JOURNAL OF CAMEL PRACTICE AND RESEARCH

www.camelsandcamelids.com • www.indianjournals.com

Volume 23 June 2016 Number 1

In This Issue

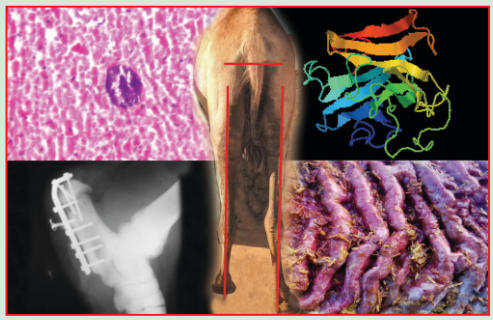

ISSN 0971-6777 (Print)
ISSN 2277-8934 (Online)

JOURNAL OF CAMEL PRACTICE AND RESEARCH

www.camelsandcamelids.com • www.indianjournals.com

Volume 23 December 2016 Number 2

In This Issue

ISSN 0971-6777 (Print)
ISSN 2277-8934 (Online)

JOURNAL OF CAMEL PRACTICE AND RESEARCH

www.camelsandcamelids.com • www.indianjournals.com

Volume 24 April 2017 Number 1

In This Issue

ISSN 0971-6777 (Print)
ISSN 2277-8934 (Online)

JOURNAL OF CAMEL PRACTICE AND RESEARCH

www.camelsandcamelids.com • www.indianjournals.com

Volume 24 August 2017 Number 2

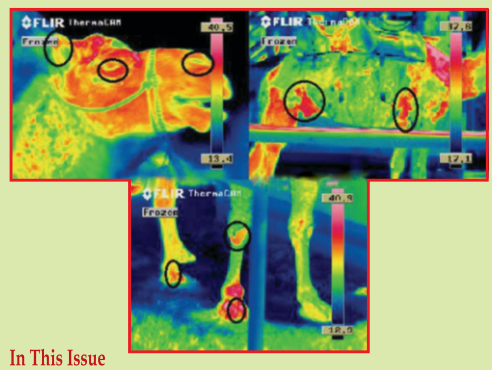

In This Issue

See the details of list of contents of all previous issues of JCPR on our website
www.camelsandcamelids.com

Kindly refer querries to: Dr. T.K. GAHLOT, Editor, JCPR
email: tkcamelvet@yahoo.com

DOI : 10.5958/2277-8934.2022.00033.9 Vol 29 No 2, p 237-244

EPIDIDYMAL BASED CHANGES IN SPERMATOZOA OF DROMEDARY CAMELS

Dina E.M. Rashad[1], Mohamed M.M. Kandiel[1*], Ahmed R.M. El-Khawagah[1], Karima Gh. M. Mahmoud[2], Yousef F. Ahmed[2], Abou El-Roos Mahmoud E.A.[1] and Gamal A.M. Sosa[1]

[1]Theriogenology Department, Faculty Veterinary Medicine, Benha University, Egypt

[2]Animal Reproduction and Artificial Insemination, National Research Centre, Dokki, Giza, Egypt[4,5]

ABSTRACT

This study was aimed to declare the role of epididymal passage on semen features, DNA integrity and ultra-structures changes in dromedary camel. The testes with attached epididymis of mature dromedary camels (n=50) were collected during the rutting season from December to April. The harvested spermatozoa from the three-main anatomical epididymal segments (Head, body and tail) were assessed for semen characters, DNA integrity as well as, ultra-structural changes. A significant difference in semen features (individual motility, sperm count, membrane and acrosome intactness, viability, normality, maturity, abnormalities and acrosome length and perimeter) among different epididymal segments. Spermatozoa from epididymal tail showed a significantly ($p<0.05$) lower DNA fragmentation than those collected from head segment while agarose gel electrophoresis revealed non-significant difference in DNA intensity between spermatozoa from the three epididymal regions. Ultra-structures of the epididymal spermatozoa showed changes in acrosome shape, sub-acrosomal space, chromatin condensation and protoplasmic droplet during epididymal passage. The protoplasmic droplets varied in size, density and position with the epididymal segments. In conclusion, epididymal passage (from the head to the tail) is an essential pre-request for dromedary camels' spermatozoa to attain high fertilising capacity through its great influence on spermatozoa characteristics and the fine cytological structures.

Key words: DNA integrity, dromedary camel, epididymis, spermatozoa, ultra-structures

Collection of epididymal spermatozoa received an increasing interest by many researchers to be adopted for several assisted reproductive techniques (El-Badry *et al*, 2015; Scholkamy *et al*, 2016). Sperm cells obtained from any epididymal segment have been assessed (Tajik *et al*, 2008). Epididymal spermatozoa recovery from slaughtered/dead animals, cryopreservation and subsequent IVF helps to preserve the genetic material either from highly productive animals and/or from endangered species (Martins *et al*, 2007a). Researchers studied acceptable motility and viability of spermatozoa recovered from the epididymis which have been maintained at room temperature or 5°C in camel (Waheed *et al*, 2011; Shahin *et al*, 2021), bull (Martins *et al*, 2009) and stallion (Muradás *et al*, 2006). However, researchers found that quality of epididymal spermatozoa varied according to breeding season (Abd and Ibrahim, 2014), temperature (Lone *et al*, 2011) and epididymal segment (Waheed *et al*, 2011; Rashad *et al*, 2018).

The current study was aimed to record the changes in semen features, DNA integrity and ultra-structures in relation to epididymal segment in mature dromedary camels during rutting season.

Materials and Methods

Epididymal semen collection and evaluation

Testes and epididymis (n=50) were collected from apparently healthy slaughtered camels aged 5 to 10 years during the rutting season (December – April). The epididymis was dissected, rinsed with 0.9% saline (Yu and Leibo, 2002) and epididymal anatomical segments (head, body and tail) were distinguished (Zayed *et al*, 2012). Each epididymal parts was incised and the spermatozoa were collected separately.

Semen evaluation

Sperm motility

The sperm individual progressive motility was determined by light microscope (×40) on a warm stage at 35°C (Melo *et al*, 2005).

Sperm count

Sperm count was determined with an improved Neubauer haemocytometer chamber after dilution with coloured hypertonic saline solution according to Atiq *et al* (2011).

SEND REPRINT REQUEST TO MOHAMED M.M. KANDIEL email: kandiel75@hotmail.com

Sperm viability and abnormality

The sperm viability and morphology were evaluated in Eosin (5%) and Nigrosin (10%) stained film sand examined under oil immersion lens (×100) according to Skidmore *et al* (2013).

Plasma membrane integrity

Plasma membrane integrity was assessed by hypo-osmotic swelling test (HOS test) as described by Jeyendran *et al* (1984) with some modifications (Zubair *et al*, 2013). Briefly, 10 µl of each semen sample was mixed with 90 µl of a pre-warmed hypo-osmotic solution (0.735 g of sodium citrate dihydrate and 1.351 g of fructose in 100 ml of de-ionised water) and incubated at 37°C for one hour. The positive HOS cells indicated by swelling and coiling of the sperm tail (Lodhi *et al*, 2008).

Acrosome integrity evaluation

The rate of spermatozoa acrosome integrity was determined using Giemsa stain (×100) as described by Chowdhury *et al* (2014).

Evaluation of DNA fragmentation

Acridine orange technique

Acridine orange stain was used to assess DNA integrity of the harvested epididymal spermatozoa as described by Martins *et al* (2007b). Damaged DNA gave red or orange fluorescence and normal double-strand DNA structure gave green fluorescence (Andrazek *et al*, 2014).

Gel electrophoresis

DNA was extracted from spermatozoa collected from the three regions of epididymis according to Trommelen *et al* (1993) with some modifications (Weyrich, 2012).The concentration and purity of extracted genomic DNA were determined spectrophotometrically (BIO RAD, USA).

Transmission electron microscopy (TEM)

Small blocks for spermatozoa from each epididymal segment were initially fixed for 2-3 h with 2% glutaraldehyde in PBS, washed three times with PBS (pH 7.4) for 5 min at 4ºC and re-fixed in 1% osmium tetroxide for 1-2 h at 4°C (Boonkusol *et al*, 2010). All samples were dehydrated in ascending grade of ethanol (50, 70, 90 and 100%) and propylene oxide for 1 h and embedded in epoxy resin. Ultrathin sections were cut using the Leica EM UC6 ultramicrotome and stained with uranyl acetate and lead citrate.

Statistical analysis

Data (expressed as mean ± SE) were statistically analysed with one-way ANOVA followed by Tukey (HSD) test using IBM-SPSS for Windows (Ver. 21, 2017). The statistical significance was noted ($P<0.05$).

Results

Epididymal semen features

The epididymal semen characteristics in dromedary camels reorded in present study are presented in table 1.

Epididymal spermatozoa motility ($P< 0.01$), count ($P< 0.001$), membrane integrity ($P< 0.0001$), acrosome intactness ($P< 0.005$), viability ($P< 0.05$), maturity ($P< 0.0001$), normality ($P< 0.0001$) varied markedly between its compartments. There was a tremendous improvement in all previous mentioned parameters in epididymal tail compared with head and body parts. Moreover, the rate of sperm head ($P< 0.005$) and tail ($P< 0.001$) abnormalities greatly reduced in body and tail of epididymis in comparison with head segment. Acrosomal length and perimeter were highly significant ($P<0.001$) between epididymal segments.

Epididymal sperm DNA fragmentation

DNA fragmentation rate as examined by acridine orange showed a tendency ($P=0.099$) of variation between epididymal segment (Fig 1). Epididymal spermatozoa from head region possessed higher ($P<0.05$) fragmented DNA than those from the tail region.

The intensity of extracted sperm DNA did not show any variation between epididymal segments by gel electrophoresis (Fig 2).

Epididymal sperm ultra-structure

Alternations in spermatozoa ultra-structural during epididymal transit were mainly noticed in the acrosome shape, sub-acrosomal space, nuclear chromatin condensation and protoplasmic droplets (Figs 3-4). The acrosome appeared projected anteriorly at head segment, but the acrosome projection was absent at the tail segment. The sub-acrosomal space decreased progressively in spermatozoa from head to tail of epididymis (Fig 3 e, f). Plasma membrane of most spermatozoa was noticed somewhat elevated at epididymal tail region. Spermatozoa with a homogeneously densely packed nucleus were predominant in the tail of the epididymis than upper segments (Fig 4a-c). The protoplasmic droplets were numerous and dense in appearance in the head

Table 1. Epididymal spermatozoa features in dromedary camels.

Item	Head	Body	Tail	P value
Spermatozoa motility (%)	13.33±2.25^{c}	39.17±1.68^{b}	58.13±2.82^{a}	0.01
Sperm cell count (×10^{6}/ml)	58.75±10.87^{b}	96.63±16.64^{b}	224.70±24.86^{a}	0.001
Membrane integrity (%)	70.58±2.06^{b}	83.71±0.99^{a}	87.28±0.87^{a}	0.0001
Acrosome integrity (%)	90.61±0.45^{b}	91.53±0.58^{b}	95.68±0.99^{a}	0.005
Livability (%)	49.95±1.35^{c}	73.65±1.58^{b}	82.84±2.97^{a}	0.05
Immaturity (%)	19.08±1.06^{a}	11.60±0.89^{b}	8.00±0.78^{c}	0.0001
Sperm normality (%)	47.07±2.31^{c}	55.73±1.78^{b}	66.67±2.47^{a}	0.0001
Head abnormality (%)	10.21±2.50^{a}	4.87±0.68^{b}	2.94±0.46^{b}	0.005
Tail abnormality (%)	41.91±1.82^{a}	39.02±1.75^{a}	30.38±2.24^{b}	0.001
Acrosome length (µm)	4.76±0.13^{a}	4.27±0.06^{b}	4.00±0.07^{c}	0.001
Acrosome perimeter (µm)	19.02±0.28^{a}	17.70±0.14^{b}	17.00±0.18^{c}	0.001
DNA fragmentation %	1.62±0.14^{a}	1.42±0.21^{ab}	1.09±0.36^{b}	0.005

Data was presented as mean ± SE (n=50). Values with different superscript letters within the same row were significantly different.

region, few and dark in the body region and few and light in the tail region. Protoplasmic droplets were situated at a higher position of sperm tail and centered around axoneme at head and body segments. Yet, few spermatozoa showed eccentric position around axoneme. Protoplasmic droplets at tail segment mostly situated at distal position and often at the mid-way of sperm tail and eccentrically placed around the axoneme (Fig 4d-e).

Discussion

The current investigation proved that progressive sperm motility radically increased from the epididymal head to tail and this came in accordance with former studies in camel (Waheed *et al*, 2011; El-Badry *et al*, 2015), bull and ram (Amann, 1987), horse (Johnson *et al*, 1980) and donkey (Contri *et al*, 2012). These findings slightly matched with that mentioned by El-Badry *et al* (2015) for the spermatozoa from the epididymal tail and body and slightly lower for spermatozoa from epididymal head. The motility percentage of spermatozoa from tail value was also close to those reported by Turri *et al* (2013).

The present study showed that epididymal sperm count was higher in tail segment than in body and head segments. These values matched with those of Ibrahim *et al* (2012), who claimed that the epididymal tail acts as sperm depot in dromedary camel. This finding was in a strong agreement with Bitto and Okpale (2006), Ahemen and Bitto (2007), Ugwu (2009) and Ibrahim *et al* (2012), but not in agreement with finding of Osman and El-Azab (1974), who indicated that the camel epididymal body incubated more spermatozoa than head and tail. The variations were perhaps due to different harvesting method where dissection was associated with high sperm count.

In our study, there was significant difference in the sperm livability percentage among the three epididymal segments. This finding was not in agreement with Tajik *et al* (2008) and El-Badry *et al* (2015) in dromedary camel. Moreover, in the present study, live sperm percentage from epididymal tail was slightly higher than that recorded by Ziapour *et al* (2014) and El-Badry *et al* (2015). Nevertheless, the mean sperm livability rate herein was slightly lower in harvested spermatozoa from epididymal head and body than that recorded by El-Badry *et al* (2015).

The present research showed that sperm normality rate was higher in epididymal cauda than corpus and caput while the sperm deformities were higher in epididymal head and body than the tail. Tingari *et al* (1986) found that the percentage of spermatozoa with protoplasmic droplet was higher in epididymal head than body and tail. This finding was in a strong agreement with McKinnon *et al* (1994). In contrary, El-Badry *et al* (2015) recorded that the morphologically abnormal sperm percentage did not vary between the three epididymal segments and the proportion of spermatozoa with protoplasmic droplets was higher in the cauda than in the corpus or caput epididymis. Nevertheless, Tajik *et al* (2008) found no significant difference in the percentage of spermatozoa with protoplasmic droplets between three regions of the epididymis. Some authors reported that cytoplasmic droplets in sperm cells might be considered as an abnormality (Bravo *et al*, 1997; Flores *et al*, 2002), while others didn't agree with them (Tingari *et al*, 1986).

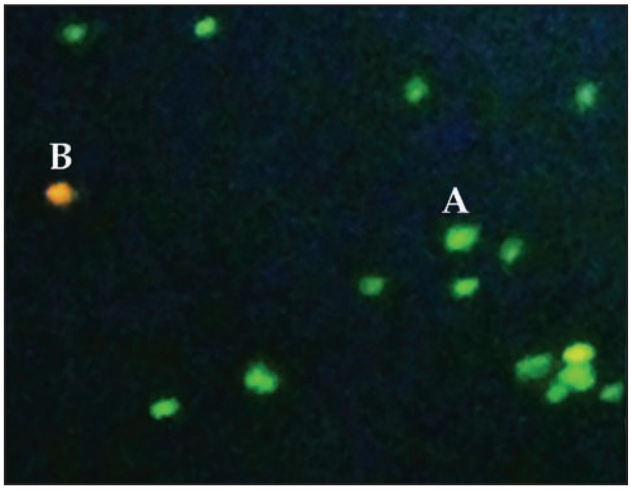

Fig 1. Representative photomicrograph for sperm DNA fragmentation stained with acridine orange stain and examined by florescent microscope. (A) refers to sperm with non-fragmented (emitted green fluorescence) DNA while (B) refers to sperm with fragmented DNA (emitted variable shades of fluorescence from yellow-green to red).

Former works considered the assessment of sperm plasma membrane integrity by the HOS test an indication of male fertility (Revell and Mrode, 1994; Perez-Llano *et al*, 2001). The present study showed that the proportion of sperm cells with an intact plasma membrane was higher for sperms from epididymal tail than head and body. The recorded values here were higher than that reported by El-Badry *et al* (2015) for camel epididymal sperm cells and Ziapour *et al* (2014) for camel ejaculatory sperms. This difference may be due to the method of evaluation.

The current study showed that percentage of spermatozoa with intact acrosome was higher in epididymal tail than those from body and head. These results were marginally higher than that recorded by El-Badry *et al* (2015), who noticed that there were no significant differences among spermatozoa with an intact acrosome between epididymal parts. Also, Morton *et al* (2010) recorded that large proportion of alpaca epididymal semen had an intact acrosome. Our study revealed that there was a very highly significant difference between the acrosome lengths of spermatozoa from different epididymal regions. Similar values were recorded by Osman and Plöen (1986), although these values were lower than that reported by Abdel-Raouf and El-Naggar (1965).

In this study, the epididymal sperm DNA didn't show differences in DNA intensity between epididymal compartments though nuclear

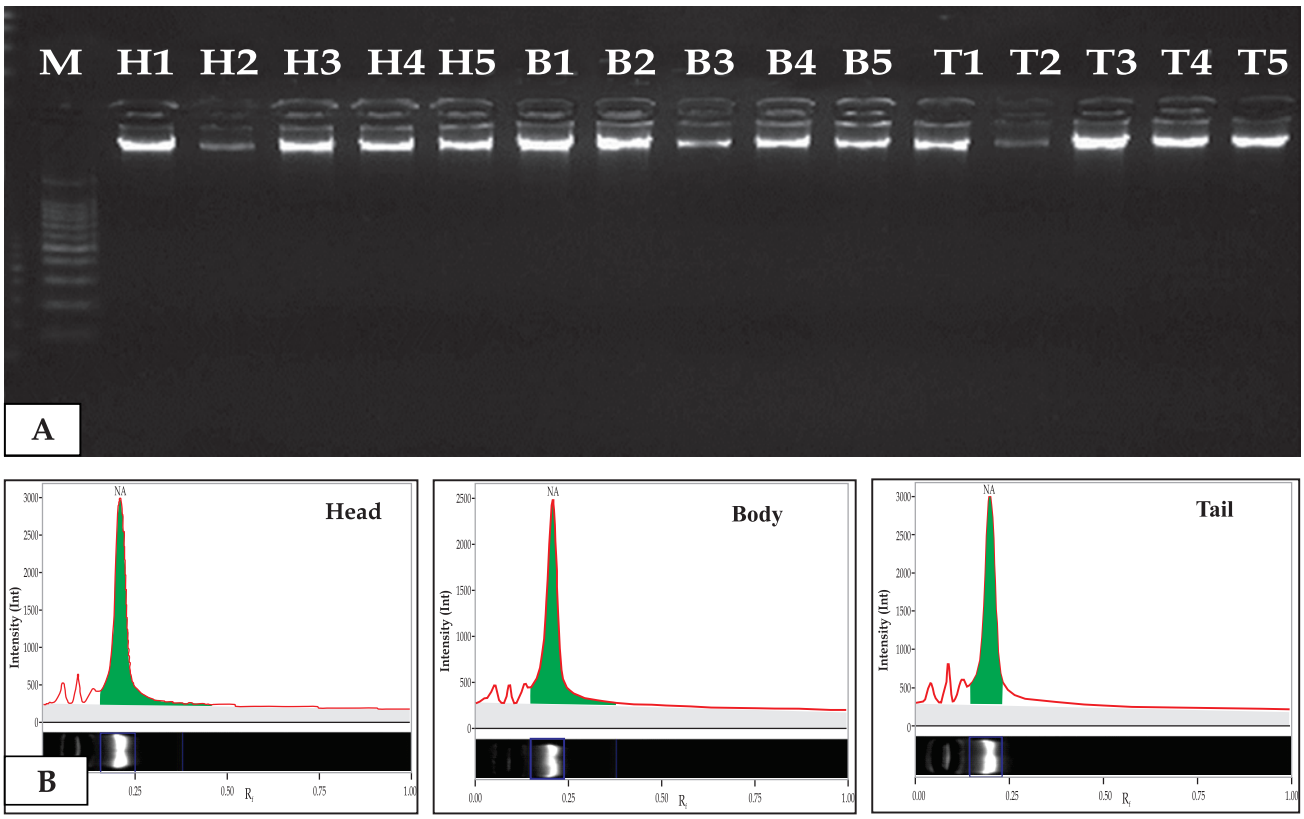

Fig 2. (A)Agarose gel stained with ethidium bromide showed sperm cell DNA extraction product. M: 100-bp ladder. Lanes: H (1-5), B (1-5) and T (1-5) represented DNA extracted from spermatozoa collected from head, body and tail of camel epididymis, respectively. Fig 2(B): Computer aided DNA band density assessment of sperm cell DNA extraction product.

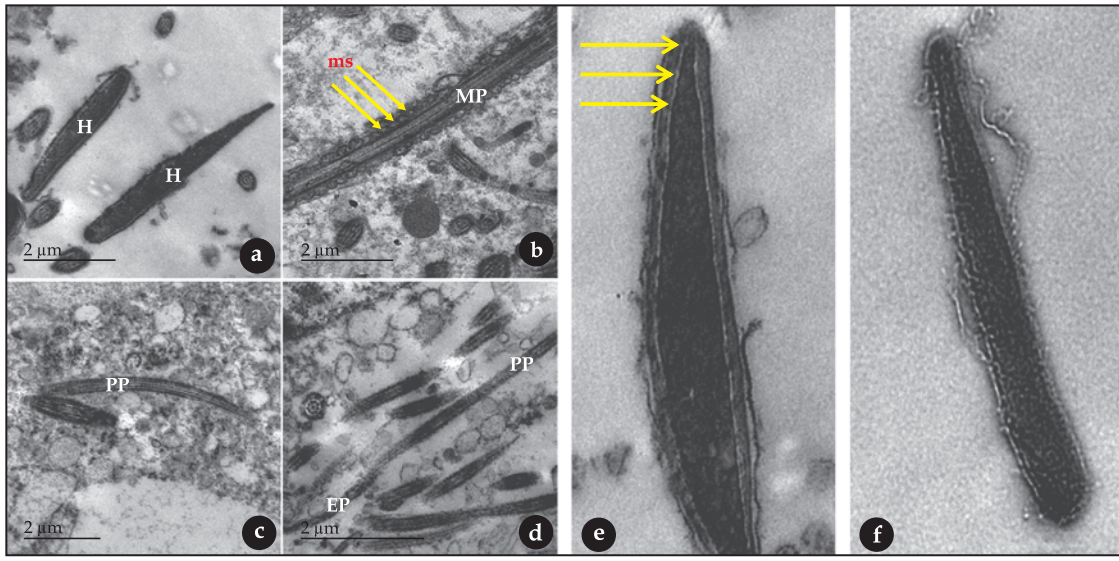

Fig 3. Representative transmission electron micrographs showed sagittal sections at camel epididymal spermatozoa parts. (H) sperm head, (mp) mid piece, (ms) mitochondrial sheath, (pp) principle piece and (EP) end piece. Notice the wide sub-acrosomal space (Fig 3e) in camel epididymal spermatozoa (arrows) that became ultimately disappeared at final epididymal transit (Fig f).

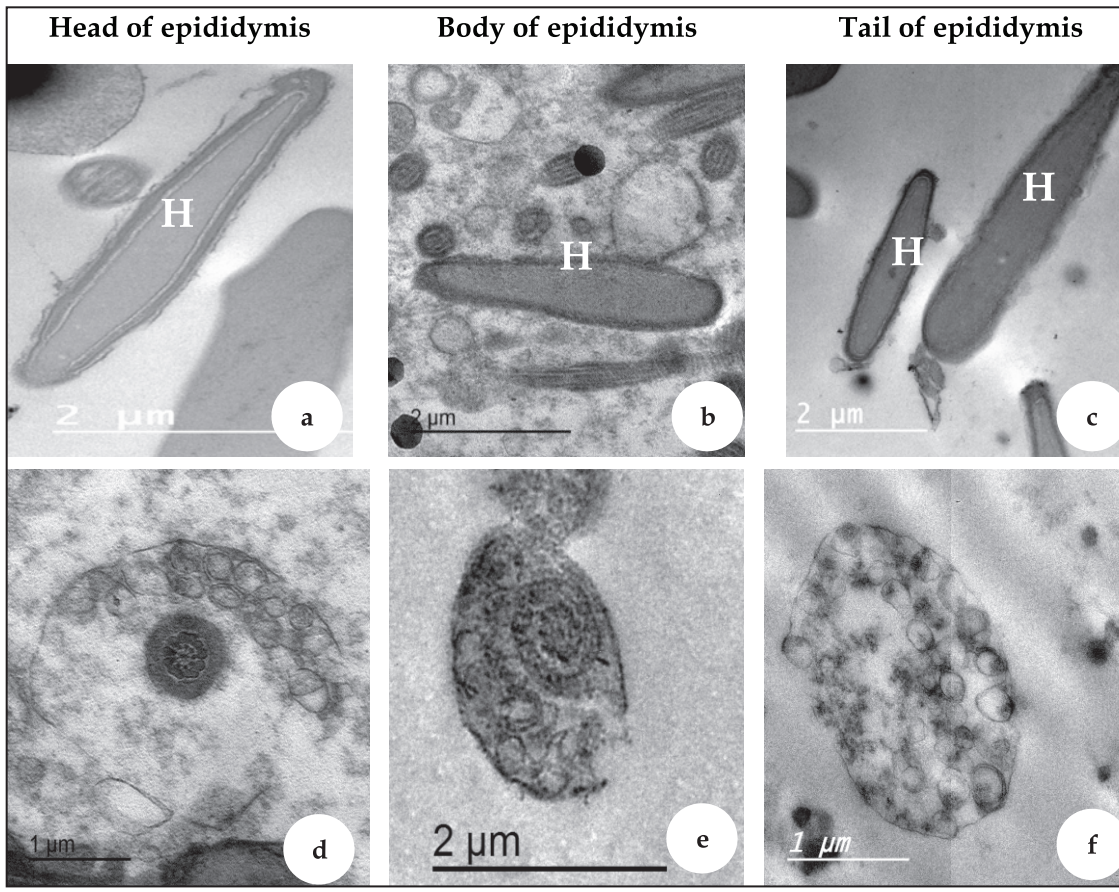

Fig 4. Representative transmission electron microscopic images of the changes in camel spermatozoa nuclear DNA decondensation (a-c) and protoplasmic droplets (d-f) during epididymal passage. There was little variation in nuclear decondensation in samples obtained from the head (a) and body (b) epididymal regions. Spermatozoa from tail of the epididymis showed a homogeneously dense nucleus (c). Protoplasmic droplet appeared proximal eccentric position (d), distal eccentric position (e) and shed-off (f) as spermatozoa passed from head to body and tail segments, respectively.

fragmentation was higher in head than tail of the epididymis. These findings indicated high stability of camel sperm DNA during epididymal passage. Aberrant chromatin packing during spermatogenesis results in sperm DNA fragmentation (Gorczyca *et al*,1993; Sailer *et al*, 1995). Accordingly, El-Badry *et al* (2015) reported that dromedary camel epididymal spermatozoa from cauda epididymis had higher DNA integrity in comparison to corpus and caput epididymal spermatozoa. Our findings agreed with Yanagimachi (1994), who stated that the mammalian spermatozoa nuclei were very stable and highly condensed with a unique DNA organisation (a six-fold more compact than somatic cells). This unique DNA packing was important to protect the sperm cell and minimise damages caused by exogenous agents before fertilisation.

Electron microscope application in reproductive research was helpful in recognising the monomorphic and polymorphic sperm defects beside understanding of spermatozoa physiology and pathology (Moretti *et al*, 2016). In the current study, camel epididymal spermatozoa showed ultra-structural variations between epididymal segments in association with the maturational changes and most of these modifications were confined to acrosome, plasma membrane and protoplasmic droplet. In epididymal head, acrosome projected anteriorly with wider sub-acrosomal space and the protoplasmic droplets were numerous, condensed and dark in appearance at a higher position of sperm tail. On the other hand, in epididymal tail, acrosome projection faded with a very narrow sub-acrosomal space, plasma membrane was somewhat elevated and the protoplasmic droplet were few and light in colour at the midway of sperm tail and eccentrically placed around the axoneme. Osman and Plöen (1986) reported that the cytoplasmic droplet was proximal immediately behind the neck region at the initial epididymal segment and centered around the axoneme then became more eccentric, migrated distally and was eventually shed as the spermatozoa move through the camel epididymis.

Conclusions

Semen characteristics as well as spermatozoa morphology were greatly modified during epididymal passage and this was an essential pre-request for successful fertilisation by the ejaculated semen. Epididymal tail spermatozoa showed an improved fertilising capacity (cytologically and molecularly) that ensure its suitability for assisted reproductive techniques e.g., IVF or ICSI in camels.

Conflict of interest

The Authors declare that there is no conflict of interest.

References

Abd AA and Ibrahim NS. Effect of age and season on the epididymal sperm and testosterone level in camel (*Camelus dromedarius*). Iraqi Journal of Veterinary Medicine. 2014; 38(1):24-29.DOI: https://doi.org/10.30539/iraqijvm.v38i1.250

Abdel-Raouf M and El Naggar MA. Studies on reproduction in camels (*Camelus dromedarius*). II. The morphology of the camel spermatozoon. Journal of Veterinary Science. U.A.R. 1965; 2(1):1-11.doi: 10.1530/jrf.0.0430109.

Ahemen T and Bitto II. Sperm production rate, gonadal and extra gonadal sperm reserves of the West African Dwarf rams in Makurdi. Proceedings of the 32nd Annual Conference of Nigerian Society for Animal Production, March 18-21, 2007; pp 99-101.

Amann RP. Function of the epididymis in bull and rams. Journal of Reproduction and Fertility. 1987; 34:115-131.

Atiq N, Ullah N andrabi SMH and Akhter S. Comparison of photometer with Improved NeubauerHaemocytometer and Makler counting chamber for sperm concentration measurement in cattle. Pakistan Veterinary Journal. 2011; 31(1):83-84.

Bitto II and Okpale MI. Sperm production rate, gonadal and extragonadal sperms reserves in slaughtered White Fulani (Bunaji) bulls in a low land tropical environment. Nigerian Journal of Animal Production. 2006; 33(2):300-307.doi:10.51791/njap.v33i2.942

Boonkusol D, Saikhun K and Ratanaphumma P. Effect of extender and storage time on motility and ultrastructure of cooled-preserved boar spermatozoa. Kasetsart Journal of Natural Science. 2010; 44:582-589.

Bravo PW, Flores U, Garnica J and Ordonez C. Collection of semen and artificial insemination of alpacas. Theriogenology. 1997; 47:619-626. https://doi.org/10.1016/S0093-691X(97)00020-4.

Chowdhury S, Das S, Gupta T, Sana D and Bose S. Evaluation of frozen semen by acrosomal integrity and sperm concentration–two vital quality parameters of male fertility in bovines. Exploratory Animal and Medical Research. 2014; 4(1):101-107.

Contri A, Gloria A, Robbe D, De Amicis I and Carluccio A. Characteristics of donkey spermatozoa along the length of the epididymis. Theriogenology. 2012; 77:166-173. doi: 10.5455/ajvs.178345.

Deen A and Sahani MS. Preliminary attempts to collect and cryopreserve camel semen. Journal of Camel Practice and Research. 2000; 7:181-186.

El-Badry DA, Scholkamy TH, Anwer AM and Mahmoud KGhM. Assessment of freezability and functional integrity of dromedary camel spermatozoa harvested from caput, corpus and cauda epididymis. Alexandria Journal of Veterinary Sciences. 2015; 44:147-158. doi:10.5455/ajvs.178345

El-Hassanein E. An invention for easy semen collection from

dromedary camels, El-Hassanein Camel Dummy. In: Skidmore, JA and Adams, GP (Eds), Recent Advances in Camel Reproduction. International Veterinary Information Service (IVIS). 2003; Document No. A1014.0203.

Flores P, Garcia-Huidobro J, Munoz C, Bustos-Obergon E and Urquieta B. Alpaca semen characteristics previous to a mating period. Animal Reproduction Science. 2002; 72:259-266.

Gorczyca W, Traganos F, Jesionowska H and Darzynkiewicz Z. Presence of DNA strand breaks and increased sensitivity of DNA *in situ* to denaturation in abnormal human sperm cells: analogy to apoptosis of somatic cells. Experimental Cell Research. 1993; 207(1):202-205. doi: 10.1006/excr.1993.1182

Ibrahim AA, Aliyu J, Hassan AM and Salisu N. Gonadal and extra gonadal sperm reserves of camel (*Camelus dromedarius*) in the semi-arid region of Nigeria. ARPN. Journal of Agricultural and Biological Science. 2012; 7(5):346-350.

Jeyendran RS, Vander-Ven HH, Perez-Pelaez M,Crabo BG and Zanevld LJD. Development of an assay to assess the functional integrity of the human sperm membrane and its relationship to other semen characters. Journal of Reproduction and Fertility. 1984; 70:219-228. doi: 10.1530/jrf.0.0700219.

Johnson L, Amann RP and Pickett BW. Maturation of equine epididymal spermatozoa. American Journal of Veterinary Research. 1980; 41:1190-1196.

Lodhi LA, Zubair M, Qureshi ZI, Ahmed I and Jamil H. Correlation between hypo-osmotic swelling test and various conventional semen evaluation parameters in fresh Nili-Ravi buffalo and Sahiwal cow bull semen. Pakistan Veterinary Journal. 2008; 28(4):186-188.

Lone FA, Islam R, Khan MZ and Soli KA. Effect of transportation temperature on the quality of caudal epididymal spermatozoa of ram. Animal Reproduction Science. 2011; 123:54-59. https://doi.org/10.1016/j.anireprosci.2010.10.012

Martins CF, Rumpf R, Pereira DC and Dode MN. Cryopreservation of epididymal bovine spermatozoa from dead animals and its uses *in vitro* embryo production. Animal Reproduction Science. 2007a; 101: 326-331. doi: 10.1016/j.anireprosci.2007.01.018..

Martins CF, Dode MN, Báo SN and Rumpf R. The use of the acridine orange test and the TUNEL assay to assess the integrity of freeze-dried bovine spermatozoa DNA. Genetics and Molecular Research. 2007b; 6(1):94-104.

Martins CF, Driessen K, Melo Costa P, Carvalho-Neto JO, de Sousa RV, Rumpf R and Dode MN. Recovery, cryopreservation and fertilisation potential of bovine spermatozoa obtained from epididymides stored at 5^{0}C by different periods of time. Animal Reproduction Science. 2009; 116:50-57.

McKinnon AO,Tinson AH and Nation G. Embryo transfer in dromedary camels. Theriogenology. 1994; 41:145-150. https://doi.org/10.1016/S0093-691X(05)80060-3.

Melo MIV, Henry M and Beker ARCL. Hypoosmotic test to predict viability of equine chilled semen in different extenders. ArquivoBrasileiro de MedicinaVeterinária e Zootecnia. 2005; 57(6):757-763.

Moretti E, Sutera G and Collodel G. The importance of transmission electron microscopy analysis of spermatozoa: Diagnostic applications and basic research. Systems Biology in Reproductive Medicine. 2016; 62(3):171-183. doi: 10.3109/19396368.2016.1155242.

Morton KM, Evans G and Maxwell WMC. Effect of glycerol concentration, Equex STM® supplementation and liquid storage prior to freezing on the motility and acrosome integrity of frozen-thawed epididymal alpaca (Vicugnapacos) sperm. Theriogenology. 2010; 74:311-316. DOI: 10.1016/j.theriogenology.2010.02.015.

Muradás PR, Weiss RR, Kozicki LE, Granemann LC, Santos IW and Pimpão CT. Some viability parameters from equine spermatozoa harvested by artificial vagina and by epididymal tail washing. Archives of Veterinary Science. 2006; 11(3):69-74.

Osman AM and El-Azab EA. Gonadal and epididymal sperm reserves in the camel (*Camelus dromedarius*). Camel (*Camelus dromedarius*). Journal of Reproduction and Fertility. 1974; 38: 452 - 430.doi: 10.1530/jrf.0.0380425

Osman DI and Plöen L. Fine structure of epididymal spermatozoa in the camel (*Camelus dromedarius*). Animal Reproduction Science. 1986; 10:177-184.

Perez-Llano B, Lorenzo JL,Yenes P and Garcia-Casado P. A short hypoosmotic swelling test for the prediction of boar sperm fertility. Theriogenology. 2001; 56:387-398. doi: 10.1016/s0093-691x(01)00571-4.

Rashad DEM, Kandiel MM, Agag MA, El-Khawagah ARM, Mahmoud KGhM, Ahmed YF, Abdou El-Roos MEA, Sosa GAM. Histomorphometry of dromedary camel epididymis and its correlation with spermatozoa characteristics during their epididymal transport. Benha Veterinary Medical Journal. 2018; 35:1-11. doi: 10.21608/bvmj.2018.35823

Revell SG and Mrode RA. An osmotic resistance test for bovine semen. Animal Reproduction Science.1994; 36: 77–86.https://doi.org/10.1016/0378-4320(94)90055-8

Sailer BL, Jost LK and Evenson DP. Mammalian sperm DNA susceptibility to in situ denaturation associated with the presence of DNA strand breaks as measured by the terminal deoxynucleotidyl transferase assay. Journal of Andrology. 1995; 16:80-88.

Scholkamy TH, El-Badry DA and Mahmoud KGhM. Developmental competence of dromedary camel oocytes fertilised *in vitro* by frozen-thawed ejaculated and epididymal spermatozoa. Iranian Journal of Veterinary Research. 2016; 17(4):253-258.

Shahin MA, Khalil WA, Saadeldin IM, Swelum AA, and El-Harairy MA. Effects of vitamin C, vitamin E, selenium, zinc, or their nanoparticles on camel epididymal spermatozoa stored at 4 °C. Tropical Animal Health and Production. 2021; 53:86. doi: 10.1007/s11250-020-02521-1

Skidmore JA, Morton KM and Billah M. Artificial insemination in dromedary camels. Animal Reproduction Science. 2013; 136:178-186.doi: 10.1016/j.anireprosci.2012.10.008.

Statistical Package for Social Science (IBM- SPSS) Program Ver. 21 for Windows, SPSS Inc., USA. 2017.

Tajik P and Hassan-Nejad Lamsoo MR. Assessment of epididymal sperm obtained from dromedary camel. Iranian Journal of Veterinary Research. 2008; 9(1):46-50.

Tingari MD, El Manna MMM, Rahim ATA, Ahme AK and Hamad MH. Studies on camel semen. I: Electro-ejaculation and some aspects of semen characteristics. Animal Reproduction Science.1986; 12:213-222.https://doi.org/10.1016/0378-4320(86)90042-4

Trommelen GJ, Den Daas NH, Vijg J and Uitterlinden AG. Identity and paternity testing of cattle: application of a deoxyribonucleic acid profiling protocol. Journal of Dairy Science. 1993; 76(5):1403-1411.doi: 10.3168/jds.S0022-0302(93)77471-8.

Turri F, Kandil OM, Abdoon AS, Sabra H, El Atrash A and Pizzi F. Conservation of camel genetic resources: Epididymal sperm recovery. The Camel Conference, SOAS (Egypt), 29 April 2013; pp 27-32.

Ugwu SOC. Relationship between scrotal circumferences, in situ testicular measurement and sperm reserves in the West African Dwarf bucks. African Journal of Biotechnology. 2009; 8(7):1354-1357.

Waheed MM, Al-Eknah MM and El-Bahr SM. Some biochemical characteristics and preservation of epididymal camel spermatozoa (*Camelus dromedarius*). Theriogenology. 2011; 76:1126-33. doi: 10.1016/j.theriogenology. 2011.05.021. PMID: 21762979.

Weyrich A. Preparation of genomic DNA from mammalian sperm. Current Protocols in Molecular Biology. 2012; 2(13):11-13doi:10.1002/0471142727.mb0213s98.

Yanagimachi R. Fertility of mammalian spermatozoa: its development and relativity. Zygote. 1994; 2: 71-372. doi: 10.1017/s0967199400002240.

Yu L and Leibo SP. Recovery of motile, membrane-intact spermatozoa from canine epididymides stored for 8 days at 4 degrees C. Theriogenology. 2002; 57(3):1179-1190.DOI: 10.1016/s0093-691x(01)00711-7.

Zayed AE, Aly K, Ibrahim IA and Abd El-Maksoud FM. Morphological studies on the seasonal changes in the epididymal duct of the one-humped camel (*Camelus dromedarius*). Veterinary Science Development. 2012; 2(1): 1-13. https://doi.org/10.4081/vsd.2012.3997.

Ziapour S, Niasari-Naslaji A, Mirtavousi M, Keshavarz M, Kalantari A and Adel H. Semen collection using phantom in dromedary. Animal Reproduction Science. 2014; 151:15-21.doi: 10.1016/j.anireprosci.2014.09.016.

Zubair M, Lodhi LA, Ahmad E and Muhammad G. Hypoosmotic swelling test as screening for evaluation of semen of bull. Journal of Entomology and Zoology Studies. 2013; 1(6):124-128.

DOI : 10.5958/2277-8934.2022.00034.0 *Vol 29 No 2, p 245-250*

GROSS AND MORPHOMETRIC STUDY OF ADRENAL GLAND OF CAMELS (*Camelus dromedarius*)

Sanwar Mal[1], Sanjeev Joshi[2], Pankaj Kumar Thanvi[2], Devendra Singh[1], Mahendra Kumar Saini[2] and Vijay Kumar Yogi[3]

[1]Department of Veterinary Anatomy, Sekhawati Veterinary College, Sikar, India
[2]Department of Veterinary Anatomy, college of Veterinary and Animal Science, Rajasthan University of Veterinary and Animal Sciences, Bikaner-334001, India
[3]Department of Veterinary Anatomy, Post Graduate Institute of Veterinary Education and Research, Jaipur-302031, India

ABSTRACT

The investigation was carried out on adrenal glands of 6 recently died adult camels. The adrenal glands of camel located bilaterally in the retroperitoneum, cranial and above the kidney. The cranial part of the right adrenal gland was partially covered by the liver thus making an impression upon the liver. The right adrenal gland was irregular triangular in shape while the left adrenal gland was flat oval in shape and each gland was reddish-grey in colour. The right adrenal gland was heavier, longer, thicker and narrower than the left adrenal gland. Statistical differences between right and left adrenals for all recorded values have been analysed. The difference between right and left adrenal volume, weight and length were statistically significant.

Key words: Adrenal gland, gross, one humped camel

Adrenal glands produce hormones that help regulate your metabolism, blood pressure, immune system, response to stress and other essential functions. It regulates many physiological functions, both in foetal and postnatal life (Hill, 2007).

The adrenal glands of mammals are located near the cranial pole of the kidneys. They consist of two distinct parts, the outer cortex and inner medulla, which differ in morphology, function and origin. Morphological studies of adrenal gland of prenatal developed gland (El-Nahla *et al,* 2011) and gland of adult dromedary camels has been extensively studied (Abdalla and Ali, 1989; Nabipour *et al,* 2008; Rehan and Qureshi 2007; Osman *et al,* 2019).

The anatomical structures of adrenal gland is eventhough studied in few countries but their studies are important because it plays a pivotal role in adaptation of camels located at different geographical locations and in different extreme environments. Present study is aimed to study the morphological details of adrenal gland of dromedary camels of Rajasthan.

Materials and Methods

The adrenal glands were collected from 6 recently died adult camels from VCC, CVAS, Bikaner, Rajasthan. The recommendations of the ethical committee were followed for present research and investigation of the organs were carried out in the Department of Veterinary Anatomy, CVAS, Bikaner. Morphometrical and other gross anatomical studies of adrenal gland intended topography and morphological features, such as, weight, length and breadth were carried out. Weight was taken with the help of physical balance and length, width and thickness were measured by digital Vernier's caliper. Volume was measured by water displacement method.

Results and Discussion

The adrenal glands of camel were located bilaterally in the retroperitoneum, cranial and dorsal to the kidney (Figs 1 and 2). The finding was in partial harmony with the findings of Ye *et al* (2017) who found that the gland was located bilaterally in the retroperitoneum superior and above the kidney in Bactrian camel.

The right adrenal was found superior and medial to the right kidney, not attached to it (Fig 1). Similar findings were reported by Abubakar (2015) in camel. On the contrary, Raghavan (1964) observed that in ox the right adrenal lie in contact with the medial part of the cranial end of right kidney. Nandeshwar *et al* (2017) reported that the right

SEND REPRINT REQUEST TO PANKAJ KUMAR THANVI email: drpankajthanvi@gmail.com

adrenal was found in contact with the medial part of the cranial end of right kidney in goat.

The cranial part of the right adrenal gland was partially covered by the liver thus making an impression upon the liver (Fig 1). Similar observations were also made by Abubakar (2015) in camel and Barszcz *et al* (2016) in European Bison. On the contrary, Raghavan (1964) observed that in ox, the right adrenal occupied a part of the renal impression on the liver.

The right adrenal gland was situated more cranially than the left gland in animals of present study. On the contrary, in pigs, both adrenals were situated at the medial border of the corresponding kidney from the hilus forward (Sisson and Grossman, 2012).

The left adrenal gland was found to be superior medially away from the left kidney in camels of present study (Fig 2). The result was in agreement with that of Abubakar (2015) in camel. However, Raghavan (1964) observed that in ox, the left adrenal was not in contact with the left kidney but lied about 5-7.5 cm in front of it. Sisson and Grossman (2012) found that the left adrenal was medial in position in cattle and was usually longer and not in contact with the left kidney but situated about 5 cm cranial to it, in sheep.

Shape and colour

The right adrenal gland was irregular and triangular in shape while the left adrenal gland was flat oval in shape (Fig 3 and 4). Similar observations were made by Abubakar (2015) in dromedary camel, Ye *et al* (2017) in Bactrian camel and Kumar and Sharma (2017) in Gohilwadi goat. The present study was in contradiction with the observation of Budras and Habel (2003) who found that the right adrenal was more or less heart shaped and the left adrenal was comma-shaped in bovine. Ashok *et al* (2005) reported that right adrenal gland of crossbred goat was roughly triangular in shape and the left one was elongated in crossbred goat. Dangi *et al* (2008) stated that left gland in goat was roughly triangular and the right was elongated in shape. Karakurum *et al* (2008) described that the adrenal gland of donkey was almost oval or circular. Sisson and Grossman (2012) mentioned that the right gland was pyramidal in shape and left adrenal was heart shaped in cattle. In sheep, both the glands were bean shaped similar to kidney. Barszcz *et al* (2016) mentioned that the shape of left adrenal gland resembled that of number "1" and the right adrenal gland was triangular in shape in European Bison. Barreiro-Vázquez (2020) stated that the right adrenal gland had a typically triangular, "V" or heart-shaped appearance and the left adrenal gland was sometimes "C" or comma-shaped in Holstein Friesian Cow. Elkbashi (2020) observed that the right adrenal gland was oval or bean-shaped, whereas the left one ranged from rounded, triangular, pyramidal, to nearly heart- shaped in dromedary camel.

The adrenal glands in camels of present study were reddish-grey in colour (Fig 3 & 4). It differed in colour in other species, i.e. reddish brown in ox (Raghavan, 1964), reddish brown to dark grey in bovines (Budras and Habel, 2003), dark brown in goats (Nandeshwar *et al,* 2017) and red colour in Bactrain camels (Ye *et al,* 2017).

Right adrenal gland was more elongated than the left one (Figs 3 and 4), but the left one was usually longer in sheep (Sisson and Grossman, 2012) and goat (Dangi *et al,* 2008).

The right adrenal gland had 3 surfaces, 3 borders and 2 extremities (Figs 3 and 4). Al-Bagdadi (1968) found dorsal and ventral surfaces in right adrenal gland of dromedary camel.

The lateral surface of right adrenal gland was roughly flat (Figs 3 and 4), the medial surface was convex and the ventral surface was flat. Al-Bagdadi (1968) found that the dorsal and ventral surfaces of the right adrenal were flat in dromedary camel more or less like that of the sheep. On the ventral surface towards the cranial and caudal end, the dorsal and ventral adrenal artery entered into the gland, respectively.

The medial, dorsal and lateral borders were convex (Figs 3 and 4). On the contrary, Al-Bagdadi (1968) found that the right adrenal gland had rounded borders at their dorsal and ventral surfaces, and the inner medial surface was smooth in dromedery camels. The cranial extremity appeared broad and convex, while the caudal extremity was pointed.

The left adrenal gland had 2 surfaces, 2 borders and 2 extremities. Its dorsal surface was convex and ventral surface was flat (Figs 3 and 4). The finding was in partial harmony with the findings of Al-Bagdadi (1968) in camel who found that the dorsal and ventral surfaces of the left gland were convex. Towards the caudal end of ventral surface, the ventral adrenal artery entered. The lateral and medial borders were convex. The cranial and caudal extremities were rounded and convex.

Topography

The right adrenal gland was located between the right kidney and liver (Fig 1), which simulated the

finding of Raghavan (1964) in ox, Abubakar (2015) in camel, Kumar and Sharma (2017) in Gohilwadi goat and Barreiro-Vázquez (2020) in Holstein Friesian cow.

The dorsal surface of both right and left adrenal gland faced towards the retroperitoneal part of roof of the abdominal cavity. This was in conformity with the findings of Budras and Habel (2003) in bovine.

The ventral surface of the right and left adrenal gland was close to caudal vena cava, which was also noticed by Barszcz *et al* (2016) in European Bison and it was in harmony with the finding of Barreiro-Vázquez *et al* (2020) who found a notch for the caudal vena cava on ventral surface of adrenal gland of Holstein Friesian cow.

Cranial pole of right adrenal gland was embedded into the ventral surface of the liver (Fig 1). This finding resembled with the reports of Karakurum *et al* (2008) in donkey and Ye *et al* (2017) in Bactrian camel. This finding was in partial harmony with the report of Al-Bagdadi (1968) who revealed that the right adrenal was in contact with the liver at the medial border of the renal impression of the liver in camel.

The caudal pole of right and left adrenal glands was connected with the cranial pole of the corresponding kidney by a fibrous cord like structure (Fig1). The finding was in partial harmony with the findings of Wenling *et al* (2015) in Bactrian camel, who found that a novel connection between the adrenal gland and the kidney that mainly consisted of fibrous tissue, blood vessels and nerve bundles in Bactrian camel and named it fibrous tissue-blood vessels-nerve bundles (FBN bundle).

The medial border of the right adrenal gland was in contact with aorta. The lateral border was in

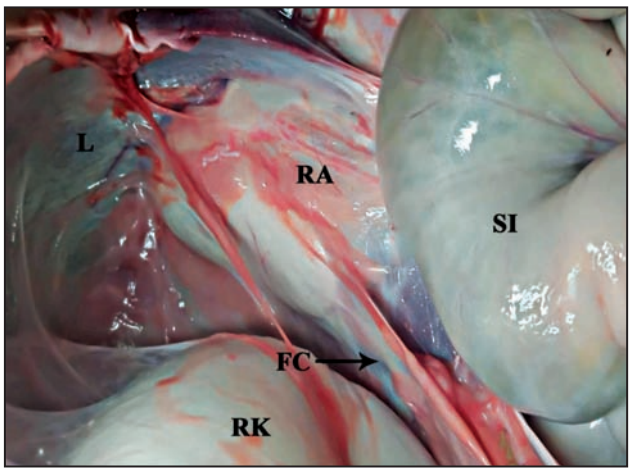

Fig 1. Photograph showing *in-situ* attachment of right adrenal gland of the camel. RA – Right adrenal gland, RK – Kidney, SI – Small intestine, L – Liver, FC – Fibrous cord.

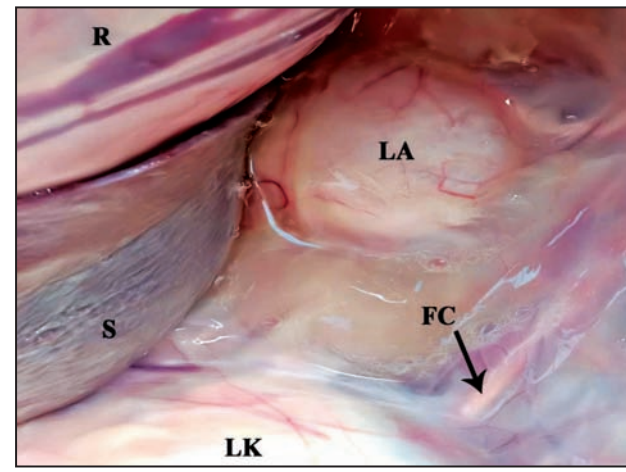

Fig 2. Photograph showing *in-situ* attachment of left adrenal gland of the camel. S – Spleen, LA – Left adrenal gland, R – Rumen, LK – Left kidney, FC – Fibrous cord.

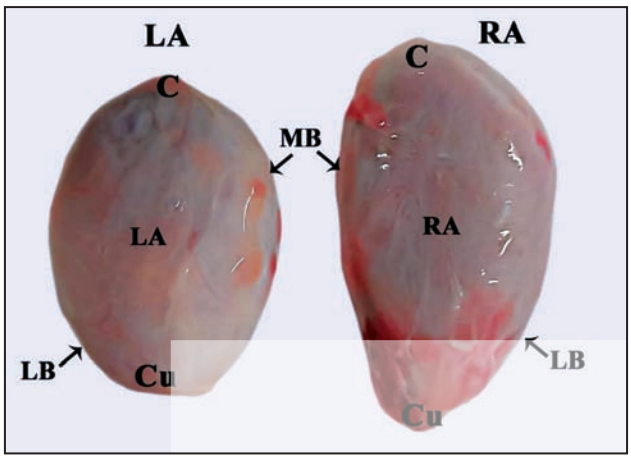

Fig 3. Photograph showing the dorsal surface of the adrenal glands in camel. LA – Left Adrenal, RA – Right Adrenal, C – Cranial end, Cu – Caudal end, MB – Medial Border, LB- Lateral Border.

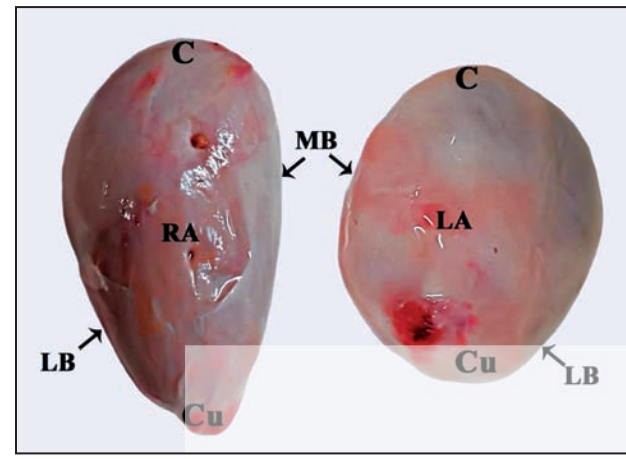

Fig 4. Photograph showing the ventral surface of the adrenal glands in camel. LA – Left Adrenal, RA – Right Adrenal, C – Cranial end, Cu – Caudal end, MB – Medial Border, LB- Lateral Border.

contact with ventral surface of liver. Cranial pole of left adrenal gland was in contact with lateral surface of the spleen. The medial border was present towards abdominal aorta. The lateral border was in contact with medial surface of spleen. It was in disagreement with the finding of Barszcz *et al* (2016) who found that the medial border of left gland was positioned next to the caudal vena cava and lateral border was adjacent to the rumen in European Bison.

Weight

The average weight of the left adrenal gland was 38.19 ± 3.80 gm, ranged from 27.45 to 49.47 gm. The average weight of right adrenal gland was 46.91 ± 3.15 gm, ranged between 37.50 to 56 gm (Table 1). However, Budras and Habel (2003) observed that the weight of each adrenal gland was 15-23 gm in bovine. Dangi *et al* (2008) recorded the average weight of adrenal as 1.73 gm in goat and Ye *et al* (2017) reported that the weights of left and right adrenal were about 12.52 ± 2.24 gm and 12.39 ± 2.02 gm, respectively in Bactrian camel.

Table 1. Average weight of left and right adrenal glands.

Sr. no.	Weight of left adrenal (gm)	Weight of right adrenal (gm)
1.	49.47	56.00
2.	36.88	46.70
3.	27.45	37.50
4.	48.33	54.66
5.	38.12	47.74
6.	28.90	38.85
Mean ± S.E.	**38.19 ± 3.80**	**46.91 ± 3.15**

The difference was statistically significant between left and right, showed that the right adrenal gland was heavier than the left one (Table 4). Whereas, Budras and Habel (2003) in bovine, Ashok *et al* (2005) in crossbred goat, Dangi *et al* (2008) in goat, Kumar and Sharma (2017) in Gohilwadi goat and Barreiro-Vazquez *et al* (2020) in Holstein Friesian cow showed that the left gland was heavier than the right gland. It was contradictory to the statement of Ye *et al* (2017) that there was no significant difference in the gland weight (P > 0.05) in Bactrian camel.

Length

The length of left and right adrenals ranged between 51.37 to 56.90 mm and 62.56 to 75.46 mm, respectively. The average length of the left and right adrenal gland was 54.03 ± 0.84 mm and 68.99 ± 2.06mm, respectively (Table 2). Al-Bagdadi (1968) found that the length of left and right gland was 48 mm and 42 mm, respectively in dromedary camels. Dangi *et al* (2008) found the average length of the adrenal gland that was 2.01 cm in goats and Ye *et al* (2017) found that the length of left and right gland was 4.20-5.60 and 5.20-7.10 cm, respectively in Bactrian camel.

The difference between left and right adrenal length was statistically significant hence the right adrenal was longer than the left adrenal (Table 4), which was in close agreement with the report of Elkbashi (2020) in camel. Contrarily, the left gland was longer than the right one in goats (Dangi *et al,* 2008) and sheep (Sisson and Grossman, 2012).

Width

The average width of the right and left adrenal glands were recorded as 34.58 ± 2.42 mm and 39.56 ± 1.79 mm, respectively that ranged between 27.55 to 44.18 mm and 34.51 to 46.46 mm, respectively (Table 2). Al-Bagdadi (1968) revealed that average width of the right and left adrenal glands were mentioned as 40mm and 35mm, respectively in camel. The average width of adrenal gland was 1.17 cm in goat (Dangi *et al,* 2008) whereas Ye *et al* (2017) observed in Bactrian camel that the width of left and right glands were 3.30-4.00 cm and 2.10-3.00 cm, respectively. The difference was statistically significant between left and right, hence the right adrenal gland was narrower than the left adrenal gland (Table 4). It was

Table 2. Average measurements of gross parameters of adrenal glands.

S. No.	Length(mm)		Thickness(mm)		Width(mm)	
	Left	Right	Left	Right	Left	Right
1.	56.90	75.46	25.85	28.88	46.46	44.18
2.	54.69	69.92	25.17	27.45	40.28	37.24
3.	52.45	64.33	23.18	25.46	37.53	33.77
4.	55.53	73.56	24.36	27.90	42.30	35.30
5.	53.24	68.15	23.58	26.47	36.25	29.46
6.	51.37	62.56	22.73	24.33	34.41	27.55
Mean ±S.E	**54.03±0.84**	**68.99±2.06**	**24.15±0.49**	**26.75±0.68**	**39.56±1.79**	**34.58±2.42**

in congruence with the observations of Dangi *et al* (2008) in goat.

Table 3. Average volume of left and right adrenal glands.

Sr. no.	Volume of left adrenal (ml)	Volume of right adrenal (ml)
1.	45	53
2.	42	50
3.	41	47
4.	44	51
5.	41	48
6.	40	46
Mean ± S.E.	**42.17 ± 0.79**	**49.17 ± 1.08**

Table 4. Statistical analysis of biometrical observation of various parameters of adrenal glands of dromedary camel.

Character	Adrenal	Range	Mean ± S.E.	Paired t^2 test
Weight of adrenal (gm)	Right	37.50-56.00	46.91 ± 3.15	12.01^S
	Left	27.45-49.47	38.19 ± 3.80	
Length of adrenal (mm)	Right	62.56-75.46	68.99 ± 2.06	12.07^S
	Left	51.37-56.90	54.03 ± 0.84	
Width of adrenal (mm)	Right	27.55-44.18	34.58 ± 2.42	-5.58^S
	Left	34.51-46.46	39.56 ± 1.79	
Thickness of adrenal (mm)	Right	24.33-28.88	26.75 ± 0.68	9.29^S
	Left	22.73-25.85	24.15 ± 0.49	
Volume of adrenal (ml)	Right	46-53	42.16 ± 0.79	19.17^S
	Left	40-45	49.17 ± 1.08	

At the 5% level. NS - Non significant S – Significant

Thickness

Thicknesses of left and right adrenal glands were ranged between 22.73 to 25.85 mm and 24.33 to 28.88 mm, respectively. The average thicknesses of left and right adrenals were 24.15 ± .49 mm and 26.75 ± 0.68 mm, respectively (Table 2). Ye *et al* (2017) observed that the left and right adrenal gland of Bactrian camel were 1.00-1.50 cm and 1.30-1.70 cm thick, respectively.

The difference between the left and right adrenal length was statistically significant and accordingly the right adrenal was thicker than the left adrenal (Table 4). This was in accordance to the findings of Elkbashi (2020) and Al-Bagdadi (1968) in camels. Dangi *et al* (2008) mentioned that the left adrenal was thicker than the right in goat.

Volume

Average volumes of the left and right gland were estimated as 42.17 ± 0.79 ml and 49.17 ± 1.08 ml, respectively that ranged from 40 to 45 ml and 46 to 53 ml, respectively (Table 3). On the contrary, Ye *et al* (2017) found the volume of each adrenal gland of Bactrian camel was 13.01 ± 1.42 cm^3. The difference between right and left adrenal volume was statistically significant hence the right adrenal had large volume than the left adrenal (Table 4).

Acknowledgement

The authors are thankful to the Dean, College of Veterinary and Animal Science, Bikaner, RAJUVAS, Bikaner, Rajasthan for providing all the necessary facilities to carry out this research work.

References

Abdalla Mohamed and Ali A. Morphometric and histological studies on the adrenal gland of the camel (*Camelus dromedarius*). Acta Morphologica Neerlando-Scandinavica. 1989; 26:269-81.

Abubakar UM. Anatomical studies on thyroid, parathyroid and adrenal glands of the indigenous one humped camel (*Camelus dromedarius*). M.Sc. thesis, Ahmadu Bello University, Nigeria. 2015.

Al-Bagdadi FAK. The adrenal gland of the camel (*Camelus dromedarius*). Zentralblatt für Veterinärmedizin Reihe A. 1968; 16(4):354-364.

Ashok N, Harshan KR and Chungath JJ. Morphological studies on the developing adrenal gland in crossbred goats (*Capra hircus*). Indian Journal of Animal Science. 2005; 75:1380-1381.

Barreiro-Vazquez JD, Lois AB and Miranda M. Ultrasonography of normal adrenal glands in adult holstein–friesian cows: A Pilot Study. Animals. 2020; 10:1171; doi: 10.3390/ani10071171.

Barszcz K, Przespolewska H, Olbrych K, Czopowicz M, Nawrot JK, Harłajczuk KG and Kupczyńska M. The morphology of the adrenal gland in the European bison (*Bison bonasus*). BMC Veterinary Research. 2016; 12:161.

Budras KD and Habel RE. A Text Book of Bovine Anatomy. schlütersche. 1st ed. pp. 82-83. 2003.

Dangi A, Joshi S, Mathur R and Nama KG. Gross and morphological studies on adrenal gland of goat (*Capra hircus*) in semi-arid zone. Veterinary Practitioner. 2008; 9:1:25-27.

Elkbashi EEO. Morphological, histometric and histochemical studies on the adrenal gland of the camel (*Camelus dromedarius*). Unpublished Ph.D. Thesis, Sudan University of Science and Technology, Sudan. 2020.

El-Nahla, SM, Imam HM, Moussa EA, Elsayed AK and Abbott LC. Prenatal development of the adrenal gland in the

one-humped camel (*Camelus dromedarius*). Anatomia, Histologia, Embryologia. 2011; 40:169-186. https://doi.org/10.1111/j.1439-0264.2010.01056.x

Hill M. Endocrine development–adrenal glands. In: Embryology. University of New South Wales Publications, Sydney. 2007; pp 234-300.

Karakurum E, Ozgel O and Dursun N. Morphology and arterial vasculature of donkey (*Equus asinus* L.) adrenal gland. Turkish Journal of Veterinary and Animal Sciences. 2008; 32(6):469-473.

Kumar V and Sharma A. Gross morphometric study on postnatal development of adrenal gland in gohilwadi goat (*Capra hircus*). The Indian Journal of Veterinary Sciences and Biotechnology. 2017; 12(03):96-98.

Nabipour A, Khanzadi S and Behdegani A. Gross and histological study on the adrenal glands in camel (*Camelus dromedarius*). Journal of Camel Practice and Research. 2008; 15(1)121-125.

Nandeshwar NC, Banubakode SB, Charjan RY, Mainde UP and Rana J. Biometrical studies on adrenal gland of goat in different age groups. International Journal of Science, Environment and Technology. 2017; 6(4):2683-2687.

Osman EE, Ali HA and Ibrahim ZH. Gross anatomy of the adrenal gland of the dromedary camel (*Camelus dromedarius*). Journal of Agricultural and Veterinary Sciences Qassim University, 2019; 12:2, 3-24.

Raghavan D. Anatomy of the Ox. Indian Council of Agricultural Research, New Delhi. 1st Edn, pp 413-415. 1964.

Rehan Sarmad and Qureshi Anas Sarwar. Morphometric analysis of heart, kidneys and adrenal glands in dromedary camel calves. Journal of Camel Practice and Research. 2007; 14(1):27-31.

Sisson and Grossman JD. The Anatomy of the Domestic Animals. 5th Edn. (Revised), W.B. Saunders Company, Philadelphia and London. 2012.

Wenling Y, Fengling W, Shuangyu L, Yagi W, Shuo D and Jianlin W. A novel path of communication from kidney to the adrenal gland in Bactrian camels (*Camelus bactrianus*). International Journal of Morphology. 2015; 33(4):1460-1462.

Ye W-L, Wang F-L, Wang H-J and Wang J-L. Morphological and ultrastructure of the adrenal gland in Bactrian camel (*Camelus bactrianus*). Tissue and Cell. 2017; 49:285-295.

DOI : 10.5958/2277-8934.2022.00035.2 Vol 29 No 2, p 251-255

HISTOLOGICAL STUDY OF PRENATAL DEVELOPMENT OF THE SPLEEN IN CAMEL (*Camelus dromedarius*)

A.M. Marwa-Babiker[1,2], T.A. Althnaian[1] and A.M. Ali[1]

[1]Department of Anatomy, College of Veterinary Medicine, King Faisal University, P.O. Box 400 Al-Ahsa 31982, Saudi Arabia
[2]Department of Anatomy, College of Veterinary Medicine, University of Bahri, Khartoum-North, Sudan, P.O. Box 012, Khartoum North 12217, Sudan

ABSTRACT

Spleen development in the camel foetus was studied during the 1st, 2nd and 3rd trimesters of gestation using histological techniques. Ten spleens of camel foetuses were collected from Omran slaughterhouse, Al-Ahsa, Saudi Arabia. The samples were prepared by routine histological procedures and stained by the general histological stain (H and E) and some other special stains including Van Geison's for collagenous fibres, Verhoff's for elastic fibres, Gordon and Sweet for reticular fibres. At the 1st trimester, the spleen capsule was composed of fine connective tissue fibres, in the 2nd trimester the capsule and trabeculae showed thick connective tissue, while in the 3rd trimester the capsule also showed smooth muscle fibres and surrounded with large amount of adipose tissue. The parenchyma, at the 1st trimester consisted of randomly distributed lymphocytes and macrophages. At the 2nd and 3rd trimesters, it was arranged as white and red pulps. Megakaryocytes observed previously in the red pulp of adult dromedary camel were seen in the red pulp at the 1st, 2nd and 3rd trimesters of gestation. It was concluded that the spleen showed very important histological developmental changes throughout the three gestational stages.

Key words: Camel, development, foetus, gestational stage, histology, spleen

The mammalian spleen develops as gathering of mesenchymal cells in the dorsal mesogastrium. The mesenchymal cells differentiate and form the splenic capsule and connective tissue (McGeady *et al,* 2017). The histomorphological structure of the spleen has been reported by many authors (Bello *et al,* 2019; Jaji *et al,* 2019; Zidan, 2000a, Maina *et al,* 2014).

It has been stated that the spleen is surrounded by a capsule from which fibrous trabeculae emerge (Dijkstra and Veerman, 1990; Alshamarry, 2010). The spleen of the one humped camel consists of a thick capsule and parenchyma consists of splenic pulp, which is composed of white pulp packed with lymphocytes and red pulp consisted of three-dimensional reticular network and splenic sinuses (Zidan *et al,* 2000a).

Bello *et al* (2016) stated that the spleen of dromedary foetus had red and white pulps of variable shape and size and special feature of connective tissue inter-digitations of variable sizes into the parenchyma along the whole surface at second and third trimester. However, there was paucity in the literature on the development of the spleen in camel foetus. Therefore, the aim of this study was to provide more information about the histological structure of the prenatal development of spleen of the dromedary camel foetus.

Materials and Methods

Ten spleens of camel foetuses were collected from Omran slaughterhouse, Al-Ahsa, Saudi Arabia. The Research Ethics Committee, Deanship of scientific research, King Faisal University approved all experiments number: KFU-REC-2022-JAN-EA000343. Depending on the gestational age (GA), the foetuses were divided into three groups: first (0-130 days), second trimester (131-260 days) and third trimester (261-423.5 days). The age of the foetus was determined using the equation of crown vertebral-rump length (CVRL) GA = (CVRL + 23.99)/0.366

Small pieces (about 1cm^3 thick) were taken, then were fixed in 10% buffered formalin. The specimens (5 µm thick) were processed by routine histological procedures and stained with (H&E) and some special stains including Van Geison's for collagenous fibres, Verhoff's for elastic fibres, Gordon and Sweet for reticular fibres (Bancroft and Stevens, 2008).

SEND REPRINT REQUEST TO AM MARWA-BABIKER email: mbabakr@kfu.edu.sa

Results and Discussion

The histological details of foetal spleen obtained at different GA were noted. The foetal spleen obtained at 1st trimester was surrounded by a thin capsule of fine loose connective tissue fibres or mesenchymal connective tissue from which connective tissue trabeculae extended in the parenchyma (Fig 1). At the second trimester, the connective tissue capsule and the trabeculae became thickened in foetal spleen. The diffuse collagen connective tissue into the parenchyma was observed at the stage of 2nd trimester (Fig 2). At the third trimester, the foetal spleen capsule consisted of dense regular connective tissue with few smooth muscle fibres that also extended in the trabeculae and the spleen was surrounded with large amount of adipose tissue (Fig 3). However, at the late stages of the third trimester, the smooth muscle fibres were clearly visible in the trabeculae (Fig 3, d).

At the first trimester, the white and red zones of the foteal spleen were not clearly differentiated and the parenchyma showed large amount of randomly distributed B &T lymphocytes and large spherical macrophages with oval nuclei and eosinophilic cytoplasm (Fig 1). Giant cells (Megakaryocytes) with lobulated nuclei and highly eosinophilic cytoplasm were also observed (Fig 1).

At the 2nd trimesters, the foetal spleen parenchyma began to differentiate in a white and a red pulp. The megakaryocytes were clearly shown in the red pulp with lobulated nuclei (Fig 2).

At the 3rd trimesters, the foetal spleen parenchyma was differentiated in white and red pulps. The white pulp showed splenic corpuscles which consisted of lymphatic nodules (B-dependent zone) surrounding the central artery and periarterial sheath of non-nodular lymphoid tissue (T-dependent zone). The red pulp fills the spaces between the capsule, the trabeculae and the white pulp. The red pulp was formed of splenic venous sinuses and splenic cords in-between the sinuses that was composed of reticular net fixed to it, reticular cells and suspended aggregates of red blood cells, B & T lymphocytes and macrophages (Fig 3). In addition, the megakaryocytes were observed at the 3rd trimesters of gestation in the red pulp only (Fig 3). The number of megakaryocytes cells were increased at the 3rd trimester and some of them showed binucleated nuclei (Fig 3, c).

The present study showed that the foteal spleen at the 1st trimester of GA was surrounded with capsule which start with fine connective tissue fibres and send fine connective tissue trabeculae in the parenchyma, then at the 2nd trimester capsule and trabeculae appeared thicker. At the stage of the 3rd trimester of GA the capsule became thick and the smooth muscle fibres were surrounded with large amount of adipose tissue. The present study agreed with some previous studies (Bello *et al,* 2016) which stated that trabecular connective tissue and capsular thickness increase depending on the developmental stages. According to Jaji *et al* (2019) the capsule in the spleen of the dromedary camel foetus had an inner smooth muscle and an outer predominant connective tissue layer. However, in present study the most of the salient features of the postnatal spleen were already evident in the first growth phase and became more developed by the second phase.

In the present study, the splenic corpuscles were observed clearly at the 3rd trimester of GA where lymphatic nodules surrounded the central artery and a non-nodular zone was seen. The red pulp is formed of splenic venous sinuses, splenic cords, reticular cells, blood cells and macrophages. The splenic cords were suspended by reticular cells net with aggregates of blood cells and macrophages. According to Veerman and van Ewijk (1975) and Steiniger (2015) the composition of the white pulp of some animal species consisted of periarteriolar lymphatic sheath (PALS), follicles and marginal zone. There were three compartments, each had their specific lymphoid and non-lymphoid cells. Reticular cells and reticulin fibres, although found in all three compartments, they formed a characteristic pattern in each compartment.

The arrangements of the spleen parenchyma was also described previously in some species (Eurell and Frappier, 2006 and Steiniger, 2015). The spleen consisted of the white pulp embedded in the red pulp. In the white pulp, T and B lymphocytes formed accumulations, the periarteriolar lymphatic sheaths located around intermediate-sized arterial vessels, the central arteries. The red pulp was a reticular connective tissue containing all types of blood cells (Steiniger, 2015). In this study a large amount of randomly distributed B and T lymphocytes, macrophages and erythrocytes, megakaryocytes were shown in Ist trimester. In the 3rd trimester splenic corpuscles the white pulp consisted of lymphoid tissue formed of lymphatic nodules was surrounded the central artery.

The number of the megakaryocytes in the red pulp of adult dromedary camel decreased with

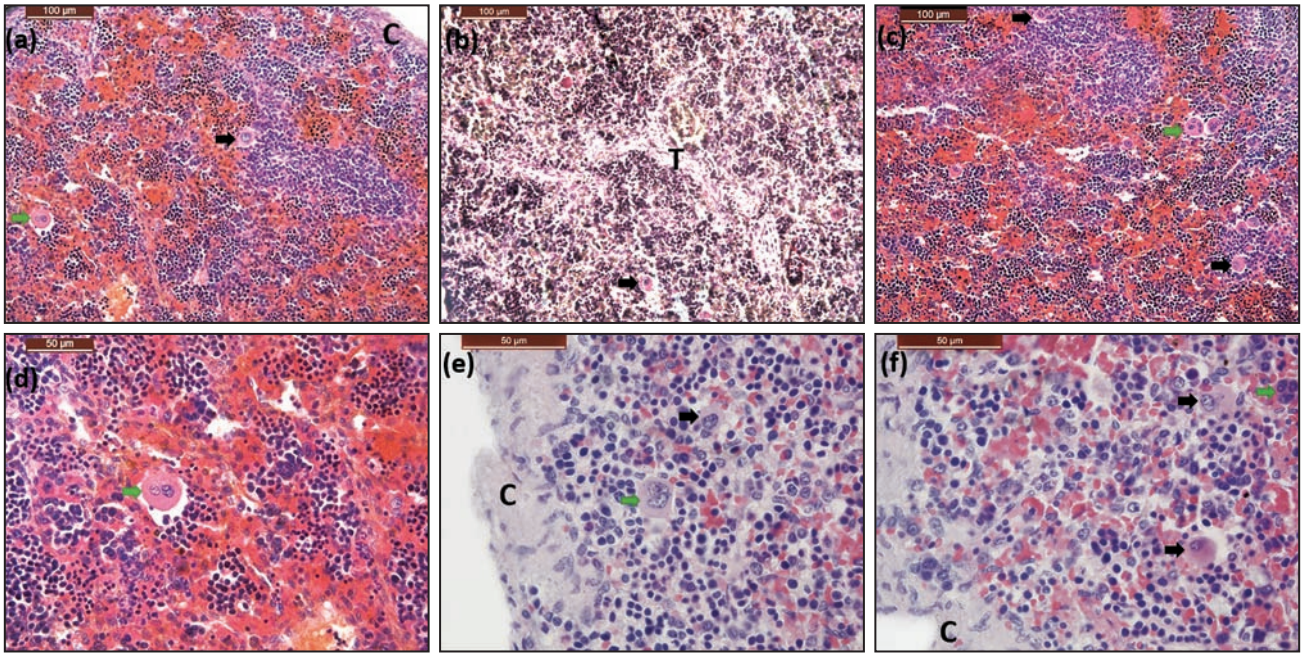

Fig 1. Photomicrographs showing spleen of camel foetus during the 1st trimester of gestation; connective tissue capsule (C) and fine connective tissue trabeculae (T), randomly distributed lymphocytes, macrophages and megakaryocytes were seen (arrows), binucleated megakaryocyte were present (green arrow). (a & c) Haematoxylin and Eosin (X20) (b) Gordon and Sweet (X20), (d) Haematoxylin and Eosin (X40), (e & f) Haematoxylin and Eosin (X100).

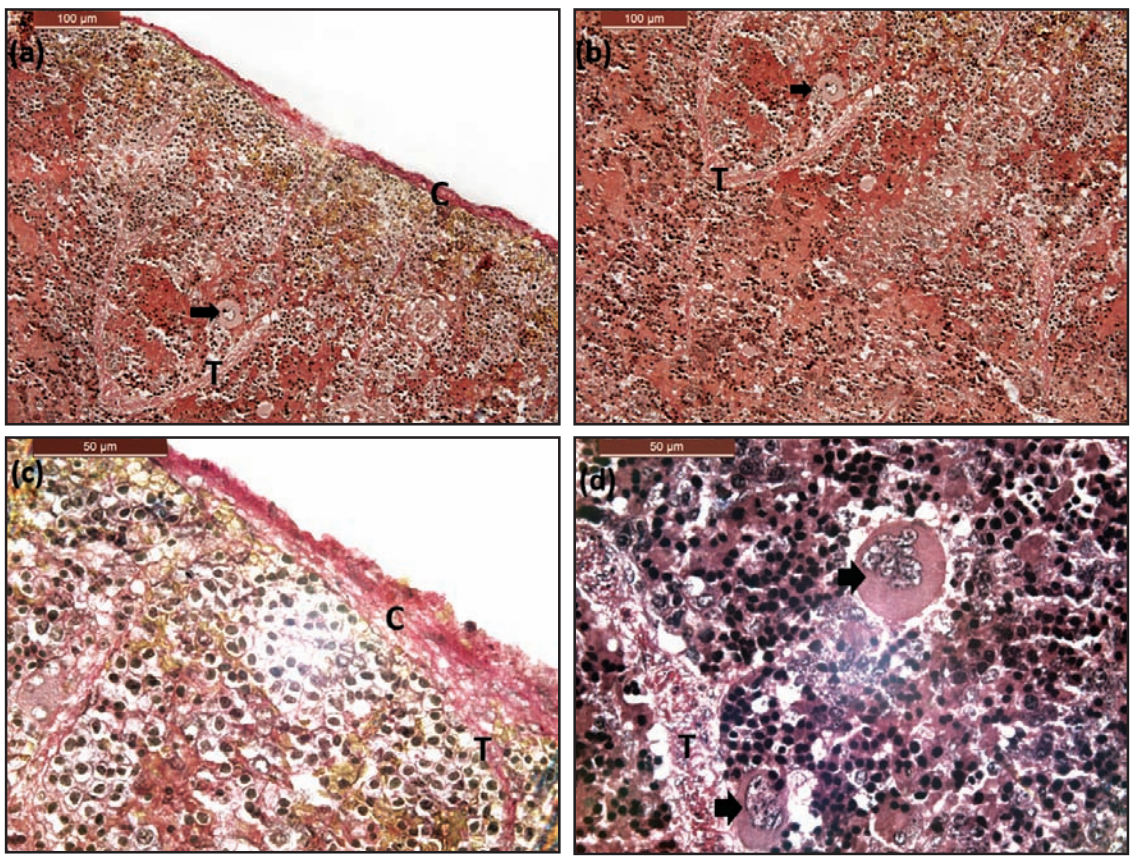

Fig 2. Photomicrographs showing spleen of camel foetus during the 2nd trimester of gestation; connective tissue capsule (C) connective tissue trabeculae (T) Especially collagen fibres. (a), (b) and (c); Megakaryocytes (arrows). (a), (b) and (c) Van Gieson's (X20, X20, X63 respectively), (d), Gordon and Sweet (X63).

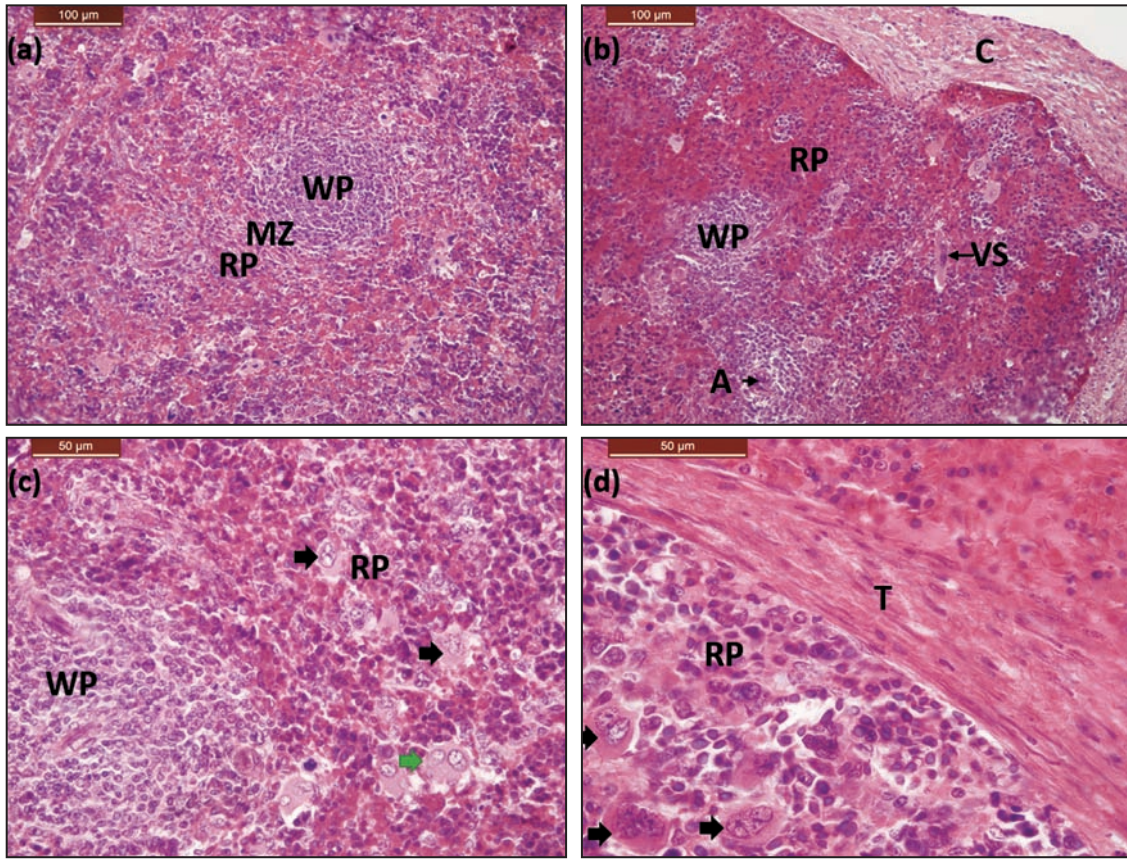

Fig 3. Photomicrographs showing spleen of camel foetus during the 3rd trimester of gestation; (a) white pulp (WP) surrounded central artery (A). (b), red pulp consists of venous sinuses (VS) at the margin of white pulp, marginal zone (MZ). Capsule (C) and trabeculae (T) consisted of smooth muscle fibres. (c and d); Megakaryocytes had lobulated nuclei (black arrows), binucleated megakaryocyte were present (green arrow). Haematoxylin and Eosin. (a) and (b): (X20), (c): (X40), (d): (X100).

age (Zidan *et al,* 2000b). However, megakaryocytes observed in the red pulp of foetal spleen of present study at the 1st, 2nd and 3rd trimesters increased in their numbers during the three GA. Binucleated megakaryocytes were observed at the 3rd trimester of GA.

The results of present study showed that the development of the spleen in 1st GA showed ordinary mesenchymal cells and undifferentiated zones of white and red pulps which later developed into differentiated zones of white and red pulps. In addition, the capsule and trabeculae developed from fine connective tissue to well-developed connective tissue. This development followed the advancement in subsequent GA from 1st to 3rd trimester.

Acknowledgement

The authors gratefully acknowledge King Faisal University, represented by the Deanship of Scientific Research, on the material support for this research under the number (GRANT574) during the academic year 1443 AH/ 2022 AD.

References

Alshamarry HA. Histological and histometric study on the spleen of Iraqi camel (*Camelus dromedarius*). Emirates Journal of Food and Agriculture. 2010; 22(1):65-70.

Bancroft DG and Stevens A. Theory and Practice of Histological Techniques. 6th ed. Edinburgh, London and New York: Bath Press, Avan. Churchill Livingston. 2008.

Bello A, Onu JE, Fawaz AM, Hena SA, Sonfada ML, Umaru MA and Shehu SA. Prenatal development of the spleen of one-humped camel (*Camelus dromedarius*): A comparative histological study. Scholarly Journal of Agricultural Science. 2016; 6(8):263-269.

Bello A, Onu JE, Onyeanusi BI, Sonfada ML, Umaru MA, Danmaigoro A and Hena SA. Unique anatomy of the spleen of one humped camel (*Camelus dromedarius*): a review. Open Access Journal of Biomedical Engineering and Biosciences. 2019; 3(3):294-298.

Dijkstra CD and Veerman AJP. Normal Anatomy, Histology, Ultrastructure, Rat. In: Monographs on Pathology of Laboratory Animals: Hemopoietic System. 1990; pp 185-93. Springer-Verlag, Berlin.

Eurell J A and Frappier BL. Dellmann's Text Book of Veterinary Histology. Blackwell Publishing. 2006; 6th Ed. 147-150.

Jaji AZ, Saidu AS, Mahre MB, Yawulda MP, Girgiri IA, Tomar P and Da'u F. Morphology, morphometry and histogenesis of the prenatal dromedary (*Camelus dromedarius*) Spleen. Macedonian Veterinary Review. 2019; 42(2):141-149.

McGeady TA, Quinn PJ, Fitzpatrick ES and Ryan MT. Textbook of Veterinary Embryology. 2nd ed. Blackwell Publishing Ltd, 9600 Garsington Road, Oxford OX42DQ, UK. 2017; pp 224-225.

Maina MM, Usende IL, Igwenagu E, Onyiche, T E, Yusuf ZM and Ntung NO. Gross, histological and histomorphometric studies on the spleen of one humped camel (*Camelus dromedarius*) found in the semi-arid region of North Eastern Nigeria. 2014; 4(10):703-711.

Steiniger BS. Human spleen microanatomy why mice do not suffice - Review. Immunology. 2015; 145(3):334-46.

Zidan M, Kassem A, Dougbag A and EL ghazzawi E. The spleen of the one humped camel (*Camelus dromedarius*) has a unique histological structure. Journal of Anatomy 196 (Pt 3), 2000a; (3):425-32.

Zidan M, Kassem A and Pabst R. Megakaryocytes and platelets in the spleen of the dromedary camel (*Camelus dromedarius*). Anatomia, Histologia, Embryologia. 2000b; 29(4):221-4.

Veerman AJ and van Ewijk W. White pulp compartments in the spleen of rats and mice. A light and electron microscopic study of lymphoid and non-lymphoid cell types in T- and B- areas. Cell and Tissue Research. 1975; 156(4):417-441.

"LA CAMELERIE"- FIRST DAIRY CAMEL FARM IN FRANCE

The first dairy camel farm "La Camelerie" producing, and processing camel milk is open in North of France close to Belgium border. It has 70 camels (dromedaries, Bactrian and hybrids). The farm in the France, had camels since several years for touristic attraction, but since June 22, milk production is started (pasteurised milk, kefir and cheese). The farm is a partner of the European project "CAMELMILK" aiming to boost the camel milk production and processing around the Mediterranean Basin. The country partners are Algeria, Turkey, France, Germany, and Croatia under the coordination of Spain and with the scientific support of Dr Bernard Faye. In Europe, dairy camel farms are already working in Netherland and in Germany. In France, camel milk production is also expected in two other farms, contributing to the diversification of milk sector in a country where camel rearing is developing recently. Due to this emergence of new camel farming out of the traditional "camel countries", Dr Bernard Faye has edited a book (in French) for all the camel farmers and vets in French-speaking countries.

The camel herd of " La Camelerie" in the North of France

Pasteurised and camel cheese making at "La Camelerie" dairy plant

INSTRUCTIONS TO CONTRIBUTORS

(Effective from year 2022)

(Journal of Camel Practice and Research - triannual -April, August and December issues every year)

The Journal of Camel Practice and Research (JCPR) is a triannual journal (April, August and December issues) published in the English language by the Camel Publishing House, 67, Gandhi Nagar West, Near Lalgarh Palace, Bikaner, 334 001 (India). It is in offset print size of 20.5x27.5 cm in two columns with a print area of 17x22 cm. It will be known as **Journal of Camel Practice and Research** with **Volume number** on yearly basis and **Number** on issues per volume basis (in exceptional cases there can be more than three issues in a volume). The editorial policies of JCPR are established by the editor-in-chief and is detailed in this section. Views expressed in papers published in JCPR represent the opinions of the author(s) and do not necessarily reflect the official policy of the author's affiliated institution, or the editor-in-chief.

Nature of coverage: This journal is dedicated to disseminate scientific information about new and old world camelids in form of **Original research** articles in camel science, health, husbandry, pastoralism, sports, specific behaviour, history and socio-economics. **Reports** on unusual clinical case(s) or unreported management of clinical case(s) are also published. Review articles will be accepted on invitation only. **Book review** directly or indirectly related to camels will be reviewed by subject-matter specialists and included if sent to the journal for this purpose. The Journal of Camel Practice and Research will occasionally contain an **invited editorial** commenting on the current research and papers in the issue.

Submission of manuscript: Manuscripts should be submitted in word files to **Dr. Tarun Kumar Gahlot**, Editor, Journal of Camel Practice and Research at tkcamelvet@yahoo.com or by online submission portals available at www.indianjournals.com or www.camelsandcamelids.com. The figures can be submitted preferably as a high pixel JPEG or other format. The manuscript should be accompanied by a covering note and author consent letter from the author responsible for correspondence. It should also contain a statement that manuscript has been seen and approved by all co-authors. Editor and members of the editorial board are not responsible for the opinions expressed by authors and reserves the right to reject any material or introduce editorial changes. Material will be accepted for publication on the understanding that it has not been published in any other form and is not being considered elsewhere. Any material once accepted for publication may not be republished in any form without prior permission of the author. **Single blind peer review policy** is used for the manuscripts submitted and the quality standards are maintained by the JCPR editorial board and by authors who submit manuscripts for publication. A preprint PDF is provided to the author in correspondence for verification of contents and corrections, if any.

Preparation of the manuscript: Manuscript should be typed in Book Antiqua font size 12 using British English, spellings and generic names of drugs. International Code of Zoological Nomenclature, Nomina Anatomica Veterinaria, International Code of Nomenclature of Bacteria, International Code of Botanical Nomenclature and International Standards should be strictly followed. All terms should be identified by their scientific names and for easy comprehension common terms/names can be used. Population data and geographical distribution of camelids should invariably be avoided in introduction, unless it is warranted. Kindly remain restricted to the relevant subject matter of given title of manuscript only. The review of literature should be up to the submission year of manuscript. Kindly check every reference for its accuracy from the relevant book, journal or through google.

Each manuscript should have the following sections:

Title page: This page should contain title of the article, name of the department/institution where work has been done, present postal address of each author and name of author with email to whom reprint request should be addressed.

Running title should be short, succinct title with not more than 45 keystrokes (characters plus spaces) in length. A title should have the first word and proper nouns capitalised. Species of subject is encouraged. The title should be unique. All authors should have preferably full names (given name, middle initial, family name). Institutions of the authors with location should be denoted with either symbols (*, †, ‡, §, #, ||, and ¶) or Roman numerals behind the author's last name. Affiliation should also include department, city, state, country, and postal code.

Following is the example:

Example:

PROTEOMIC CHARACTERISATION OF SERUM DURING THE BREEDING CYCLE IN MALE BACTRIAN CAMELS

Le Hai[1], Rendalai Si[2], Fu-Cheng Guo[1], Jing HeI, Li Yi[1], Liang Ming[1], Jun-Wen Zhou[3], La Ba[3], Rigetu Zhao[3] and Rimutu Ji[1,2]

[1]Key Laboratory of Dairy Biotechnology and Bioengineering, Ministry of Education, Inner Mongolia Agricultural University, Hohhot, Inner Mongolia, China

[2]Inner Mongolia Institute of Camel Research, Badanjiran, Inner Mongolia, China

[3]Alxa League Institute of Animal Husbandry, Alxa, Inner Mongolia, China

SEND REPRINT REQUEST TO RIMUTU JI email: yeluotuo1999@vip.163.com

Abstract and Key words: A single paragraph of no more than 2,500 keystrokes (characters plus spaces) that summarises the results in an understandable form using statistical evidence (P-values). Abbreviations are defined at first use in the ABSTRACT and again in the body of the manuscript. List up to 6 key words in alphabetical order and separated by a comma. Capitalise only proper nouns. Do not use abbreviations. Place the key words at the end of the Abstract.

Text: The proper text of the paper should commence after key words. The text should be divided into sections with headings, introduction, materials and methods, results, discussion, tables/illustrations and references.

Introduction: The logic of the introduction is to introduce the specificity and relevance of the topic to the readers. It should include the objective of the work in brief and most important related reference(s). The contents of the introduction should be lucid showing a clear justification for conducting the research with a stated hypothesis and objective(s) is required. The population data of camelids and their importance should be avoided as it is well known and is not relevant to the title in

most of the manuscripts. Authors should not write the word, "First report" as later it is found that previous reports exist. The rationale for the experiments should place the work into the context of existing literature. There is NO word limit on the section but brevity is encouraged.

Materials and Methods: Should contain details regarding materials and brief account of procedures used. The manuscript must include a statement of institutional animal care and use or ethical committee, or country-specific equivalent, approval of all animal procedures. This statement should appear as the first item in MATERIALS AND METHODS and should specify which publicly available animal care and use standards were followed. A clear description of all biological, analytical and statistical procedures is required with each section denoted by a short descriptive title (i.e., Animals and sampling, Tests used, Treatment, Experimental design and analysis, etc). Materials used must include the product name and vendor at first mention. When a commercial product is used as part of an experiment, the manufacturer name and location must be given parenthetically and the generic name should be used subsequently. No ™, ®, or © symbols should be used. Sex, breed, age, species are included in the animal descriptions. Provide evidence of assay validation, or suitable published reference, as well as inter/intra-assay CV, as needed. Appropriate statistical methods should be used with experimental unit defined. Numbers of biological and experimental replicates should be stated. State the threshold for significance ($P < 0.05$) and definition of tendency if used. In case reports, the case record sheet should also be included in materials and methods.

Results and Discussion should be presented in logical sequence with implications of findings about other relevant studies. The data or information easily attainable from the tables or graphics need not be repeated in the results. Only important observations need to be summarised. Undue repetition of the text from results to discussion has to be avoided. To preclude it, depending on article, results and discussion can be combined. In discussion only significant results should be discussed. One should not always stick to the term `statistically significant' data rather biological importance or significance of any variation should be given due importance in discussion. The section contains the interpretation of the results. It should be clear and concise, address the biological mechanisms and their significance, and integrate the results into existing literature. The Discussion may offer an interpretation that is consistent with the data. Do not include any reference to tables and figures or include P-values in the Discussion. Authors have the option to create a single RESULTS AND DISCUSSION section.

Tables: Each tables should be typed on separate sheet. Large tables should be avoided and should not exceed one page. Each table should be numbered in Indo-Arabic numerals according to their sequence in the text that refers to it. In the text it should be referred as proper noun e.g., Table 1. The title of the table should be brief and self-explanatory. Footnotes can be included to enhance understanding ability of the contents of the table.

Illustrations and Legends: All illustrations should be submitted about twice the size desired for reproduction that is 17 cm for double column or 8.3 cm for single column. Photographs should be of good quality with adequate contrast and high pixels. All illustrations should be referred as figures in the text and should also be numbered in Indo-Arabic numerals e.g., Fig 1. Legends of all these figures should be typed on a separate sheet. Each legend should be clear, concise and informative. A statement of magnifications or reductions should be given where it is applicable.

Disclosures (Conflict of Interest)

The authors must disclose any actual or potential conflicts of interest that may affect their ability to objectively present or review research or data. A succinct statement detailing any perceived conflict of interest is required. If none, please indicate as such.

References: Papers in the section must either be published or 'in press'. All references must include the DOI, if available. Authors are encouraged to use the most recent reference style for the Journal of Camel Practice and Research in the reference writing. References should be arranged in alphabetical order. Authors should not modify the title of the references. Mention full name of the journal.

Examples of correct forms of references are given below:

Periodicals: Shawaf T, El Nahas A, Melegi A, Al Bulushi S, Aiyan AA and Eljalli I. Investigation on biochemical parameters of cerebrospinal fluid in camels with neurological disorders. Journal of Camel Practice and Research. 2020; 27(2):165-171.

Wilson R Trevor. The one-humped camel in Eritrea and Ethiopia: a critical review of the literature and a bibliography. Journal of Camel Practice and Research. 2020; 27(3):229-262.

For edited symposium/congress/proceedings: Abdalla HS. Camel trypanosomiasis in the Sudan. Proceedings of the First International Camel Conference, Dubai (UAE), February 2-6, 1992; pp 401-403.

Books (Personal authors): Faye B and Bengoumi M. Camel Clinical Biochemistry and Haematology: Springer International Publishing. 2018; pp 275-286.

Chapter from multiauthored books: Wernery U, Kinne J and Schuster RK. Unusual arboviruses and other minor viral infections. In: Camelid Infectious Disorders. OIE Book. 2014; pp 319-322.

Thesis: Rathod Avni. Therapeutic studies on sarcopticosis in camels (Camelus dromedarius). Unpublished Masters Thesis (MVSc), Rajasthan Agricultural University, Bikaner, Rajasthan, India. 2006.

Commercial booklets: Anonymous/Name. Conray-Contrast Media. IIIrd Edn., 1967; pp 12-15, May and Baker Ltd., Dagenham, Essex, England.

Magazine articles: Taylor D. The Constipated Camel. Reader's Digest. Indian Edn. RDI Print & Publishing (P) Ltd., Mehra House, 250-C, New Cross Road, Worli, Bombay, India. 1985; 126:60-64

News paper articles: Christina Adams. Camel milk: a miracle cure for children with autism?. Gulf News, Published: April 09. 2014.

Personal communication: Hall LW. Reader in Comparative Anaesthesia, Department of Clinical Veterinary Medicine, Madingley Road, University of Cambridge, Cambridge, CB3 0ES, England. 1995.

Reprints or Publication charges: There is no provision for free reprints. Author or person in correspondence has to pay INR 4500/- (for Indian Citizens only) or US $ 450, in advance to receive a final PDF or for 10 reprints for the year 2022. Publication charges for colour and black and white pictures: Author(s) has to pay publication charges of colour plates in his/her manuscript as per the invoice provided to them. Publication charges would be double if a manuscript is more

than 10 printed pages in length. The publication charges can be paid into the bank account of Camel Publishing House (using cheque, demand draft or money transfer method) or through a payment portal given in our website www.camelsandcamelids.com. Author(s) will be sent final pre-published PDF for verification and corrections, if any, along with an invoice and bank account details for making advance payment, before publication of manuscript in JCPR.

Copyright: The copyright of the article will remain with the owner, Dr Tarun Kumar Gahlot and will be governed by the Indian Copyright Act.

Author Consent Letter

{Note: Kindly take print out of the Author Consent letter form, fill, scan and send along with your manuscript. Without Author Consent letter your manuscript will not be considered for publication}

To

Editor in Chief

Journal of Camel Practice and Research

Camel Publishing House

Bikaner

Sub: Submission of manuscript for publication in Journal of Camel Practice and Research reg.

Dear Sir

I hereby submit the manuscript for publication in 'Journal of Camel Practice and Research". I assure that this manuscript has neither been published in any other journal nor submitted for publication in any other journal. I also undertake along with the other authors that present study (on animals, human or laboratory animals, if any) was undertaken after the prior approval of relevant country/institutional ethical committee. I and on behalf of other co-author(s), I declare "No conflict of interest". I assure that this article do not have any plagiarism. Kindly consider the manuscript for publication in your journal. I abide all rules and regulations of the journal. In future if any litigation arises in this article I will cooperate with the editor to resolve the issue. I shall accept the decision of the editor and that would be final.

Thanking You

SIGNATURE of Corresponding Author

NAME

ADDRESS

Kindly enter the details in the following

Manuscript

TITLE:

SUBJECT:

LABORATORY/RESEARCH CENTRE/INSTITUTE:

BACK ISSUES OF JCPR AVAILABLE

ISSN 0971-6777 (Print)
ISSN 2277-8934 (Online)

JOURNAL OF CAMEL PRACTICE AND RESEARCH

www.camelsandcamelids.com • www.indianjournals.com

Volume 21 June 2014 Number 1

In This Issue

ISSN 0971-6777 (Print)
ISSN 2277-8934 (Online)

JOURNAL OF CAMEL PRACTICE AND RESEARCH

www.camelsandcamelids.com • www.indianjournals.com

Volume 21 December 2014 Number 2

In This Issue

ISSN 0971-6777 (Print)
ISSN 2277-8934 (Online)

JOURNAL OF CAMEL PRACTICE AND RESEARCH

www.camelsandcamelids.com • www.indianjournals.com

Volume 22 June 2015 Number 1

In This Issue

ISSN 0971-6777 (Print)
ISSN 2277-8934 (Online)

JOURNAL OF CAMEL PRACTICE AND RESEARCH

www.camelsandcamelids.com • www.indianjournals.com

Volume 22 December 2015 Number 2

In This Issue

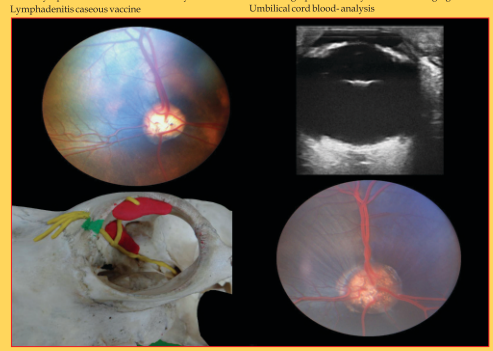

See the details of list of contents of all previous issues of JCPR on our website www.camelsandcamelids.com

Kindly refer querries to: Dr. T.K. GAHLOT, Editor, JCPR
email: tkcamelvet@yahoo.com